The 3rd Edition of the Spicy Gluons Workshop



Exotic Nuclear Structure and Decay Under Extreme Conditions

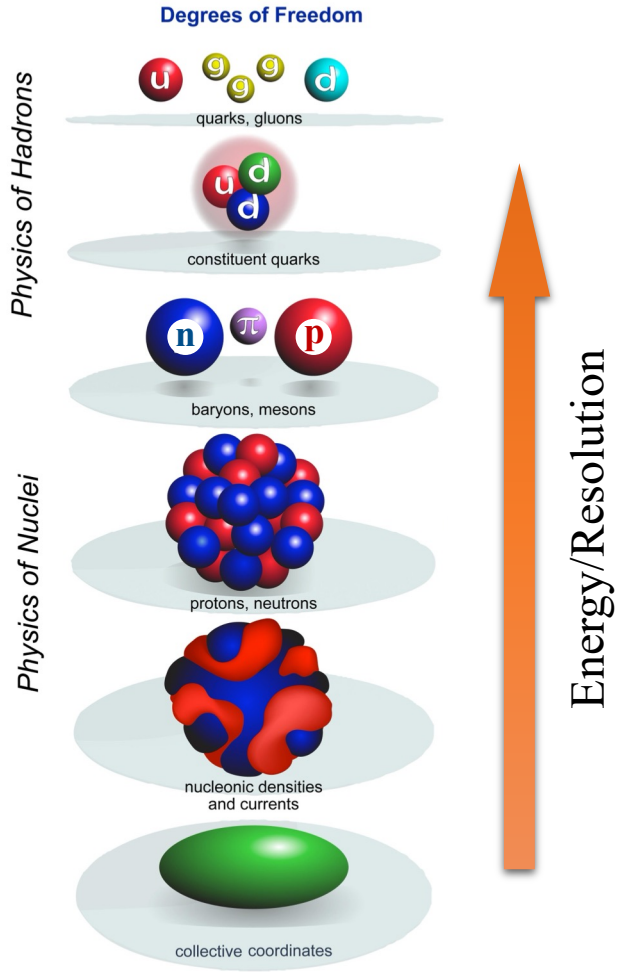
Simin Wang (S. M. Wang)

Fudan University

Collaborators: Y. G. Ma, F. R. Xu, W. Nazarewicz, M. Pfützner, Y. R. Lin, A. Gade, T. Beck, I. Mukha, R. J. Charity, A. Volya …



Nuclear degrees of freedom



Energy/Resolution

$$\Delta p \Delta x \geq \frac{\hbar}{2}$$

$$\Delta E \Delta t \geq \frac{\hbar}{2}$$

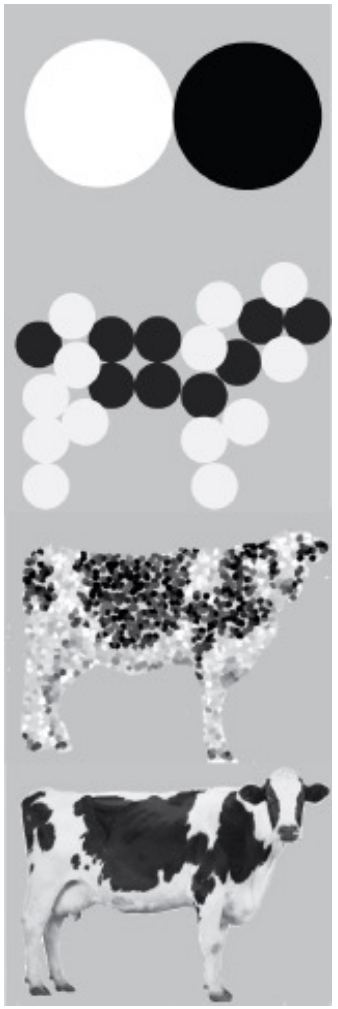
$$\hbar \approx 197\,\mathrm{MeV} \cdot \mathrm{fm}/c$$

$$2^A \times \frac{A!}{N!Z!}$$

coupled equations
in 3A dimensions

Hilbert-space
truncations
necessary

Resolution



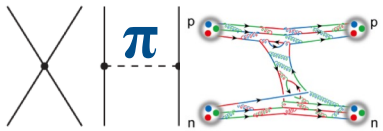
W Nazarewicz, J. Phys. G 43, 044002 (2016)

Nuclear force

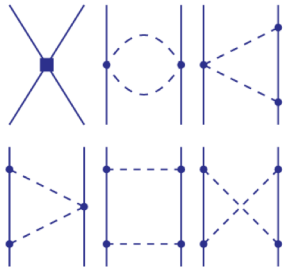
Realistic interaction: chiral EFT

2-body force

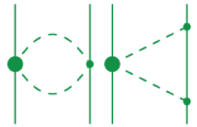
LO $(Q/\Lambda_\chi)^0$



NLO $(Q/\Lambda_\chi)^2$

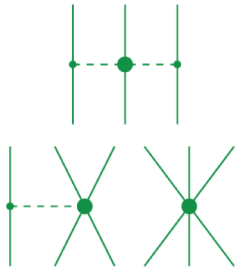


NNLO $(Q/\Lambda_\chi)^3$

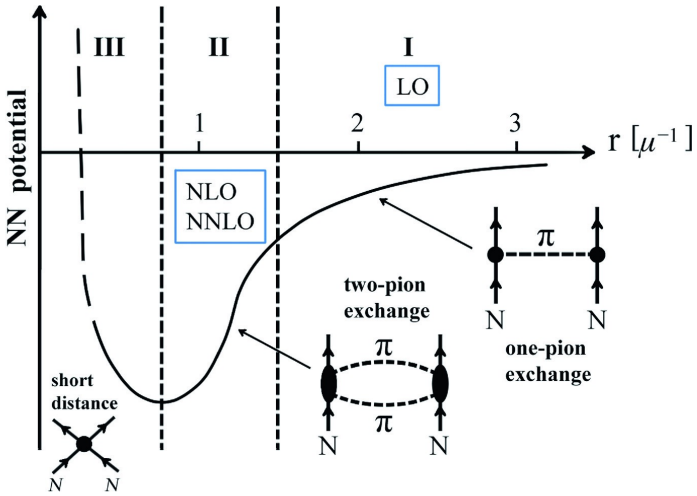


+...

3-body force



Taketani diagram



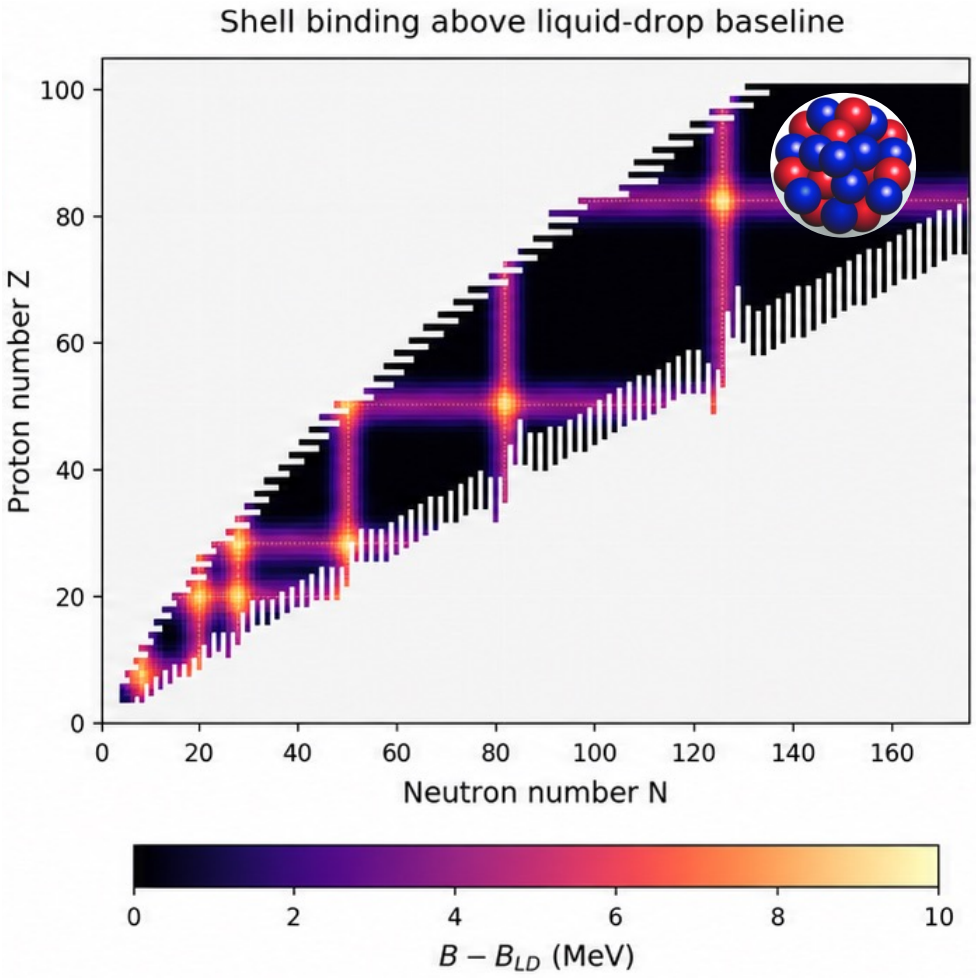
Hierarchy of scaling

$$V_{\rm LO} = V_{1\pi} + V_{\rm ct}^{(0)}$$

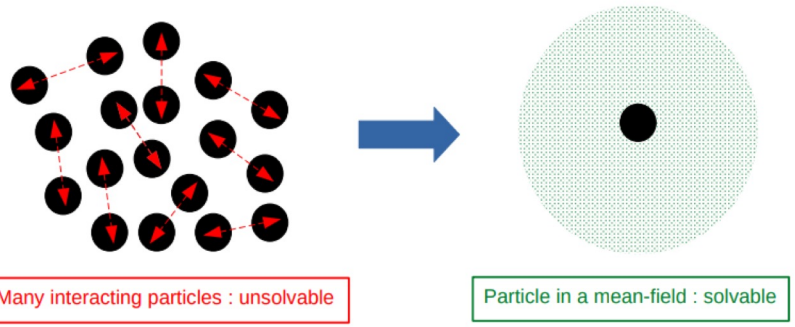
$$V_{\rm NLO} = V_{\rm LO} + V_{2\pi}^{(2)} + V_{\rm ct}^{(2)}$$

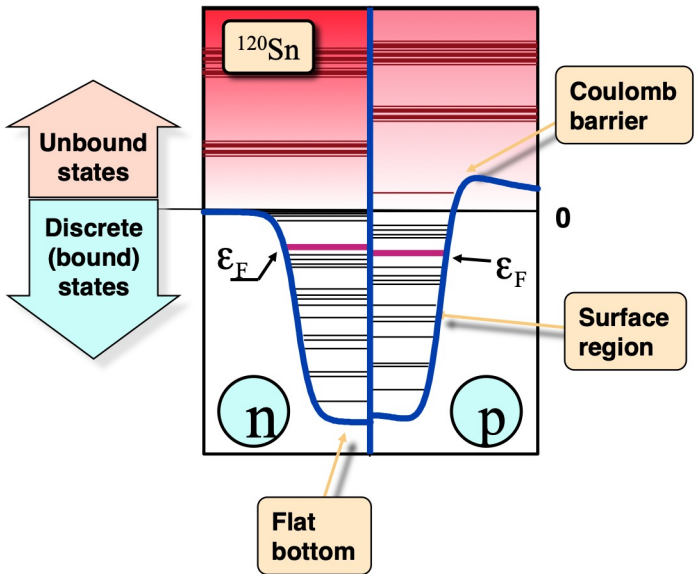
$$V_{\rm N^2LO} = V_{\rm NLO} + V_{2\pi}^{(3)}$$

Nuclear landscape

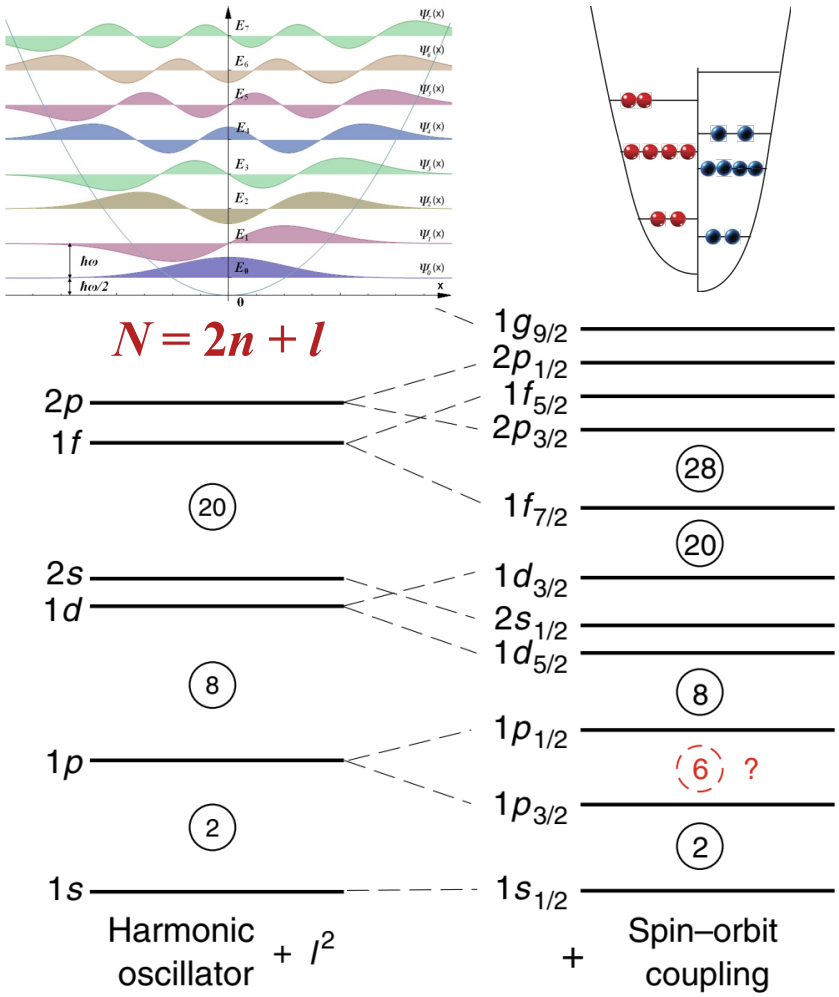


Nuclear mean field





Nuclear single-particle levels



Large energy gaps stabilize closed shells.

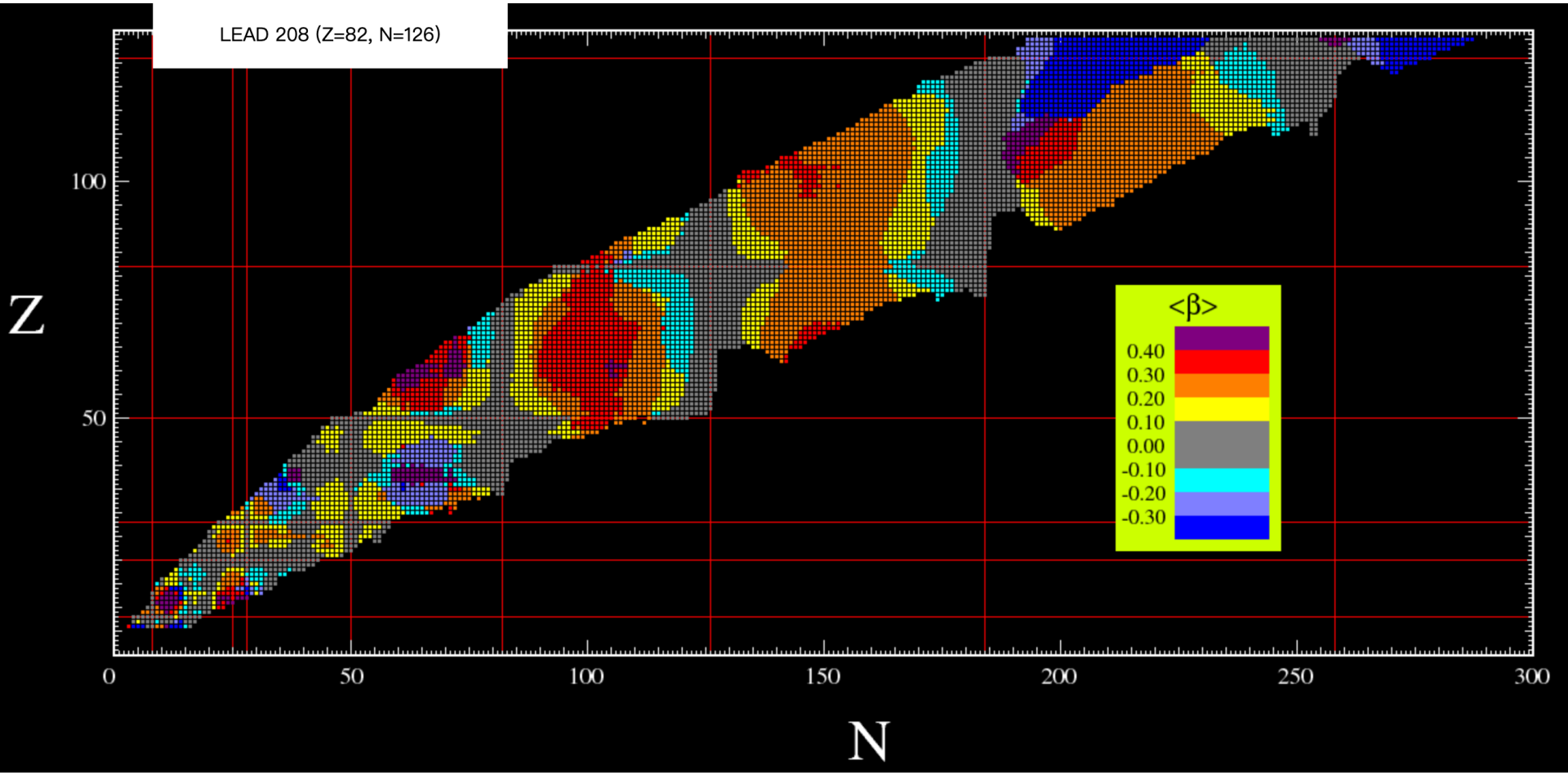
Spin–orbit coupling creates the familiar magic numbers.

Far from stability, orbital spacing and correlations evolve.

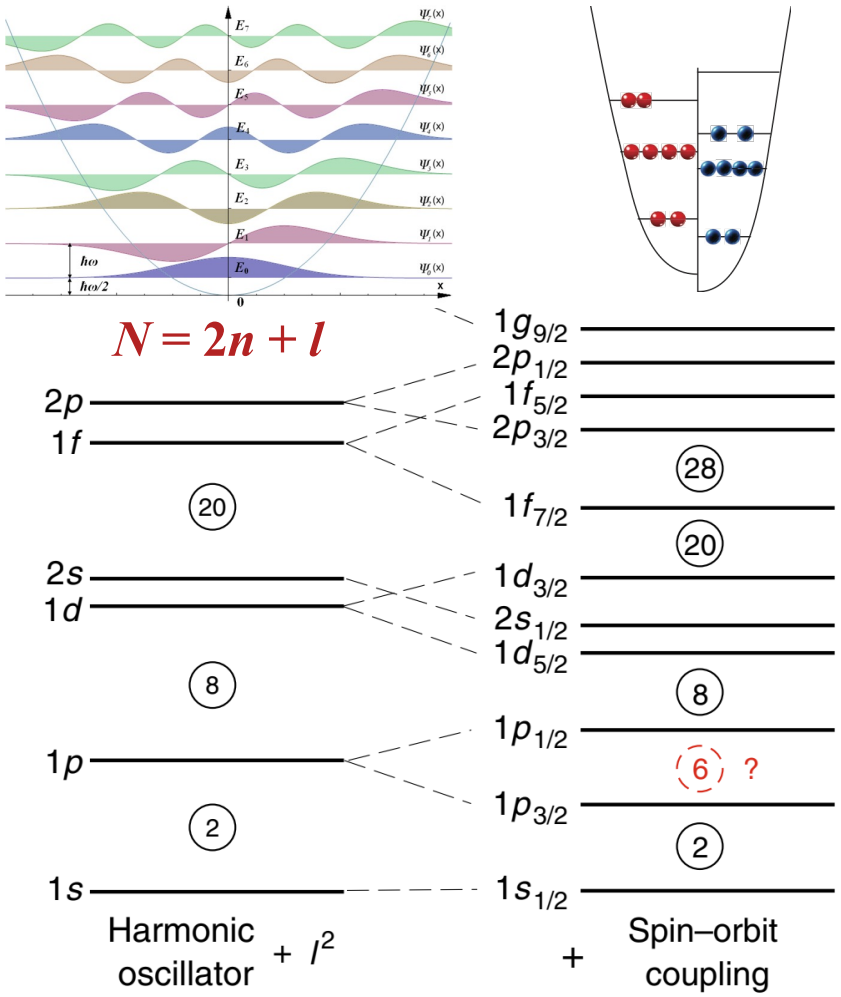
A shell gap is a property of an evolving many-body system.

D. T. Tran *et al.*, Nat. Commun. 9, 1594 (2018), Fig. 1.

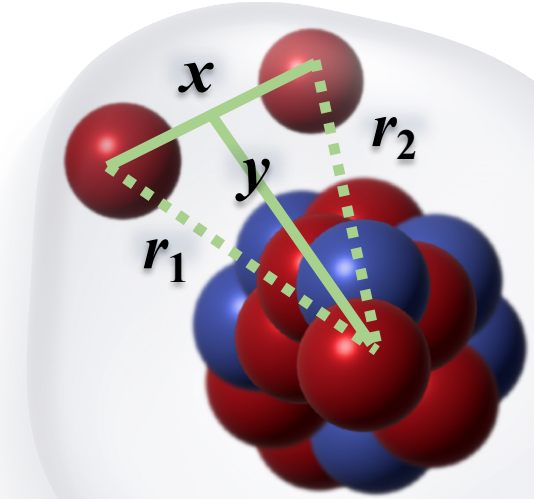
Nuclear deformation



Nuclear single-particle levels



D. T. Tran *et al.*, Nat. Commun. 9, 1594 (2018), Fig. 1.



$$R = R(\theta,\phi) = R_0\left(1 + \alpha_{00} + \sum_{\lambda=1}^{\infty}\sum_{\mu=-\lambda}^{\lambda} \alpha^*_{\lambda\mu} Y_{\lambda\mu}(\theta,\phi)\right)$$

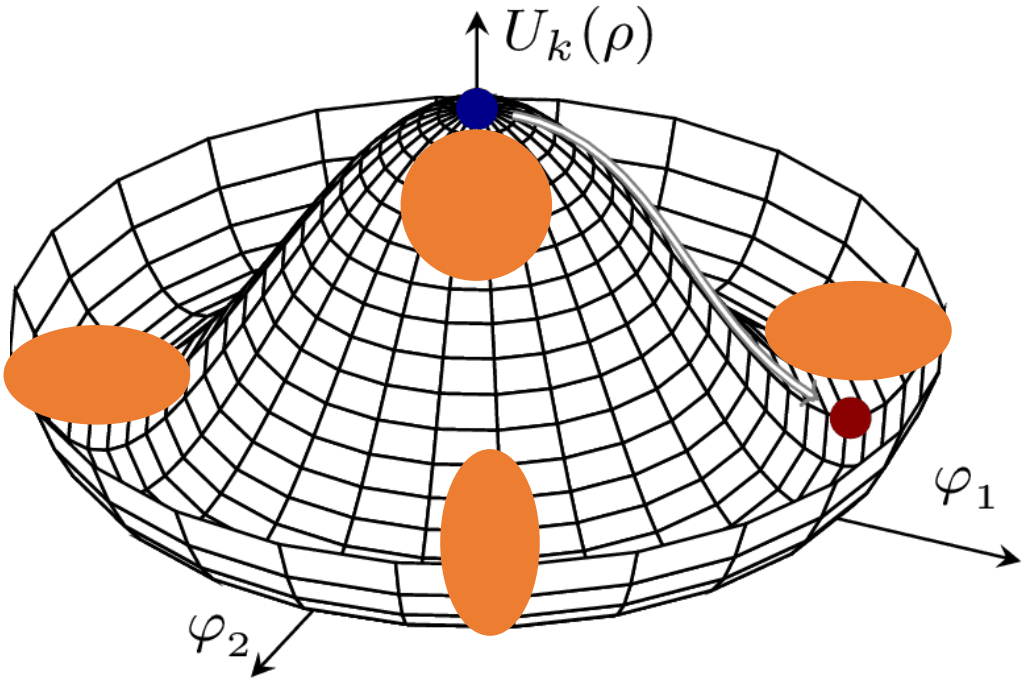
Jacobi ⟷ **Single-particle**

(ℓ_x, ℓ_y) ⟷ (ℓ_1, ℓ_2)

$(0, 0)$ ⟷ (s, s), (p, p), (d, d), (f, f)

dinucleon

Spontaneous symmetry breaking



The energy surface preserves the symmetry.

A chosen minimum selects an intrinsic orientation.

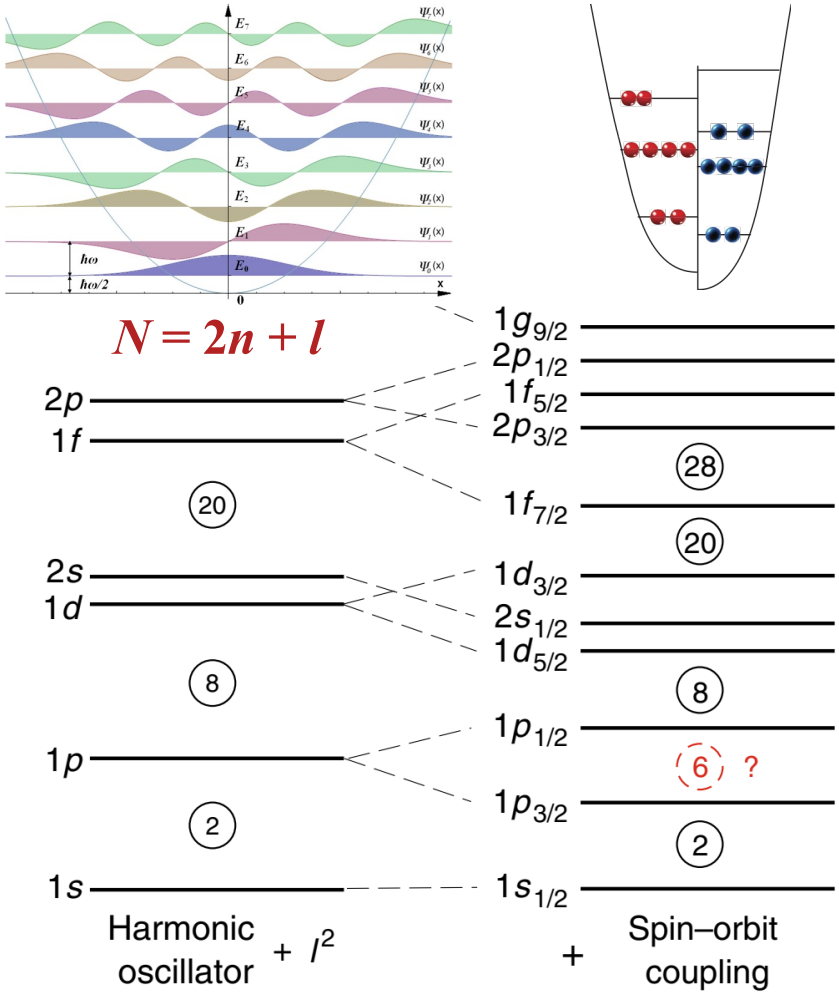
Equivalent orientations generate collective rotational motion.

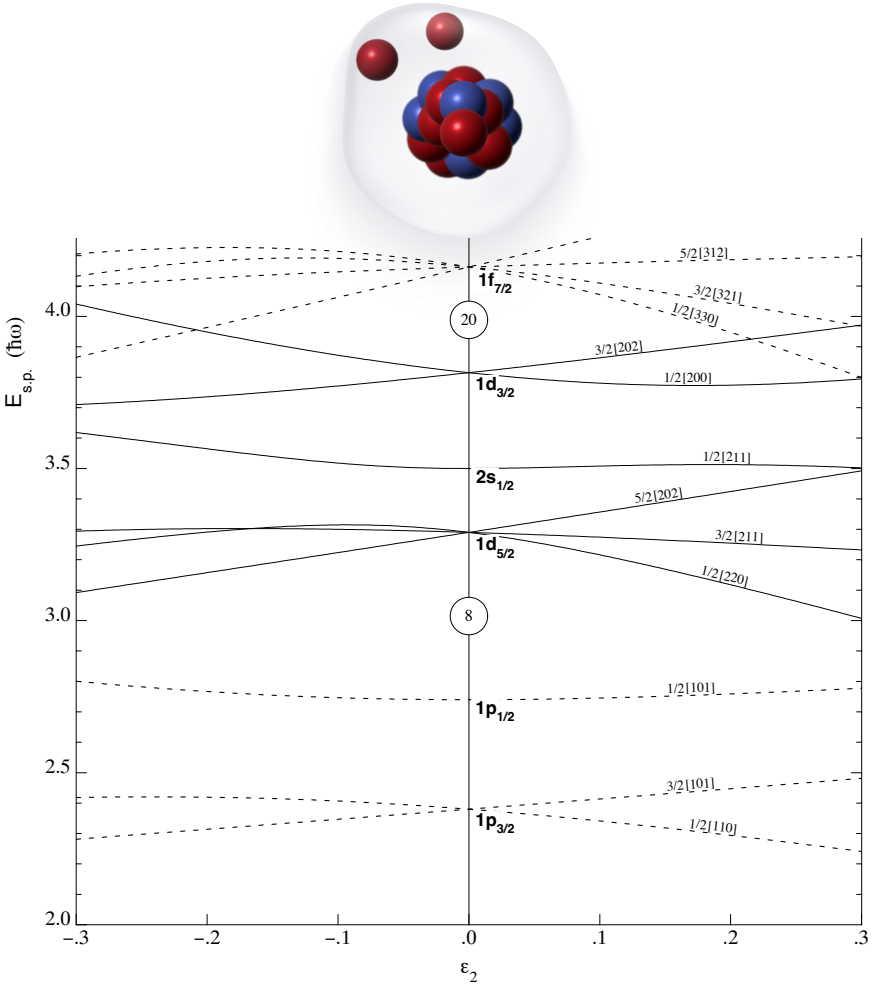
Conceptual order-parameter diagram

A finite nucleus requires symmetry restoration for states with good angular momentum.

J. Phys. G 48, 123001 (2021)

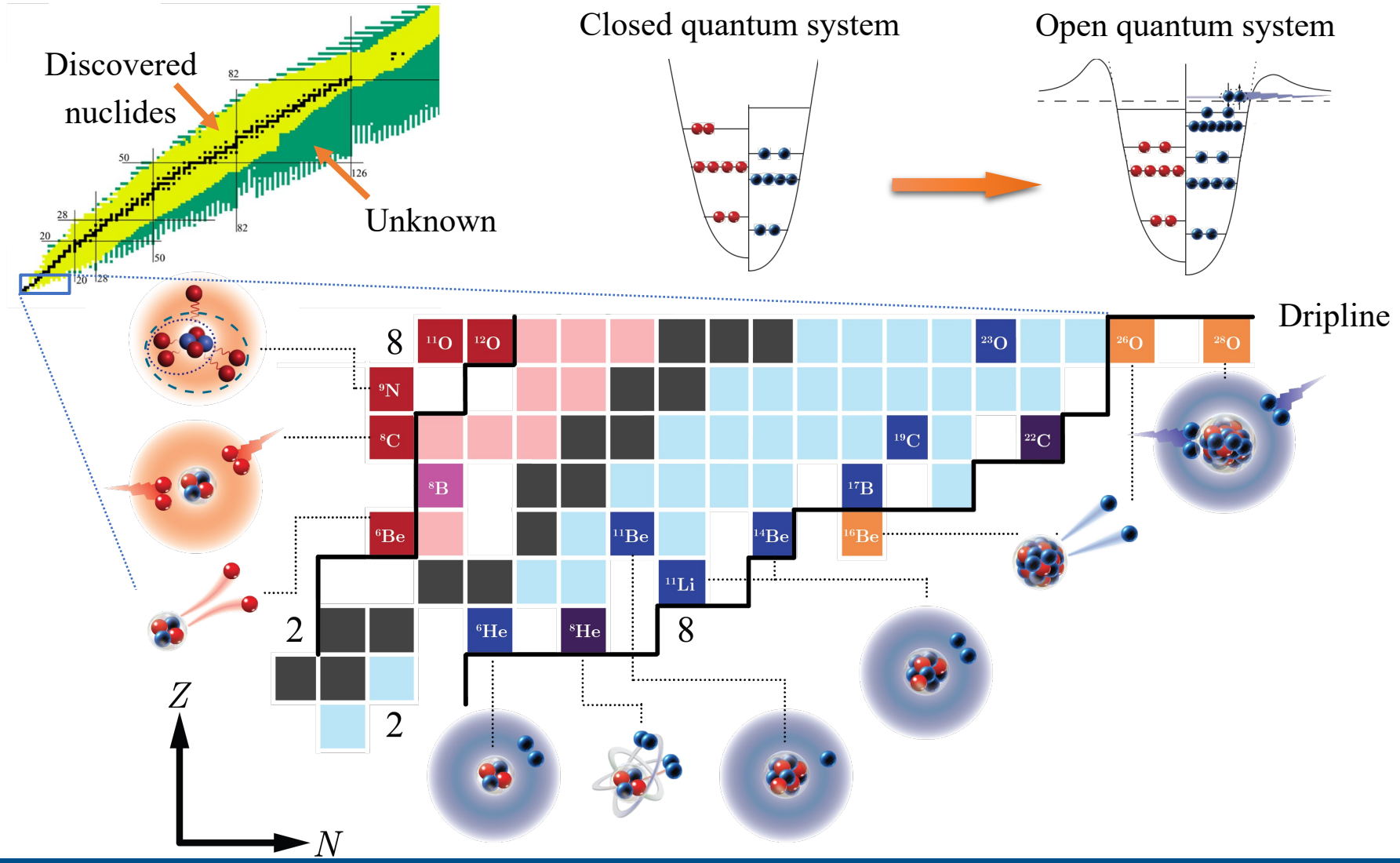
Nuclear single-particle levels



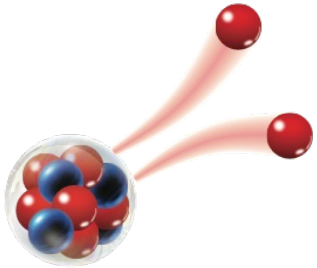


D. T. Tran *et al.*, Nat. Commun. 9, 1594 (2018), Fig. 1.

New physics towards the dripline

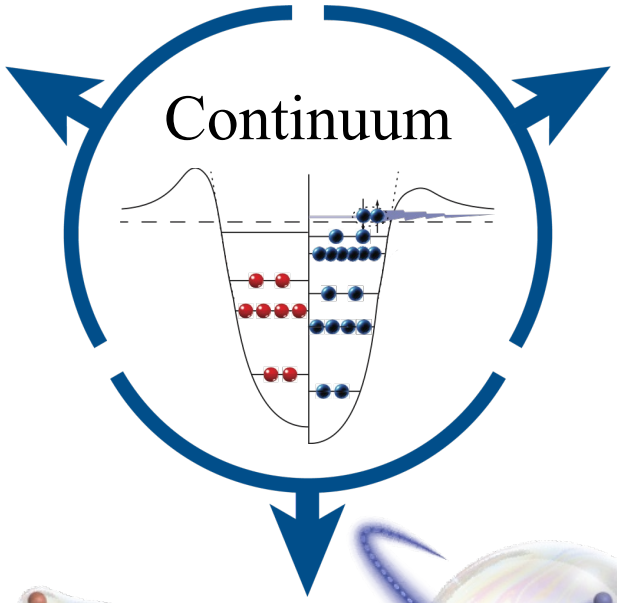


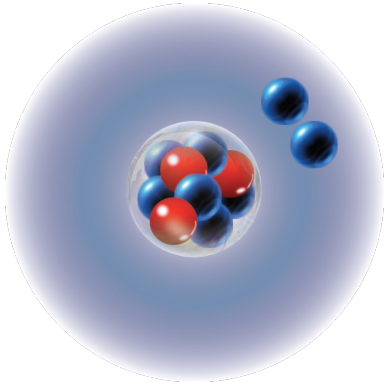
Continuum-impacted phenomena



Rare decay modes

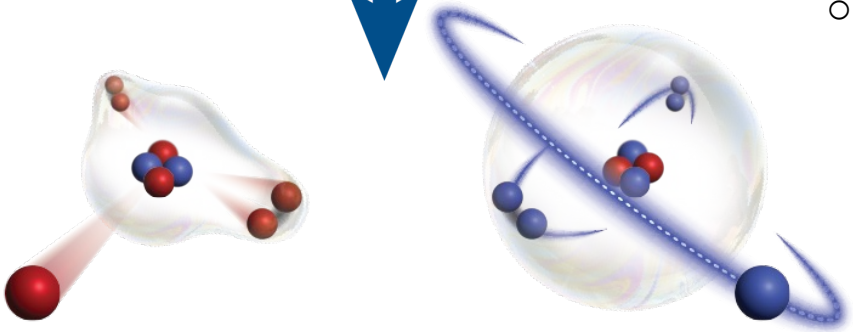
- $2p/2n$ decays
- Multi-particle emissions
- …





Exotic structures

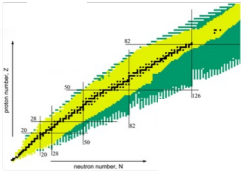
- Halo & clustering
- Deformation
- …



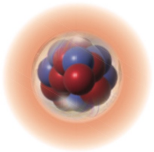
Mirror symmetry breaking

Outline

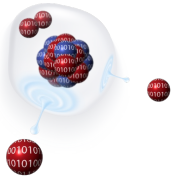
Introduction 1
- Dripline region
- Continuum coupling



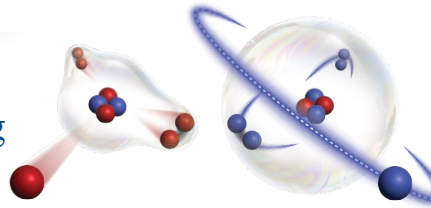
Radius 2
- Complex radius
- Halo-like enhancement



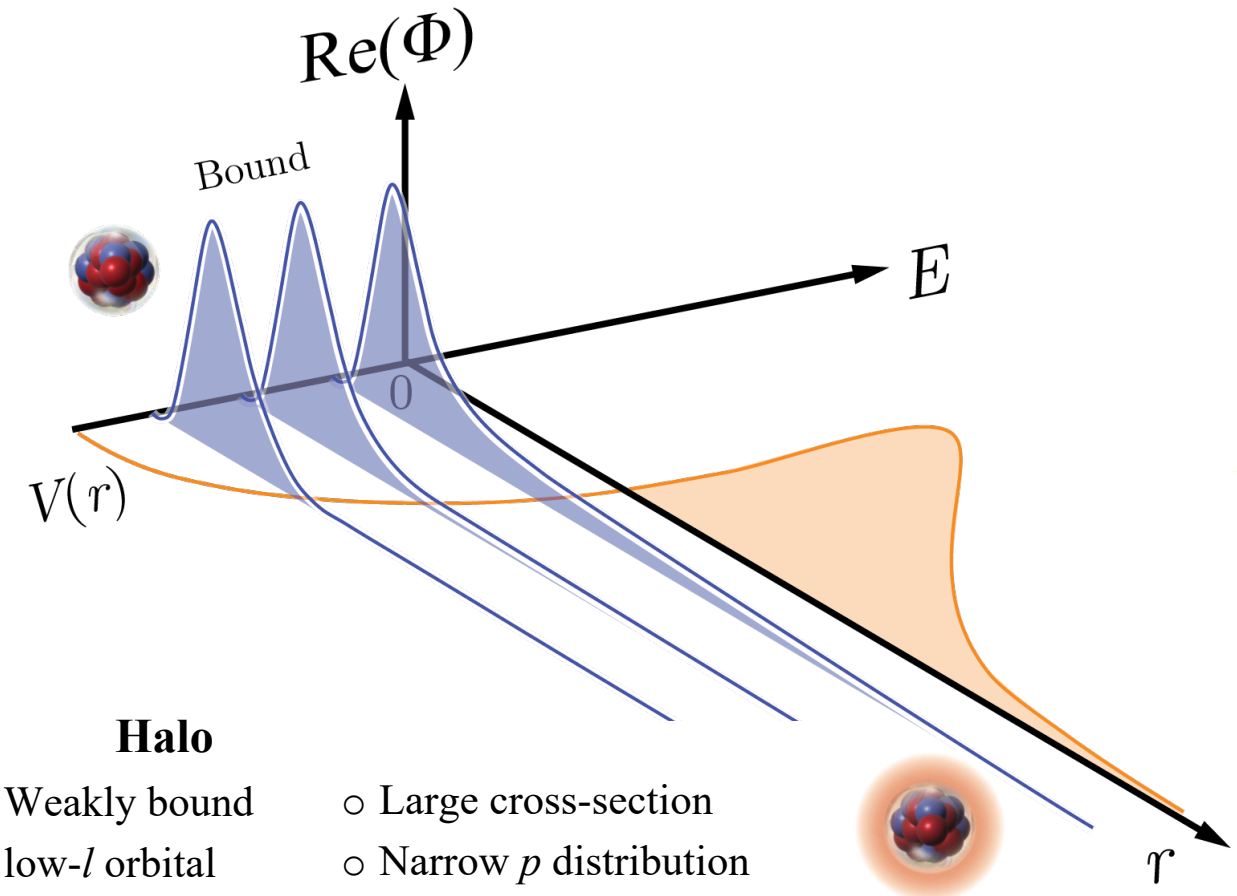
Decay 3
- 2*p* decay
- *pp* correlation

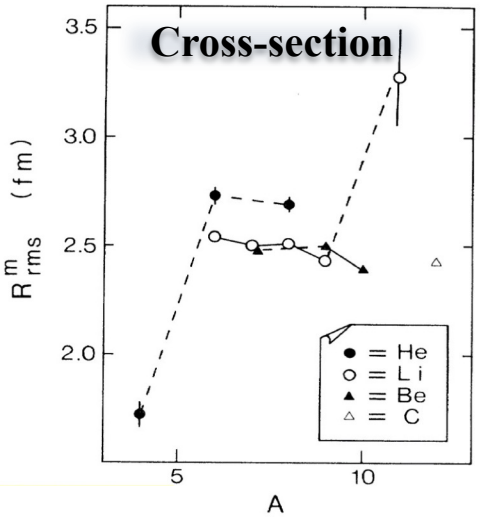


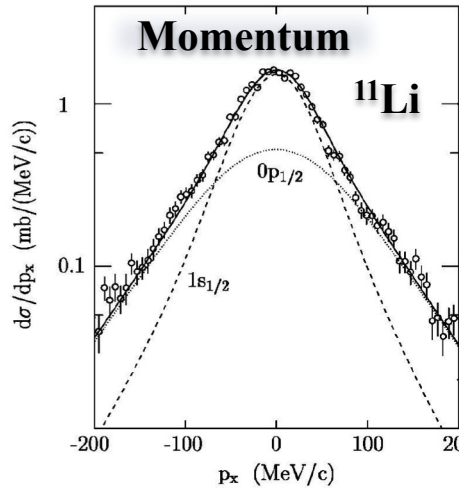
Mirror 4
- Thomas-Ehrman effect
- Mirror symmetry breaking



Contiuum effect







Halo

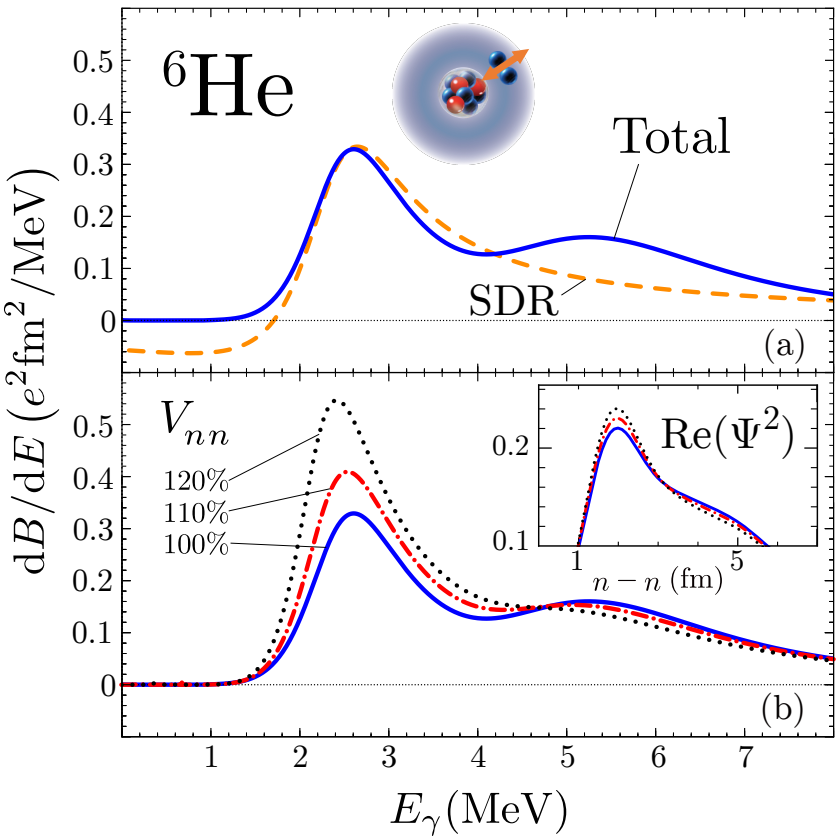
- Weakly bound
- low-*l* orbital
- Enhanced radius
- Large cross-section
- Narrow *p* distribution
- *E*1 response/MSB

$$r^2_{\mathrm{rms}} \equiv \langle \Phi | r^2 | \Phi \rangle = \int_0^\infty |r\Phi|^2 r^2 \, dr.$$

I. Tanihata *et al.*, Phys. Rev. Lett. 55, 2676 (1985)
H. Simon *et al.*, Phys. Rev. Lett. 83, 496 (1999)

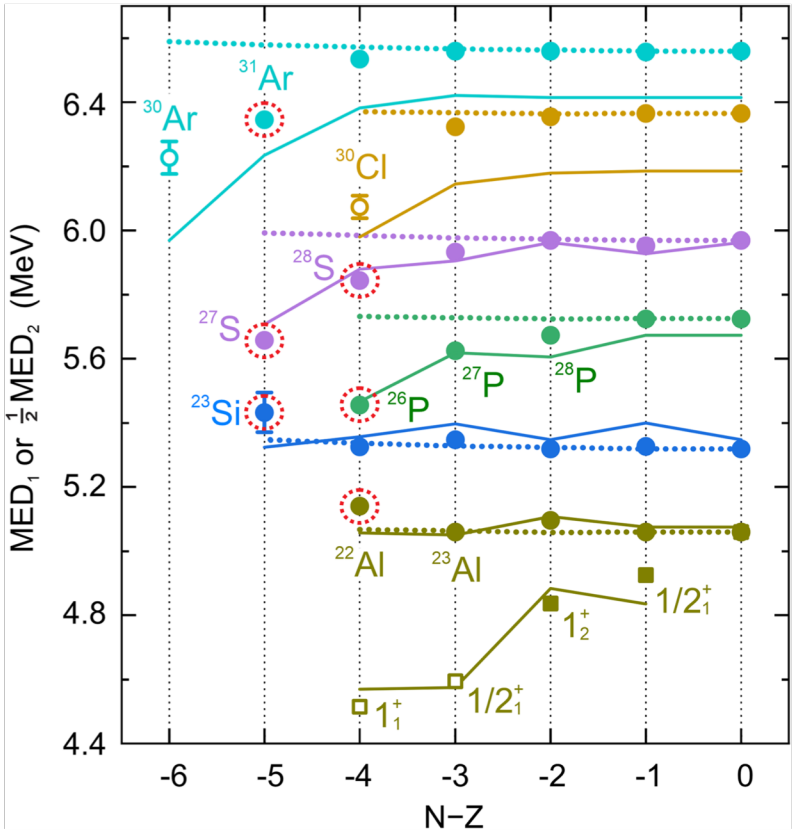
Impact of diffused density (halo)

$E1$ response



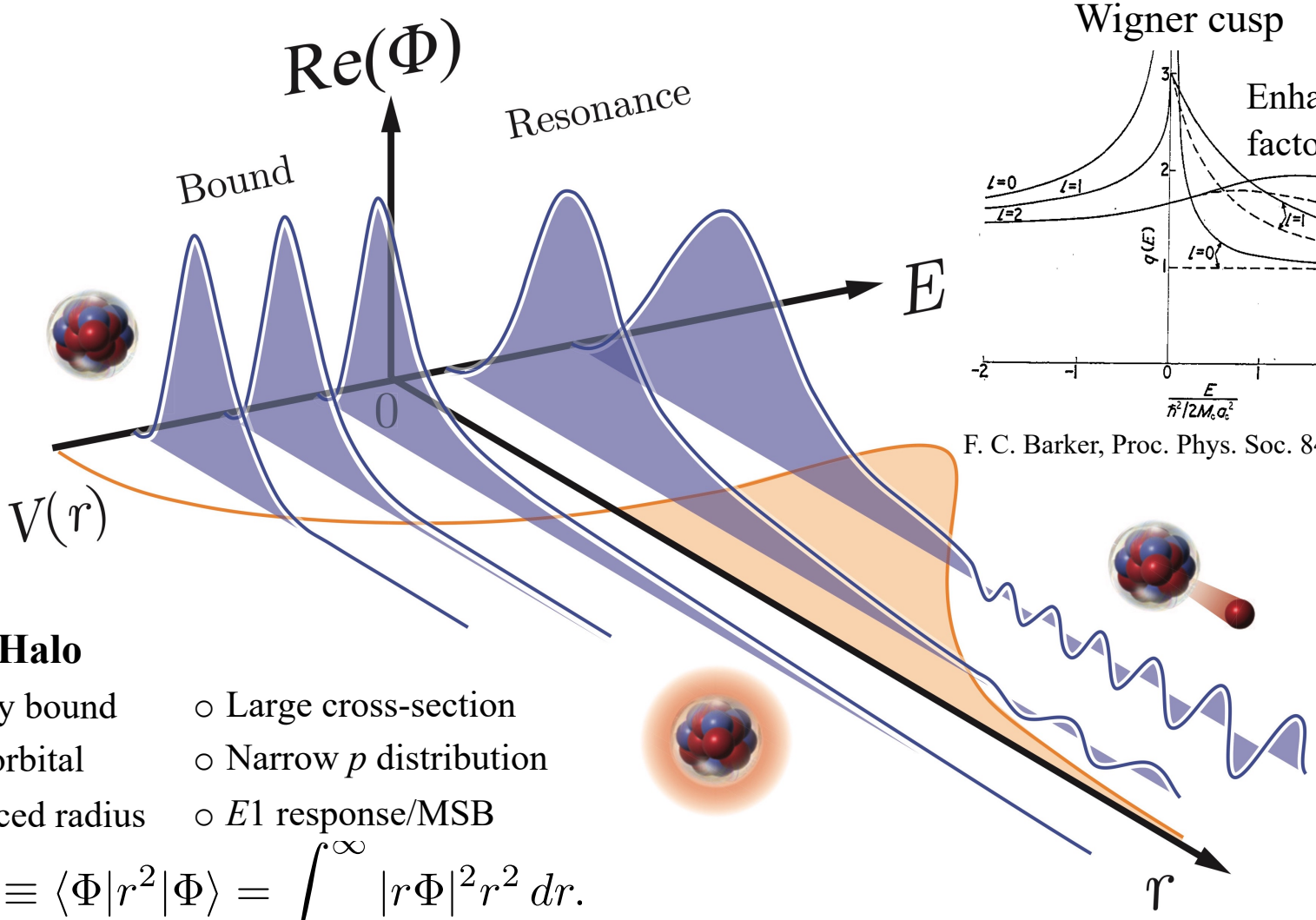
Y. H. Yang *et al.*, Eur. Phys. J. A 61, 69 (2025)
T. Nakamura *et al.*, Phys. Rev. Lett 96, 252502(2006)
Y. L. Sun *et al.*, Phys. Lett. B 814, 136072 (2021)

Mirror energy difference



Y. Yu *et al.*, Phys. Rev. Lett. 133, 222501 (2024)

Contiuum effect



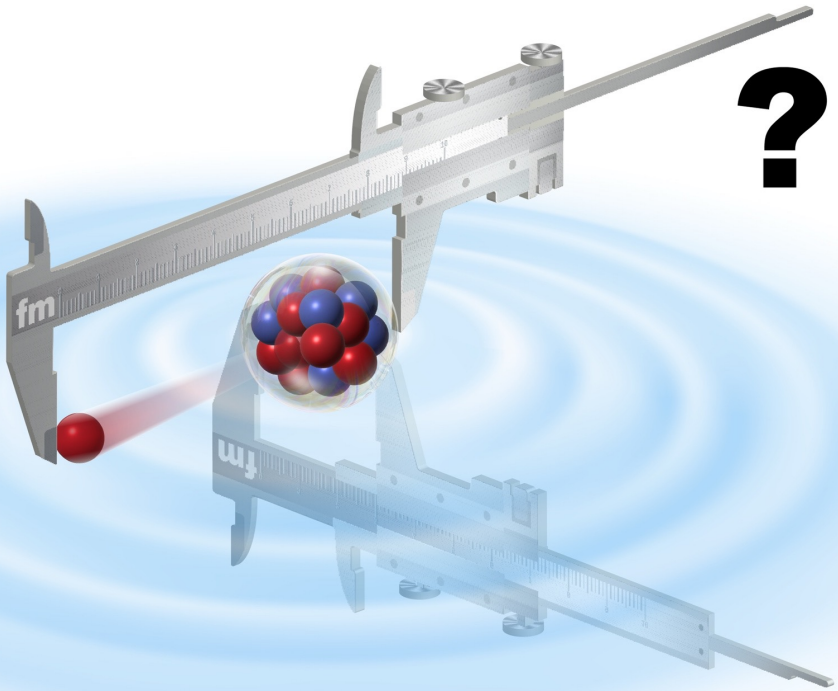
F. C. Barker, Proc. Phys. Soc. 84, 681 (1964)

Halo

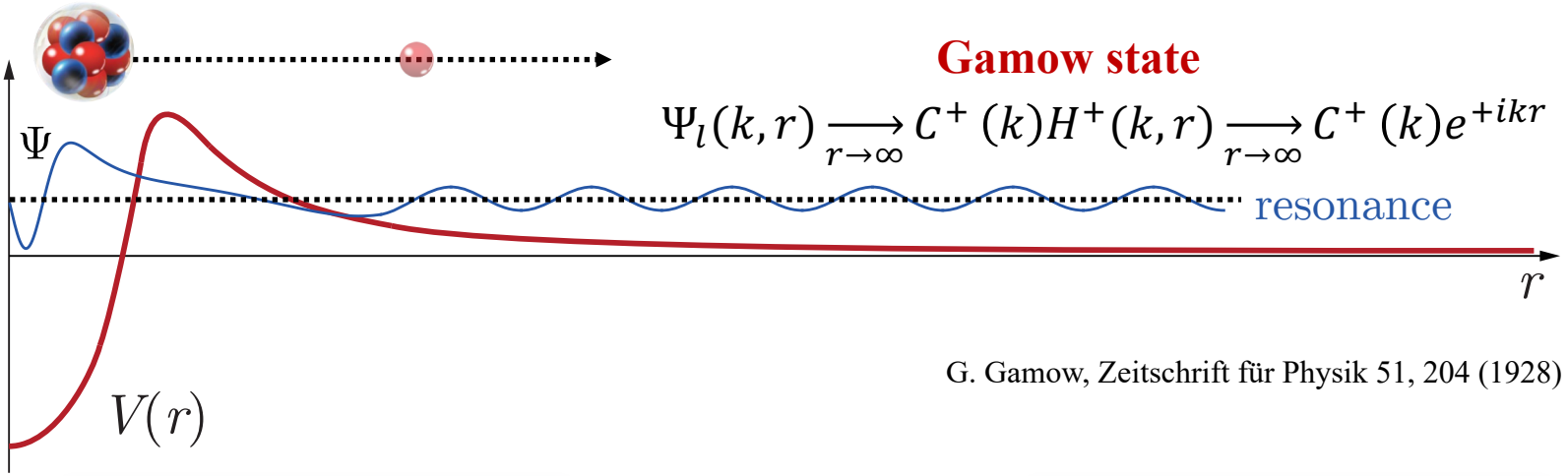
- Weakly bound
- low-l orbital
- Enhanced radius
- Large cross-section
- Narrow p distribution
- $E1$ response/MSB

$$r_{\mathrm{rms}}^2 \equiv \langle \Phi | r^2 | \Phi \rangle = \int_0^\infty |r\Phi|^2 r^2 \, dr.$$

Radius of the unbound state

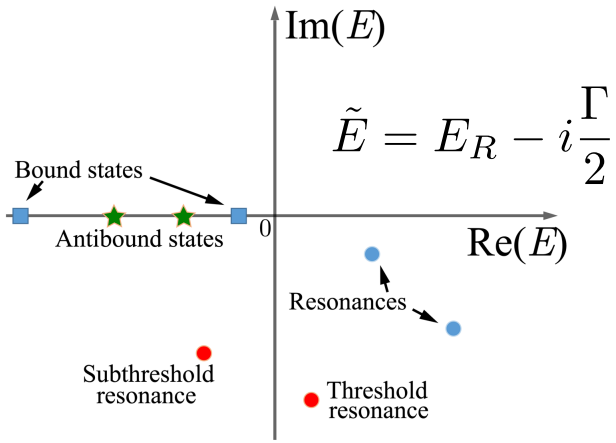


Quantum picture of decay



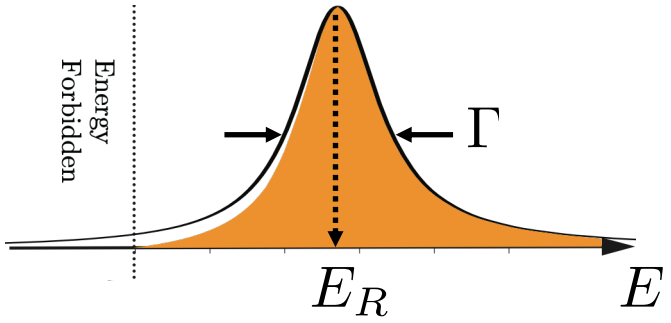
G. Gamow, Zeitschrift für Physik 51, 204 (1928)

Complex energy plane



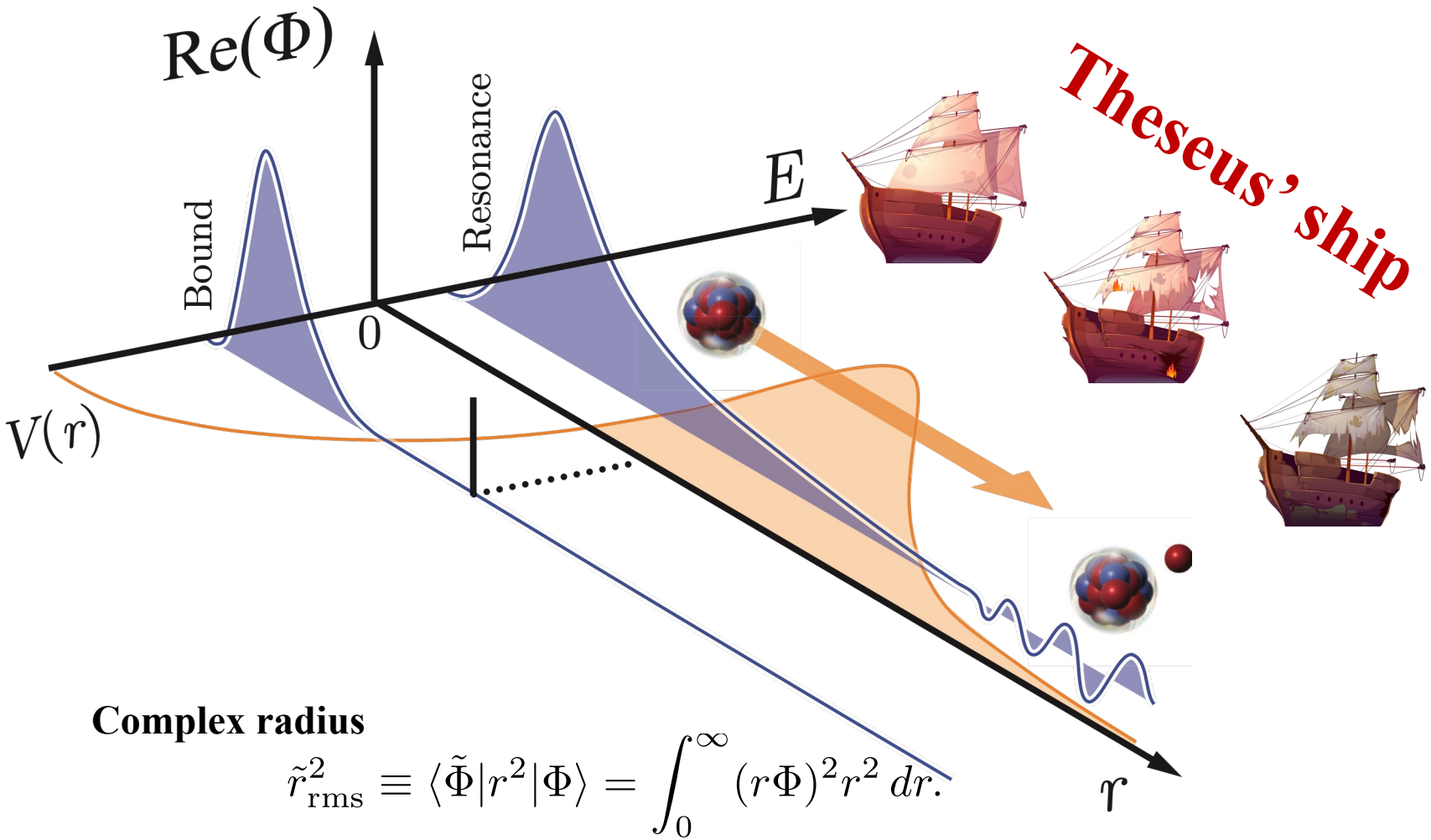
$$\Psi(t) = e^{-i\frac{\hat{H}}{\hbar}t}\Psi(0) = e^{-i\frac{E_R t}{\hbar} - \frac{\Gamma t}{2\hbar}}\Psi(0)$$

Resonance spectral function



$$\Gamma = \frac{\hbar \ln 2}{T_{1/2}}; \qquad \Delta E \Delta T \geq \frac{\hbar}{2}$$

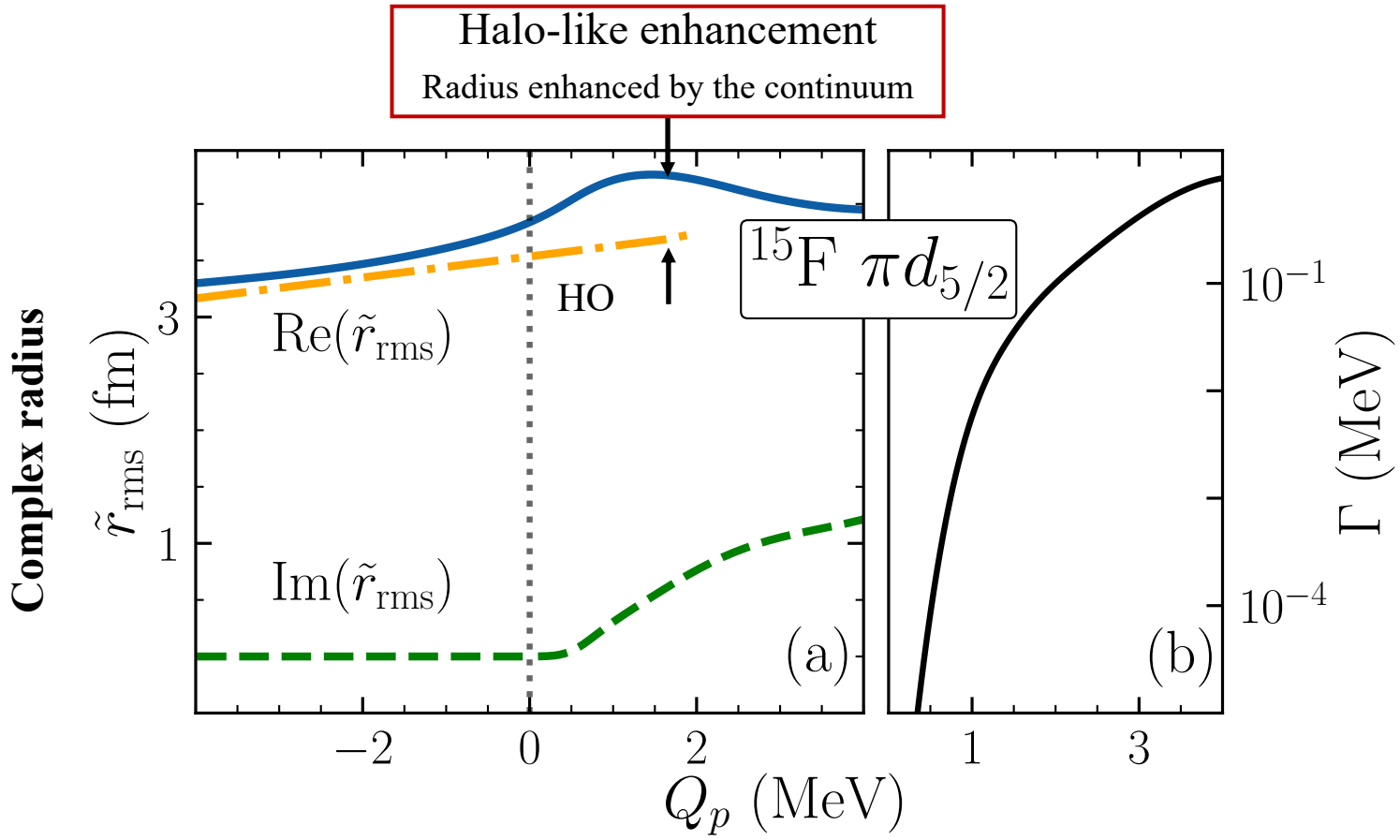
Complex radii of particle emitters



Complex radius

$$\tilde{r}^2_{\rm rms} \equiv \langle\tilde{\Phi}|r^2|\Phi\rangle = \int_0^\infty (r\Phi)^2 r^2\, dr.$$

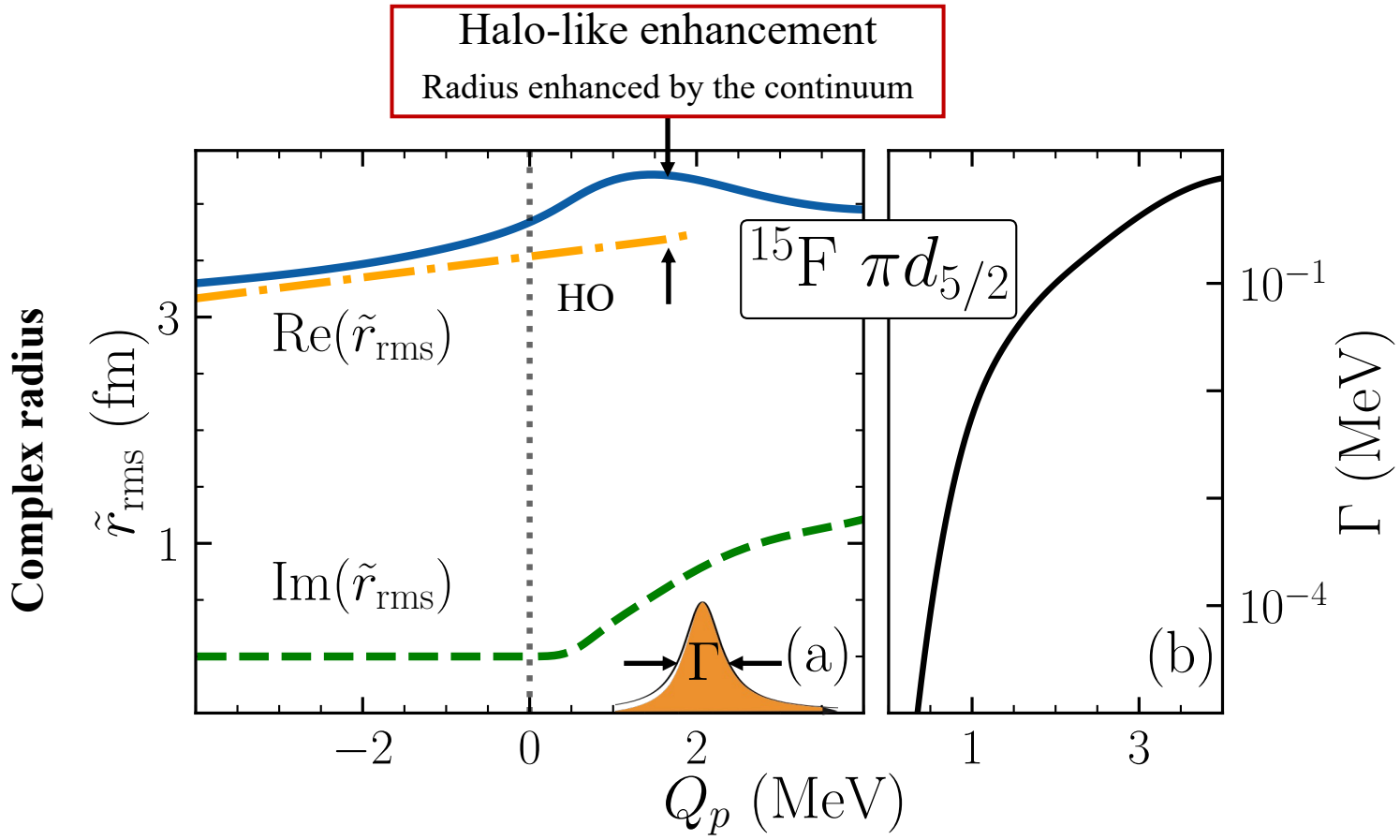
Complex radius of 1*p* emitter ^{15}F



- Contiuum coupling is enhanced near the threshold.
- Complex radius $\tilde{r}^2_{\rm rms} \equiv \langle\tilde{\Phi}|r^2|\Phi\rangle = \int_0^\infty (r\Phi)^2 r^2\, dr.$

Y. R. Lin, SW *et al.*, Phys. Rev. Lett. 136, 122501(2026)
T. Myo and K. Katō,
Prog. Theor. Exp. Phys. 2014, 083D01 (2014).

Complex radius of 1*p* emitter ^{15}F

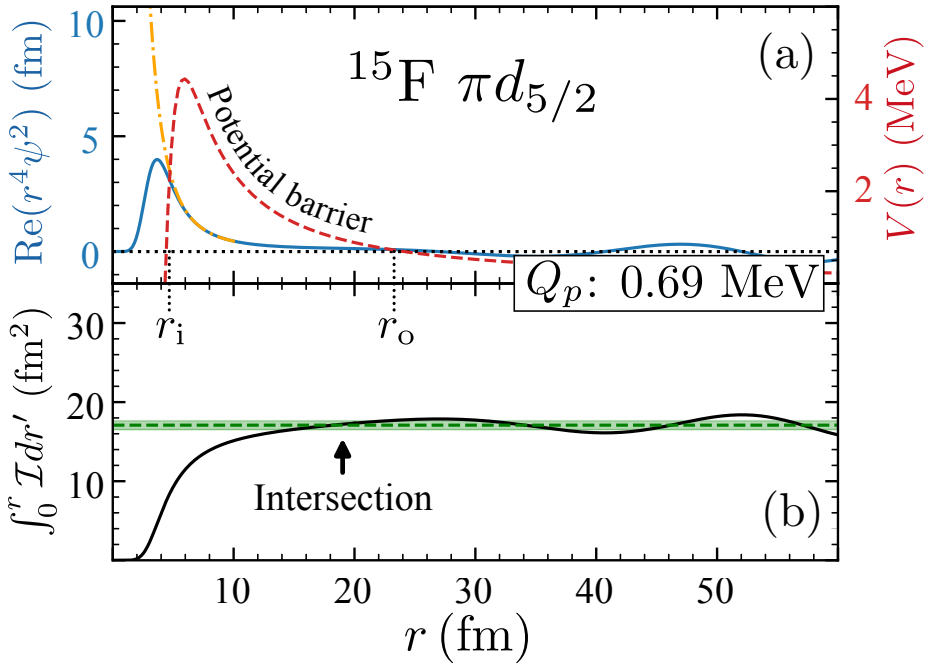


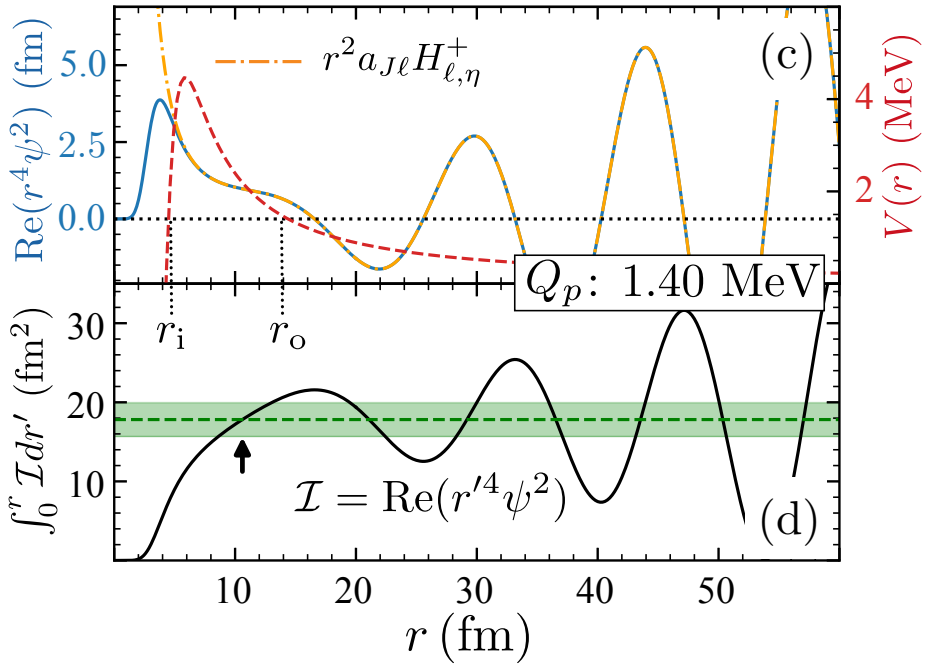
- Contiuum coupling is enhanced near the threshold.
- Complex radius $\tilde{r}^2_{\rm rms} \equiv \langle\tilde{\Phi}|r^2|\Phi\rangle = \int_0^\infty (r\Phi)^2 r^2\, dr.$

Y. R. Lin, SW *et al.*, Phys. Rev. Lett. 136, 122501(2026)
T. Myo and K. Katō,
Prog. Theor. Exp. Phys. 2014, 083D01 (2014).

Complex radius of 1*p* emitter ^{15}F

Wavefunction & radius integrand at Q = 0.69, 1.40 MeV

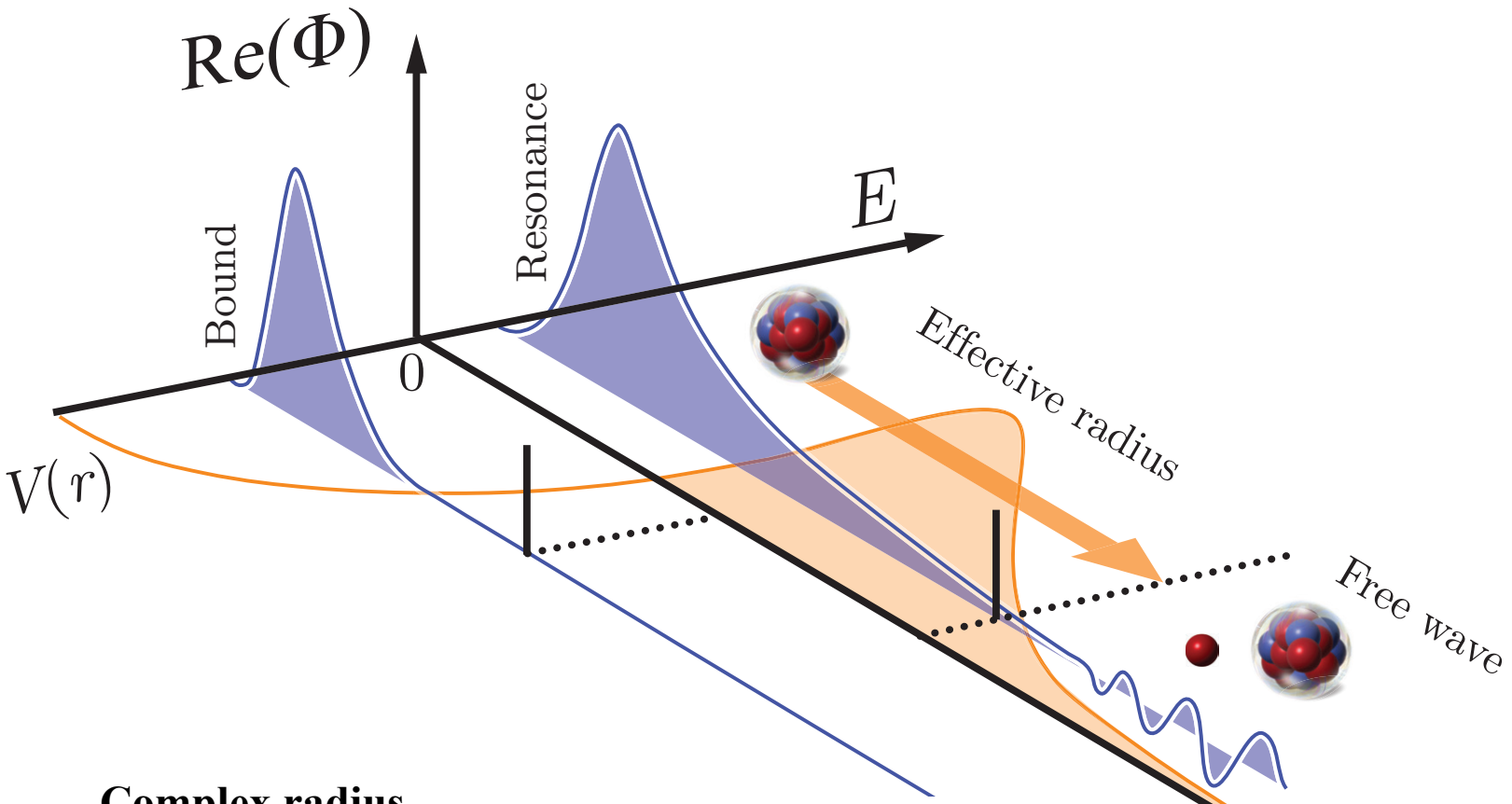




Y. R. Lin, SW *et al.*, Phys. Rev. Lett. 136, 122501(2026)

- The contribution to the complex radius from the asymptotic region is largely canceled out.
- The matching point for the complex radius is located inside the barrier.

Complex radii of particle emitters

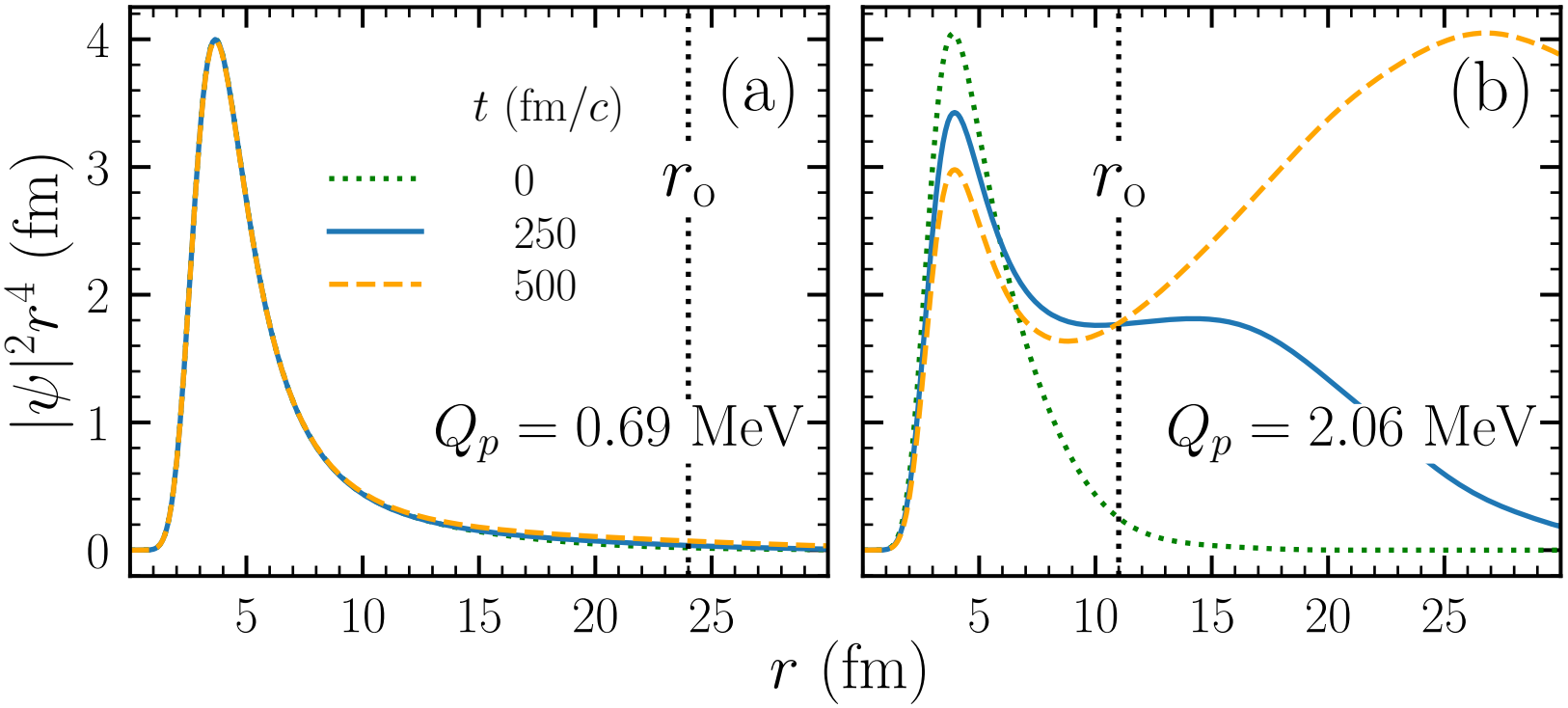


Complex radius

$$\tilde{r}^2_{\rm rms} \equiv \langle \tilde{\Phi} | r^2 | \Phi \rangle = \int_0^\infty (r\Phi)^2 r^2 \, dr.$$

RMS radius evolution during the decay

Wavefunction evolution at Q = 0.69, 2.06 MeV

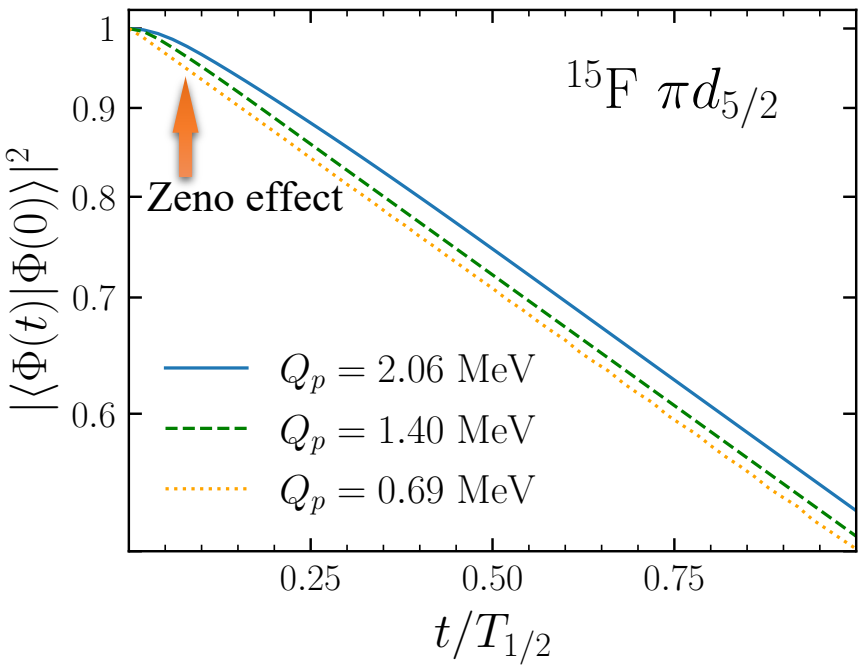


- The density inside r_i gradually decreases.
- Beyond r_o is the free space for particle emission.

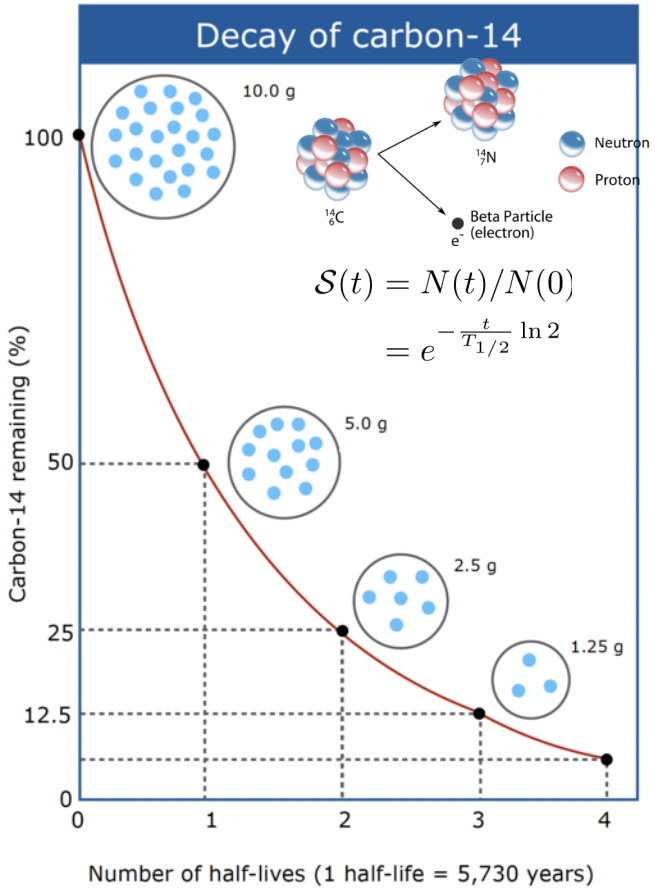
Y. R. Lin, SW *et al.*, Phys. Rev. Lett. 136, 122501(2026)

Survival probability

Survival probability



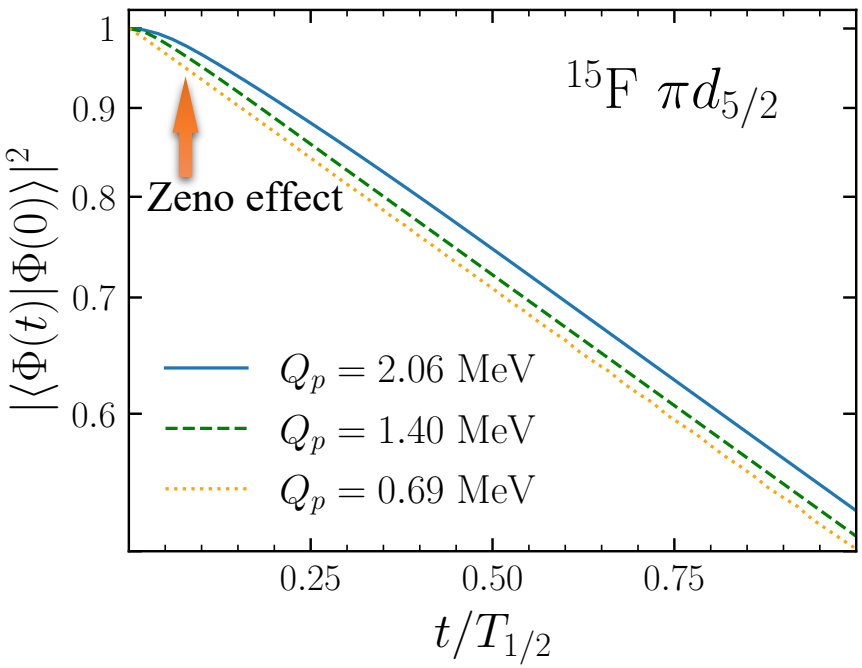
Classical picture of decay



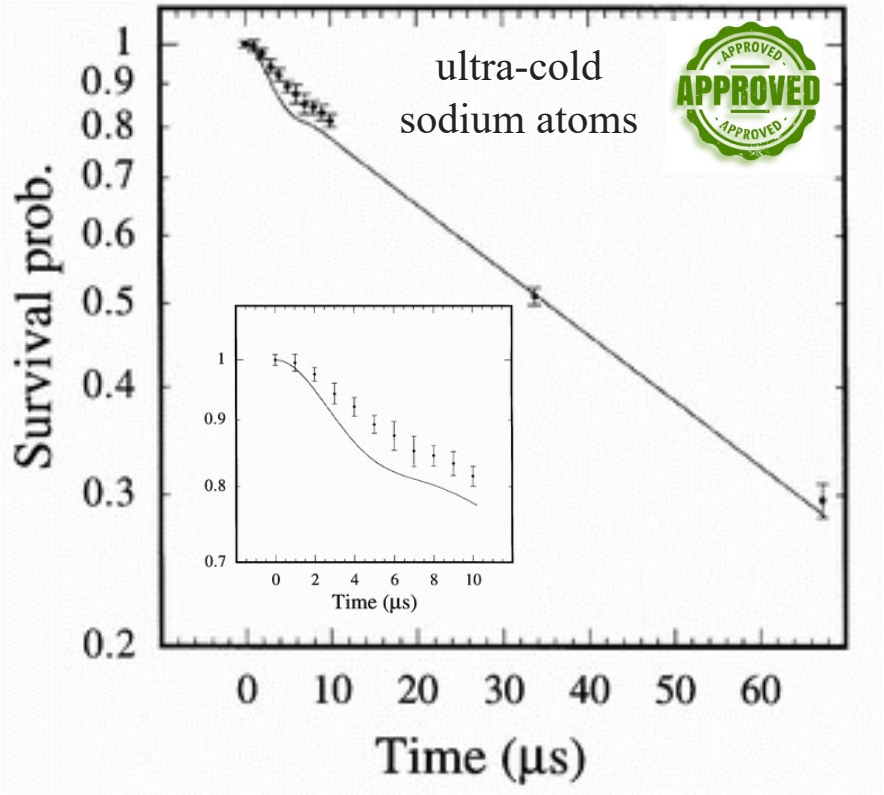
- Decay rate is a constant in classical decay.
- Memory effect in quantum decay.

Quantum Zeno effect

Survival probability



Quantum tunneling

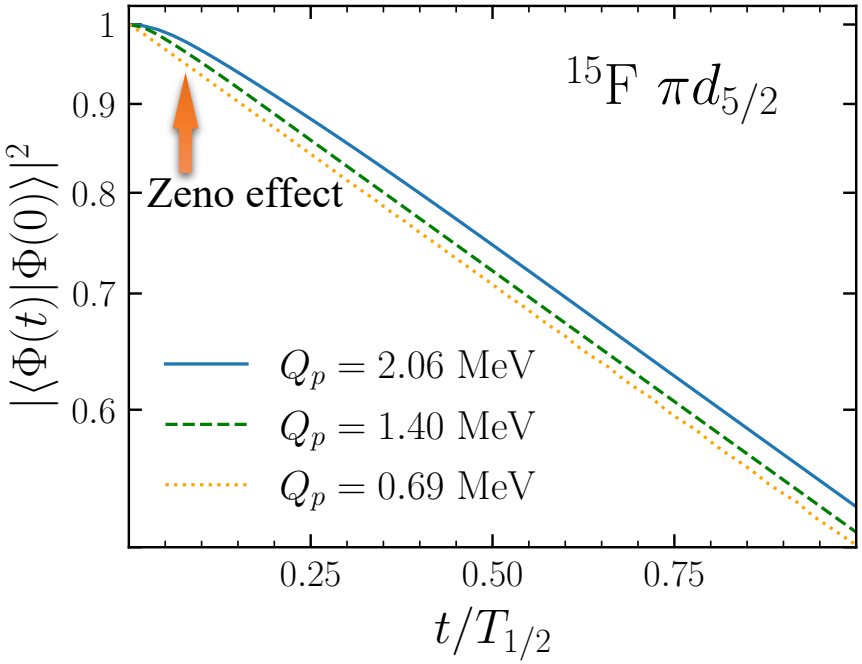


- Decay rate is a constant in classical decay.
- Memory effect in quantum decay.

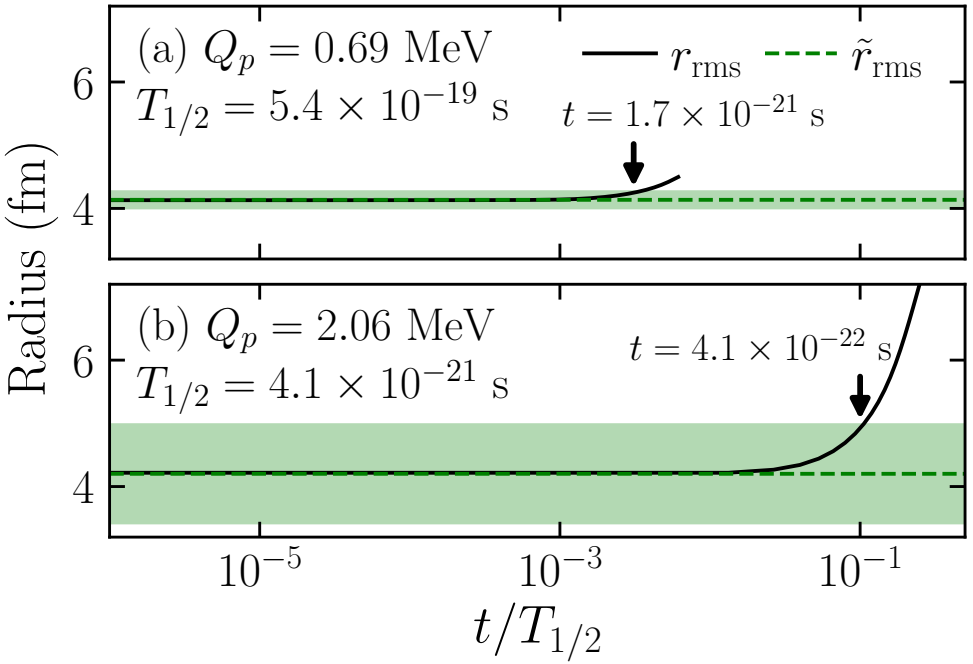
S. R. Wilkinson *et al.*, Nature 387, 575 (1997)
M. Ji and C. Xu, Chinese Phys. Lett. 38 032301 (2021)

RMS radius evolution during the decay

Survival probability



Radius evolution at Q = 0.69, 2.06 MeV



Y. R. Lin, SW *et al.*, Phys. Rev. Lett. 136, 122501(2026)

- Initially, the rms radius matches with the complex one.
- There is a plateau for the rms radius at the early stage of the decay due to the quantum Zeno effect.
- For long-lived system, one can extract the radius experimentally.

RMS radius evolution during the decay

According to the Ehrenfest theorem,

$$\frac{d}{dt}r_{\rm rms}^2 \equiv \frac{d}{dt}\langle r^2\rangle = \frac{1}{i\hbar}\langle[\mathbf{r}^2, H]\rangle$$

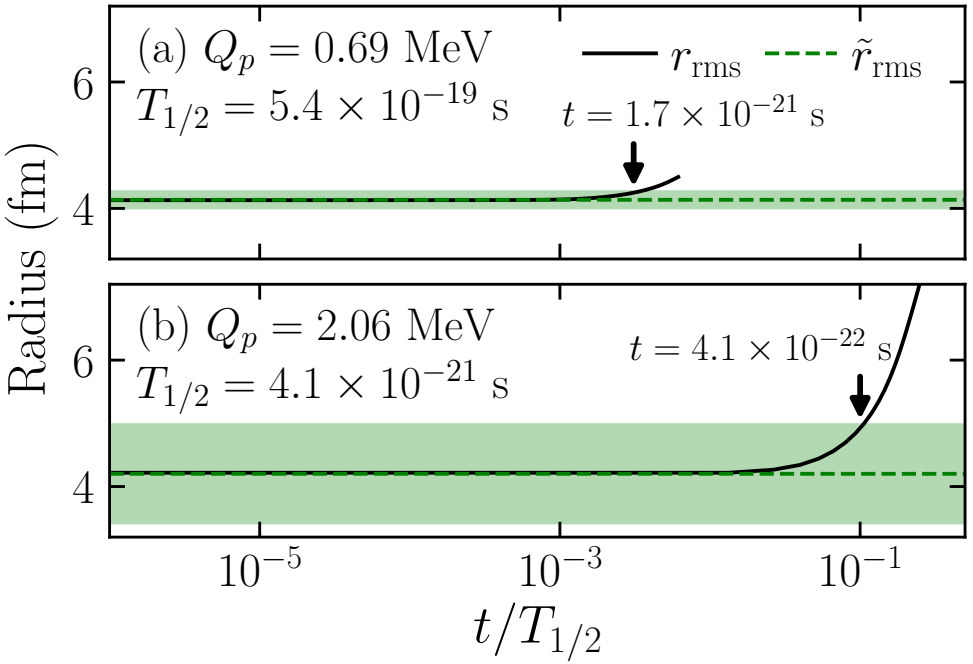
one can obtain:

$$r_{\rm rms}^2(t) \simeq r_{\rm rms}^2(0) + b_{\rm TPA}\, t^2$$

where

$$b_{\rm TPA} = \frac{1}{m}\langle \vec{r}\cdot\vec{\nabla}(V_{\rm TPA} - V)\rangle_{t=0}$$

Radius evolution at Q = 0.69, 2.06 MeV



Y. R. Lin, SW *et al.*, Phys. Rev. Lett. 136, 122501(2026)

- Initially, the rms radius matches with the complex one.
- There is a plateau for the rms radius at the early stage of the decay due to the quantum Zeno effect.
- For long-lived system, one can extract the radius experimentally.

RMS radius evolution during the decay

According to the Ehrenfest theorem,

$$\frac{d}{dt}r_{\mathrm{rms}}^2 \equiv \frac{d}{dt}\langle r^2\rangle = \frac{1}{i\hbar}\langle[\mathbf{r}^2, H]\rangle$$

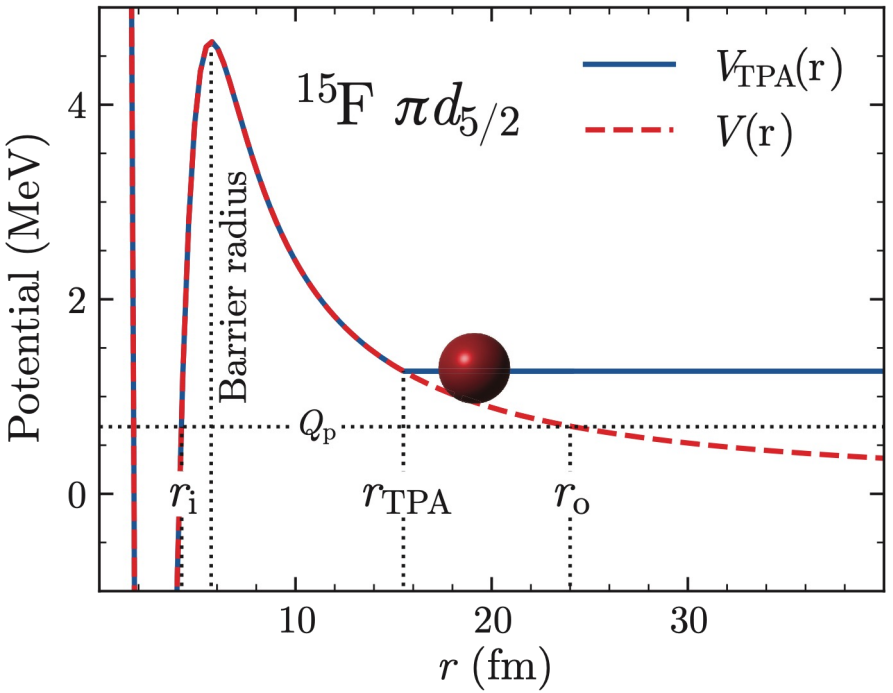
one can obtain:

$$r_{\mathrm{rms}}^2(t) \simeq r_{\mathrm{rms}}^2(0) + b_{\mathrm{TPA}}\, t^2$$

At initial stage with small t

$$r_{\mathrm{rms}}(t) \simeq r_{\mathrm{rms}}(0) + \frac{1}{2}\frac{b_{\mathrm{TPA}}}{r_{\mathrm{rms}}(0)}\, t^2$$

Classical-like acceleration



Y. R. Lin, SW *et al.*, Phys. Rev. Lett. 136, 122501(2026)

- Initially, the rms radius matches with the complex one.
- There is a plateau for the rms radius at the early stage of the decay due to the quantum Zeno effect.
- For long-lived system, one can extract the radius experimentally.

Classical-like picture of decay

According to the Ehrenfest theorem,

$$\frac{d}{dt}r_{\rm rms}^2 \equiv \frac{d}{dt}\langle r^2\rangle = \frac{1}{i\hbar}\langle[\mathbf{r}^2, H]\rangle$$

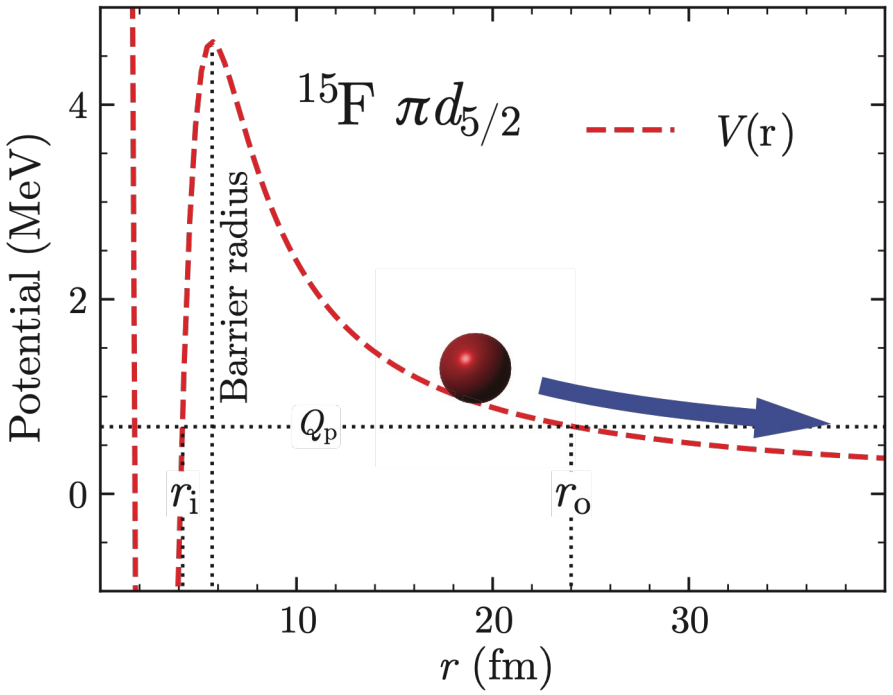
one can obtain:

$$r_{\rm rms}^2(t) \simeq r_{\rm rms}^2(0) + b_{\rm TPA}\, t^2$$

At initial stage with small t

$$r_{\rm rms}(t) \simeq r_{\rm rms}(0) + \frac{1}{2}\frac{b_{\rm TPA}}{r_{\rm rms}(0)}\, t^2$$

Classical-like acceleration

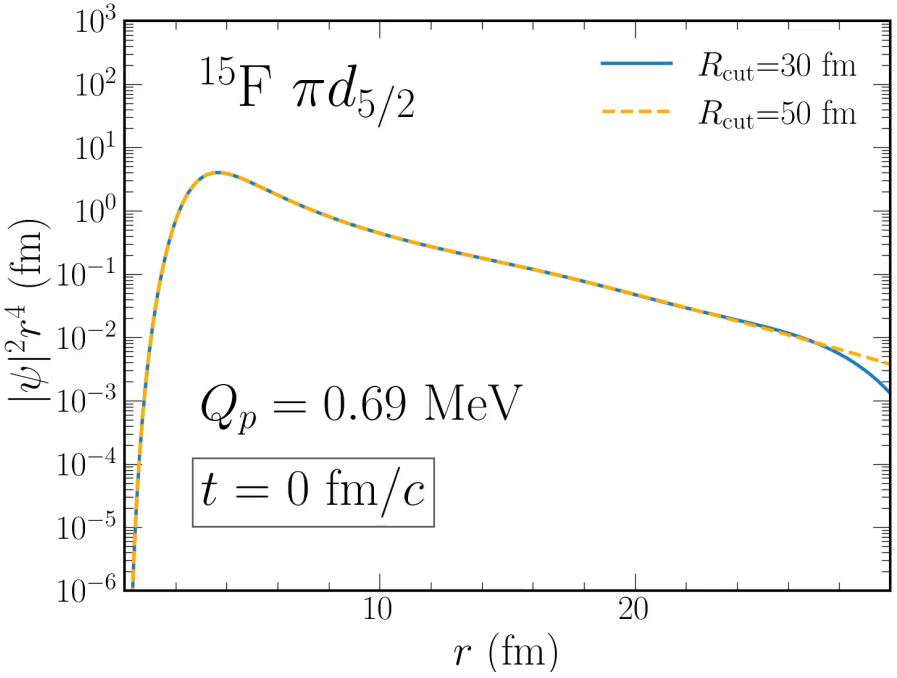


Y. R. Lin, SW *et al.*, Phys. Rev. Lett. 136, 122501(2026)

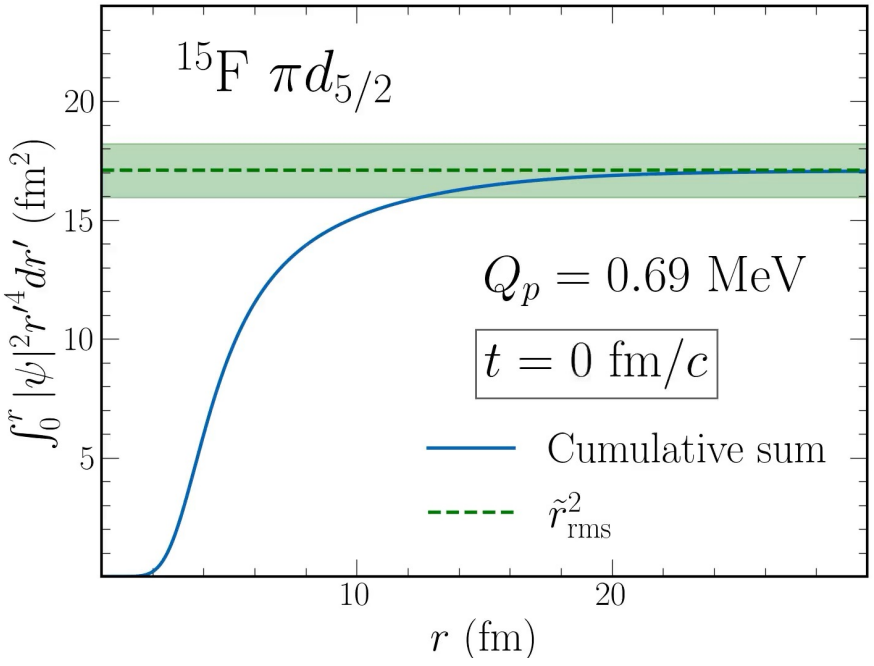
- Initially, the rms radius matches with the complex one.
- There is a plateau for the rms radius at the early stage of the decay due to the quantum Zeno effect.
- For long-lived system, one can extract the radius experimentally.

RMS radius evolution during the decay

Density evolution



Radius evolution

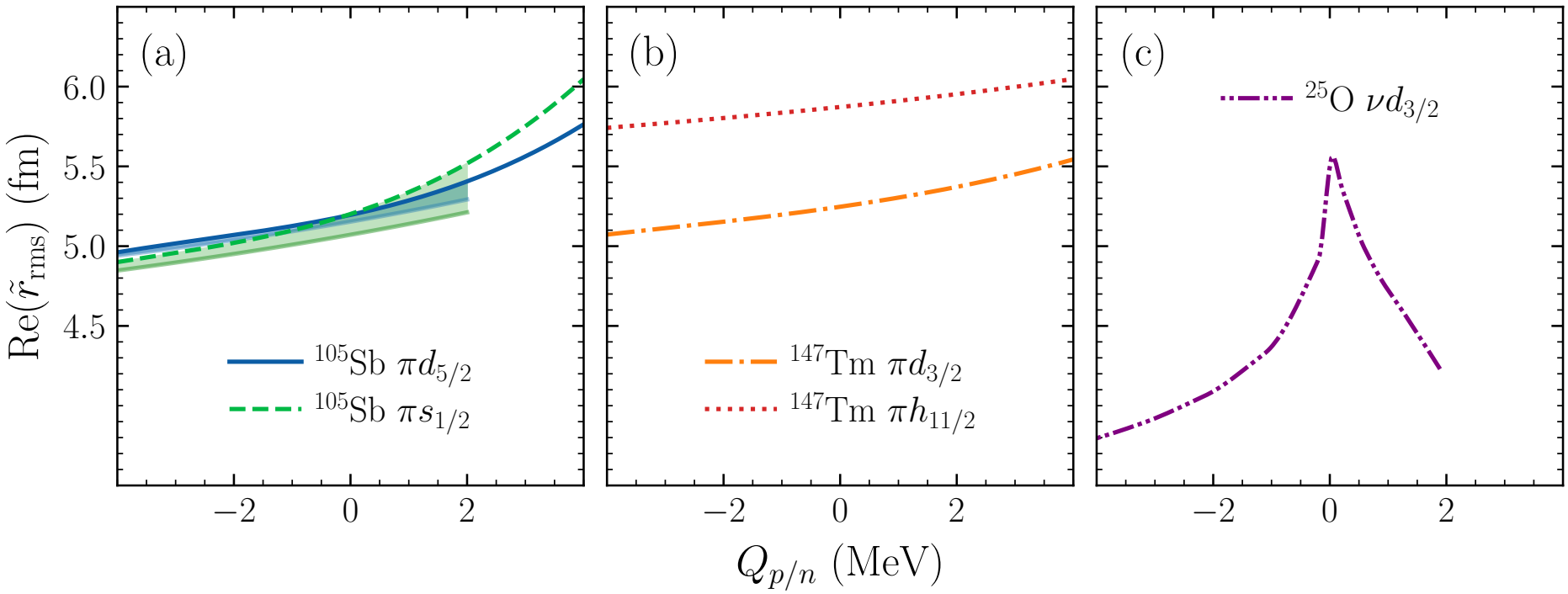


Y. R. Lin, SW *et al.*, Phys. Rev. Lett. 136, 122501(2026)

- Initially, the rms radius matches with the complex one.
- There is a plateau for the rms radius at the early stage of the decay due to the quantum Zeno effect.
- For long-lived system, one can extract the radius experimentally.

Radius enhancement around the dripline

Radius predictions for ^{105}Sb, ^{147}Tm, and ^{25}O

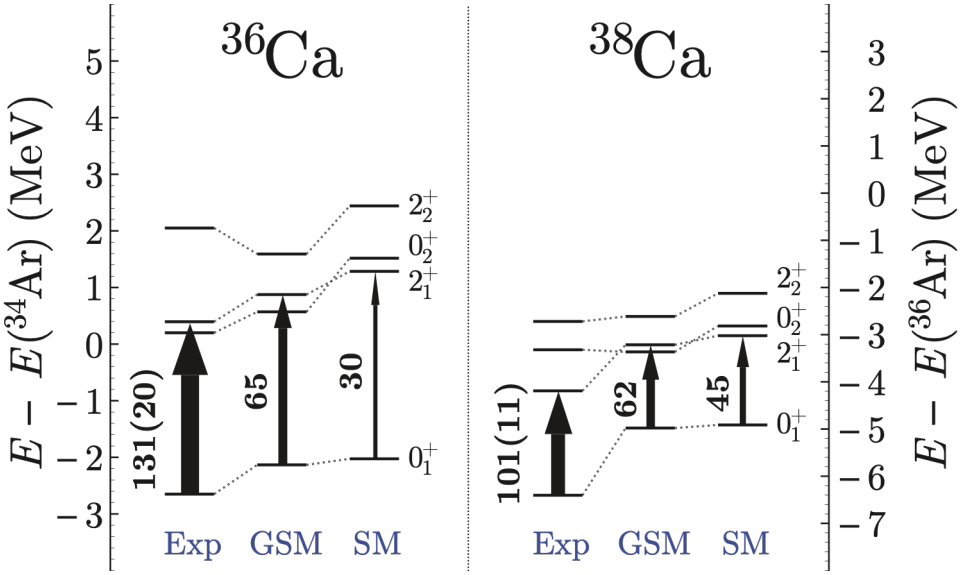


Future test with laser spectroscopy?

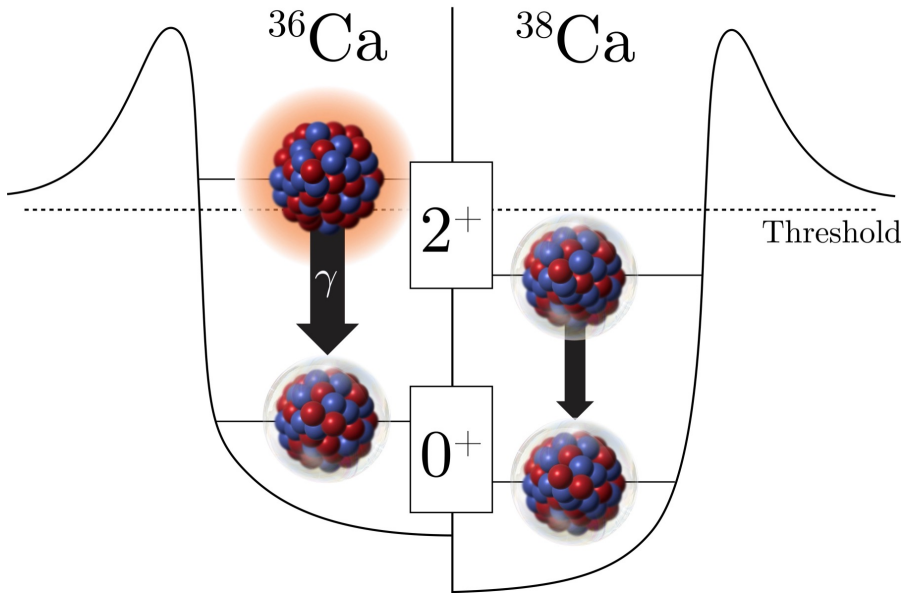
- The radii of all the dripline systems are enhanced by the continuum.
- Neutron-rich nuclei are more sensitive to the continuum.

Contiuum effect on electromagnetic transition

Spectra and $B(E2)$ values of ^{36,38}Ca



Density evolution



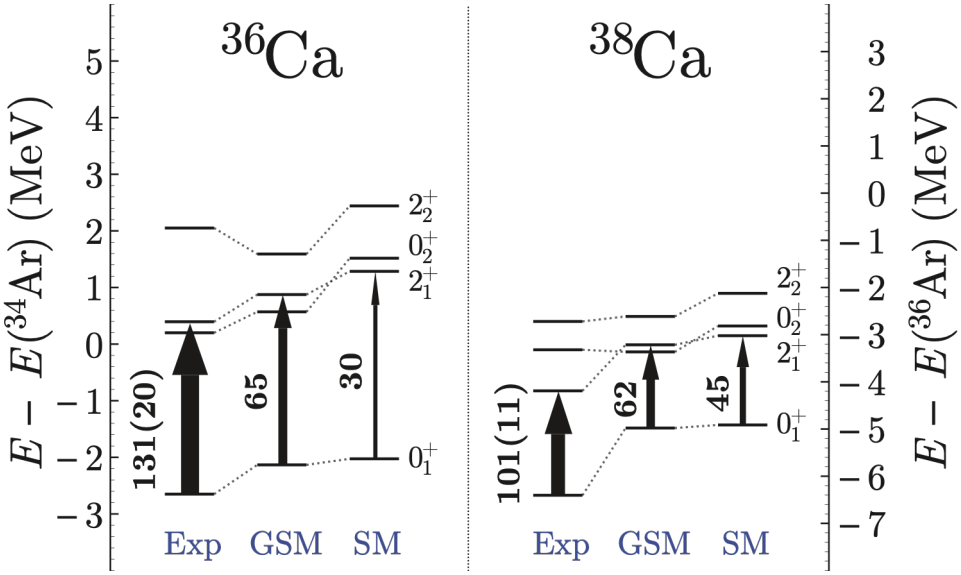
$$\rho_L(r) = \langle \Phi_f | \frac{1}{r^2} \delta(r' - r) Y_L | \Phi_i \rangle$$

$$B(EL) = \left[\frac{\hat{J}_f}{\hat{J}_i} \int_0^\infty \rho_L(r) r^{L+2} dr \right]^2$$

Z. Xu, SW *et al.*, PRC 112, L011302 (2025).
T. Beck, A. Gade *et al.*, PRC 108, L061301 (2023)
N. Dronchi, D. Weisshaar *et al.*, PRC 107, 034306 (2023)

Contiuum effect on electromagnetic transition

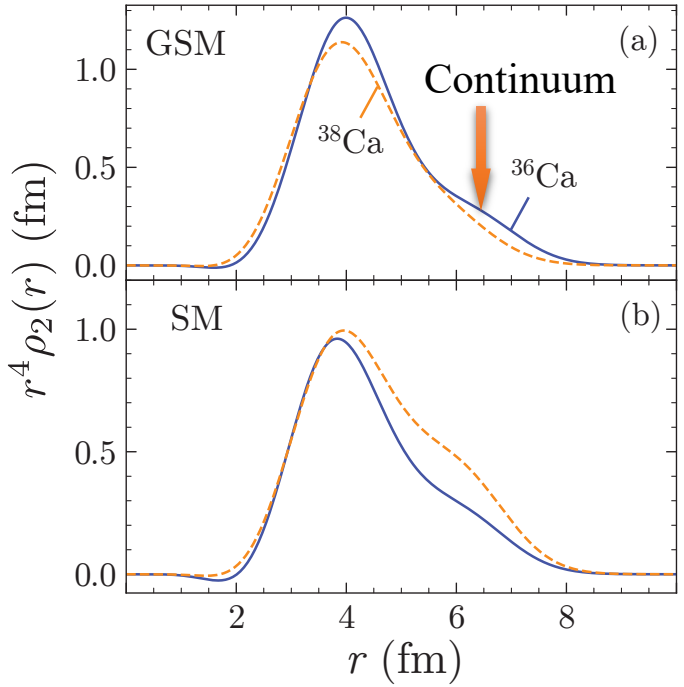
Spectra and $B(E2)$ values of ^{36,38}Ca



$$\rho_L(r) = \langle \Phi_f | \frac{1}{r^2} \delta(r' - r) Y_L | \Phi_i \rangle$$

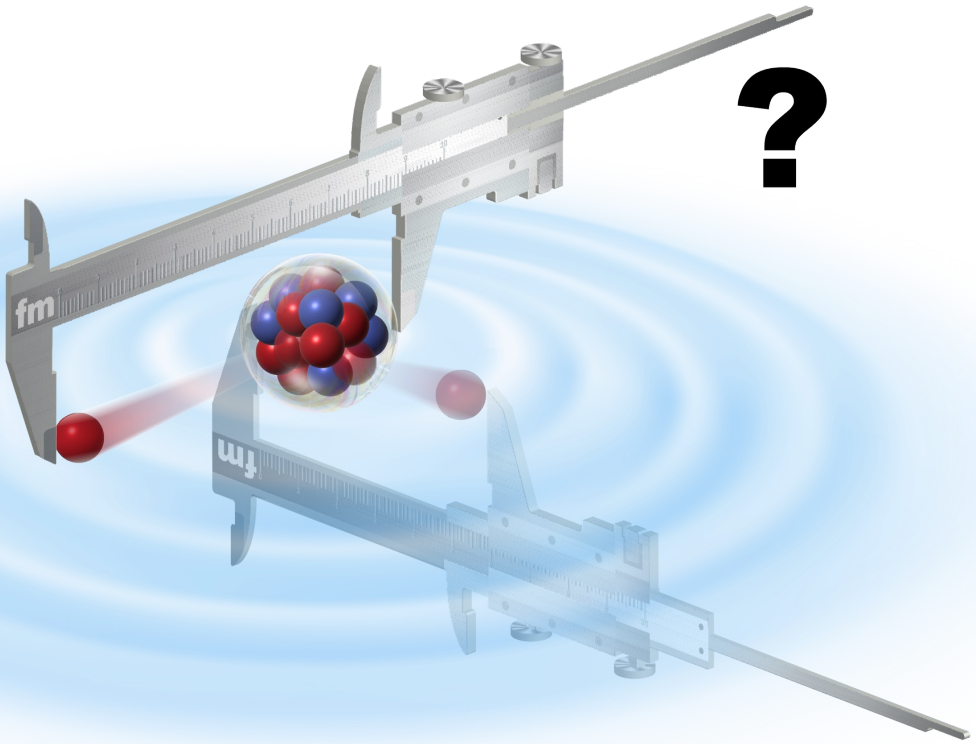
$$B(EL) = \left[\frac{\hat{J}_f}{\hat{J}_i} \int_0^\infty \rho_L(r) r^{L+2} dr \right]^2$$

***E*2 ($0^+ \rightarrow 2^+$) Transition densities**



Z. Xu, SW *et al.*, PRC 112, L011302 (2025).
T. Beck, A. Gade *et al.*, PRC 108, L061301 (2023)
N. Dronchi, D. Weisshaar *et al.*, PRC 107, 034306 (2023)

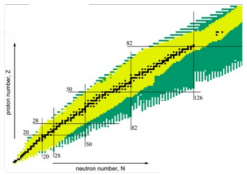
Structure of unbound nuclei



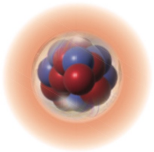
Decay properties might help

Outline

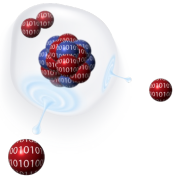
Introduction 1
- Dripline region
- Continuum effect



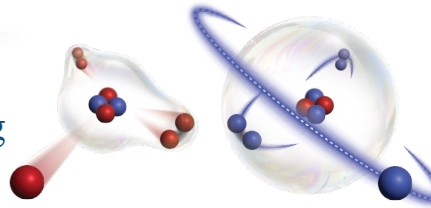
Radius 2
- Complex radius
- Halo-like enhancement



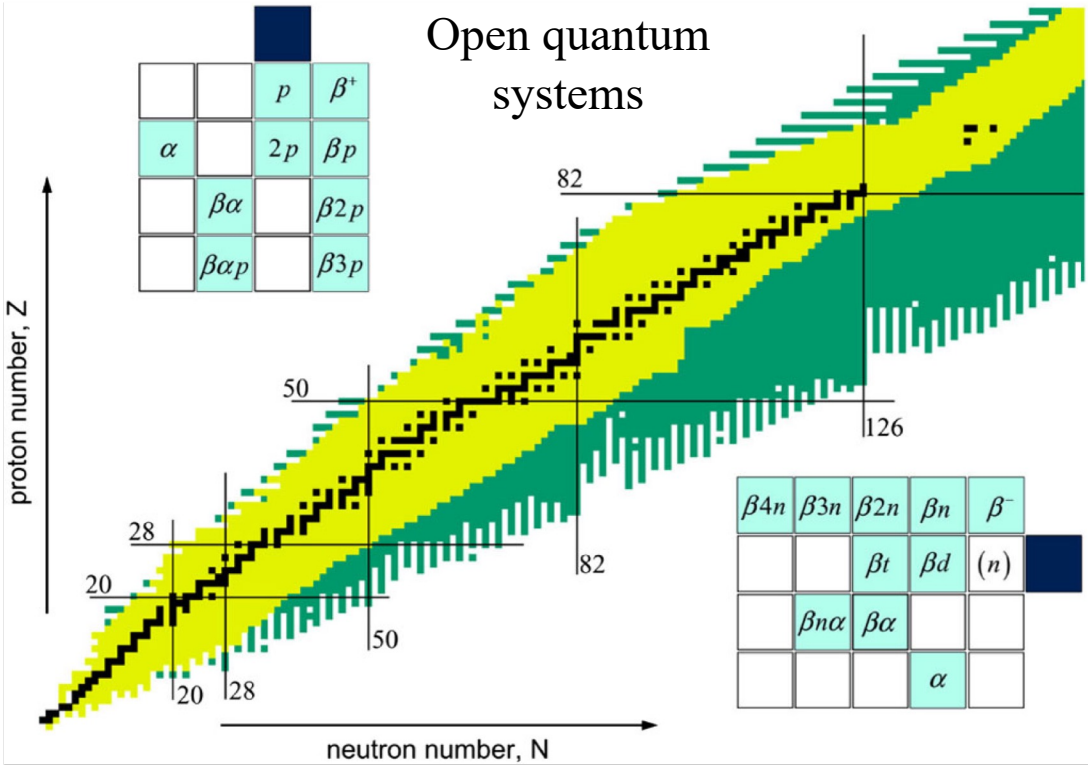
Decay 3
- 2*p* decay
- *pp* correlation



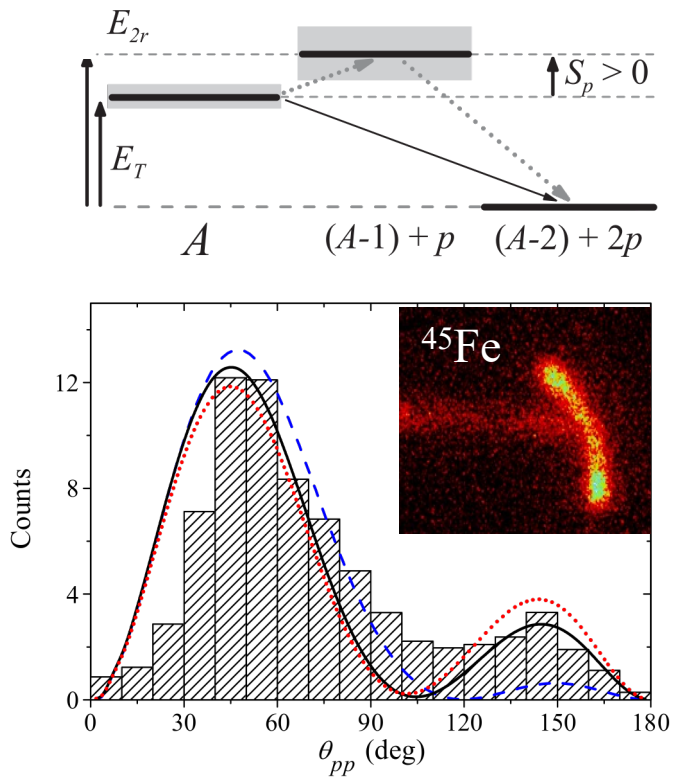
Mirror 4
- Thomas-Ehrman effect
- Mirror symmetry breaking



Two-proton (2*p*) decay



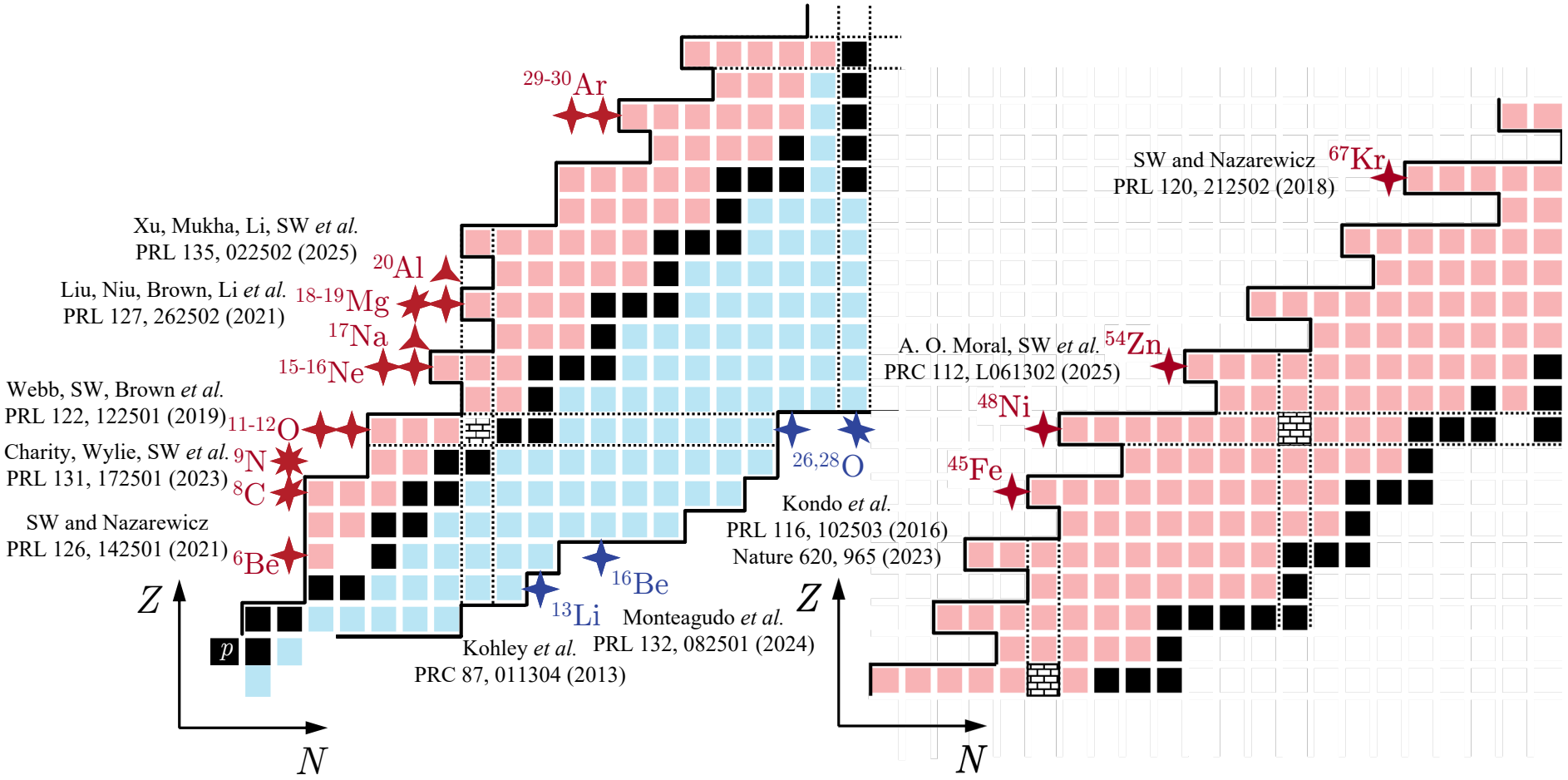
- **2*p* decay**



Y.B. Zeldovich, Sov. Phys. JETP 11, 812 (1960)
V. Goldansky, NP 19, 482 (1960)

J. Giovinazzo *et al.*, PRL 89, 102501 (2002)
K. Miernik *et al.*, PRL 99, 192501 (2007)

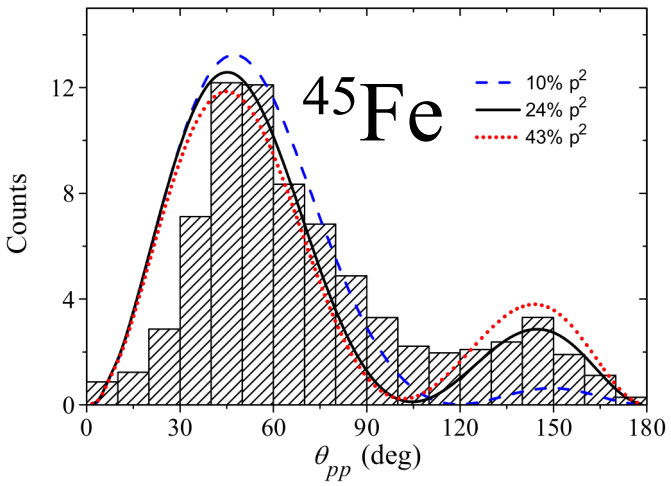
Observed 2*p* & *np* emitters



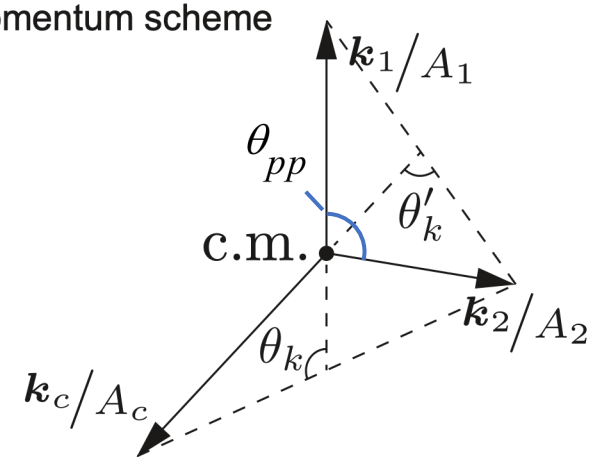
M. Pfützner, I. Mukha, SW, Prog. Part. Nucl. Phys. 132, 104050 (2023)

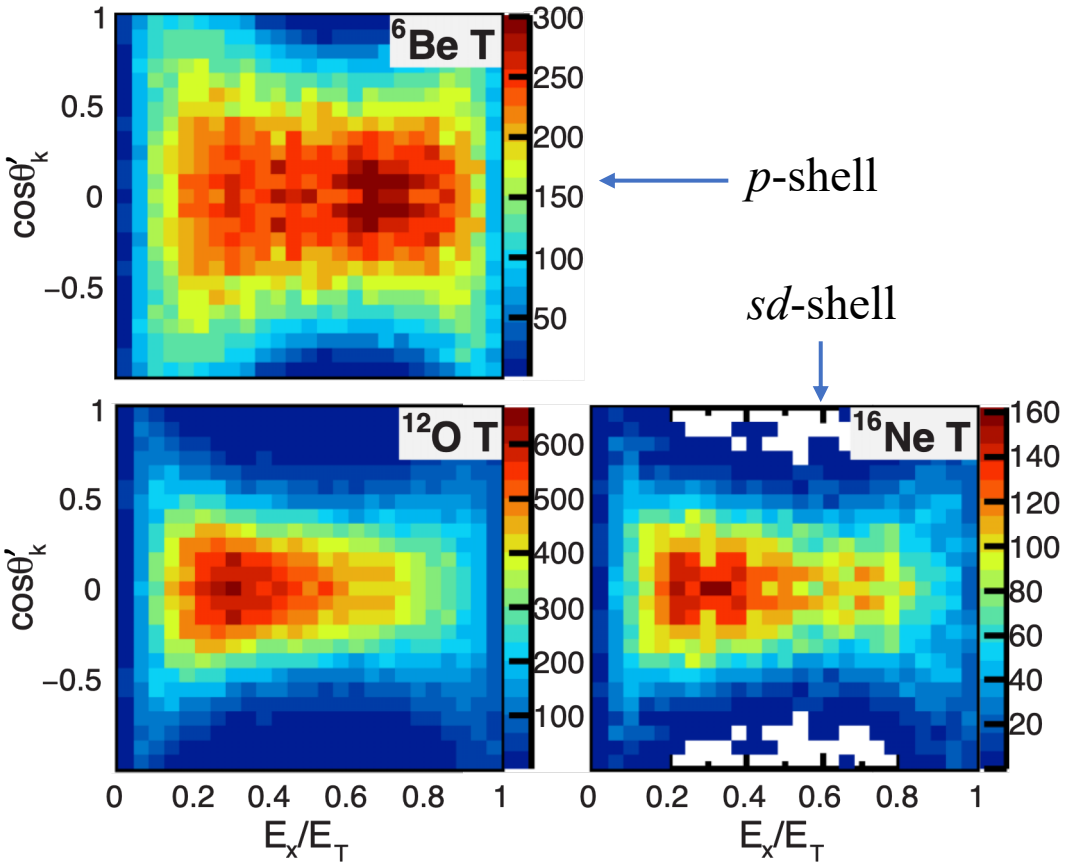
Asymptotic nucleon-nucleon correlation

K. Miernik *et al.* PRL 99, 192501 (2007)



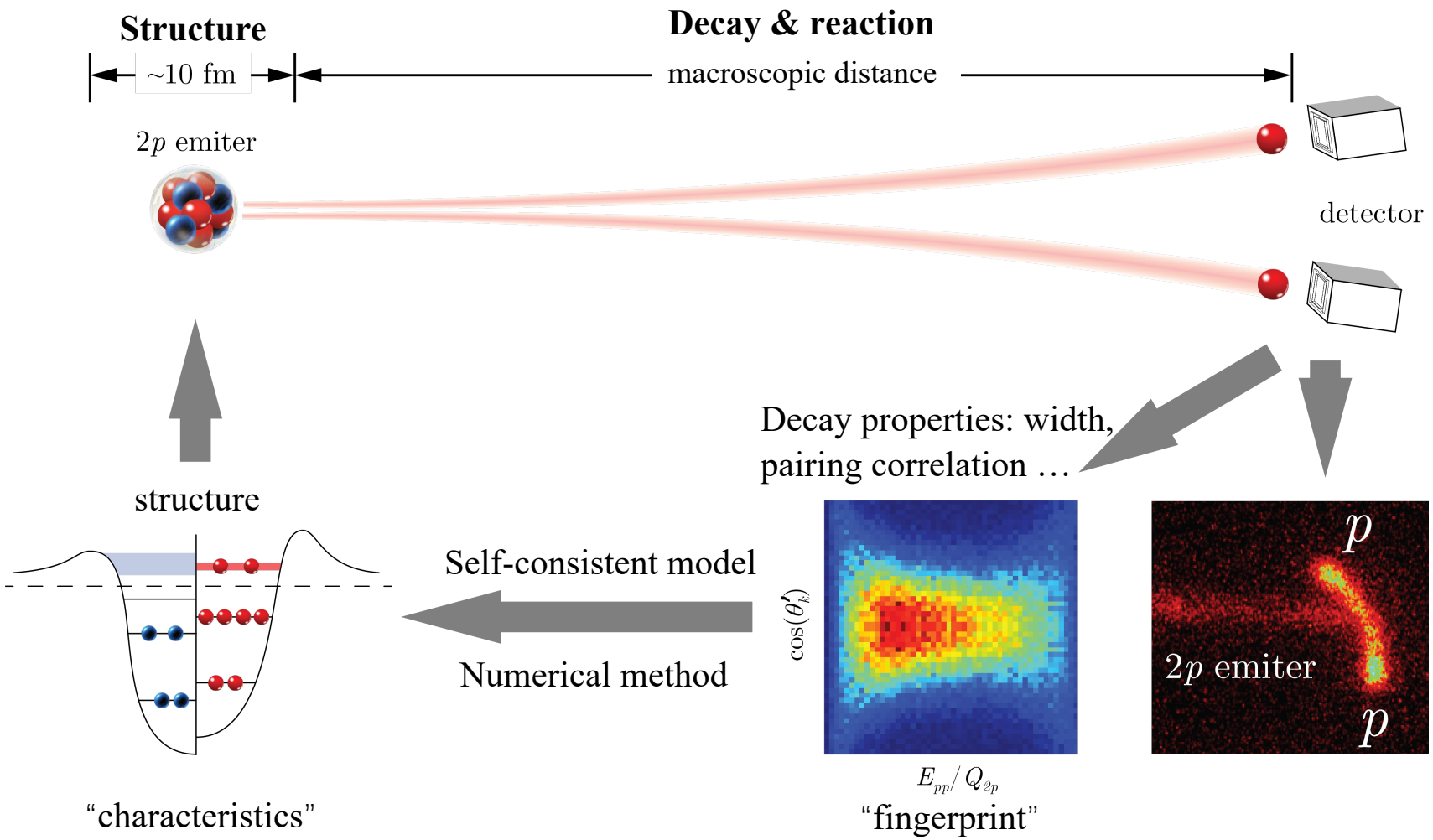
Momentum scheme





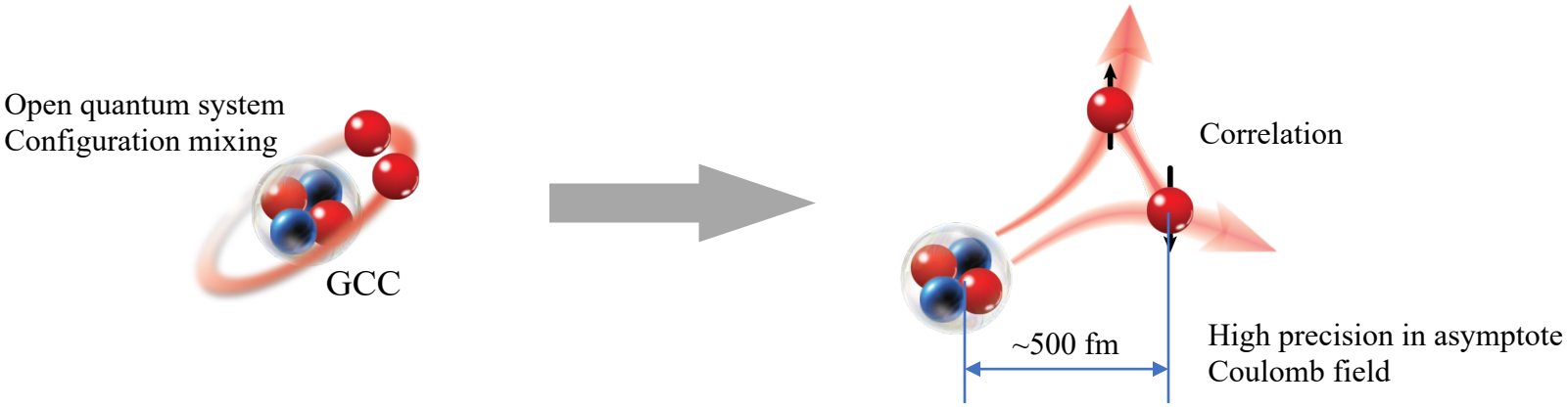
T.B. Webb *et al.* Phys. Rev. C 100, 024306 (2019)

Structure ⟷ Asymptotic observables



Time dependent (TD) approach

In order to study the dynamics of 2*p* decay



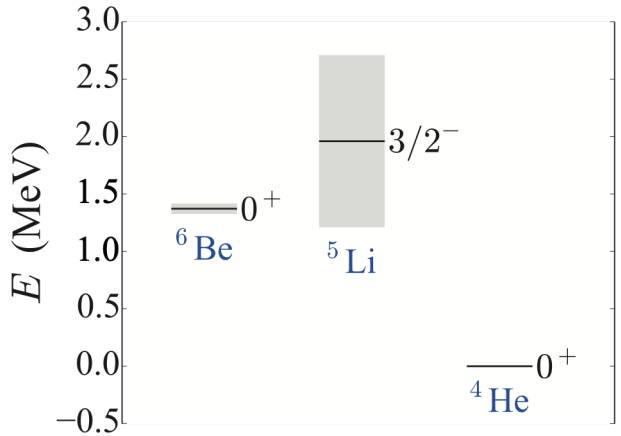
- **Time dependent approach**

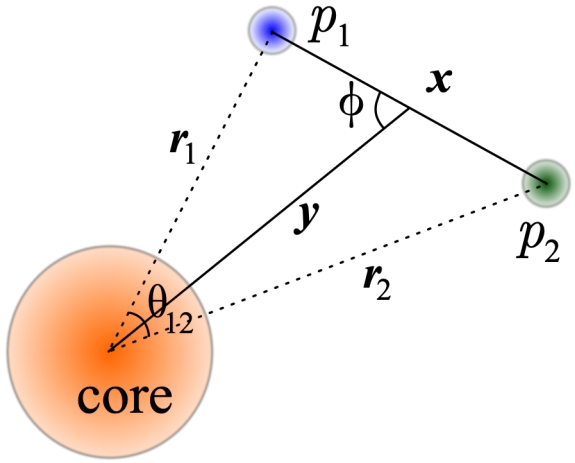
$$e^{-i\frac{\hat{H}}{\hbar}t} = \sum_{n=0}^{\infty}(-i)^n\,(2-\delta_{n0})\,J_n(t)T_n(\hat{H}/\hbar)$$

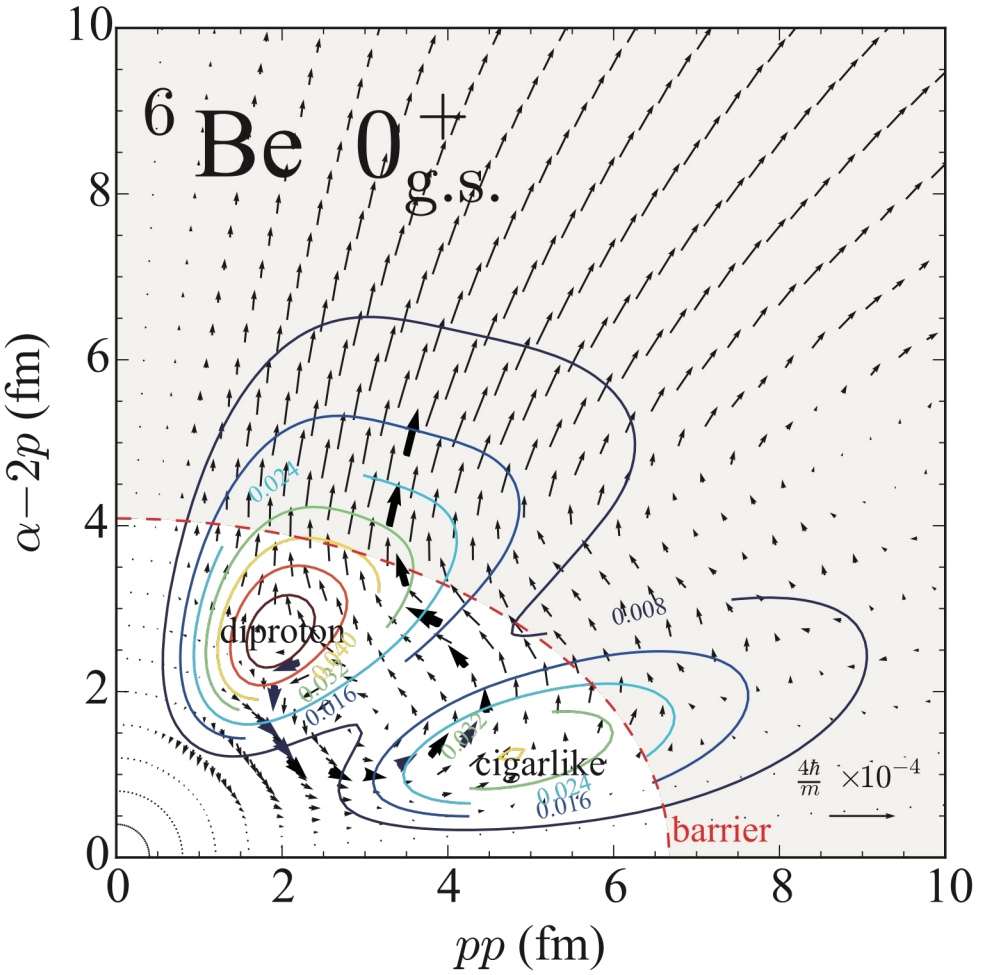
  - Time propagator can be expanded with Chebyshev polynomials.
  - Initial wave function is obtained by GCC, which includes configuration mixing and proper asymptote.
  - Two-proton wave function has been propagated to over 500 fm.

SW and W. Nazarewicz, Phys. Rev. Lett. 126, 142501 (2021)

Ground-state of ^{6}Be

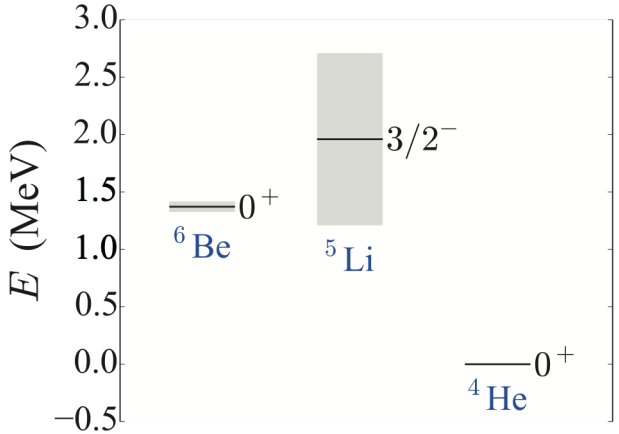


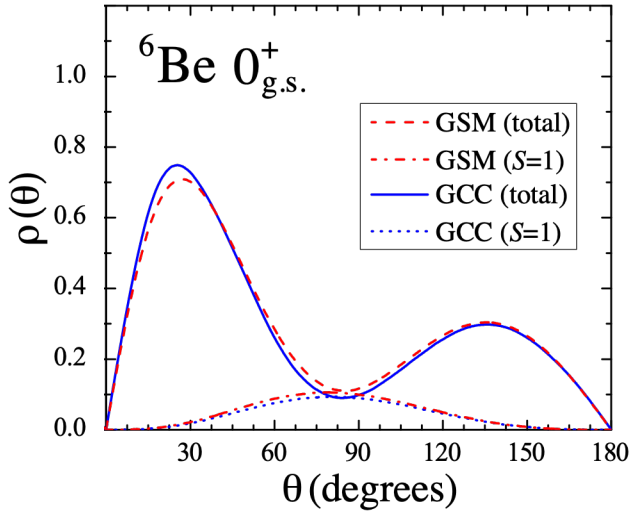


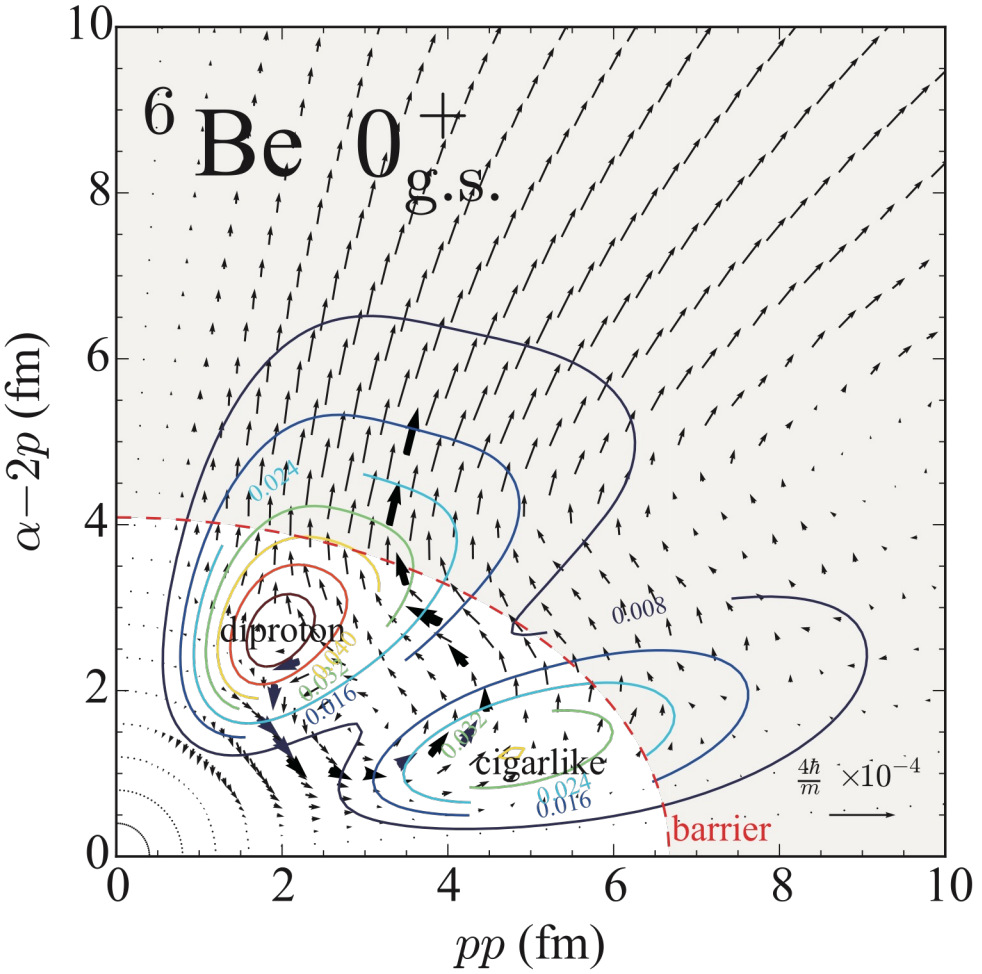


SW *et al.*, Phys. Rev. C 99, 054302 (2019)

Ground-state of ^{6}Be



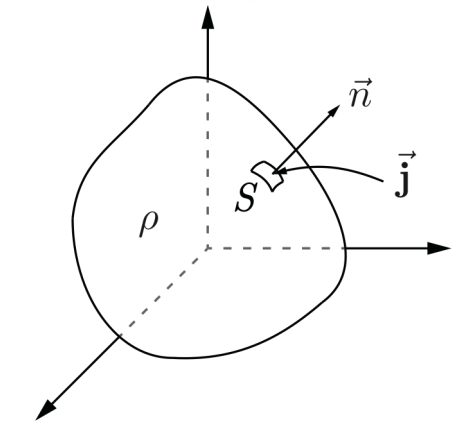




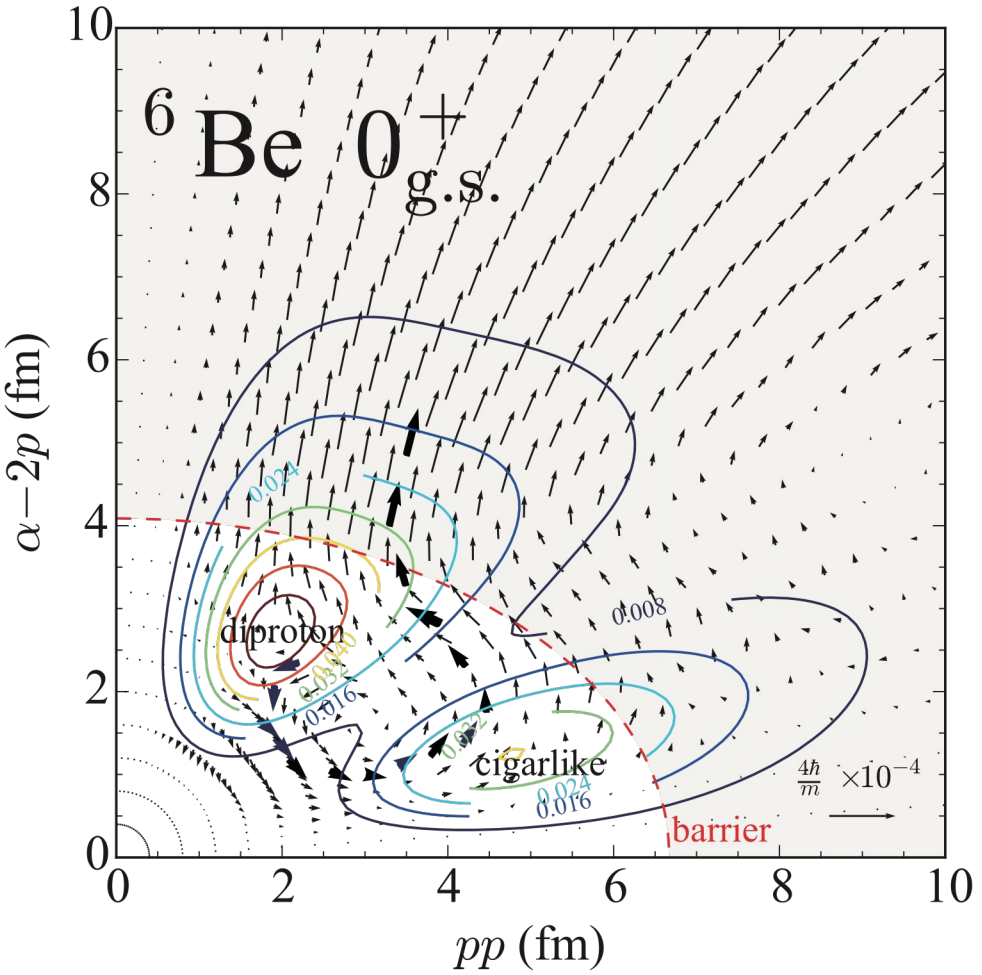
SW *et al.*, Phys. Rev. C 99, 054302 (2019)

Ground-state of ^{6}Be

Probability current

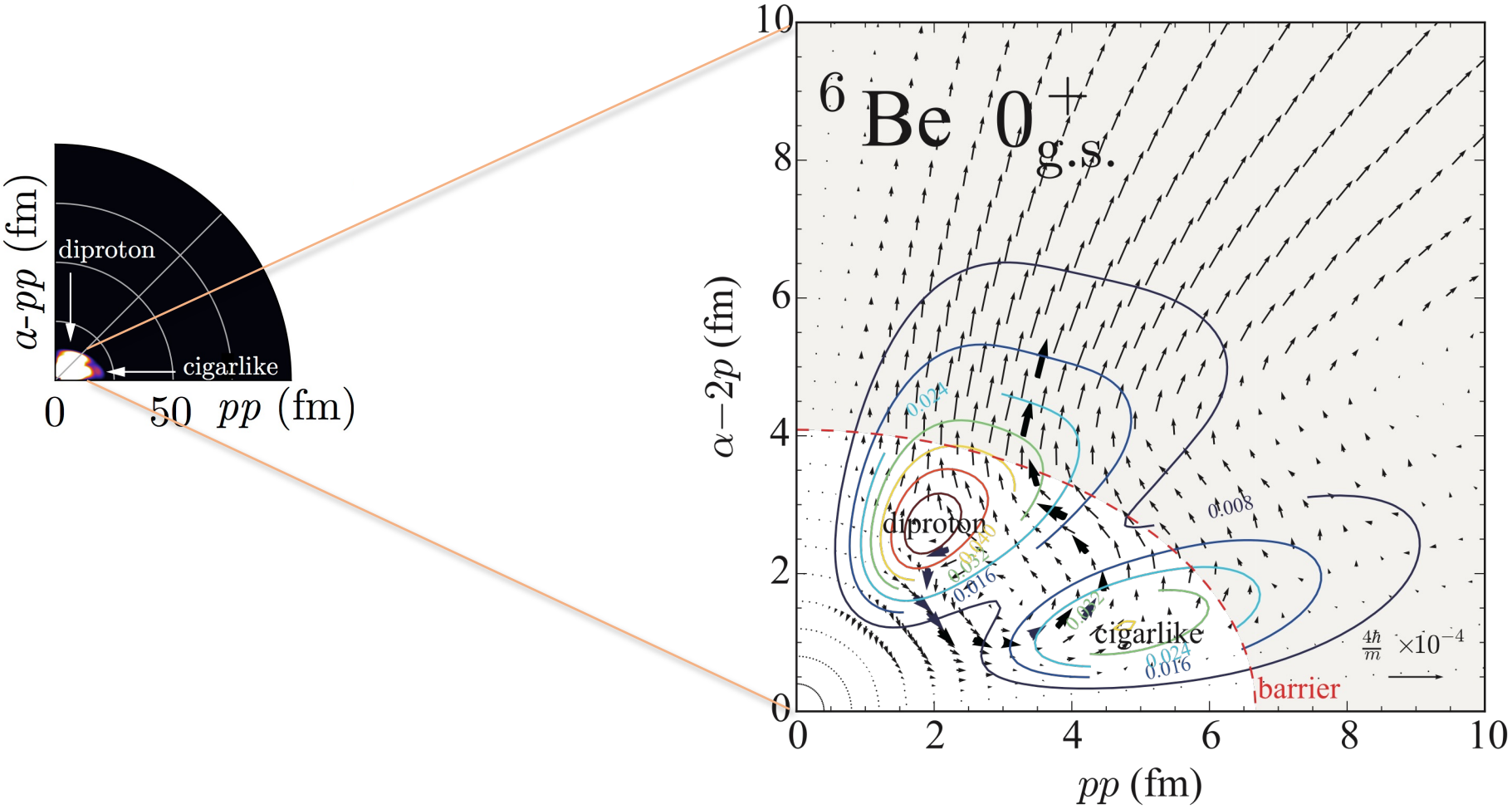


$$\iiint \frac{\partial \rho}{\partial t}\,\mathrm{d}V = -\oiint \vec{\mathbf{j}}\cdot\vec{n}\,\mathrm{d}S$$



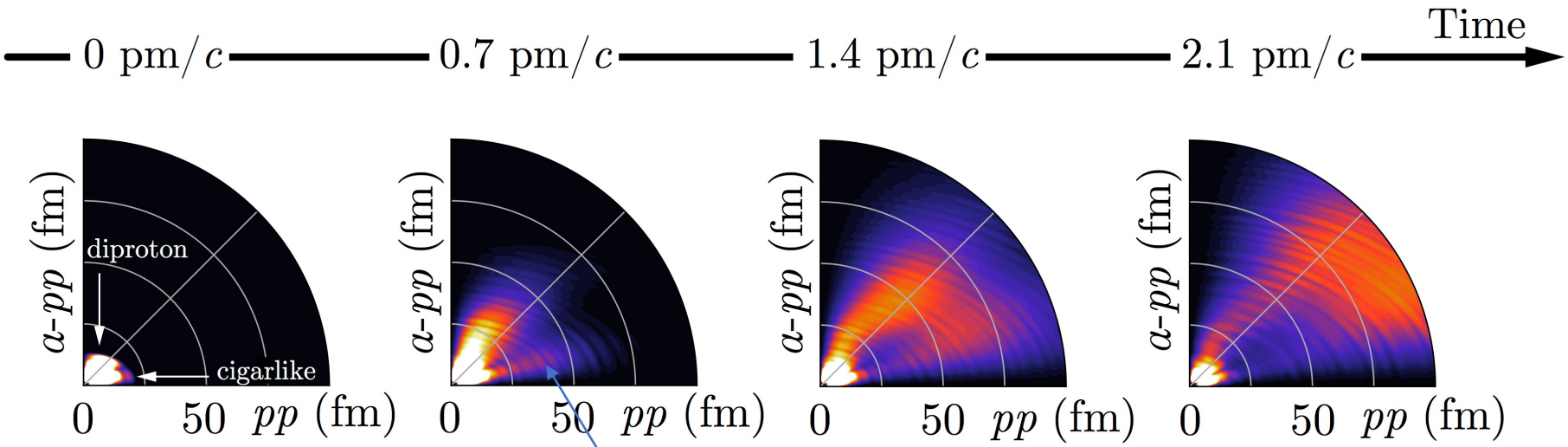
SW *et al.*, Phys. Rev. C 99, 054302 (2019)

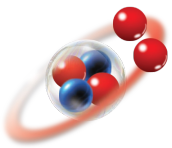
Ground-state of ^{6}Be



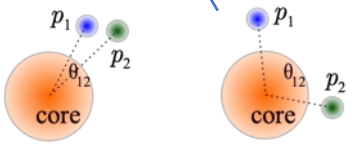
SW *et al.*, Phys. Rev. C 99, 054302 (2019)

2*p* decay in ^{6}Be

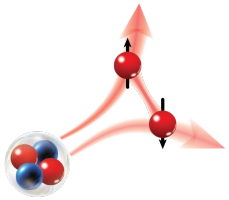




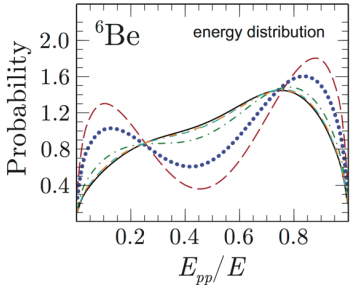
Protons inside nucleus



Two types of tunneling:
1. diproton (primarily)
2. cigarlike



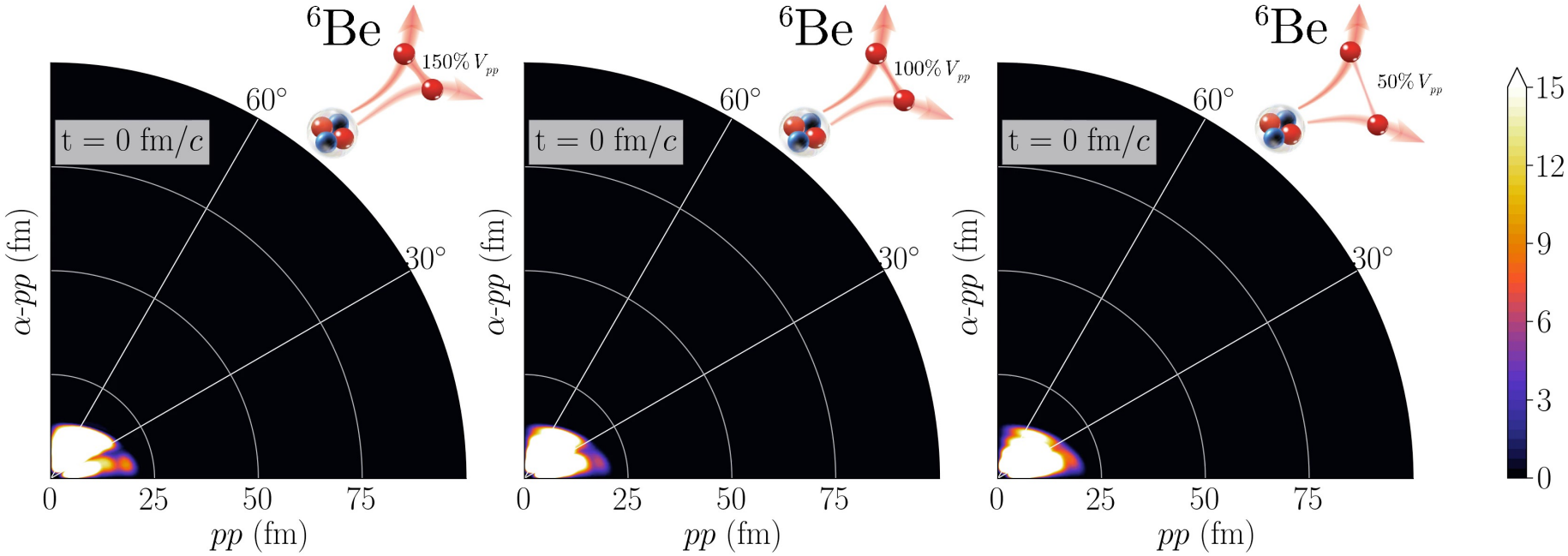
Diproton branch bends due to Coulomb repulsion



Asymptotic correlation begin to converge

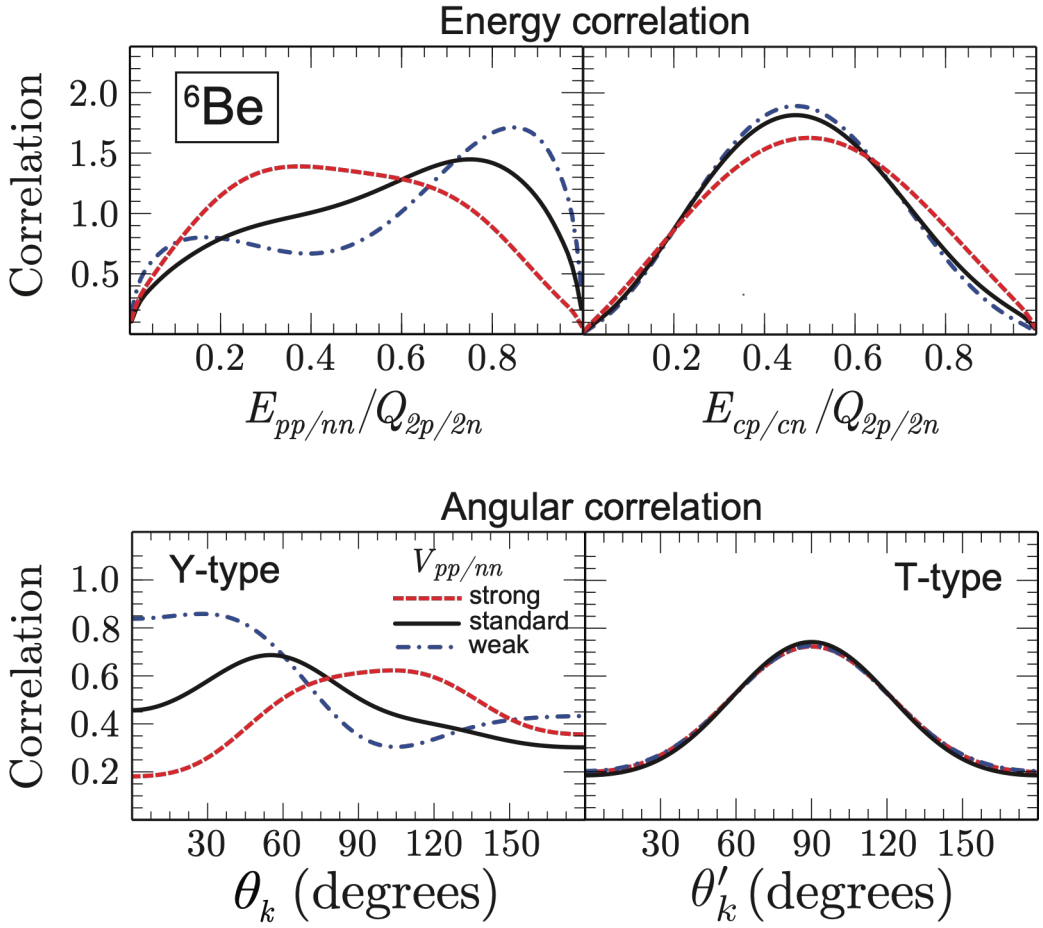
SW and W. Nazarewicz, PRL 126, 142501 (2021)

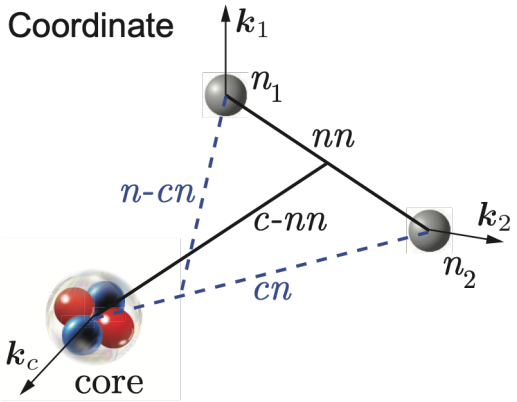
Decay dynamics depends on pairing

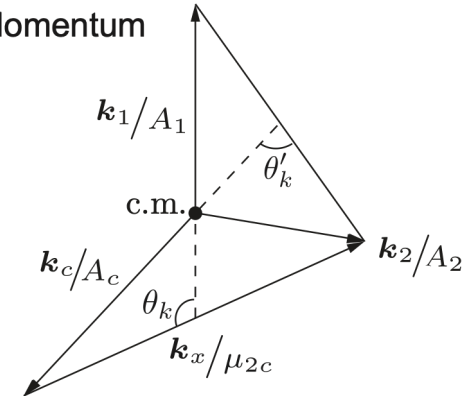


- The decay dynamics as well as correlation strongly depend on the pairing strength.
- Strong pairing results in a larger decay width, which indicates that pairing will benefit the 2p tunneling.

Asymptotic correlations



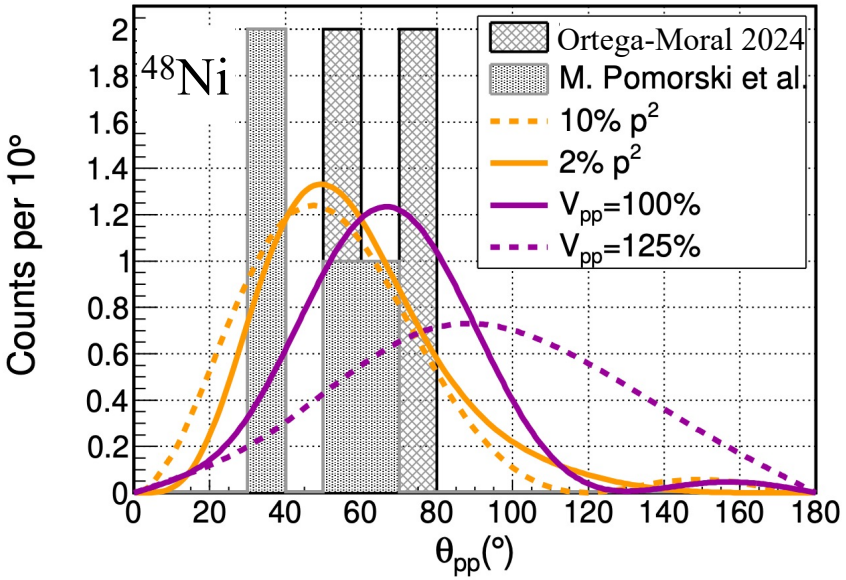




- E_{pp} and Y-type angular correlations are strongly impacted by nucleon-nucleon interaction.

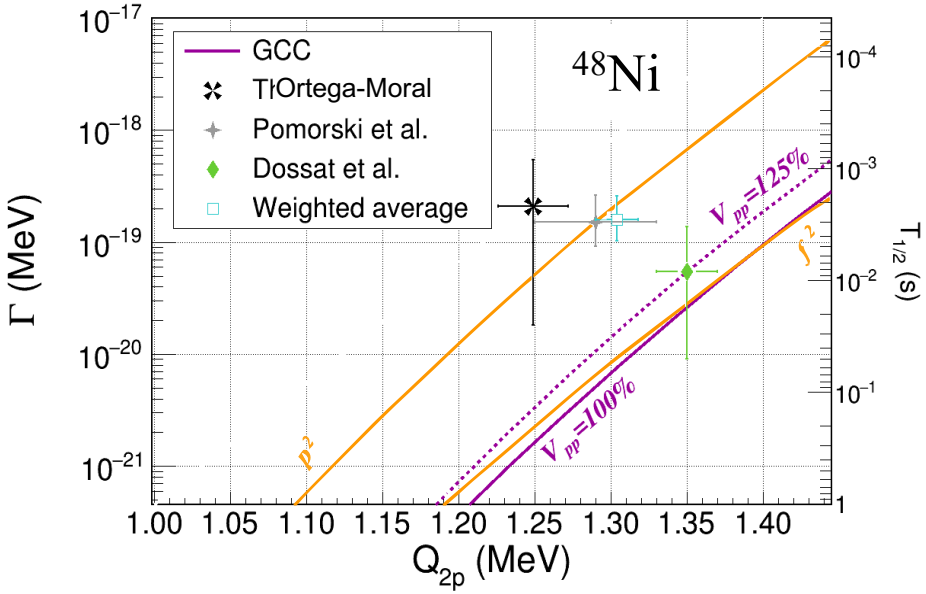
Asymptotic correlation of ^{45}Fe and ^{48}Ni

Angular correlation of ^{48}Ni



$f^2_{7/2}$	$p^2_{3/2}$	$p^2_{1/2}$	$f^2_{5/2}$	$s^2_{1/2}$
91.6%	4.7%	1.0%	1.0%	0.1%

Half-live of ^{48}Ni

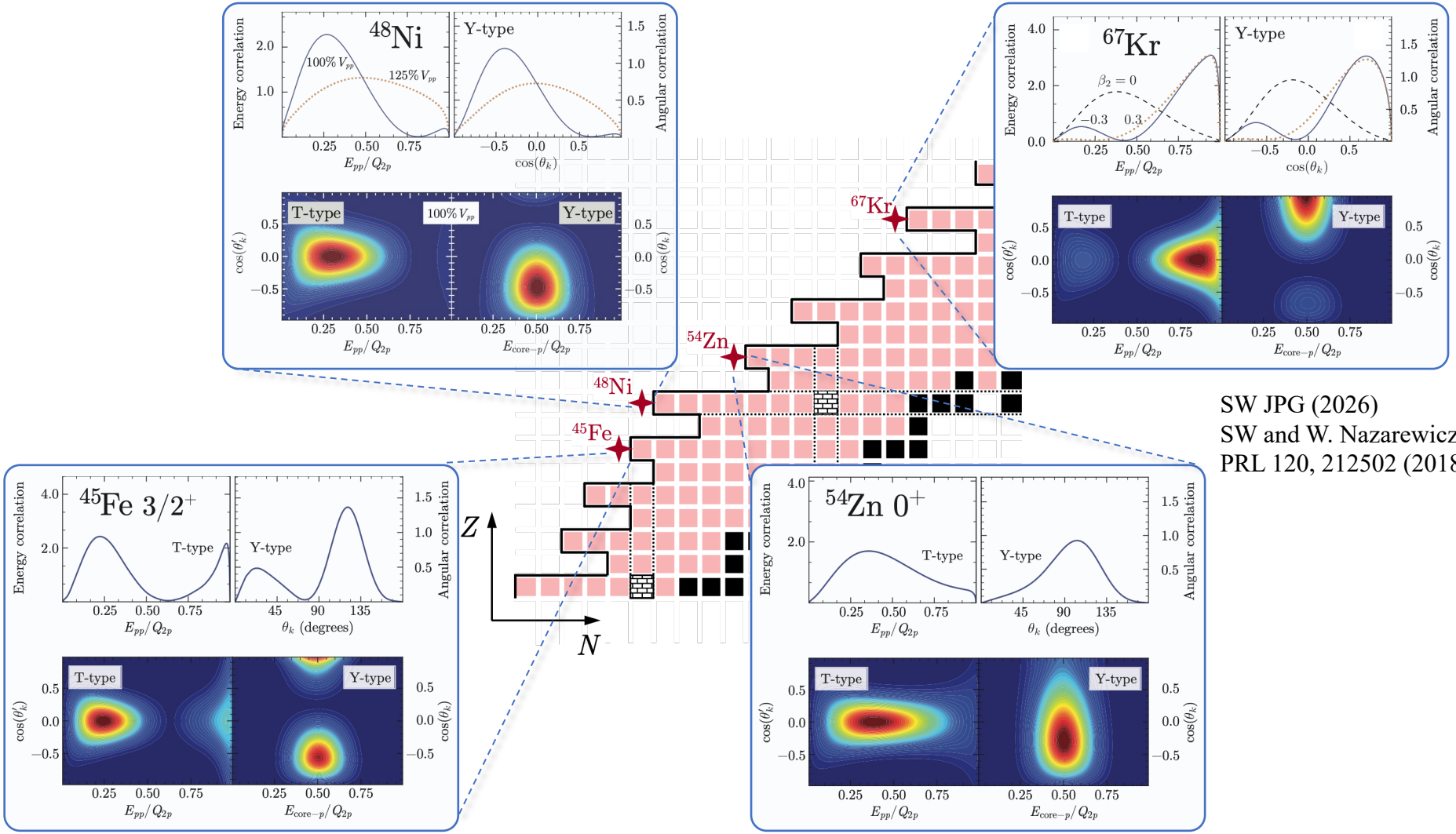


Q^{Exp}_{2p} (keV)		Q^{Cal}_{2p} (keV)		
Ortega-Moral	Pomorski	Brown	Ormand	Cole
1249(23)	1290(40)	1360(130)	1290(330)	1350(60)

- Closed shell behavior for ^{48}Ni?
- Discrepancy between correlations and half-lives.

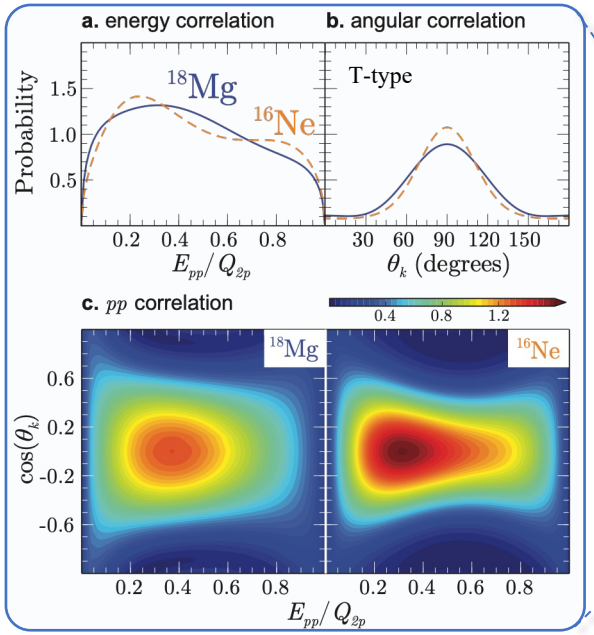
A. O. Moral, SW *et al.*, Phys. Rev. C 112, L061302 (2025)

Perspective: new data are anticipated

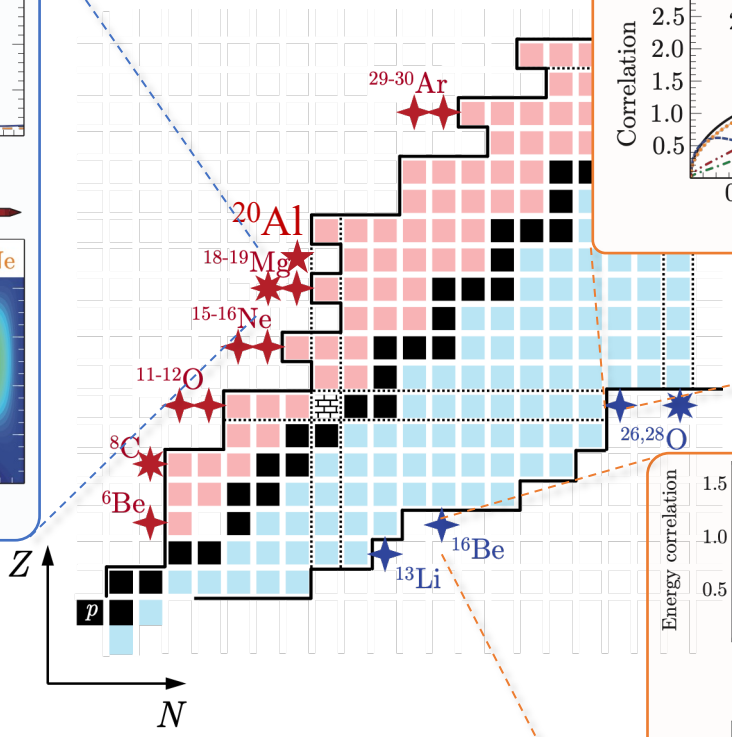


SW JPG (2026)
SW and W. Nazarewicz, PRL 120, 212502 (2018)

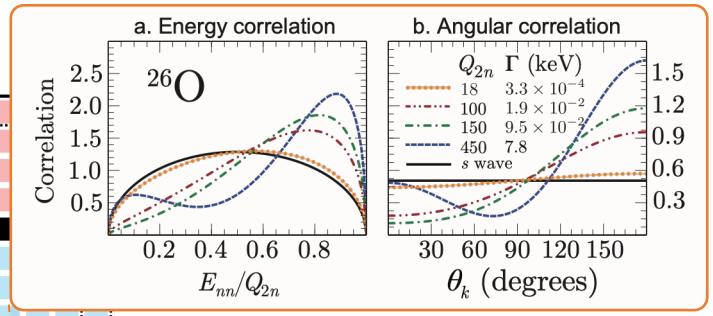
Correlations in light-mass nuclei



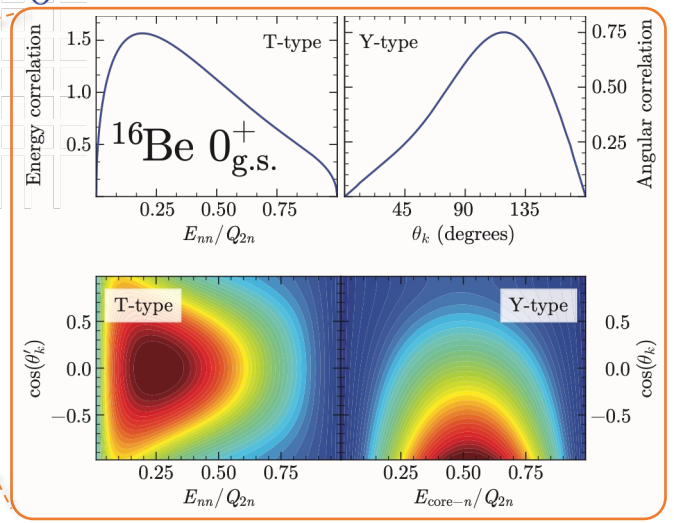
L. Zhou, SW *et al.*,
Nucl. Sci. Tech. 35, 107 (2024)



SW *et al.*, J. Phys. G 49, 10LT02 (2022)



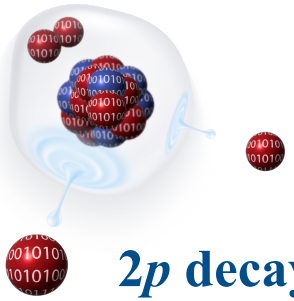
Y. R. Lin in preparation



B. Monteagudo *et al.*, Phys. Rev. Lett. 132, 082501(2024)

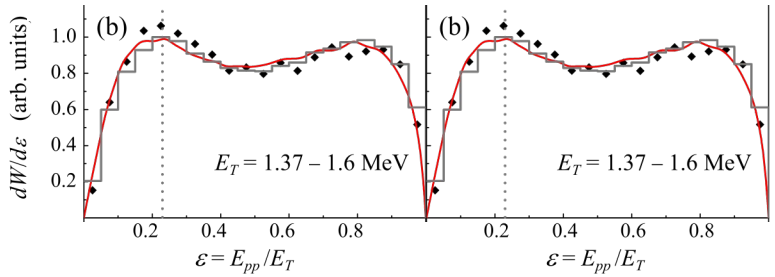
- 4p ($2p$+$2p$) decay of ^{18}Mg.
- Multi-proton emissions.
- Correlation changes when $Q \rightarrow 0$.

Exotic phenomena of 2*p* decay



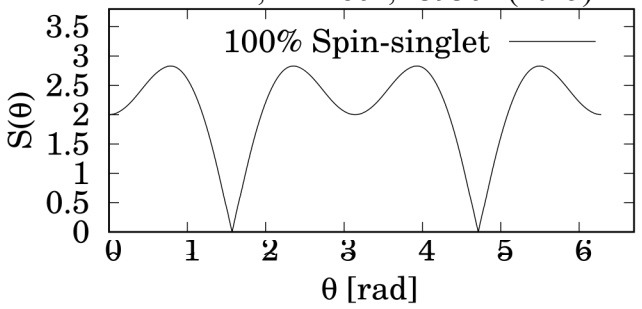
2*p* decay

I. A. Egorova *et al.*, PRL 109, 202502 (2012)



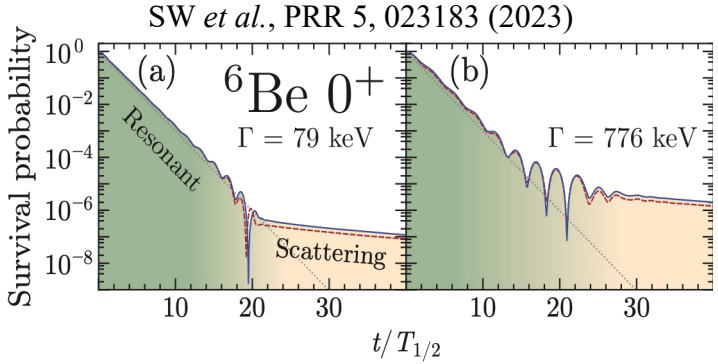
***E*-dependent *nn* correlation**

T. Oishi, PLB 862, 139361 (2025)



Entanglement

SW *et al.*, PRR 5, 023183 (2023)



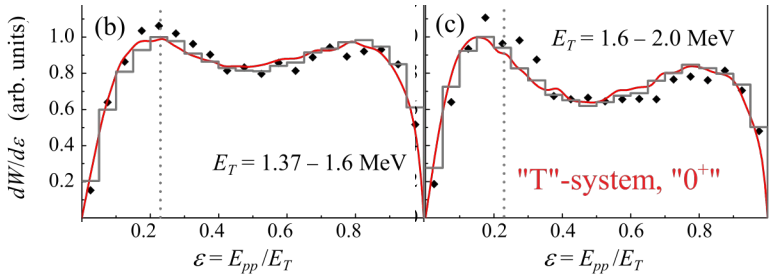
Non-exp decay

Exotic phenomena of 2*p* decay



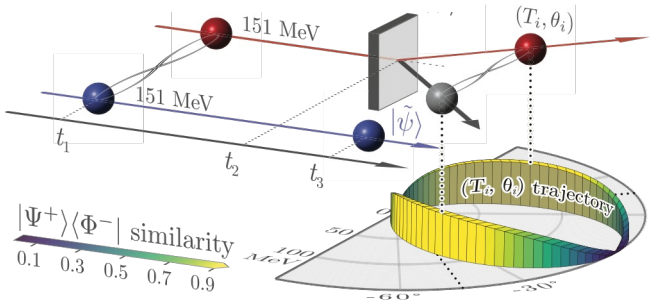
2*p* decay

I. A. Egorova *et al.*, Phys. Rev. Lett. 109, 202502 (2012)



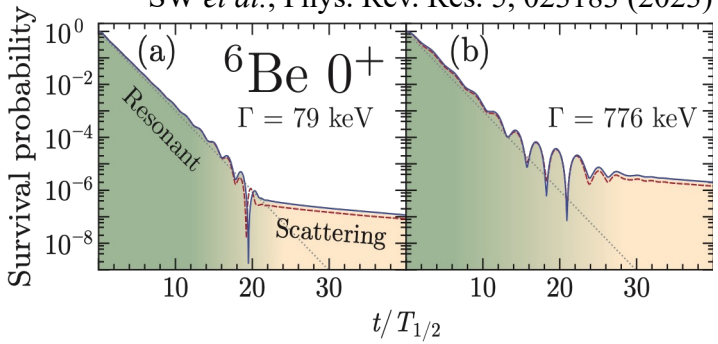
***E*-dependent *nn* correlation**

Z. X. Shen *et al.*, Arxiv 2510.24325



Entanglement

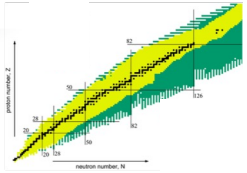
SW *et al.*, Phys. Rev. Res. 5, 023183 (2023)



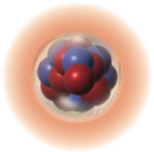
Non-exp decay

Outline

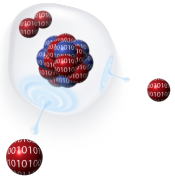
Introduction 1
- Dripline region
- Continuum effect



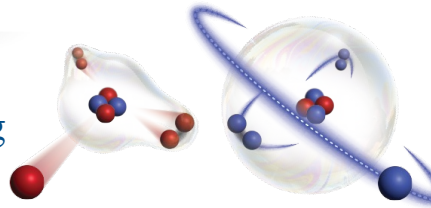
Radius 2
- Complex radius
- Halo-like enhancement



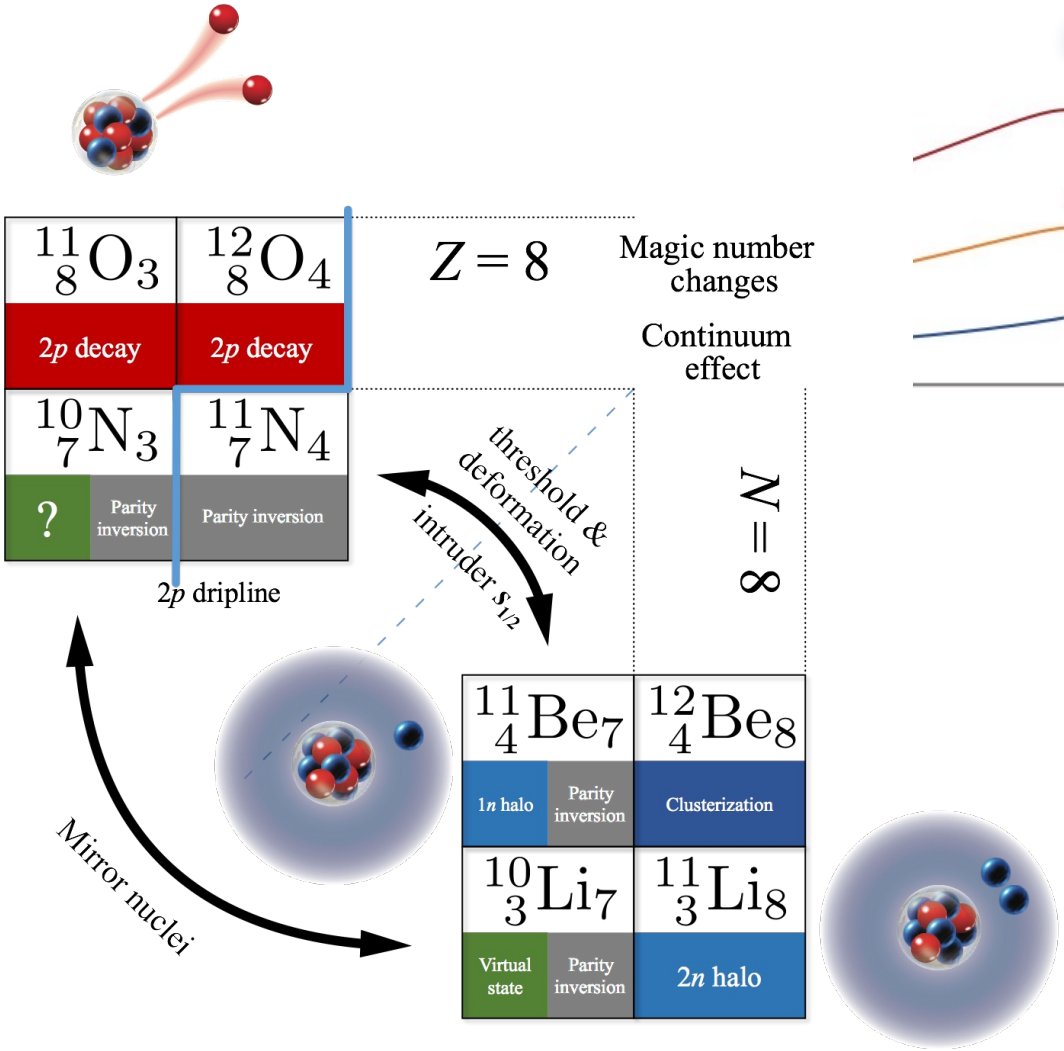
Decay 3
- 2*p* decay
- *pp* correlation

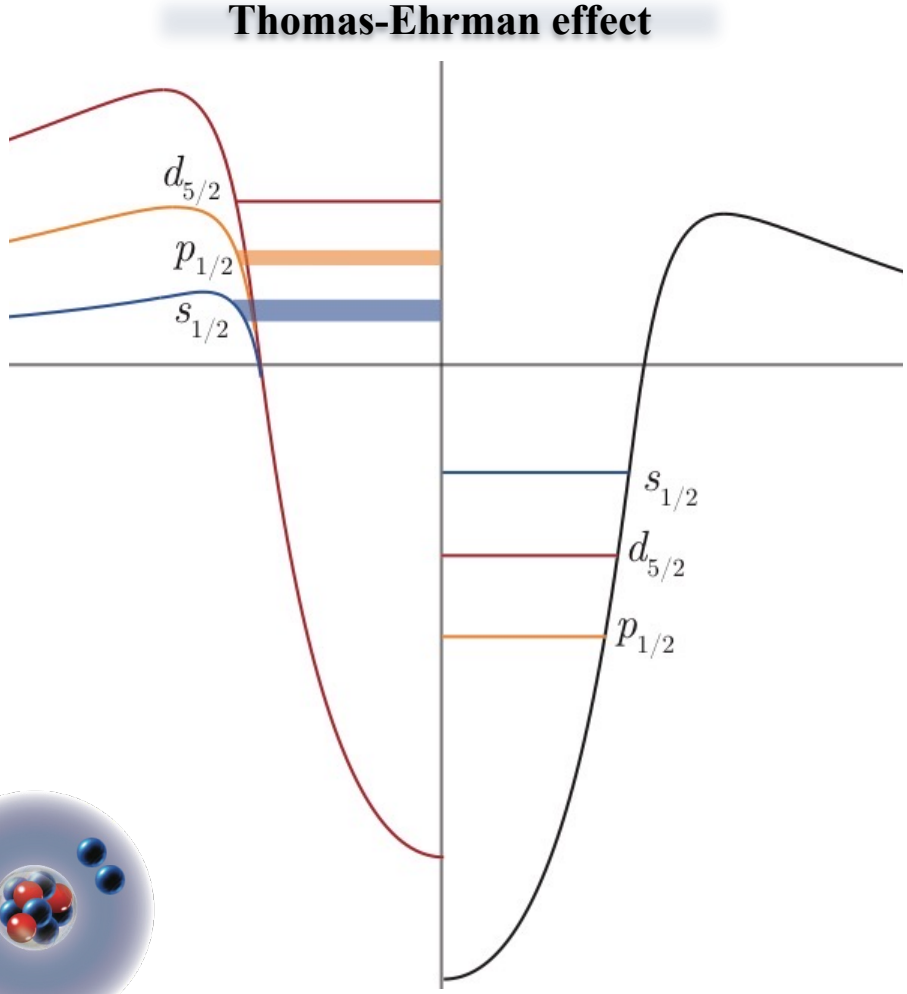


Mirror 4
- Thomas-Ehrman effect
- Mirror symmetry breaking



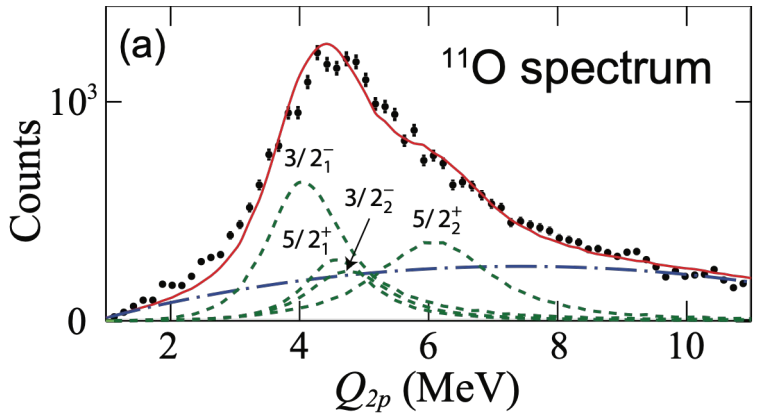
Mirror structure probed by 2*p* decay



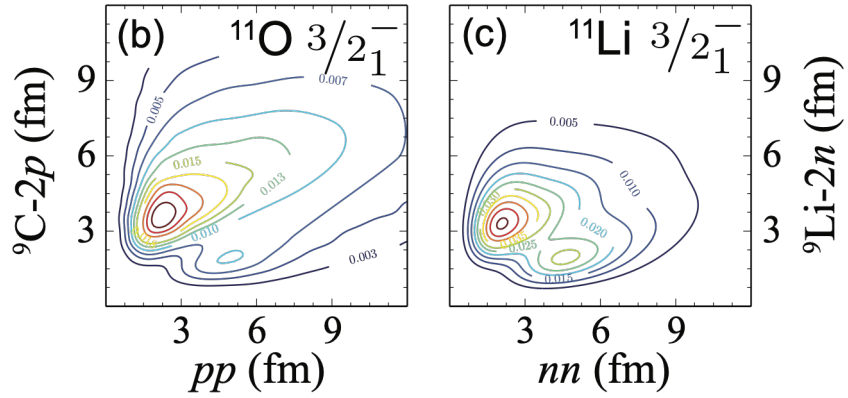


Predicted spectrum and structure of ^{11}O

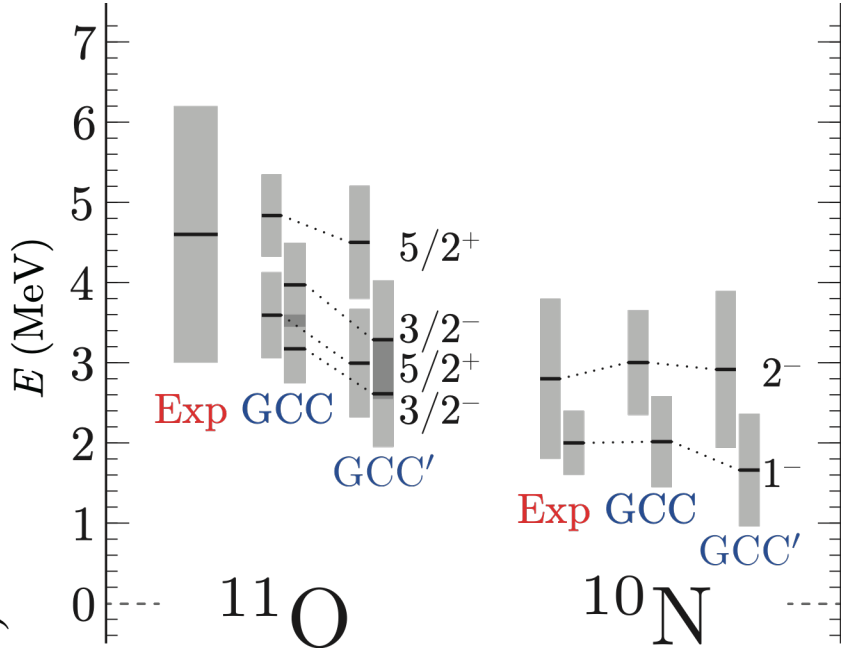
Measured spectrum of ^{11}O



Density distributions of ^{11}O and ^{11}Li



Calculated spectra of ^{10}N, ^{11}O

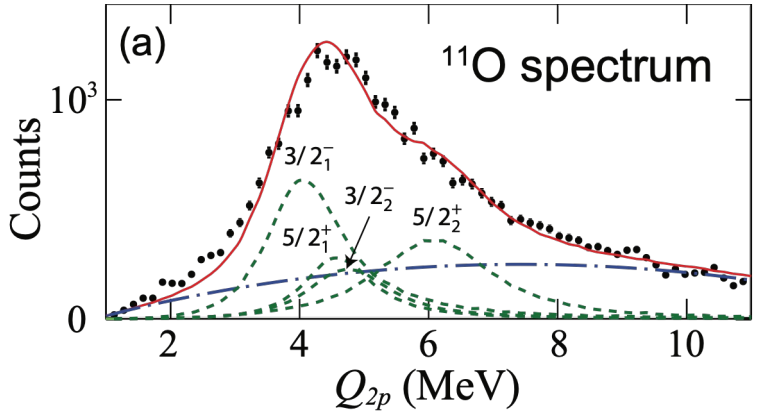


T. Webb *et al.*, PRL 122, 122501 (2019)

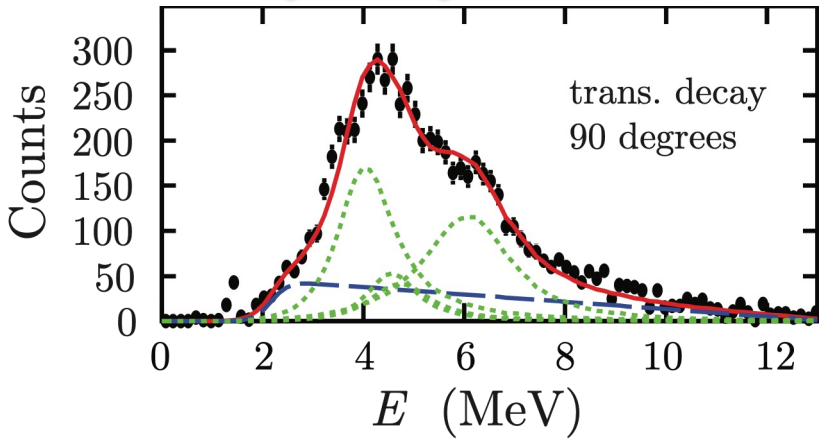
- The detected broad peak can be reproduced by four states rather than one.
- Mirror systems ^{11}O and ^{11}Li.

Predicted spectrum and structure of ^{11}O

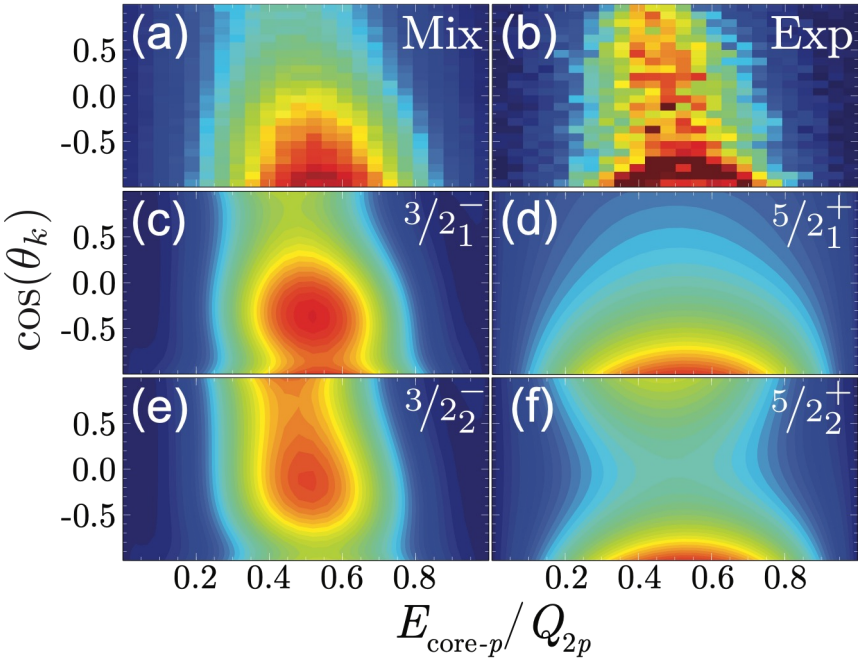
Measured spectrum of ^{11}O



Updated spectrum of ^{11}O



Asymptotic correlation of ^{11}O

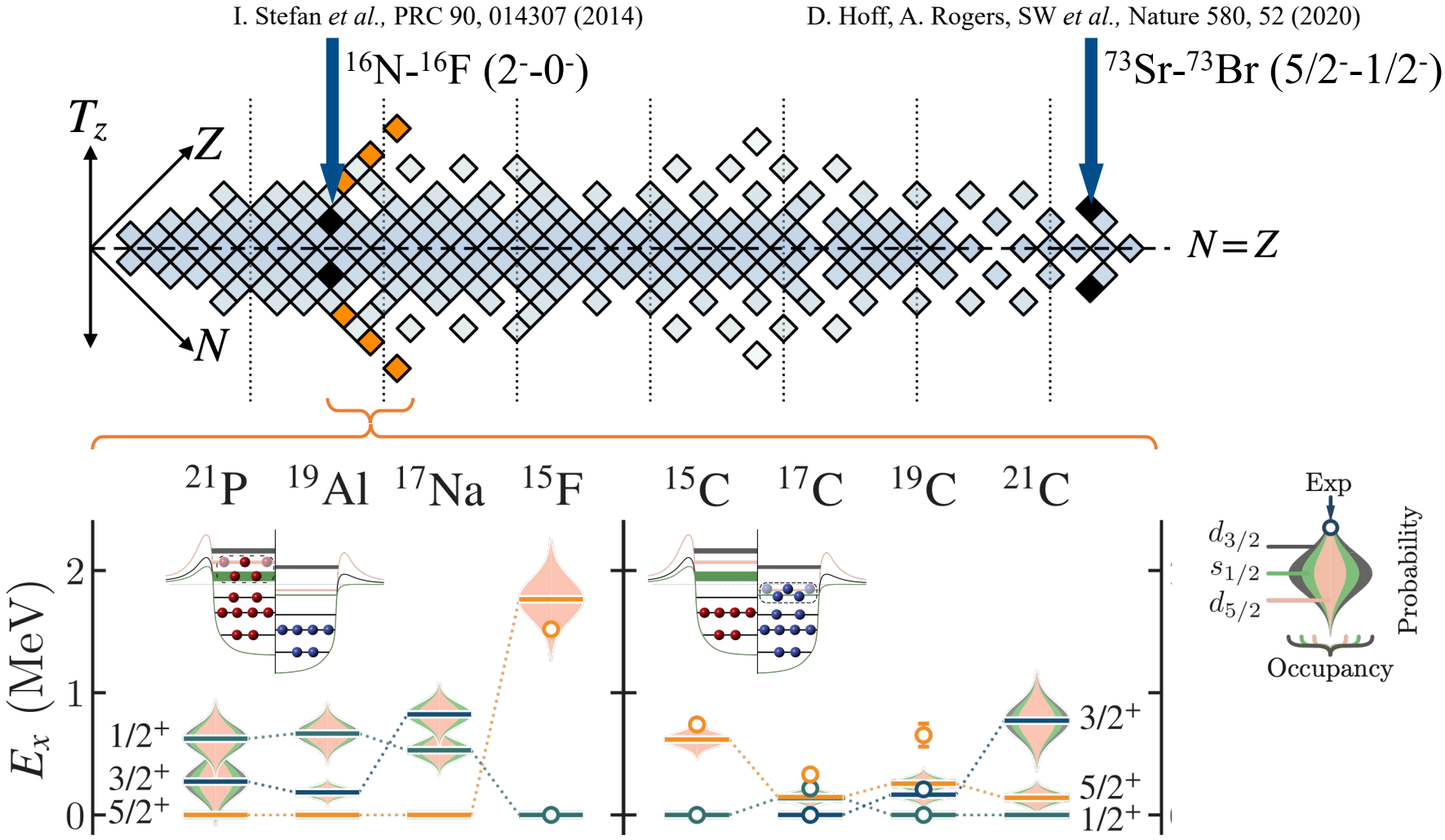


SW *et al.*, JPG 49, 10LT02 (2022)

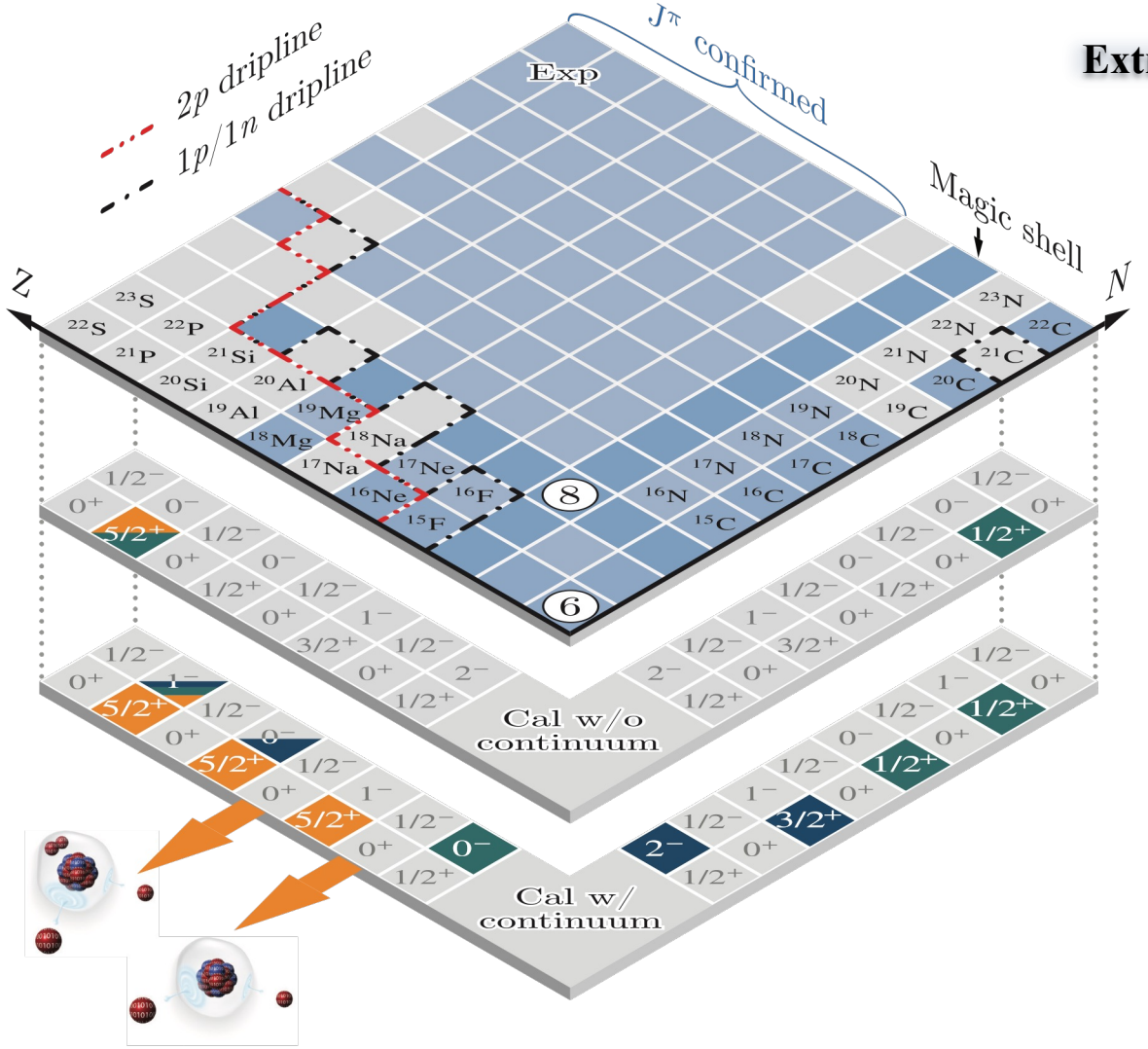
T. Webb *et al.*, PRC 101, 044317 (2020)

- The correlation and updated spectrum suggest multiple states in the broad resonance of ^{11}O.

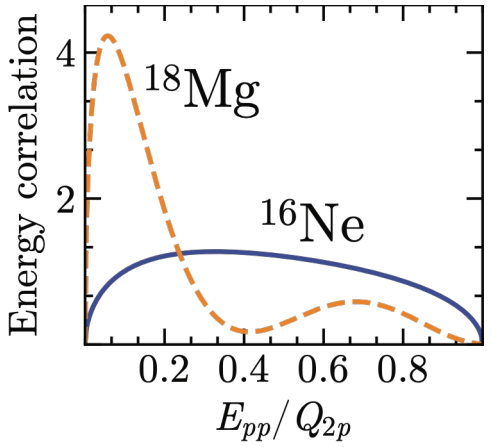
Ground-state mirror symmetry violation

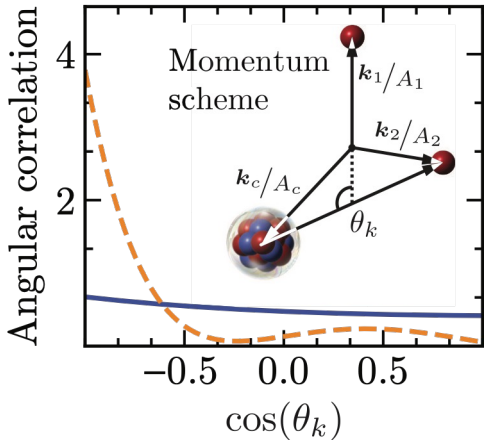


Broad region of GMSV



Extract spin/structure from correlation





Thank you for your attention!

Summary

- Continuum effects in open quantum systems
  - Complex radius
  - 2*p* decay
  - Nucleon-nucleon correlations
  - Connection between structure and decay properties

Acknowledgements

- W. Nazarewicz
- Y. R. Lin
- Z. X. Shen
- I. Mukha
- L. G. Sobotka
- Z. C. Xu
- M. Pfützner
- R. J. Charity
- A. Volya
- …



Thank you for your attention!

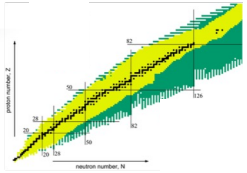
Questions

1. What's the meaning of the real and imaginary parts of complex radius?
2. What's the difference between $2p$ and $2n$ decay?
3. Correlations evolutions during the decay process
4. Any simultaneous multi-particle emissions?
5. Does decay dynamics depends on the production?
6. Entanglement evolution during the decay.
7. Other ways to extract mirror symmetry breaking.

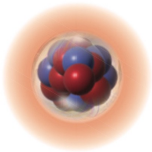


Outline

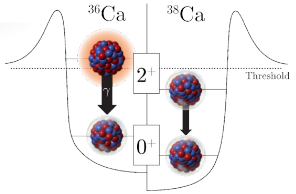
Introduction 1
- Dripline region
- Continuum effect



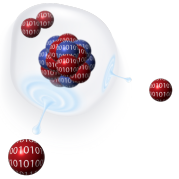
Radius 2
- Complex radius
- Halo-like enhancement



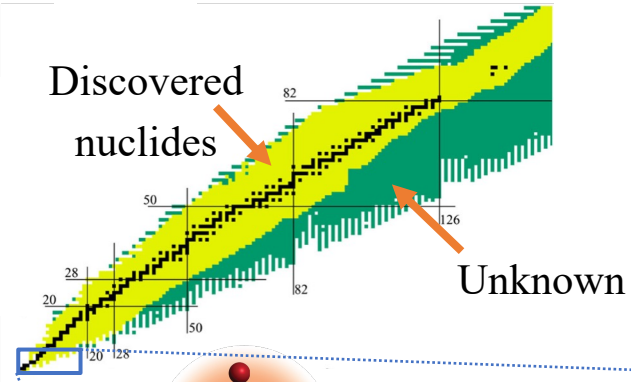
Spectroscopy 3
- *E*2 transition



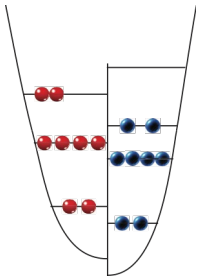
Decay 4
- 2*p*/2*n* decay
- *nn* correlation



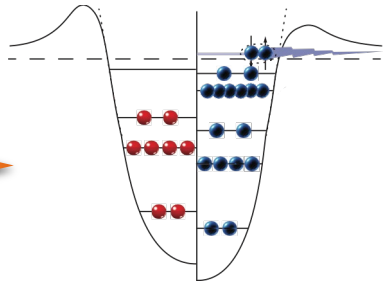
Rich phenomena towards the dripline

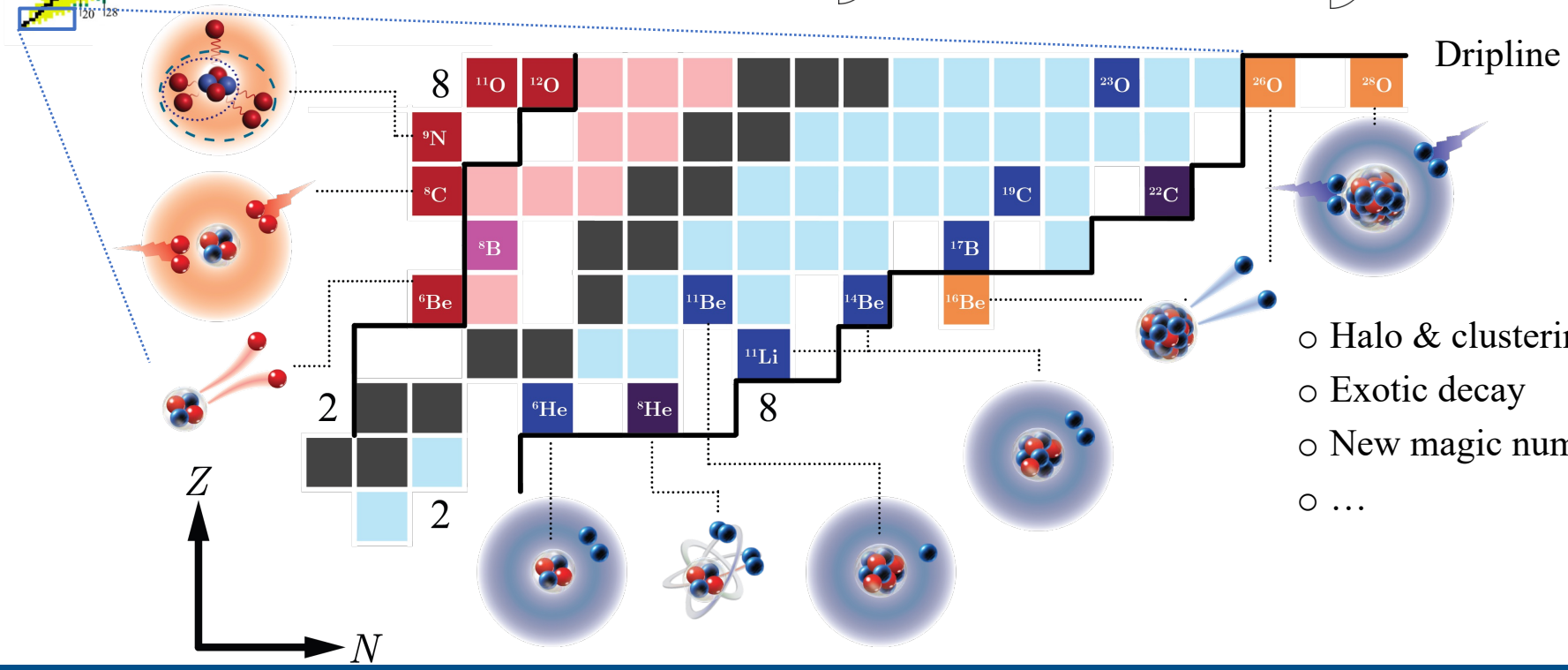


Closed quantum system



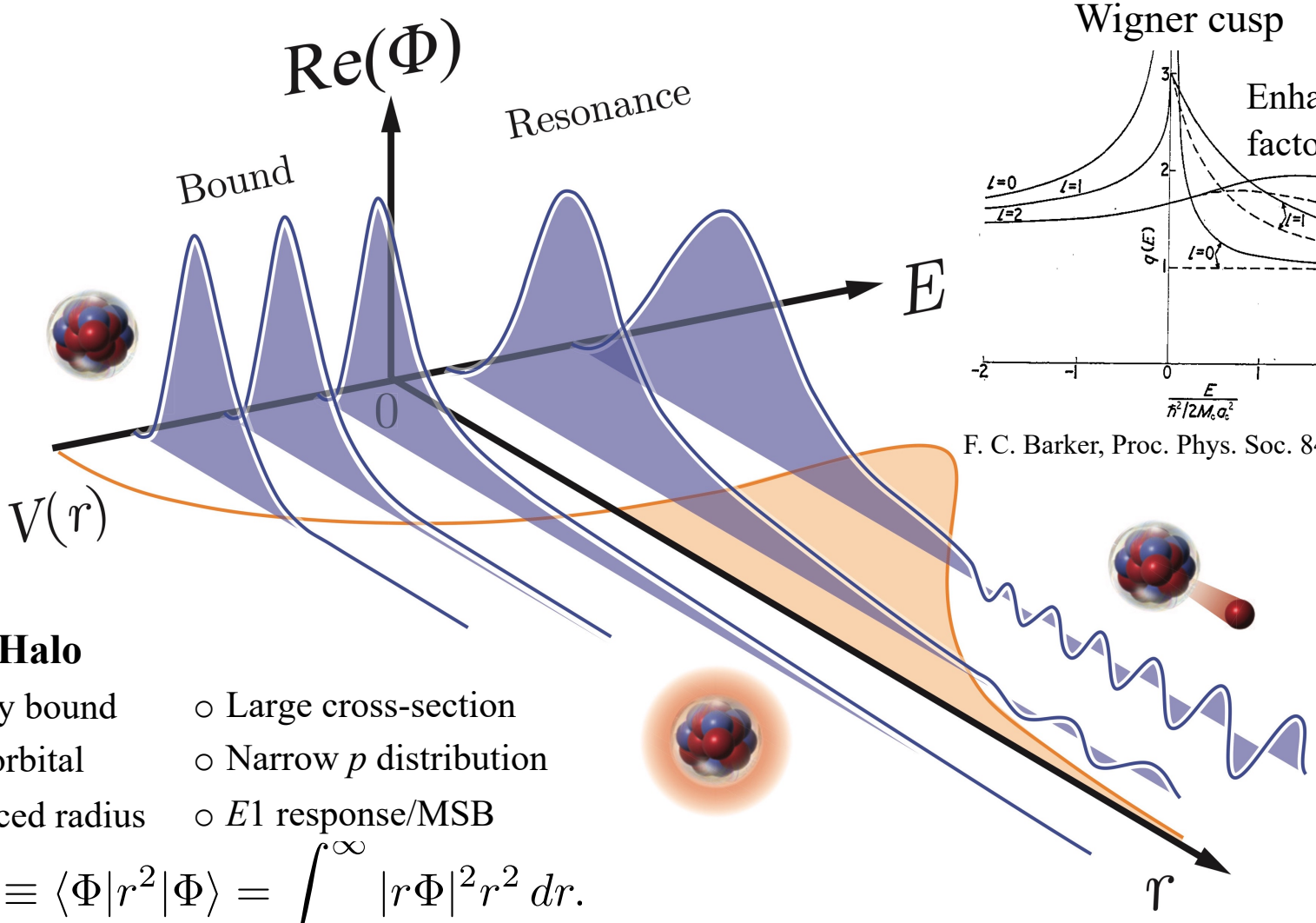
Open quantum system





- Halo & clustering
- Exotic decay
- New magic number
- …

Contiuum effect



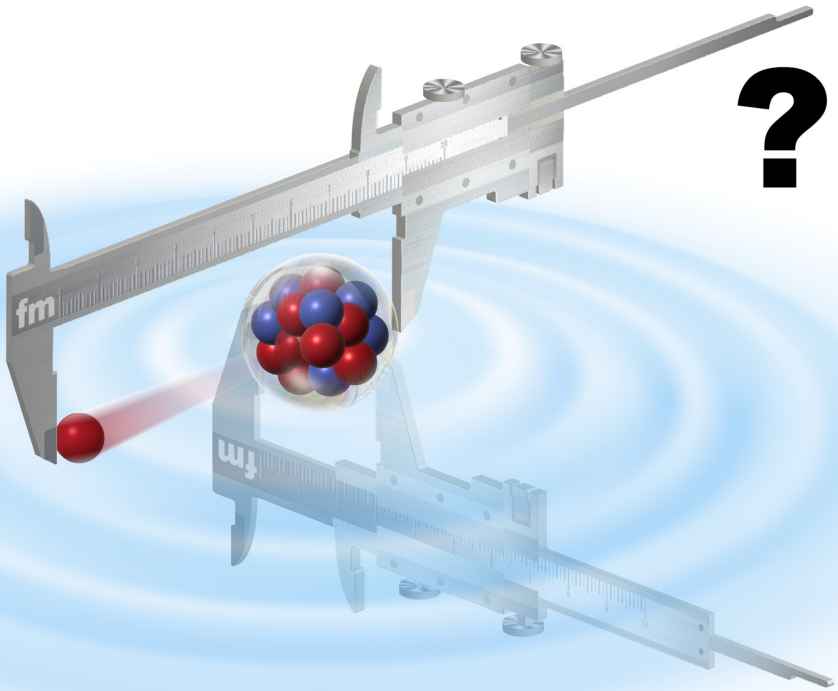
F. C. Barker, Proc. Phys. Soc. 84, 681 (1964)

Halo

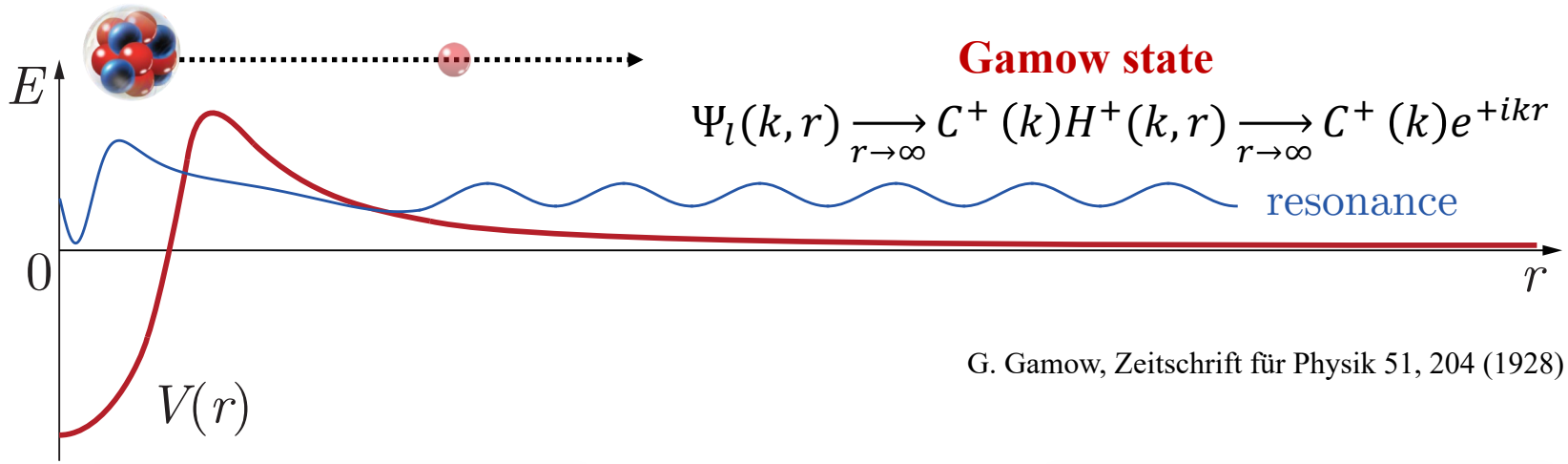
- Weakly bound
- low-l orbital
- Enhanced radius
- Large cross-section
- Narrow p distribution
- $E1$ response/MSB

$$r_{\mathrm{rms}}^2 \equiv \langle \Phi | r^2 | \Phi \rangle = \int_0^\infty |r\Phi|^2 r^2 \, dr.$$

Radius of the unbound state



Quantum picture of decay

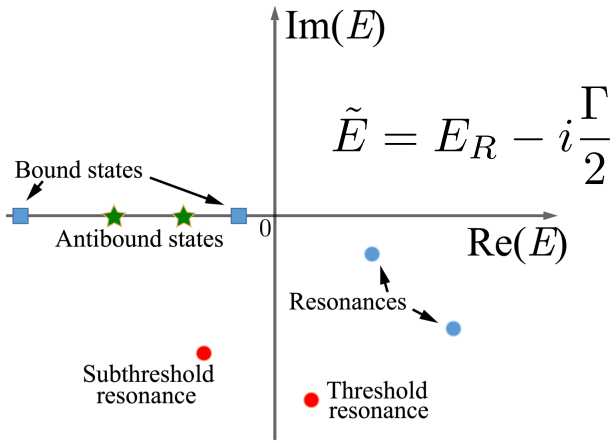


Gamow state

$$\Psi_l(k,r) \xrightarrow[r\to\infty]{} C^+(k)H^+(k,r) \xrightarrow[r\to\infty]{} C^+(k)e^{+ikr}$$

G. Gamow, Zeitschrift für Physik 51, 204 (1928)

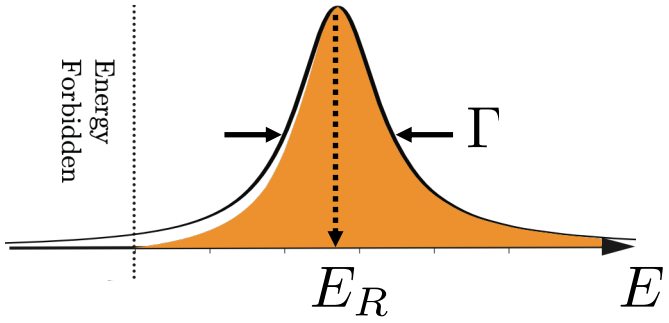
Complex energy plane



$$\tilde{E} = E_R - i\frac{\Gamma}{2}$$

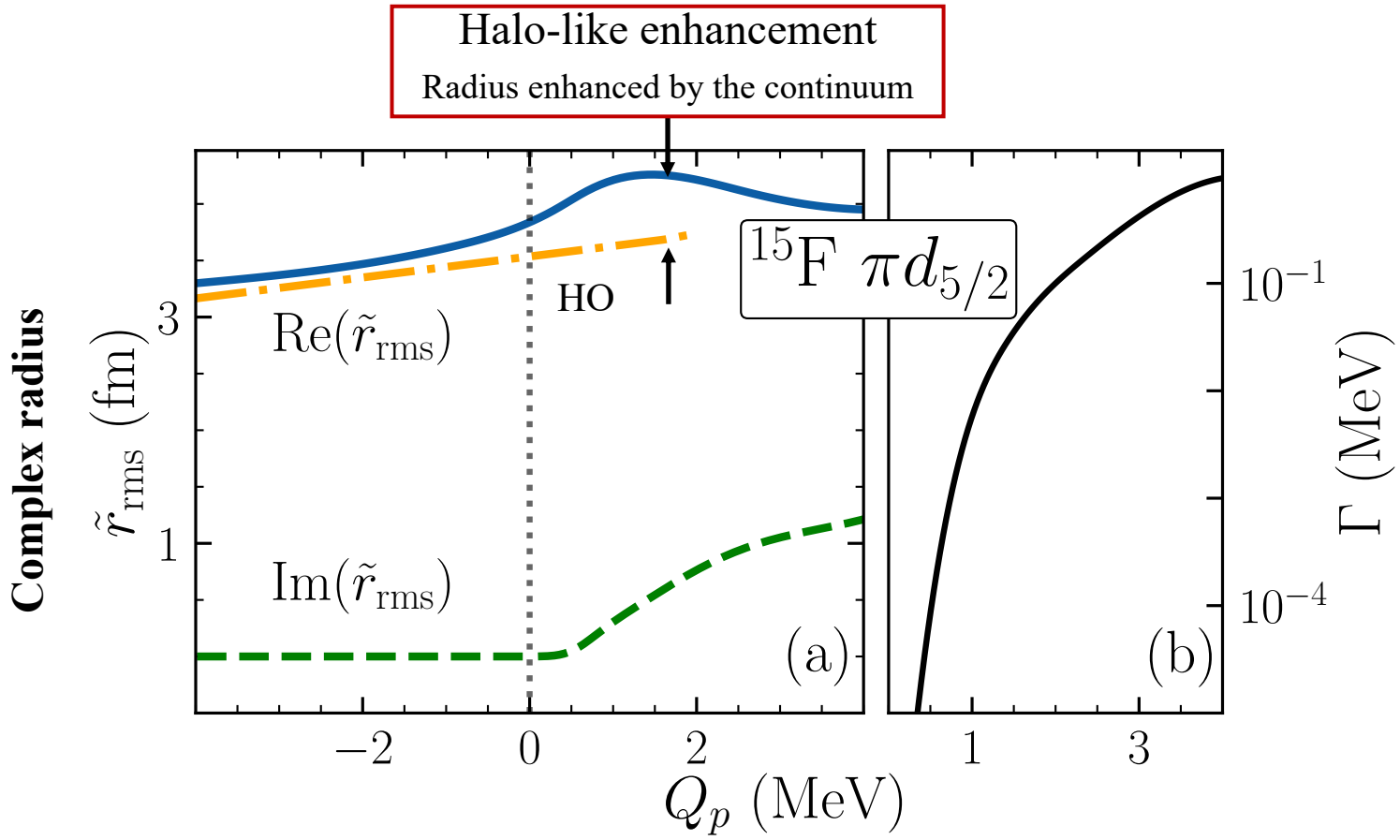
$$\Psi(t) = e^{-i\frac{\hat{H}}{\hbar}t}\Psi(0) = e^{-i\frac{E_R t}{\hbar} - \frac{\Gamma t}{2\hbar}}\Psi(0)$$

Resonance spectral function



$$\Gamma = \frac{\hbar \ln 2}{T_{1/2}}; \qquad \Delta E \Delta T \geq \frac{\hbar}{2}$$

Complex radius of 1*p* emitter ^{15}F

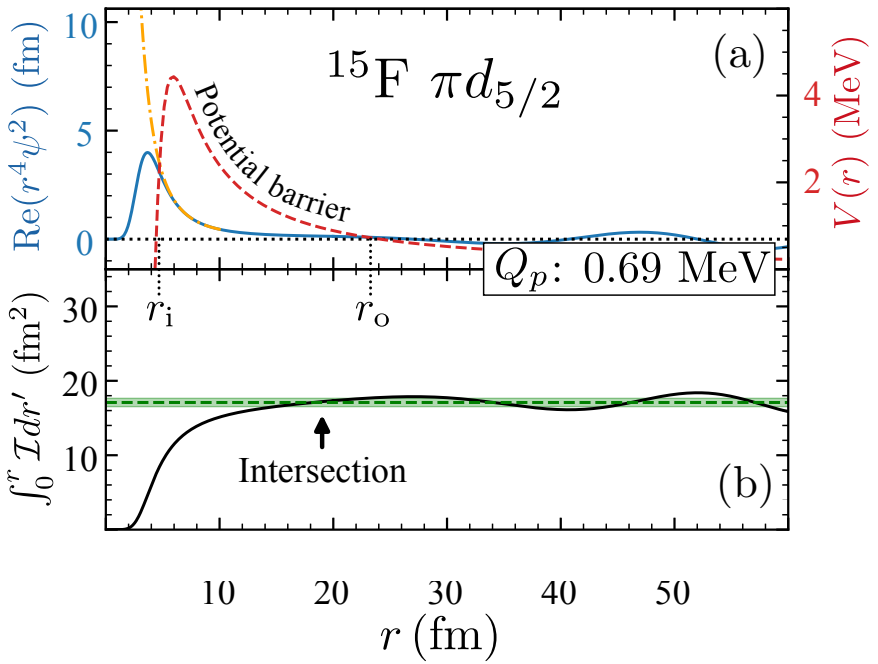


- Contiuum coupling is enhanced near the threshold.
- Complex radius $\tilde{r}^2_{\rm rms} \equiv \langle\tilde{\Phi}|r^2|\Phi\rangle = \int_0^\infty (r\Phi)^2 r^2\, dr.$

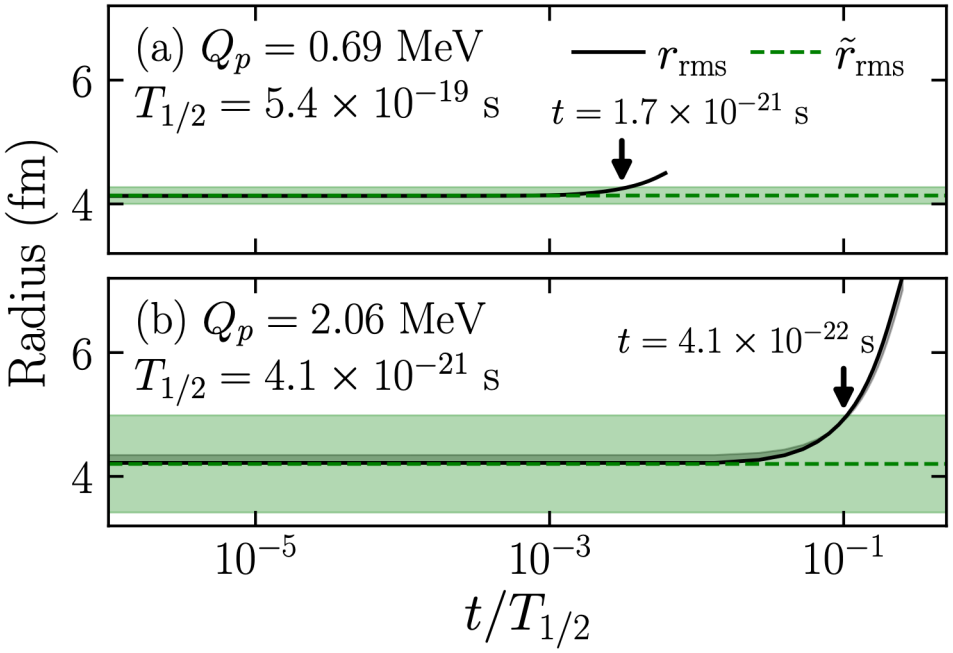
Y. R. Lin, SW *et al.*, Arxiv 2511.10238, PRL accepted
T. Myo and K. Katō,
Prog. Theor. Exp. Phys. 2014, 083D01 (2014).

Complex radius of 1*p* emitter ^{15}F

Wavefunction & radius at Q = 0.69 MeV



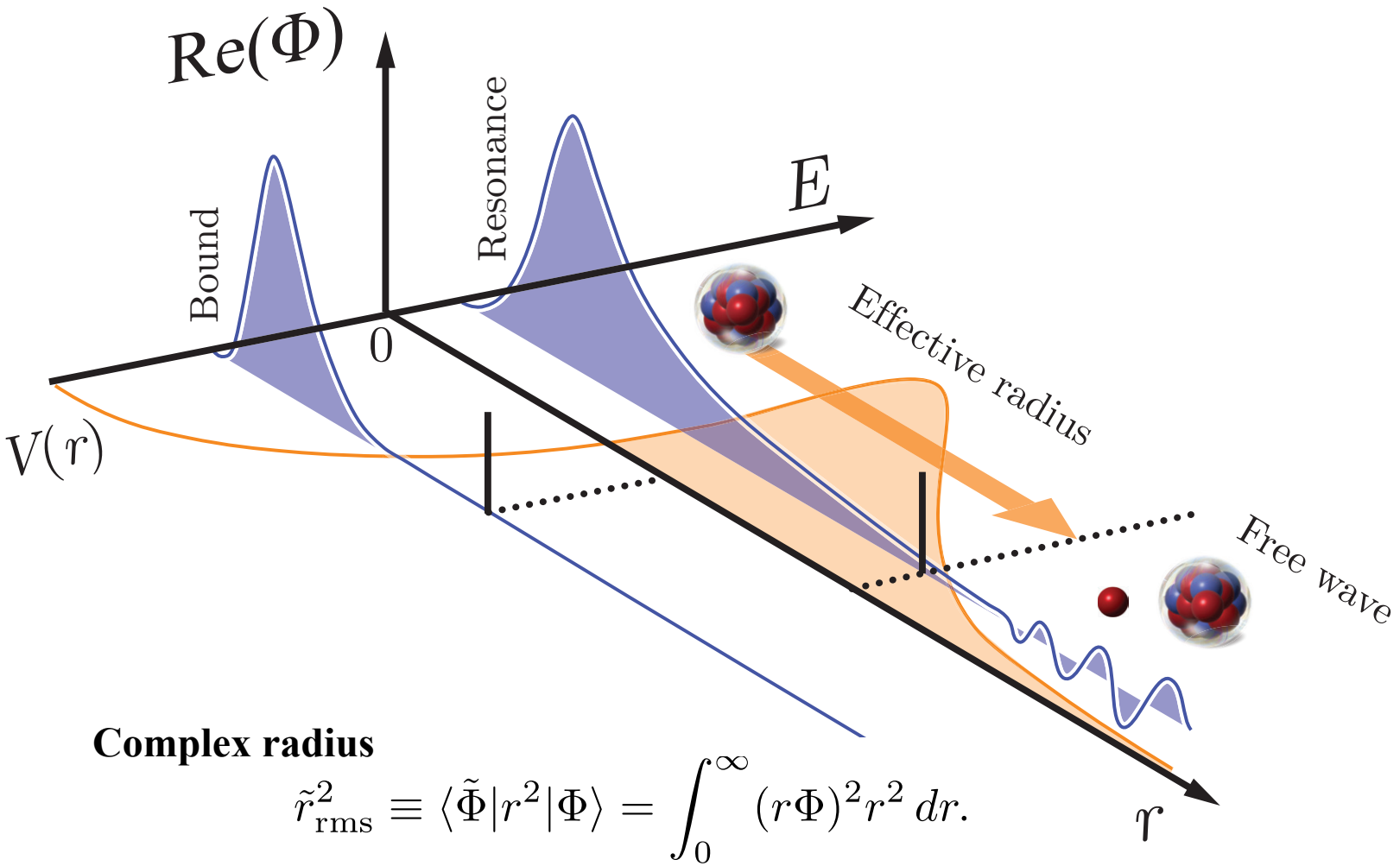
Radius evolution



Y. R. Lin, SW *et al.*, Arxiv 2511.10238, PRL accepted

- The contribution to the complex radius from the asymptotic region is largely canceled out.
- The match point for the complex radius is located inside the barrier.

Complex radii of particle emitters

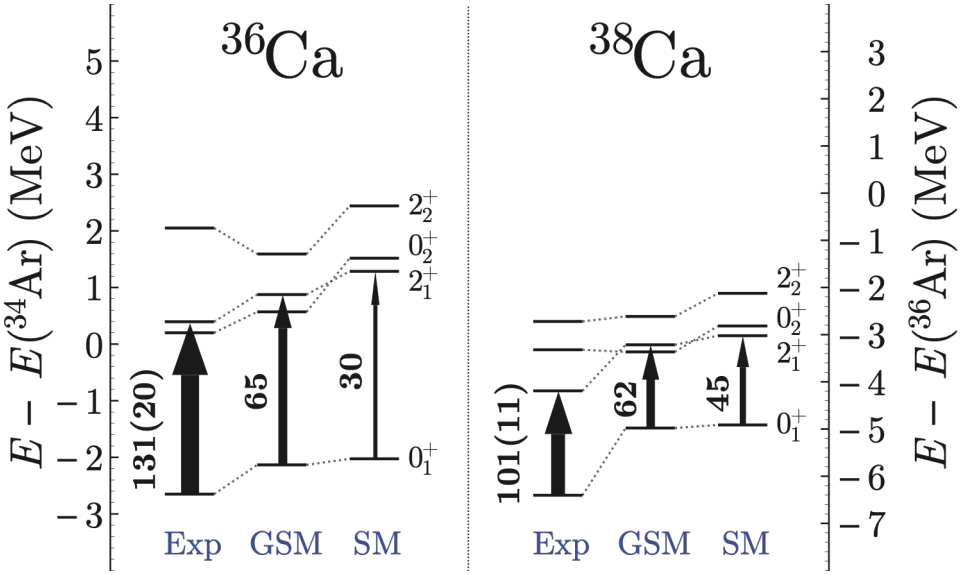


Complex radius

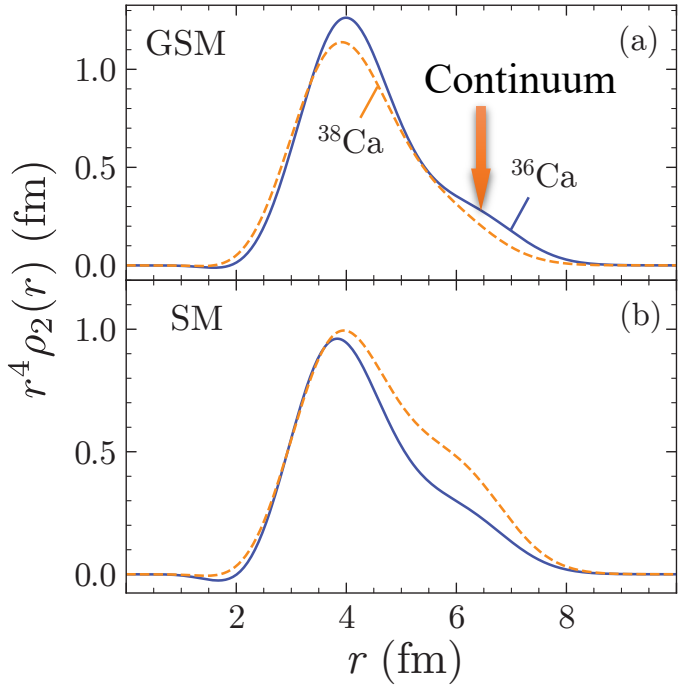
$$\tilde{r}^2_{\rm rms} \equiv \langle \tilde{\Phi} | r^2 | \Phi \rangle = \int_0^\infty (r\Phi)^2 r^2 \, dr.$$

Contiuum effect on electromagnetic transition

Spectra and $B(E2)$ values of ^{36,38}Ca



$E2$ ($0^+ \rightarrow 2^+$) Transition densities



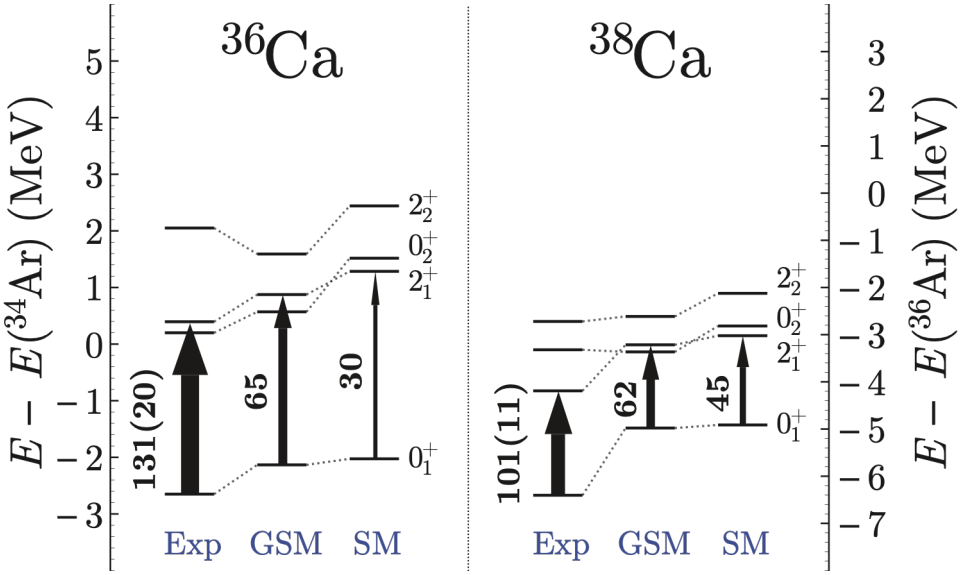
$$\rho_L(r) = \langle \Phi_f | \frac{1}{r^2} \delta(r' - r) Y_L | \Phi_i \rangle$$

$$B(EL) = \left[\frac{\hat{J}_f}{\hat{J}_i} \int_0^\infty \rho_L(r) r^{L+2} dr \right]^2$$

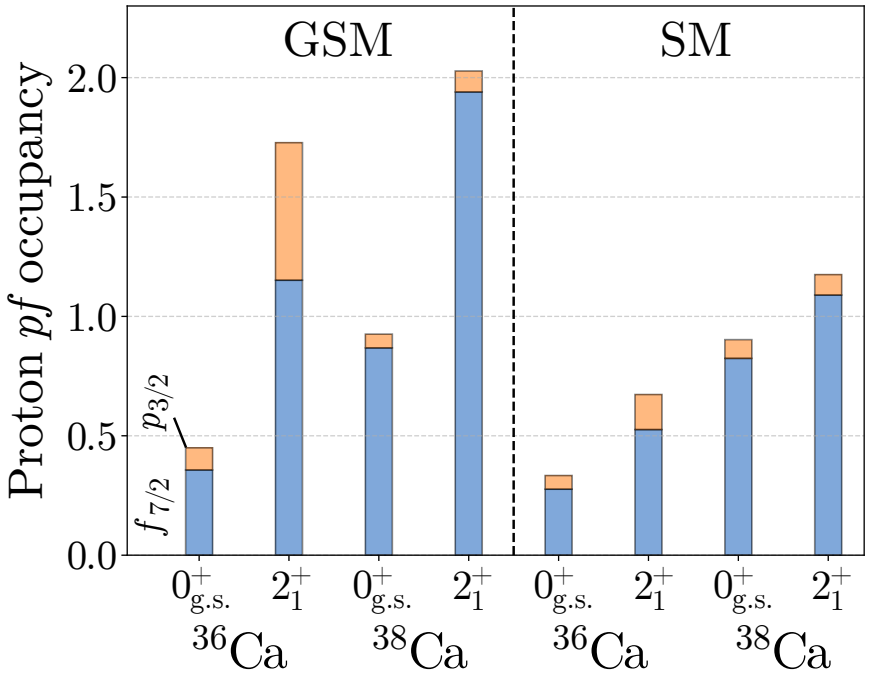
Z. Xu, SW *et al.*, Phys. Rev. C 112, L011302 (2025).
T. Beck, A. Gade *et al.*, Phys. Rev. C 108, L061301 (2023)
N. Dronchi, D. Weisshaar *et al.*, Phys. Rev. C 107, 034306 (2023)

Contiuum effect on spectroscopic factor

Spectra and $B(E2)$ values of ^{36,38}Ca



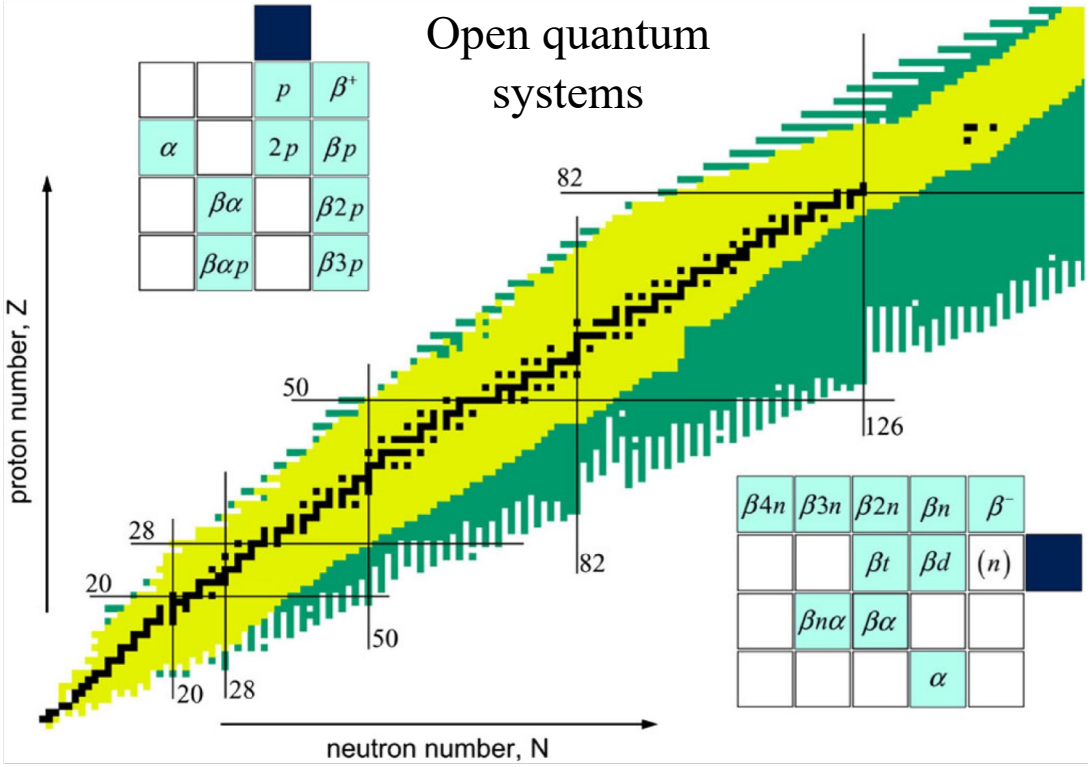
Cross-shell excitations



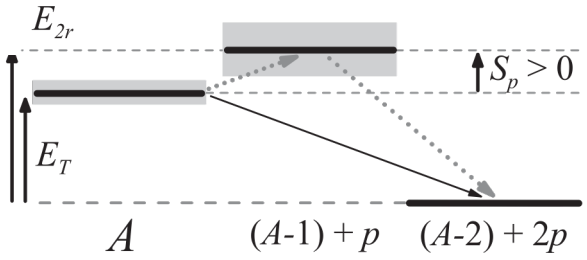
- Continuum enhances the cross-shell effect.
- p wave is strongly impacted by the continuum.

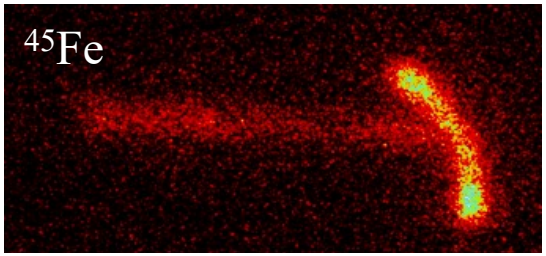
Z. Xu, SW *et al.*, Phys. Rev. C 112, L011302 (2025)
J. Wylie *et al.*, Phys. Rev. C 104, L061301
M. R. Xie *et al.*, Phys. Rev. C 110, 054301 (2024)

Exotic two-proton (2*p*) decay



- **2*p* decay**





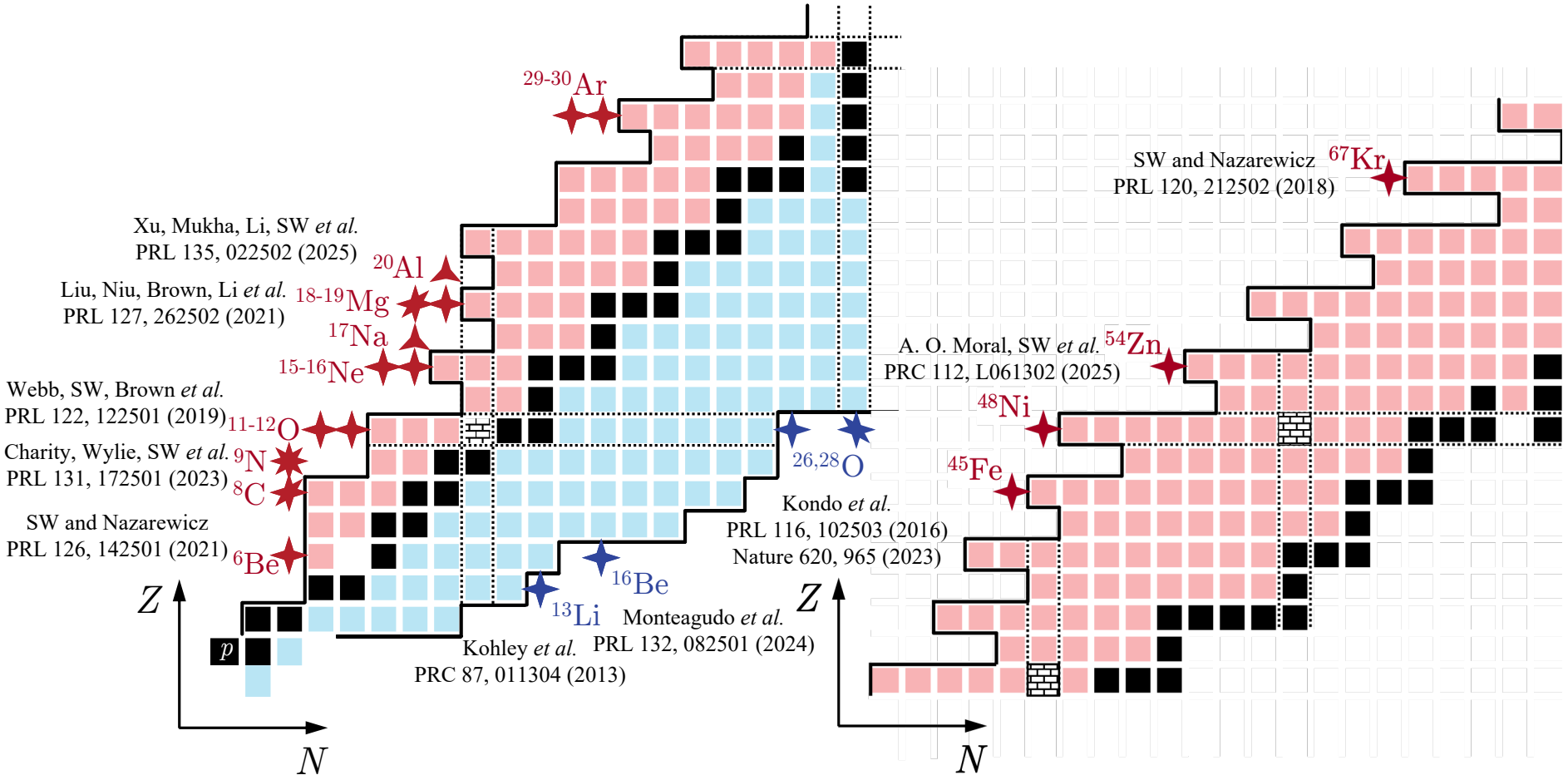
Y.B. Zeldovich, Sov. Phys. JETP 11, 812 (1960)

V. Goldansky, Nucl. Phys. 19, 482 (1960)

J. Giovinazzo *et al.*, Phys. Rev. Lett. 89, 102501 (2002)

K. Miernik *et al.*, Phys. Rev. Lett. 99, 192501 (2007)

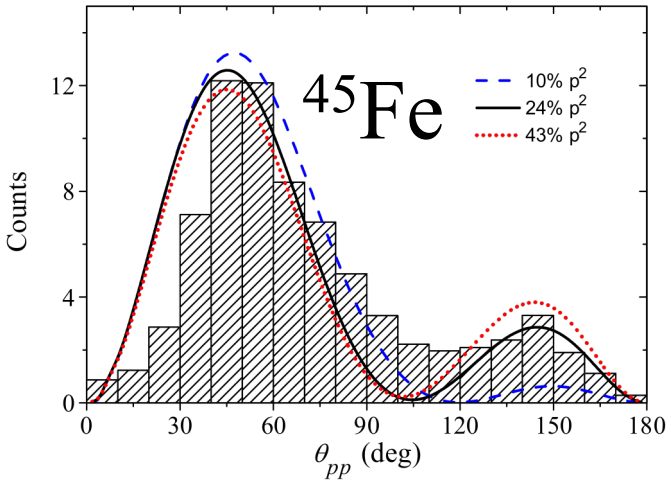
Observed 2*p* & *np* emitters



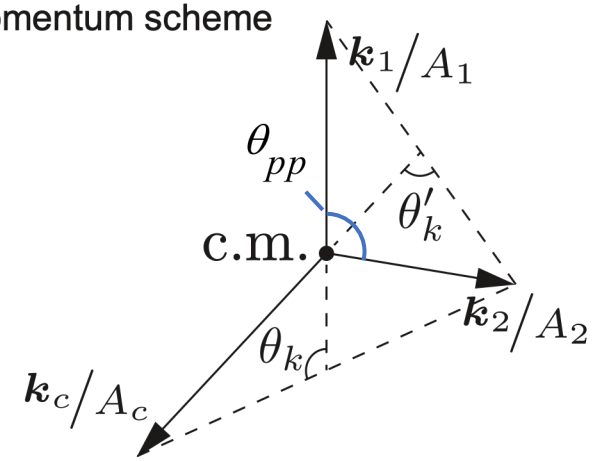
M. Pfützner, I. Mukha, SW, Prog. Part. Nucl. Phys. 132, 104050 (2023)

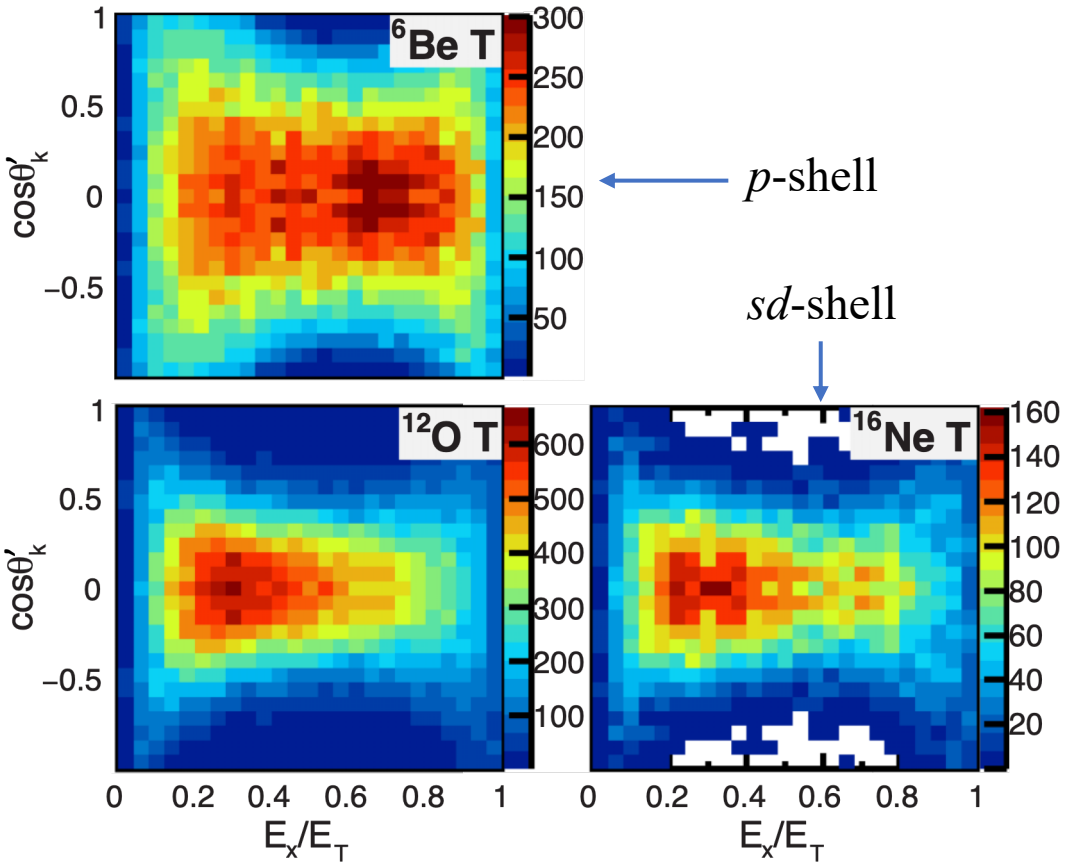
Asymptotic nucleon-nucleon correlation

K. Miernik *et al.* PRL 99, 192501 (2007)



Momentum scheme

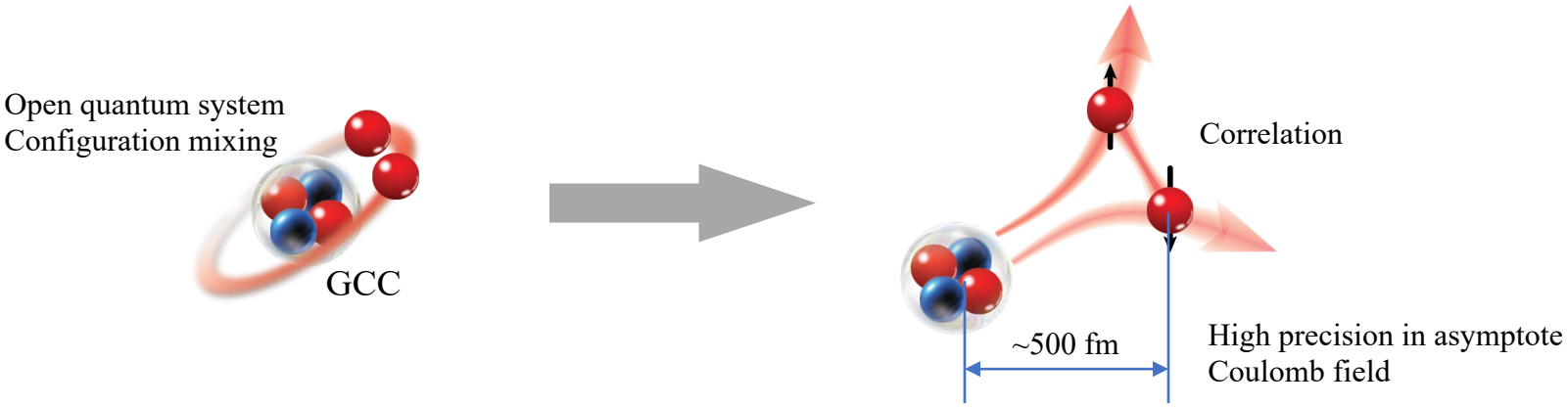




T.B. Webb *et al.* Phys. Rev. C 100, 024306 (2019)

Time dependent (TD) approach

In order to study the dynamics of 2*p* decay



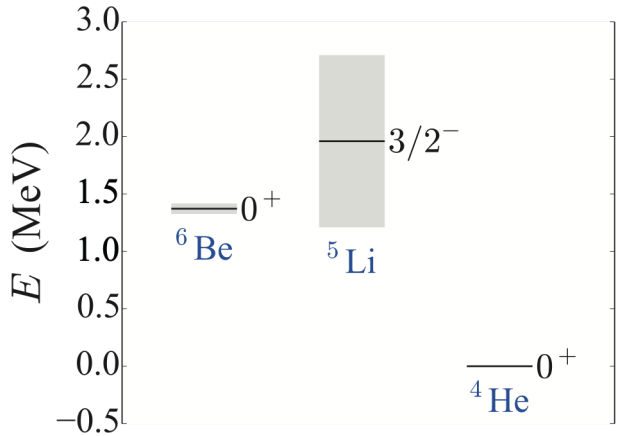
- **Time dependent approach**

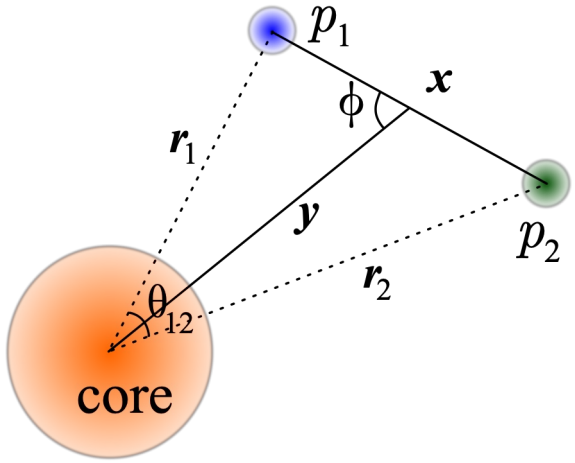
$$e^{-i\frac{\hat{H}}{\hbar}t} = \sum_{n=0}^{\infty}(-i)^n\,(2-\delta_{n0})\,J_n(t)T_n(\hat{H}/\hbar)$$

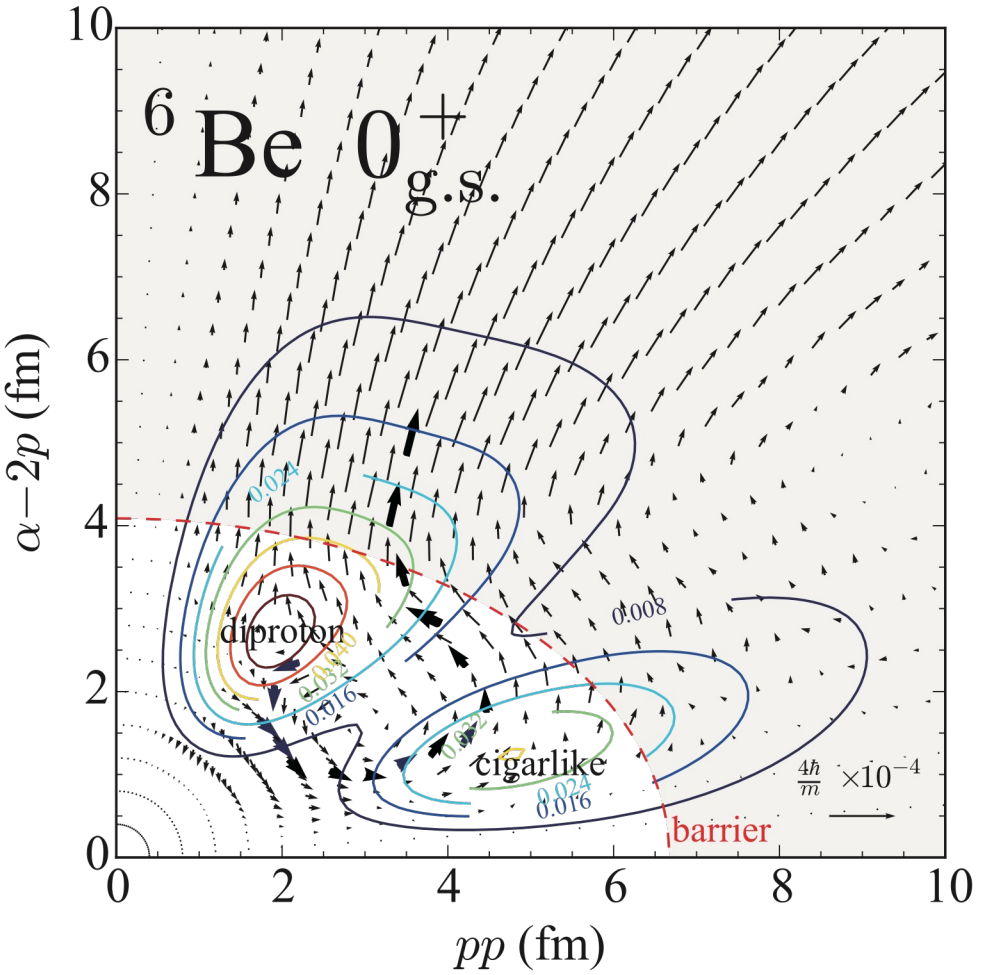
  - Time propagator can be expanded with Chebyshev polynomials.
  - Initial wave function is obtained by GCC, which includes configuration mixing and proper asymptote.
  - Two-proton wave function has been propagated to over 500 fm.

SW and W. Nazarewicz, Phys. Rev. Lett. 126, 142501 (2021)

Ground-state of ^{6}Be

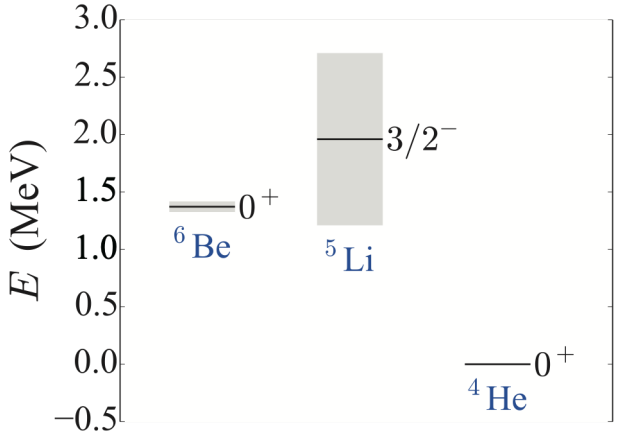


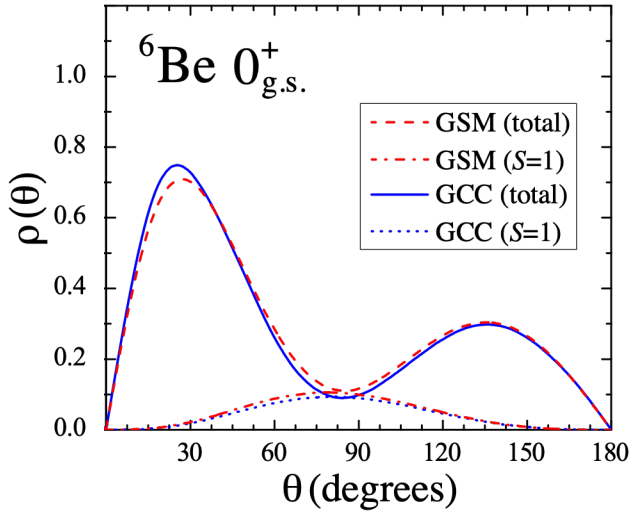


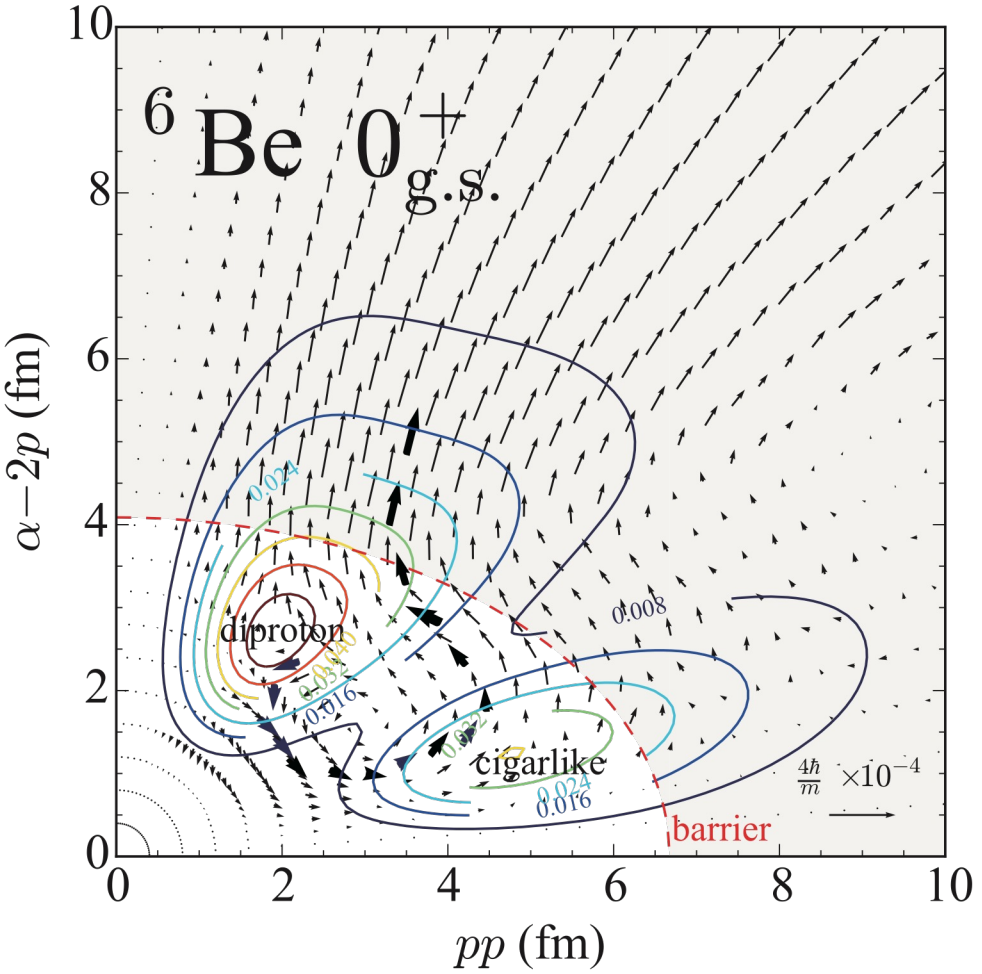


SW *et al.*, Phys. Rev. C 99, 054302 (2019)

Ground-state of ^{6}Be



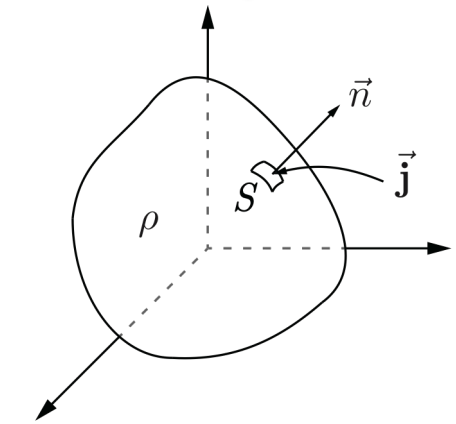




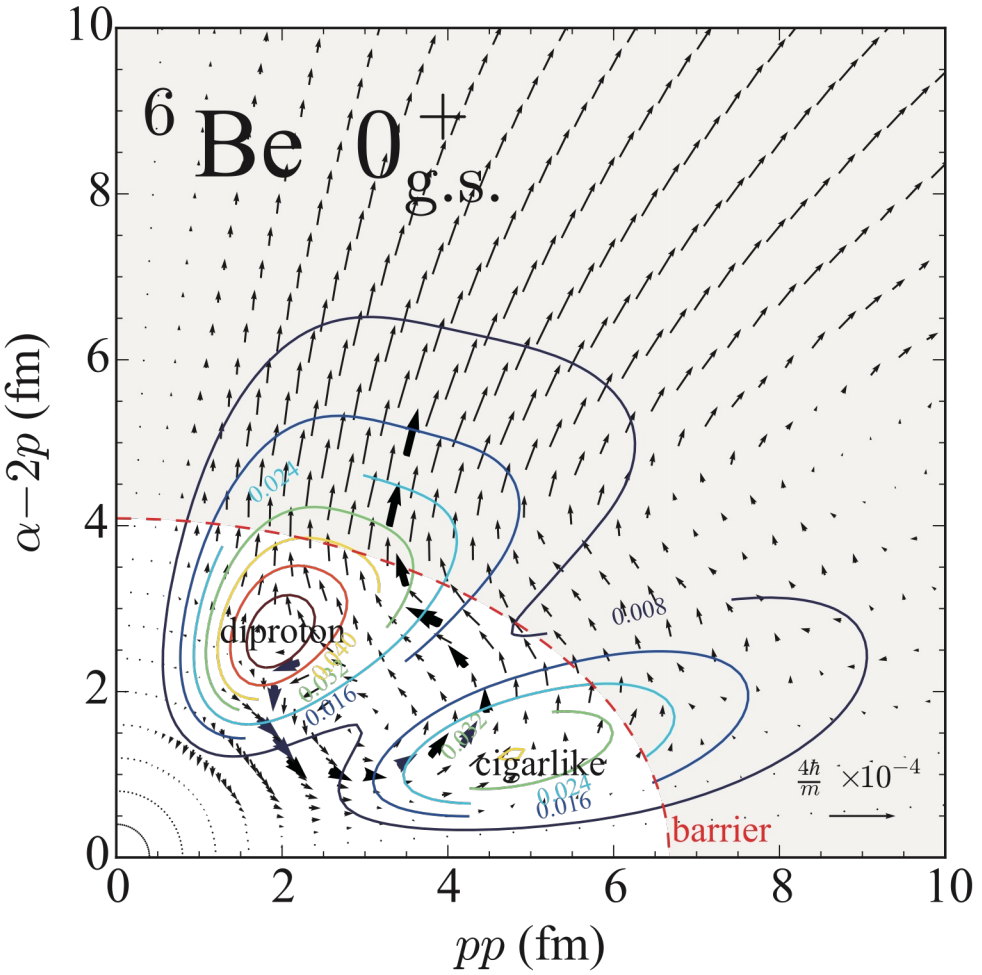
SW *et al.*, Phys. Rev. C 99, 054302 (2019)

Ground-state of ^{6}Be

Probability current

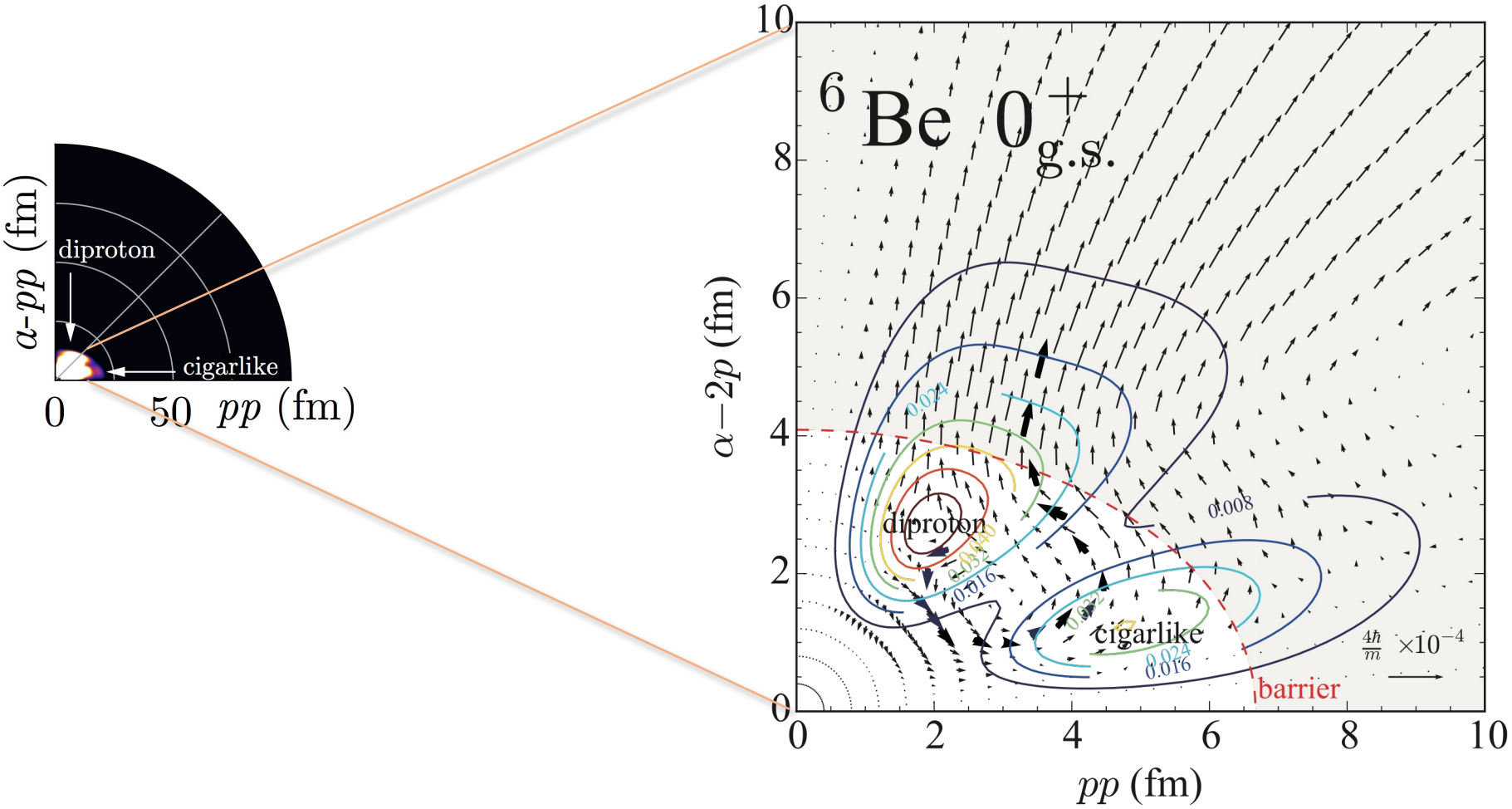


$$\iiint \frac{\partial \rho}{\partial t}\,\mathrm{d}V = -\oiint \vec{\mathbf{j}}\cdot\vec{n}\,\mathrm{d}S$$



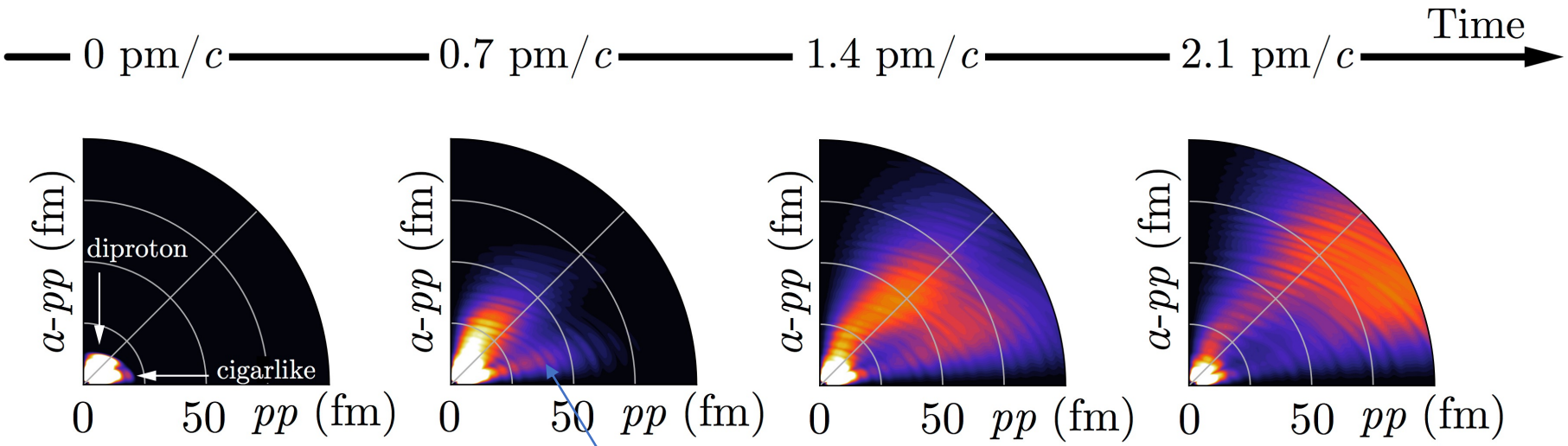
SW *et al.*, Phys. Rev. C 99, 054302 (2019)

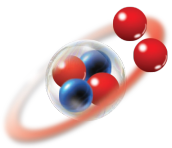
Ground-state of ^{6}Be



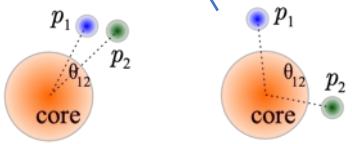
SW *et al.*, Phys. Rev. C 99, 054302 (2019)

2*p* decay in ^{6}Be

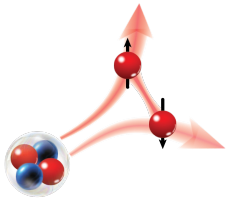




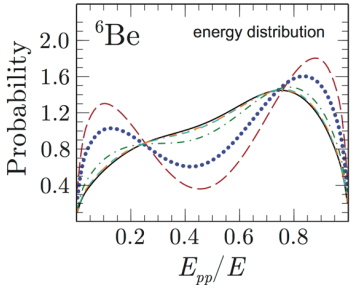
Protons inside nucleus



Two types of tunneling:
1. diproton (primarily)
2. cigarlike



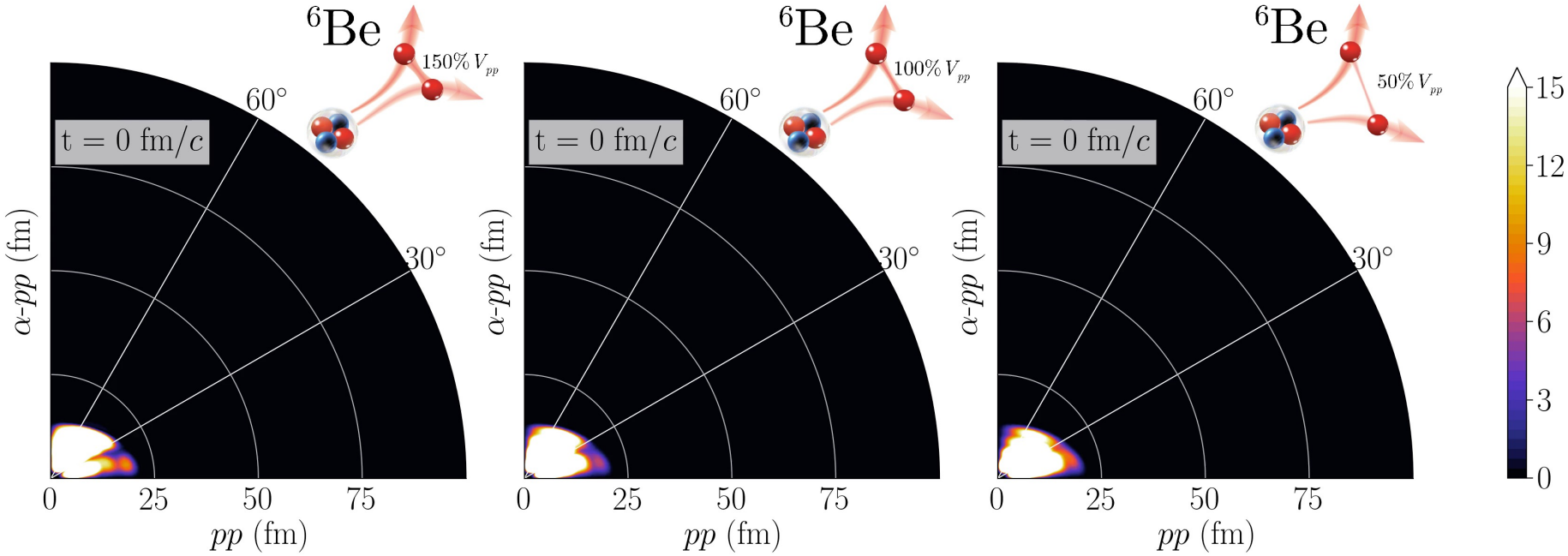
Diproton branch bends due to Coulomb repulsion



Asymptotic correlation begin to converge

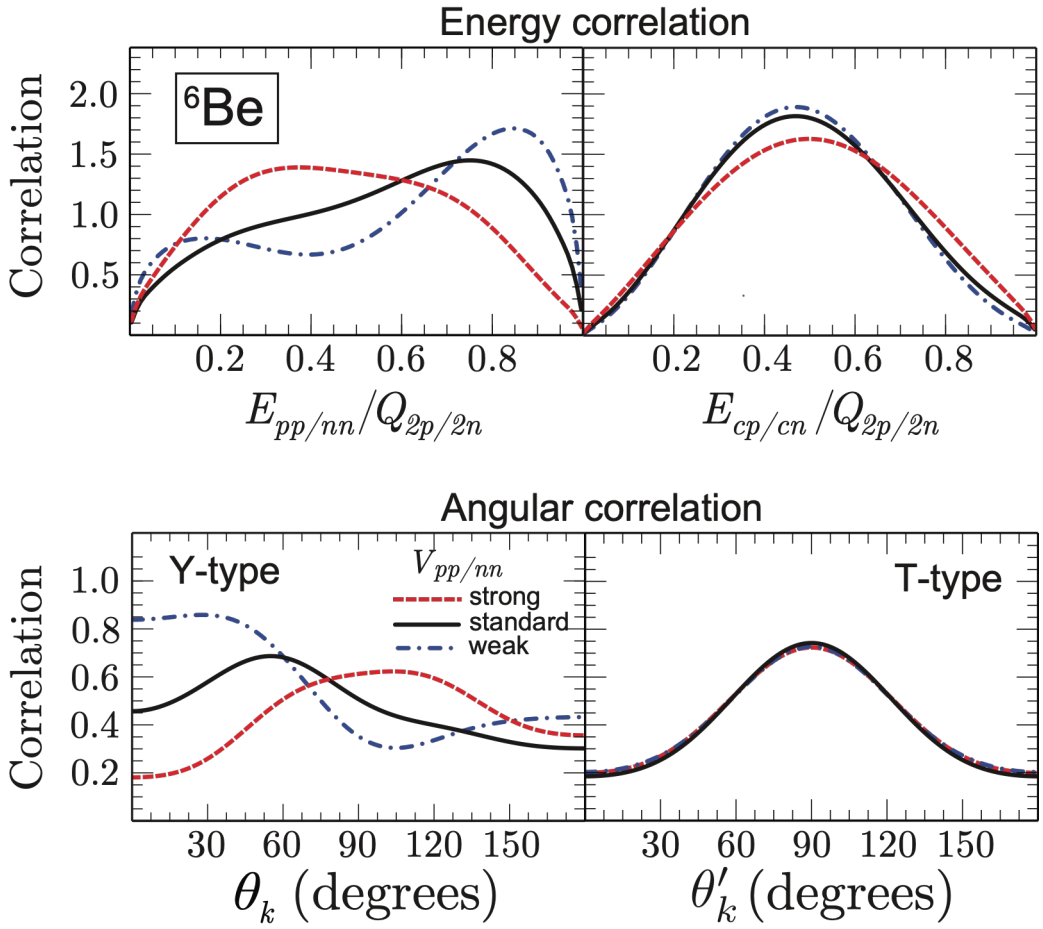
SW and W. Nazarewicz, Phys. Rev. Lett. 126, 142501 (2021)

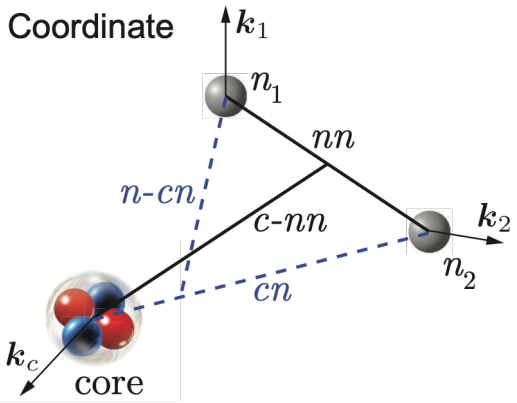
Decay dynamics depends on pairing

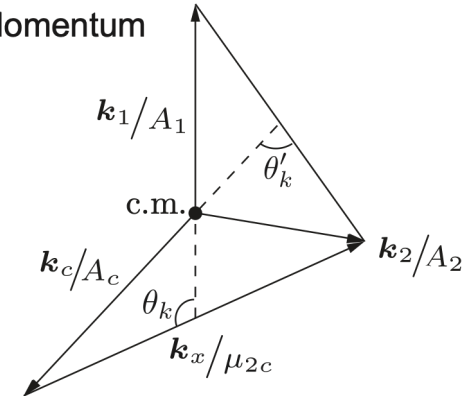


- The decay dynamics as well as correlation strongly depend on the pairing strength.
- Strong pairing results in a larger decay width, which indicates that pairing will benefit the 2*p* tunneling.

Asymptotic correlations

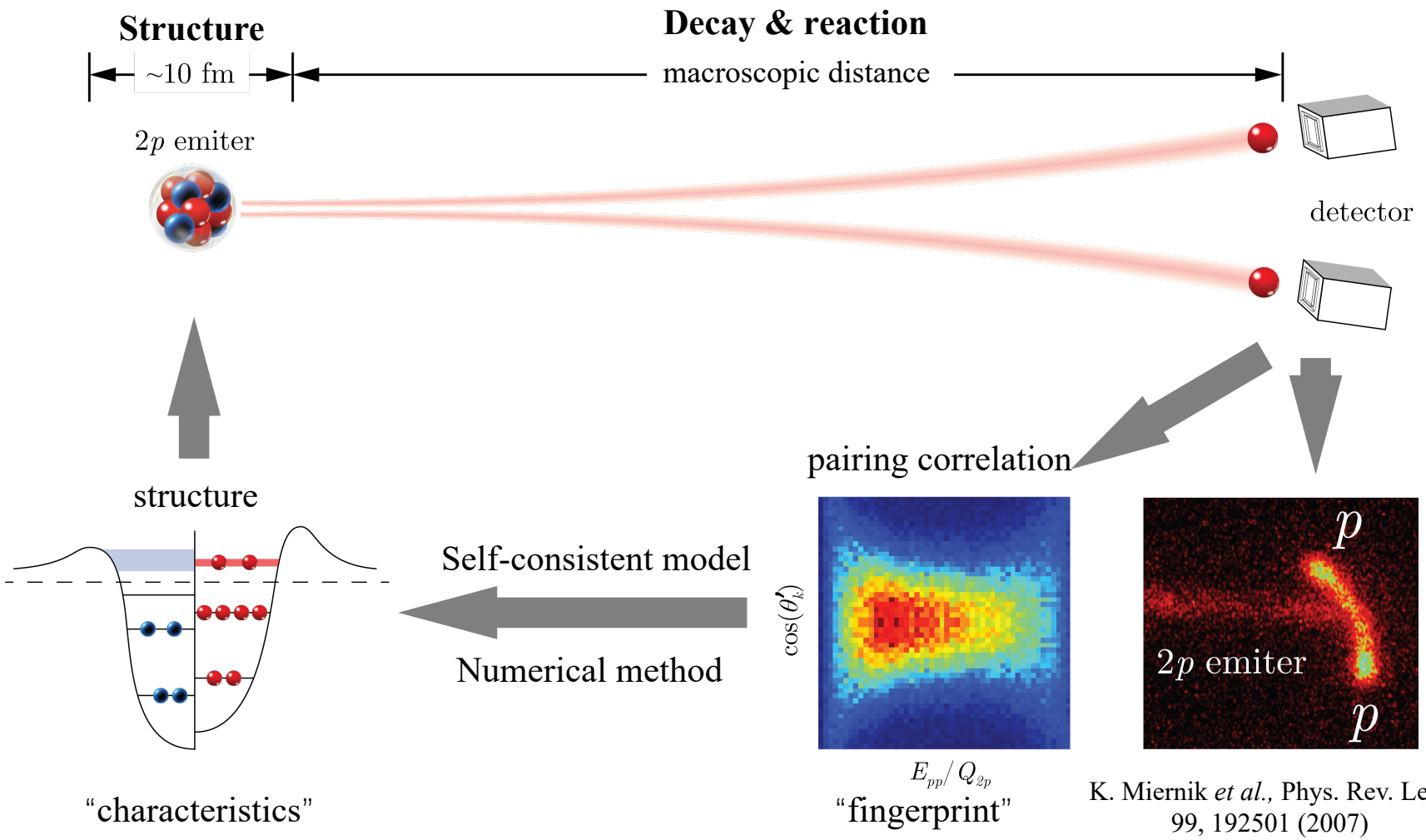






- E_{pp} and Y-type angular correlations are strongly impacted by nucleon-nucleon interaction.

Structure ⟷ Asymptotic observables



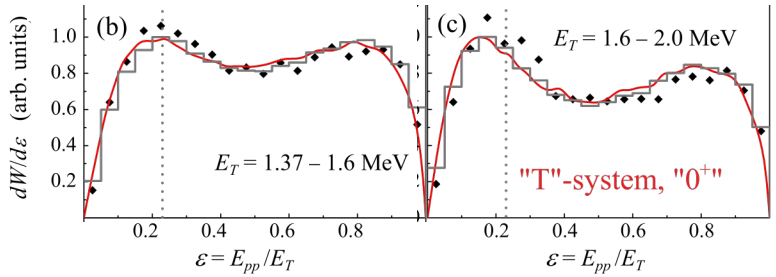
K. Miernik *et al.*, Phys. Rev. Lett. 99, 192501 (2007)

Exotic phenomena of 2*p* decay



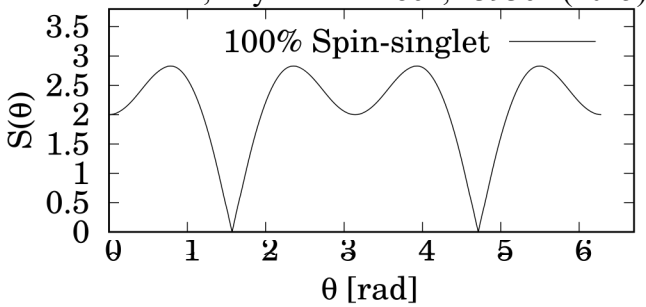
2*p* decay

I. A. Egorova *et al.*, Phys. Rev. Lett. 109, 202502 (2012)



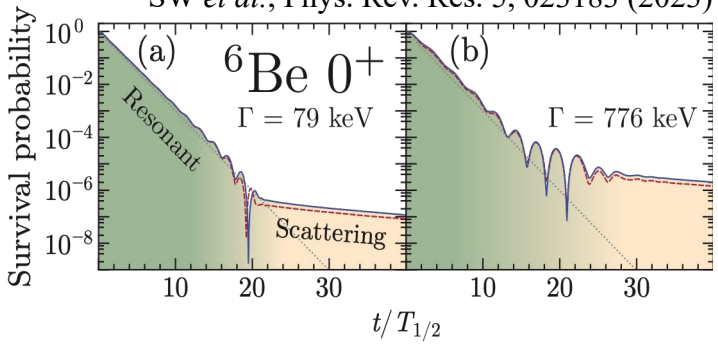
***E*-dependent *nn* correlation**

T. Oishi, Phys. Lett. B 862, 139361 (2025)



Entanglement

SW *et al.*, Phys. Rev. Res. 5, 023183 (2023)



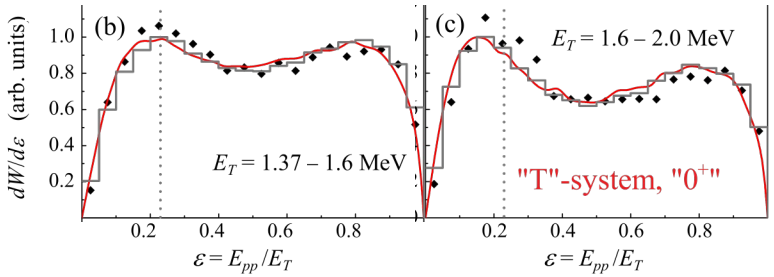
Non-exp decay

Exotic phenomena of 2*p* decay



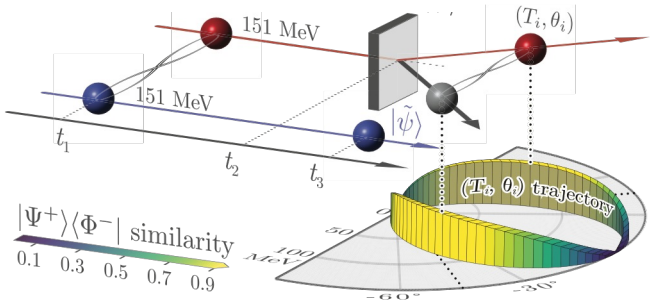
2*p* decay

I. A. Egorova *et al.*, Phys. Rev. Lett. 109, 202502 (2012)



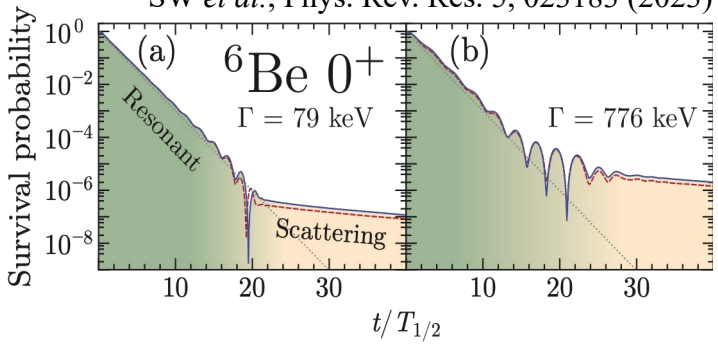
***E*-dependent *nn* correlation**

Z. X. Shen *et al.*, Arxiv 2510.24325



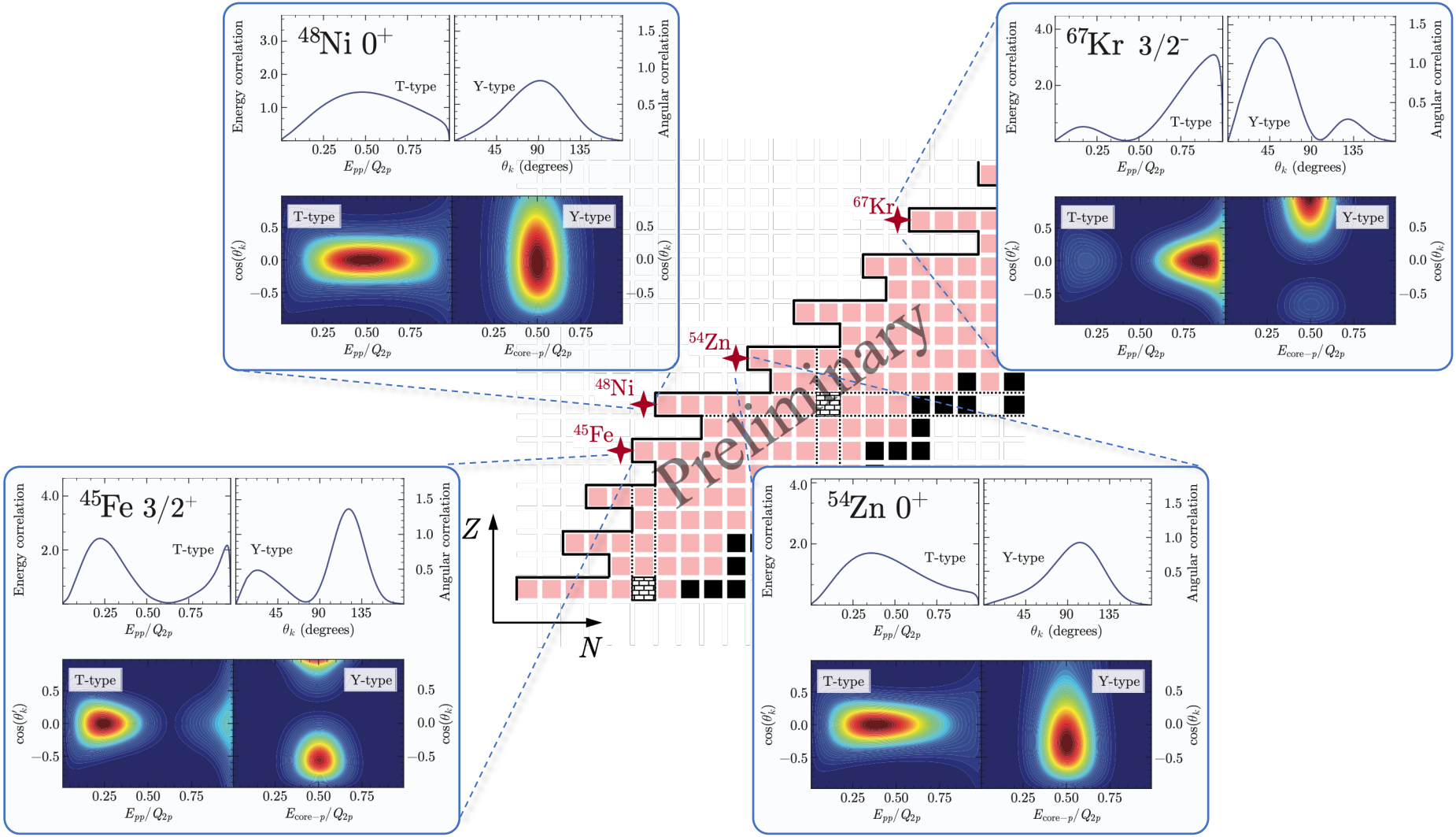
Entanglement

SW *et al.*, Phys. Rev. Res. 5, 023183 (2023)



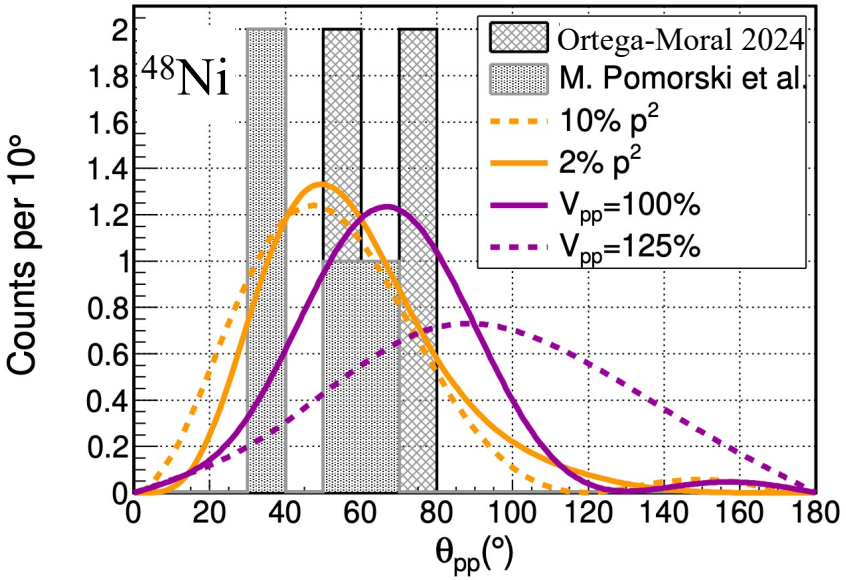
Non-exp decay

Correlations in heavy-mass nuclei



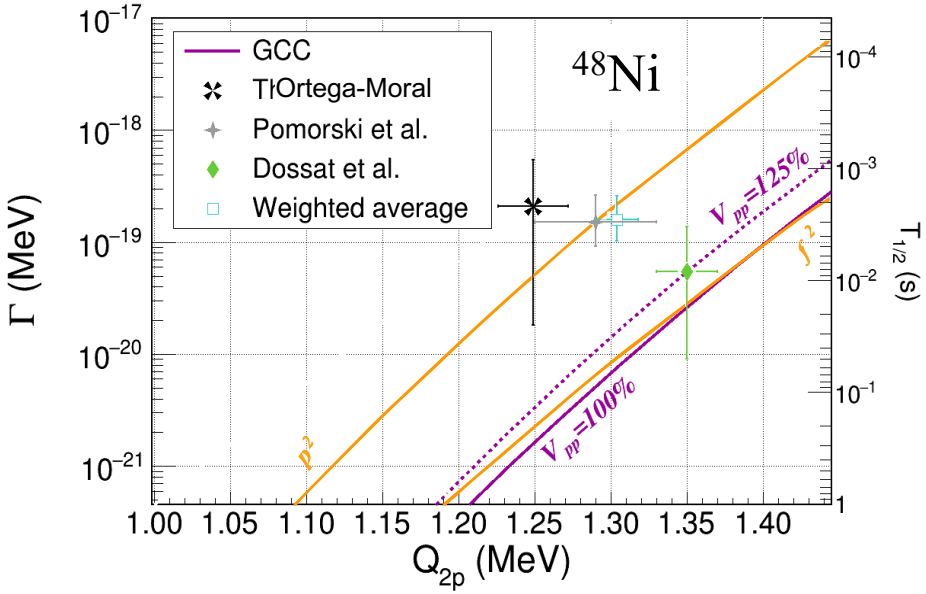
Asymptotic correlation of ^{45}Fe and ^{48}Ni

Angular correlation of ^{48}Ni



$f^2_{7/2}$	$p^2_{3/2}$	$p^2_{1/2}$	$f^2_{5/2}$	$s^2_{1/2}$
91.6%	4.7%	1.0%	1.0%	0.1%

Half-live of ^{48}Ni

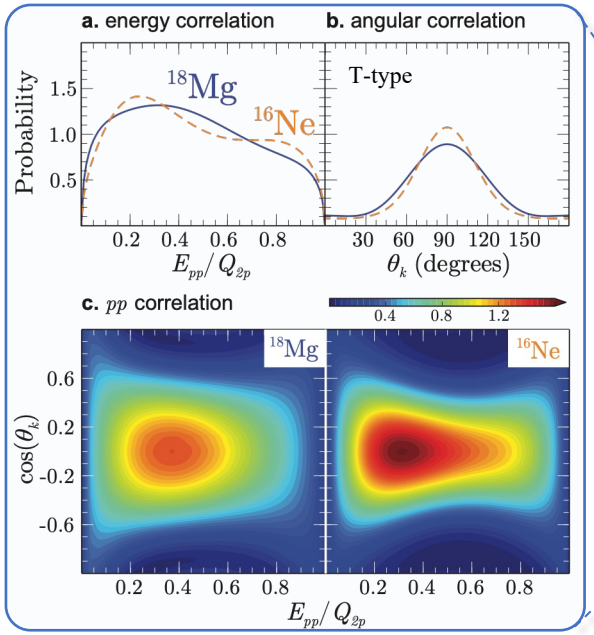


Q^{Exp}_{2p} (keV)		Q^{Cal}_{2p} (keV)		
Ortega-Moral	Pomorski	Brown	Ormand	Cole
1249(23)	1290(40)	1360(130)	1290(330)	1350(60)

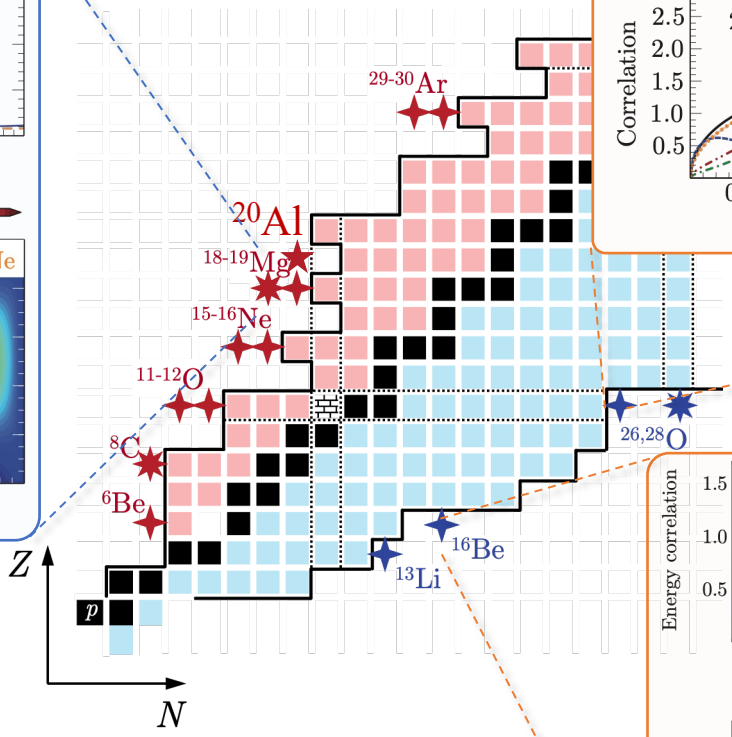
- Closed shell behavior for ^{48}Ni?
- Discrepancy between correlations and half-lives.

A. O. Moral, SW *et al.*, Phys. Rev. C 112, L061302 (2025)

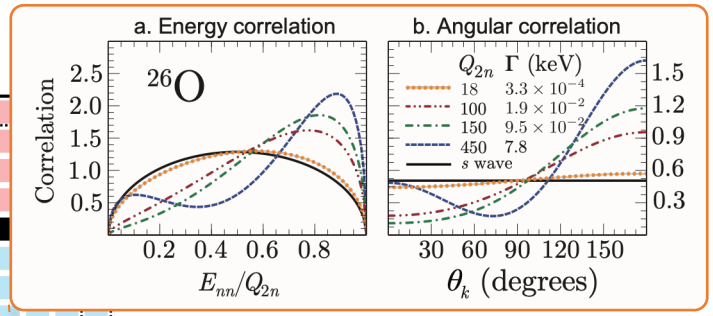
Correlations in light-mass nuclei



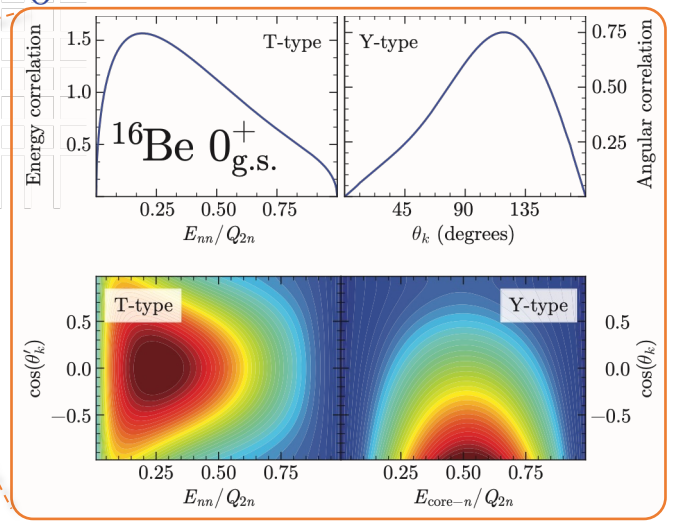
L. Zhou, SW *et al.*,
Nucl. Sci. Tech. 35, 107 (2024)



SW *et al.*, J. Phys. G 49, 10LT02 (2022)



Y. R. Lin in preparation



B. Monteagudo *et al.*, Phys. Rev. Lett. 132, 082501(2024)

- 4*p* (2*p*+2*p*) decay of ^{18}Mg.
- Multi-proton emissions.
- Correlation changes when $Q \rightarrow 0$.

2*n*/4*n* decay candidate ^{26}O/ ^{28}O

^{26}O:

$Q_{2n} = 150^{+50}_{-150}$ keV — E. Lunderberg *et al.*, PRL 108, 142503 (2012)

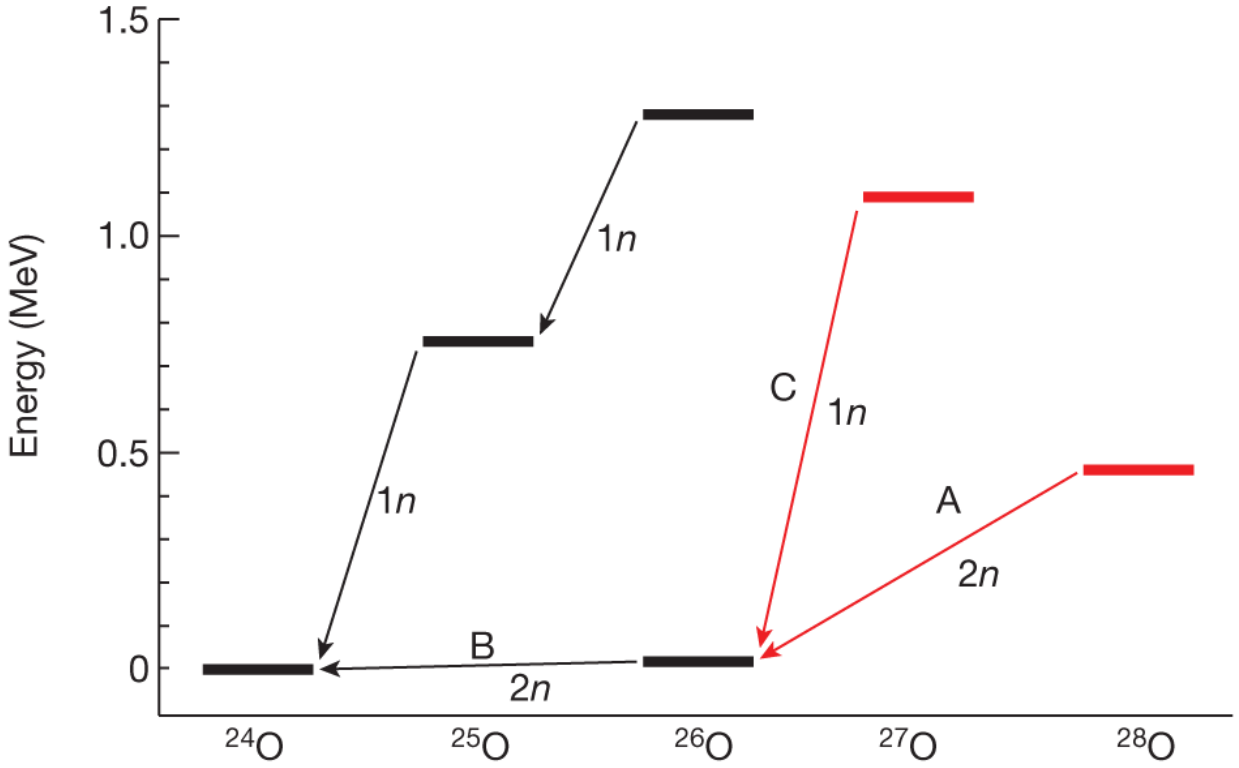
< 53 keV — Z. Kohley *et al.*, PRL 91, 034323 (2015)

$= 18 \pm 7$ keV — Y. Kondo *et al.*, PRL 116, 102503 (2016)

^{28}O:

$Q_{4n} = 0.46^{+0.05}_{-0.04}(\text{stat}) \pm 0,02(\text{syst})$ MeV

Y. Kondo *et al.*, Nature 620, 965 (2023)



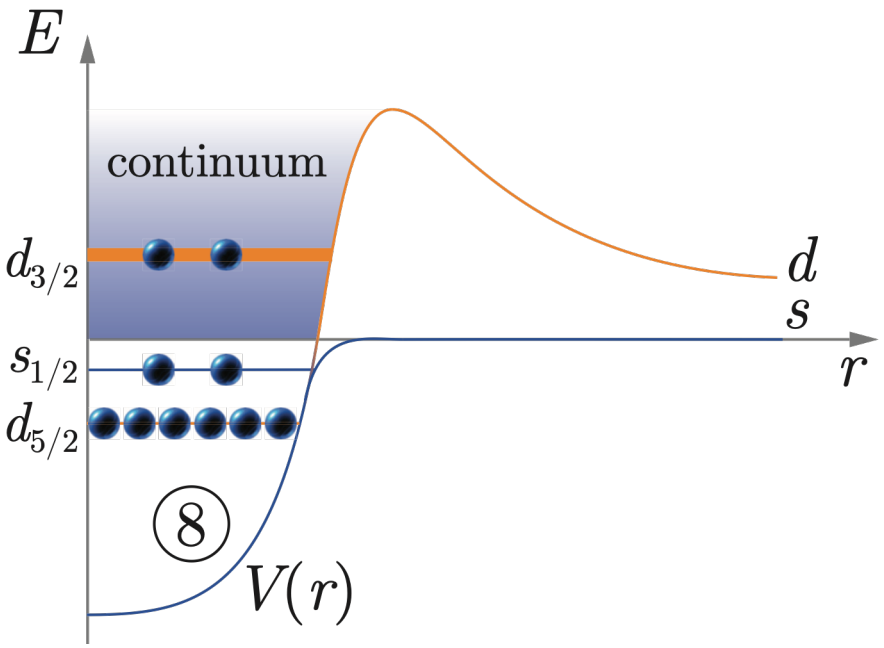
Inner structure of ^{26,28}O

- Threshold resonance:

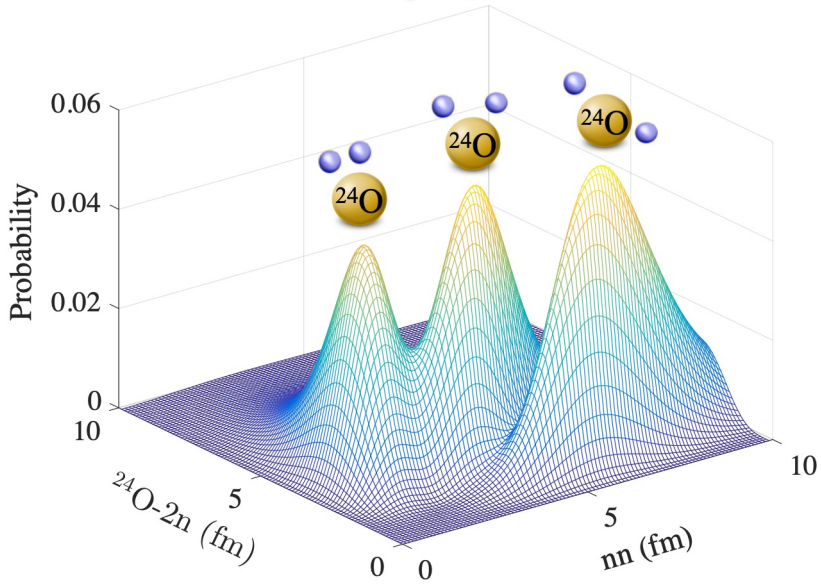
$Q_{2n} = 150^{+50}_{-150}$ keV — E. Lunderberg *et al.*, PRL 108, 142503 (2012)

< 53 keV — Z. Kohley *et al.*, PRL 91, 034323 (2015)

$= 18 \pm 7$ keV — Y. Kondo *et al.*, PRL 116, 102503 (2016)



Calculated density distribution of ^{26}O



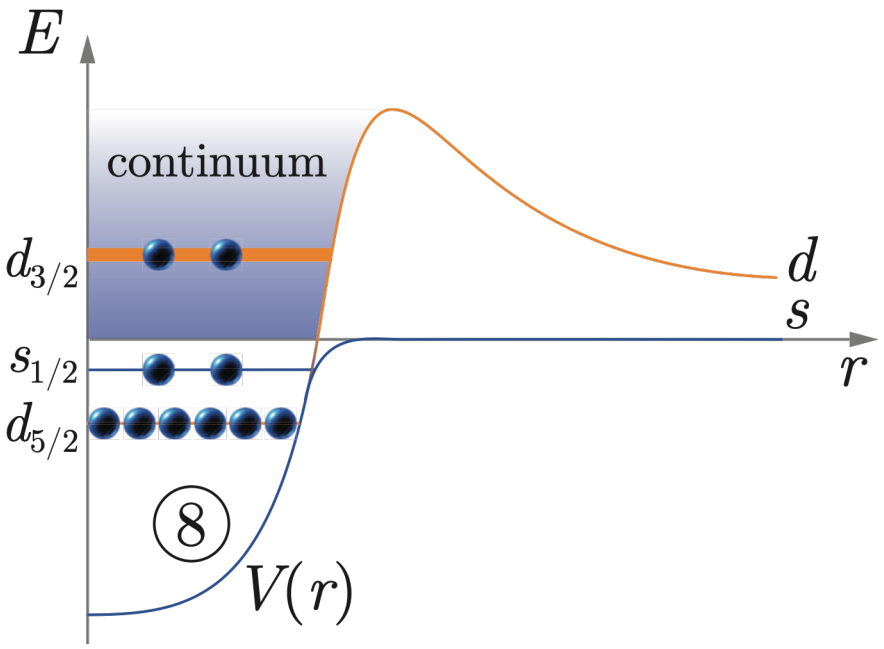
Decay dynamics of ^{26}O

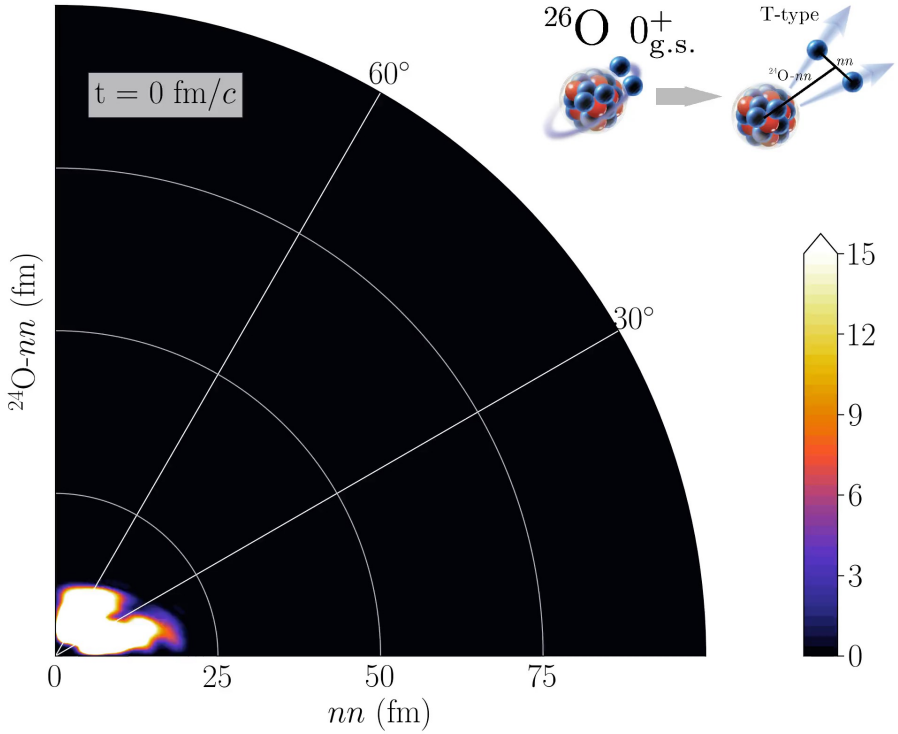
- Threshold resonance:

$Q_{2n} = 150^{+50}_{-150}$ keV — E. Lunderberg *et al.*, PRL 108, 142503 (2012)

< 53 keV — Z. Kohley *et al.*, PRL 91, 034323 (2015)

$= 18 \pm 7$ keV — Y. Kondo *et al.*, PRL 116, 102503 (2016)





Asymptotic correlations of ^{26}O

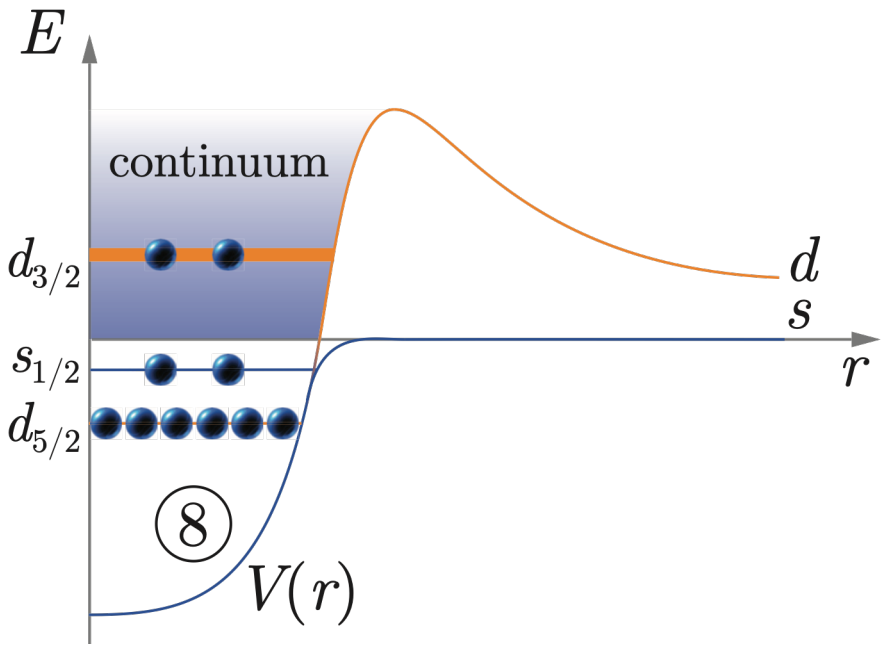
- Threshold resonance:

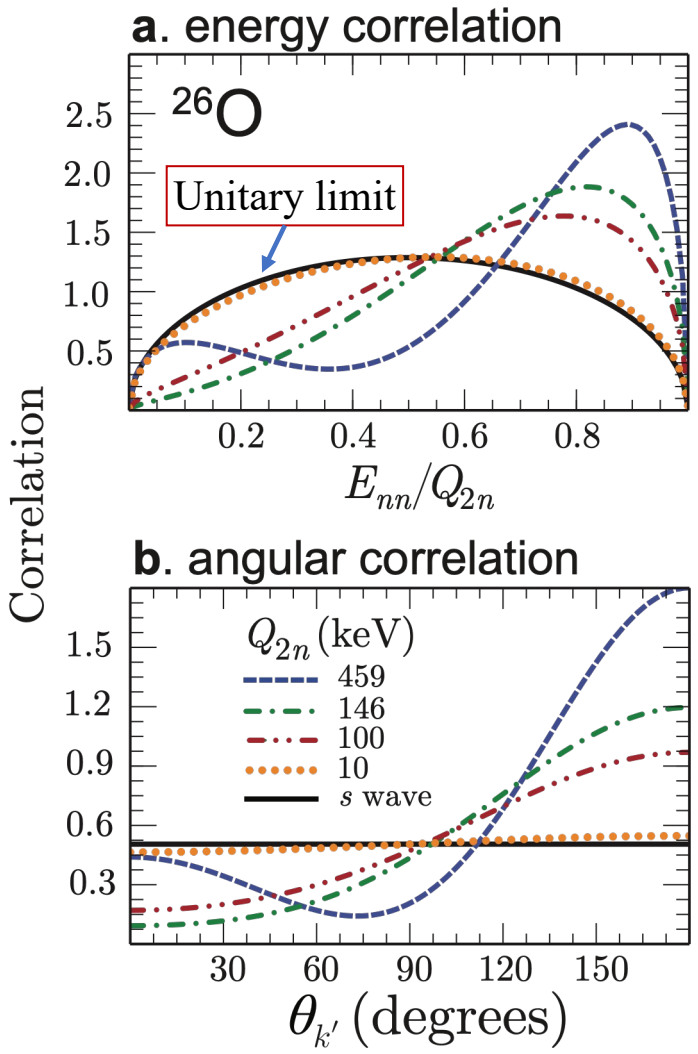
$Q_{2n} = 150^{+50}_{-150}$ keV — E. Lunderberg *et al.*, PRL 108, 142503 (2012)

< 53 keV — Z. Kohley *et al.*, PRL 91, 034323 (2015)

$= 18 \pm 7$ keV — Y. Kondo *et al.*, PRL 116, 102503 (2016)

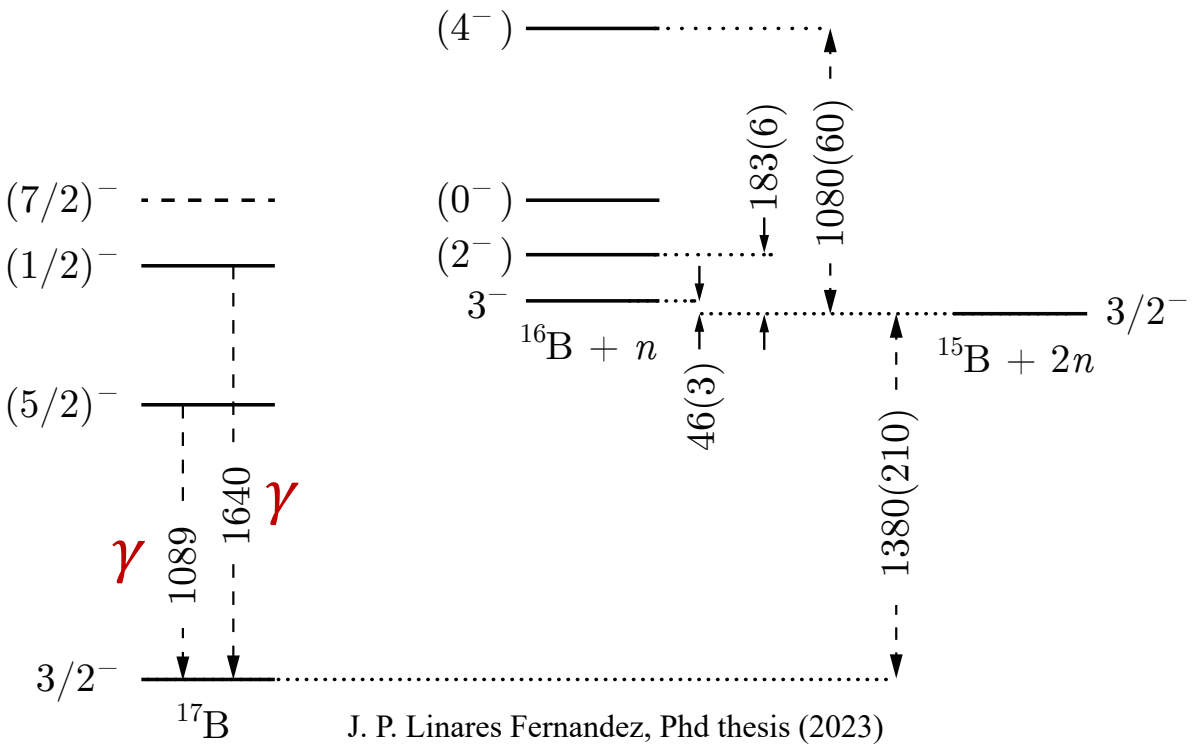
- *nn* correlations can be very different between ^{26}O and ^{28}O





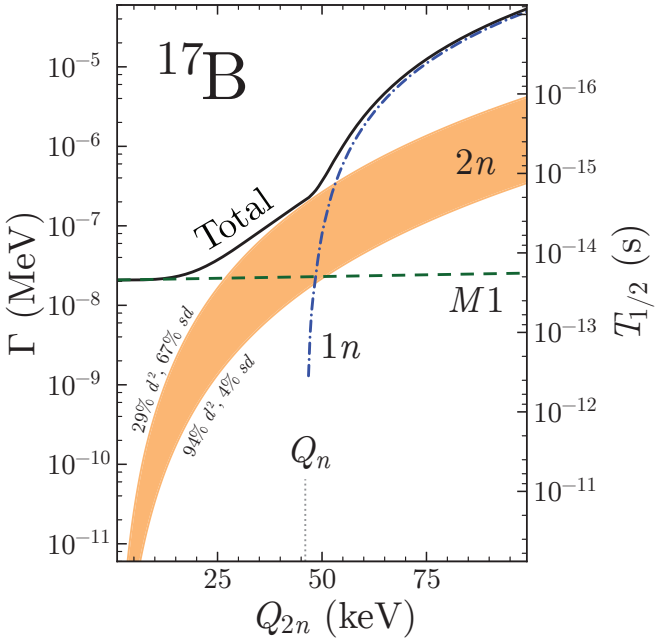
Exotic threshold resonance in ^{17}B

Spectra of ^{15,16,17}B



J. P. Linares Fernandez, Phd thesis (2023)
Z. H. Yang *et al.*, Phys. Rev. Lett. 126, 082501 (2021)

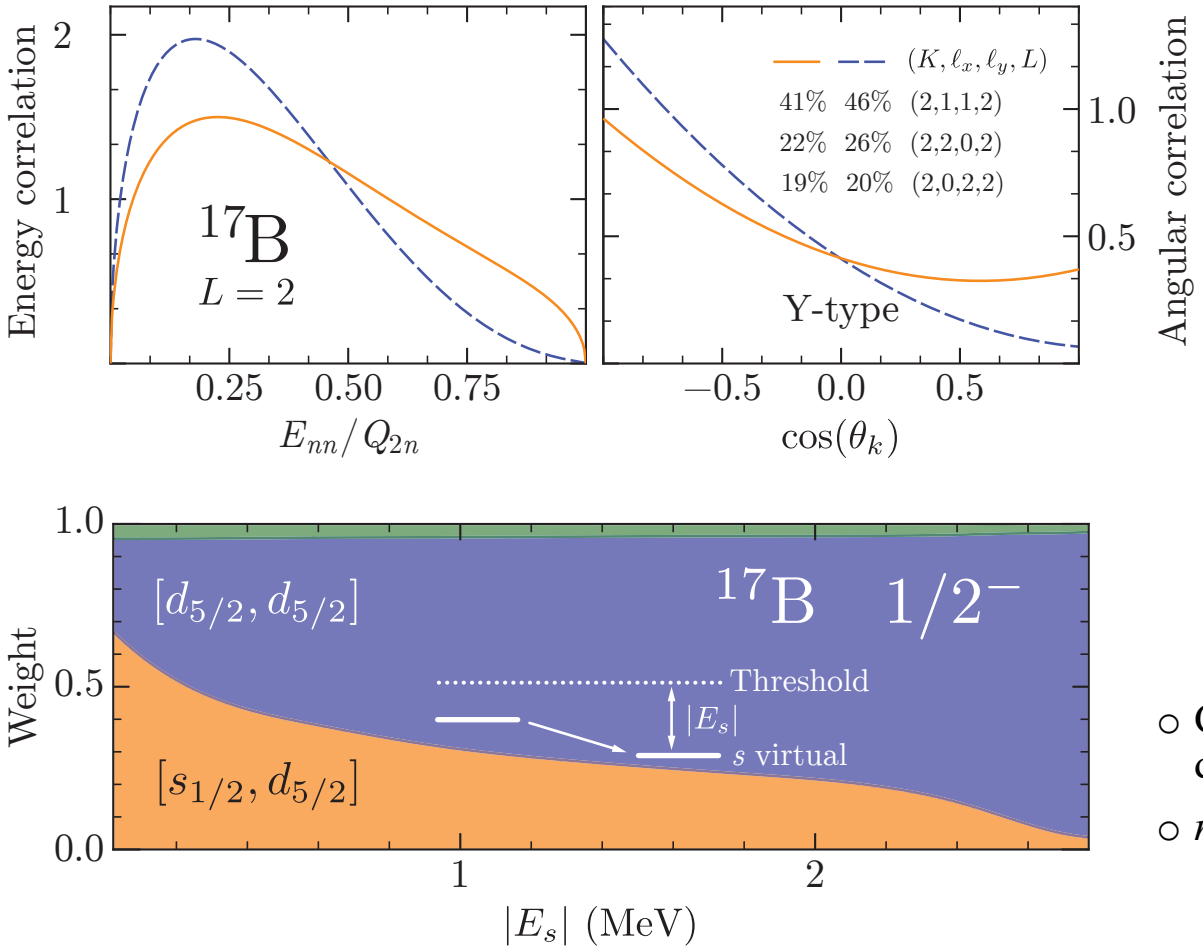
Partial decay widths

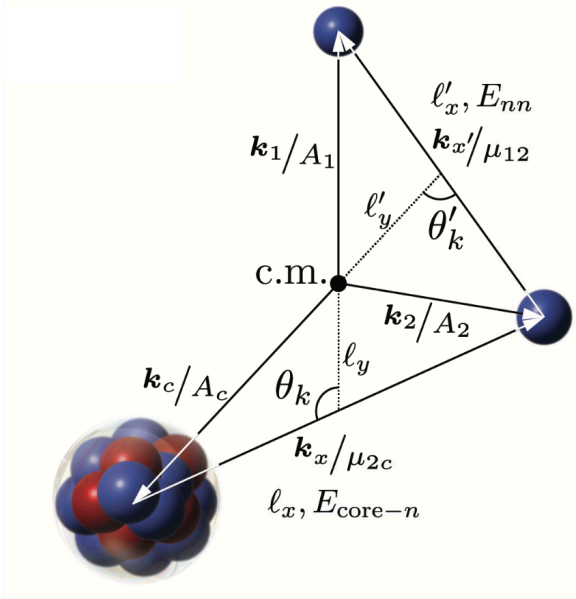


A. Volya, SW *et al.*, Phys. Rev. Res. 8, 013125 (2026)

- The excited states of ^{17}B have been observed, along with the γ decays.
- Through the branching analysis, this newly observed state is extremely close to the threshold.

$L = 2$ $2n$ decay



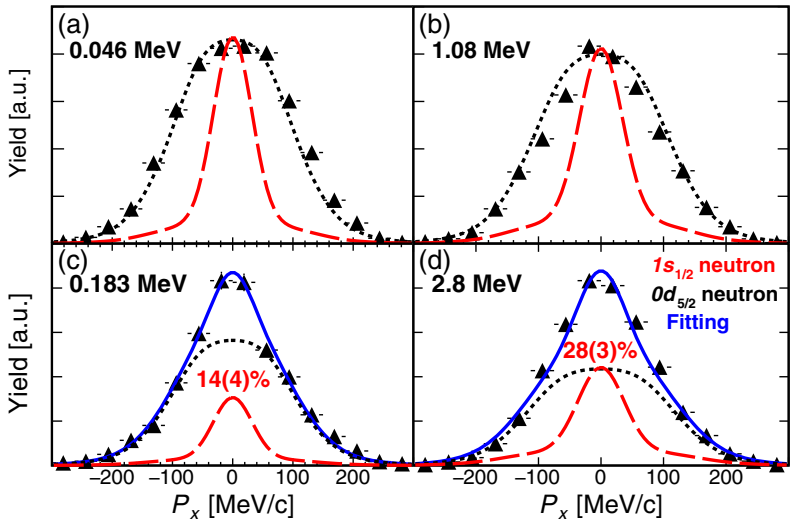


- Compared with $L = 0$ $2n$ decay, ^{17}B $2n$ decay has a different patten.
- *nn* correlation is sensitive to structure.

A. Volya, SW *et al.*, Phys. Rev. Res. Accepted (2025)

Spectroscopic factors of ^{17}B

Transverse momentum distributions for ^{16}B



Z. H. Yang *et al.*, Phys. Rev. Lett. 126, 082501 (2021)

- ^{17}B has large *s*-wave component.
- Knockout might not result in *s*-wave neutrons due the spectroscopic factor.

Spectroscopic factor

Block	ℓ	^{16}B intermediate state J^π 0^-	3^-	2^-	1^-	4^-
E_x (MeV)		1.48 0.29	0.00 0.00	0.14 0.38	2.75 1.72	1.03 1.27
$^{17}\mathrm{B} \to {}^{16}\mathrm{B}$	s	0.34 0.69	—	—	0.21 0.04	—
	d	—	0.11 0.33	0.31 0.47	0.03 0.00	—
$^{16}\mathrm{B} \to {}^{15}\mathrm{B}_{\mathrm{g.s.}}$	s	—	—	0.00 0.58	0.18 0.54	—
	d	0.08 0.08	0.42 0.53	0.60 0.40	0.51 0.27	0.74 0.74
$^{17}\mathrm{B}(p,pn)$	s	—	—	0.07 0.15	0.04 0.04	—
	d	0.01 0.02	0.86 0.75	0.60 0.10	0.12 0.04	0.68 0.51
$^{17}\mathrm{C}(p,2p)$	p	0.22 0.95	0.76 0.40	0.28 0.02	0.37 0.31	—

Continuum

Spectroscopic factor

A. Volya, SW *et al.*, Phys. Rev. Res. 8, 013125 (2026)

Thank you for your attention!

Summary

- Continuum effects in open quantum systems
  - Complex radius
  - Electromagnetic transitions
  - $2p/2n$ decay
- Nucleon-nucleon correlations
  - Connection to nuclear inner structure
  - Ability to reveal $2p/2n$ decay mechanism

Acknowledgements

- F. R. Xu
- N. Michel
- I. Mukha
- L. G. Sobotka
- W. Nazarewicz
- M. Pfützner
- R. J. Charity
- A. Volya
- …



Thank you for your attention!

Questions

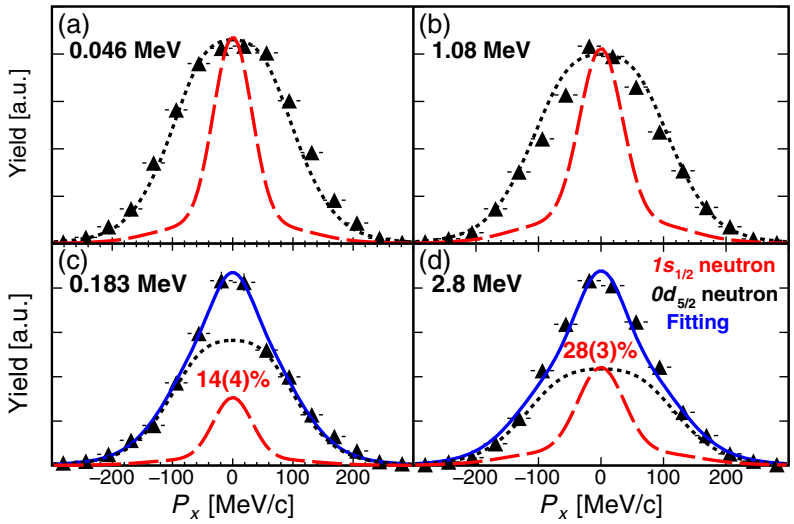
1. What's the difference between $2p$ and $2n$ decay?
2. Difference between complex scaling and Berggren basis?
3. Correlations evolutions during the decay process
4. Any simultaneous multi-particle emissions?
5. Does decay dynamics depends on the production?
6. Entanglement evolution during the decay



Backup

Spectroscopic factors of ^{17}B

Transverse momentum distributions for ^{16}B



Z. H. Yang *et al.*, Phys. Rev. Lett. 126, 082501 (2021)

- ^{17}B has large *s*-wave component.
- Knockout might not result in *s*-wave neutrons due the spectroscopic factor.

Spectroscopic factor

Block	ℓ	^{16}B intermediate state J^π 0^-	3^-	2^-	1^-	4^-
E_x (MeV)		1.48	0.00	0.14	2.75	1.03 ← Continuum
		0.29	0.00	0.38	1.72	1.27
$^{17}\mathrm{B} \to {}^{16}\mathrm{B}$	s	0.34	—	—	0.21	—
		0.69			0.04	
	d	—	0.11	0.31	0.03	—
			0.33	0.47	0.00	
$^{16}\mathrm{B} \to {}^{15}\mathrm{B}_{\mathrm{g.s.}}$	s	—	—	0.00	0.18	—
				0.58	0.54	
	d	0.08	0.42	0.60	0.51	0.74
		0.08	0.53	0.40	0.27	0.74
$^{17}\mathrm{B}(p,pn)$	s	—	—	0.07	0.04	—
				0.15	0.04	
	d	0.01	0.86	0.60	0.12	0.68
		0.02	0.75	0.10	0.04	0.51
$^{17}\mathrm{C}(p,2p)$	p	0.22	0.76	0.28	0.37	—
		0.95	0.40	0.02	0.31	

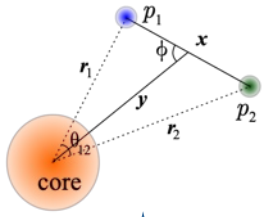
Spectroscopic factor

A. Volya, SW *et al.*, Phys. Rev. Res. Accepted (2025)

Summary: selected progresses in multi-*p* decay

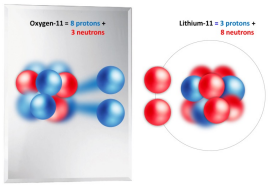
GCC model

SW, Michel, Nazarewicz *et al.*
PRC 122, 122501 (2017)



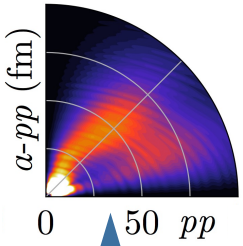
2*p* emitter ^{11}O

Webb, SW, Brown *et al.*
PRL 122, 122501 (2019)



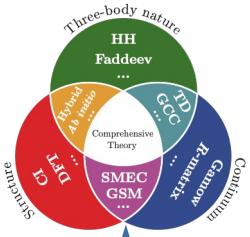
2*p* dynamics

SW and Nazarewicz
PRL 126, 142501 (2021)



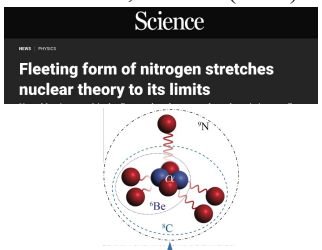
2*p* Review

Pfützner, Mukha, SW *et al.*
PPNP 132, 104050 (2023)



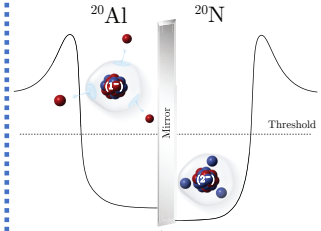
5*p* emitter ^{9}N

Charity, Wylie, SW *et al.*
PRL 131, 172501 (2023)

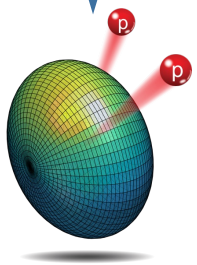


3*p* emitter ^{20}Al

Xu, Mukha, Li, SW *et al.*
PRL 135, 022502 (2025)

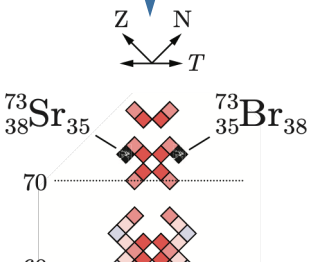


2017 2018 2019 2020 2021 2022 2023 2024 2025 2026



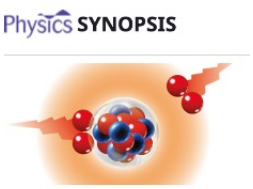
SW and Nazarewicz
PRL 120, 212502 (2018)

Deformed 2*p*



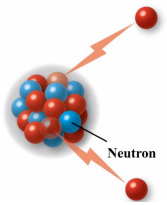
Hoff, Rogers, SW *et al.*
Nature 580, 52 (2020)

Mirror symmetry



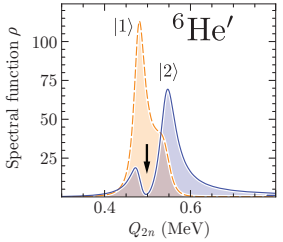
Jin, Niu, Brown, Li *et al.*
PRL 127, 262502 (2021)

4*p* emitter ^{18}Mg



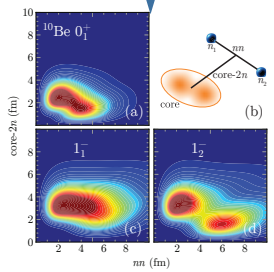
Liu, Xu, Sun, Yuan *et al.*
PRL 129, 242502 (2022)

β-delayed 2*p*



SW, Nazarewicz, Ma
PRR 5, 023183 (2023)

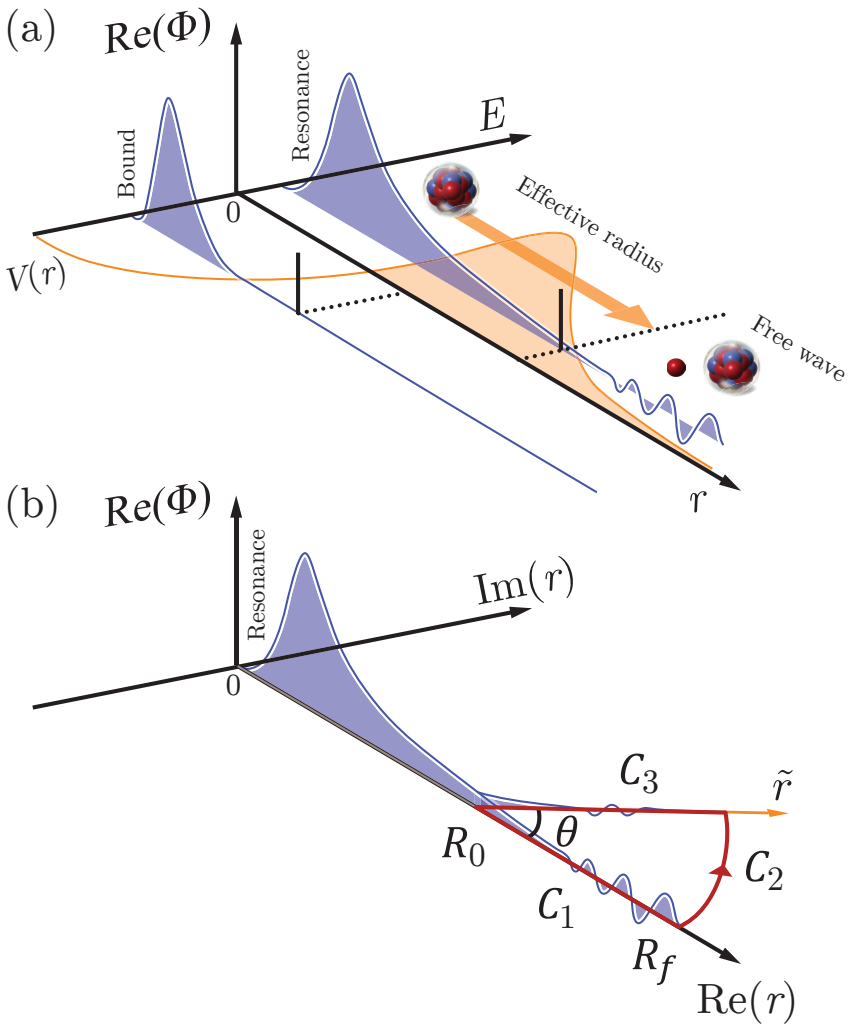
Non-exp decay

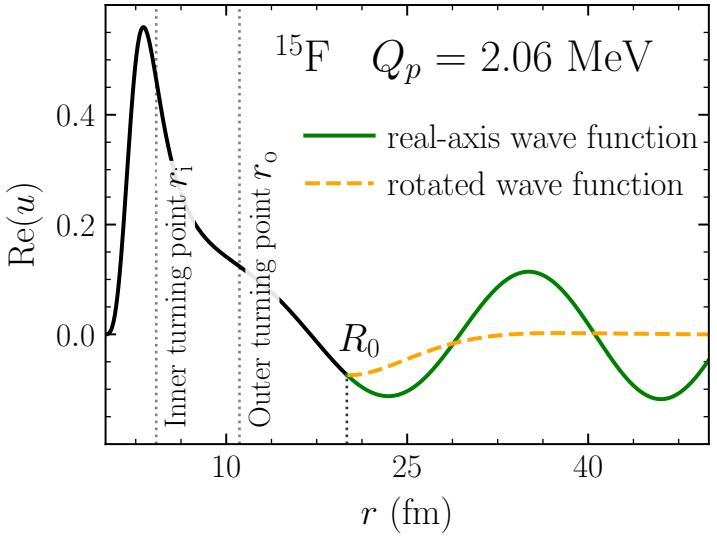


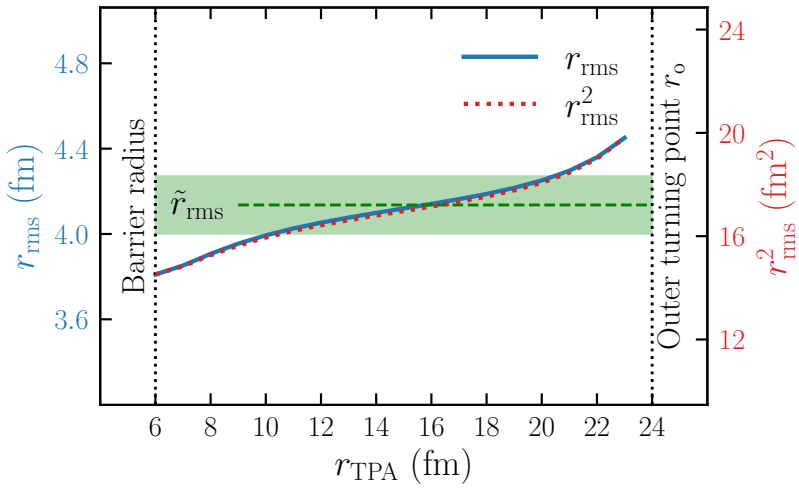
Chen, Ayyad, Bazin *et al.*
PRL 134, 012502 (2025)

Threshold 1$^-$

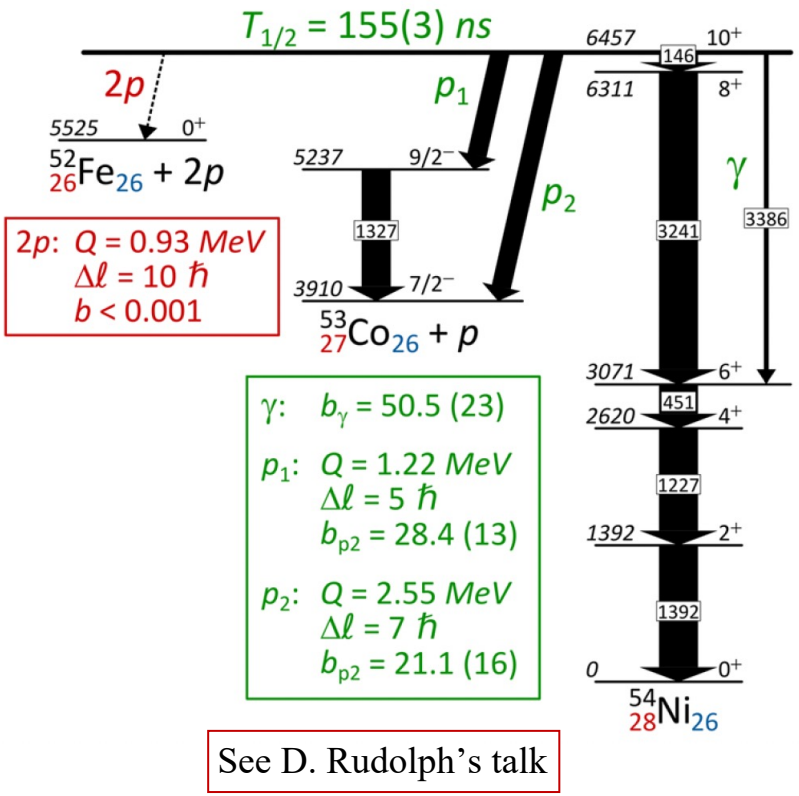
Complex radii of particle emitters





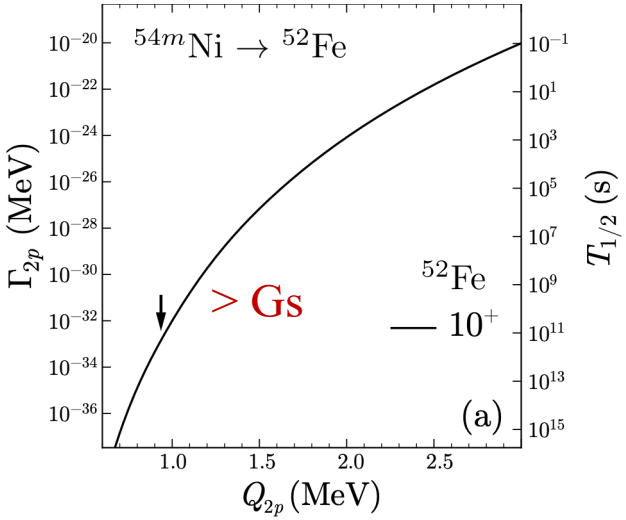


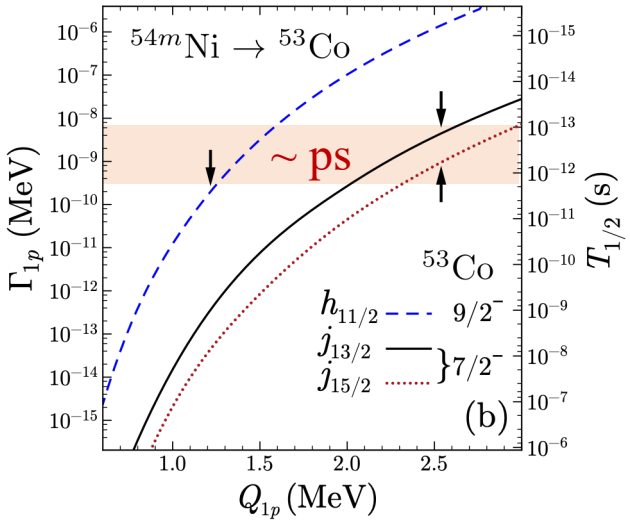
Decay property of ^{54m}Ni



See D. Rudolph's talk

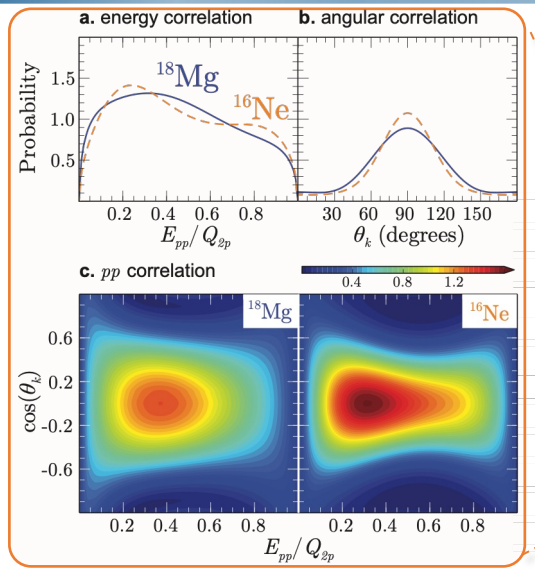
J. Giovinazzo *et al.*, Nat. Comm. 12, 4805 (2021)

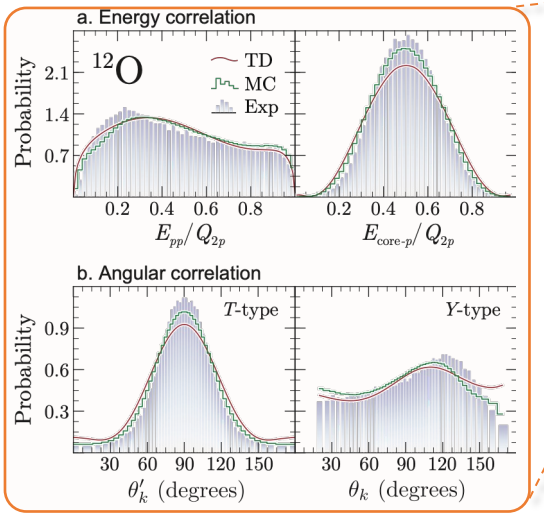


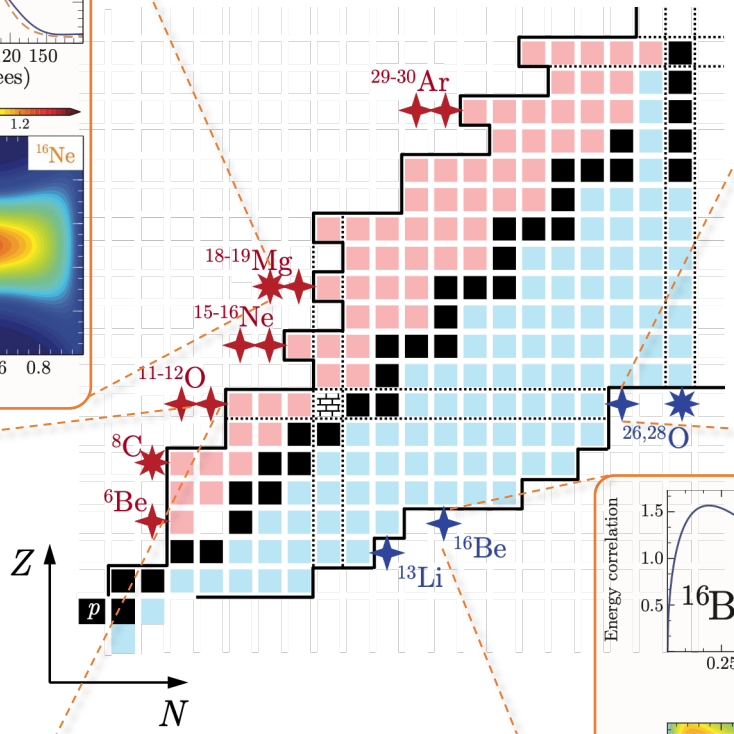


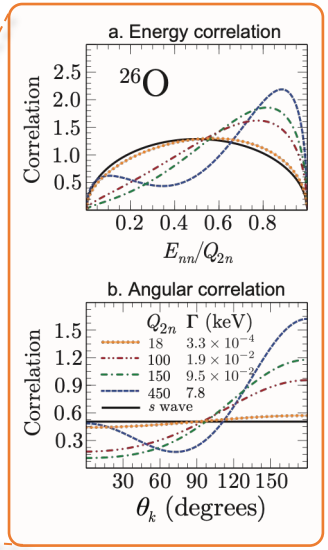
- Lifetime strongly depends on the decay energy and channels.
- Branching ratio is less than 10^{-21} for 2*p* decay.

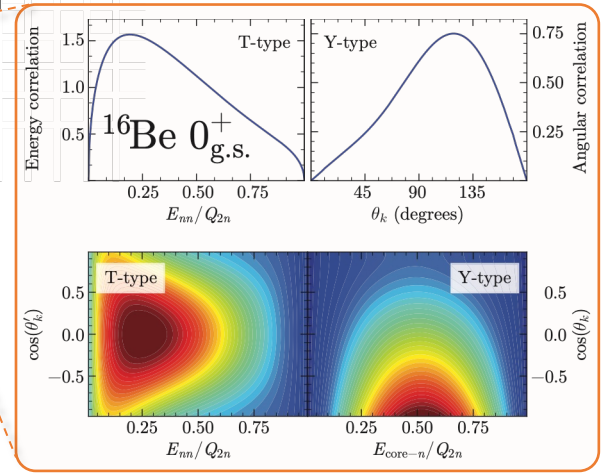
Correlations of light-mass nuclei



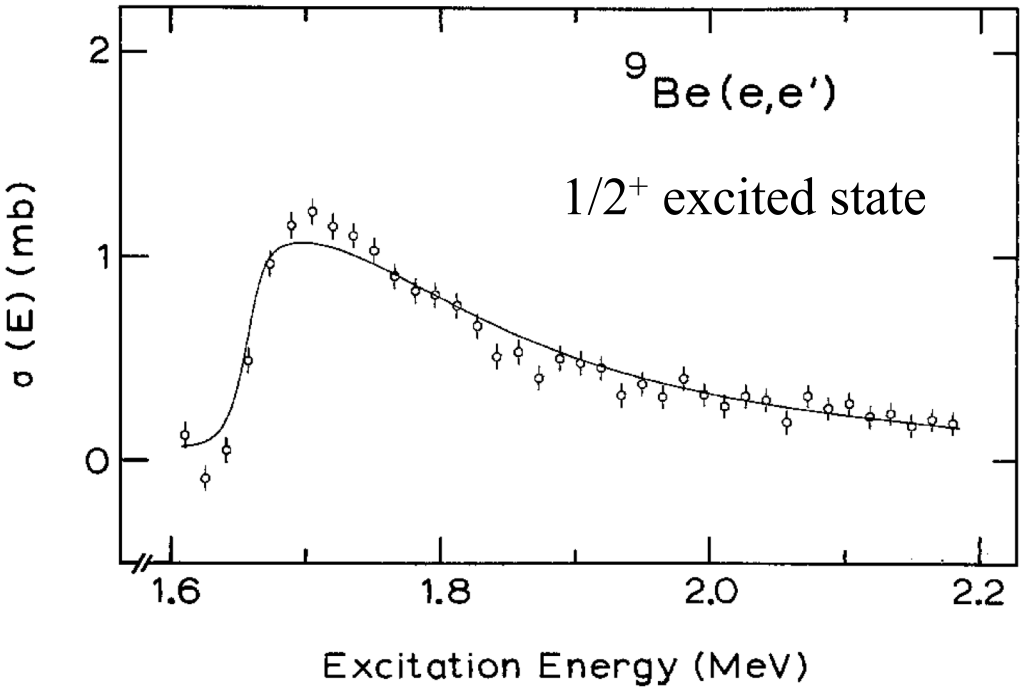




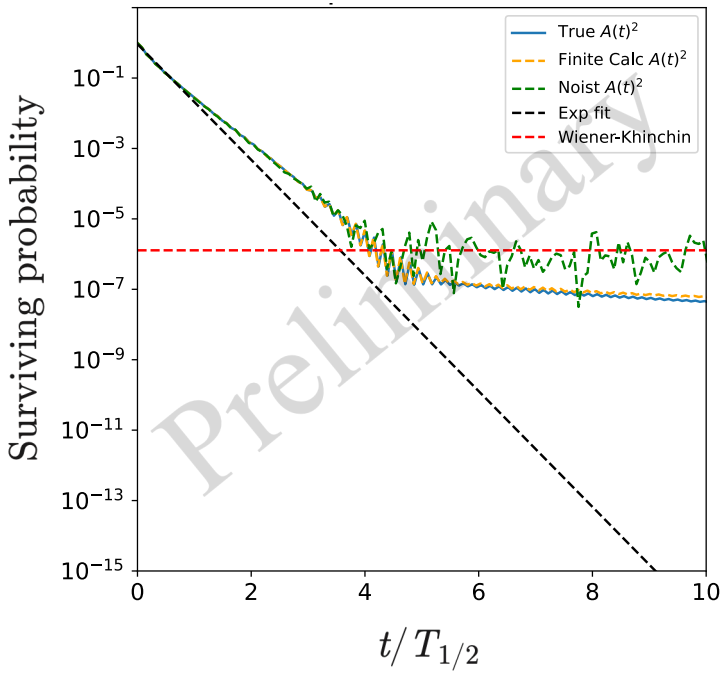




Experimental candidate

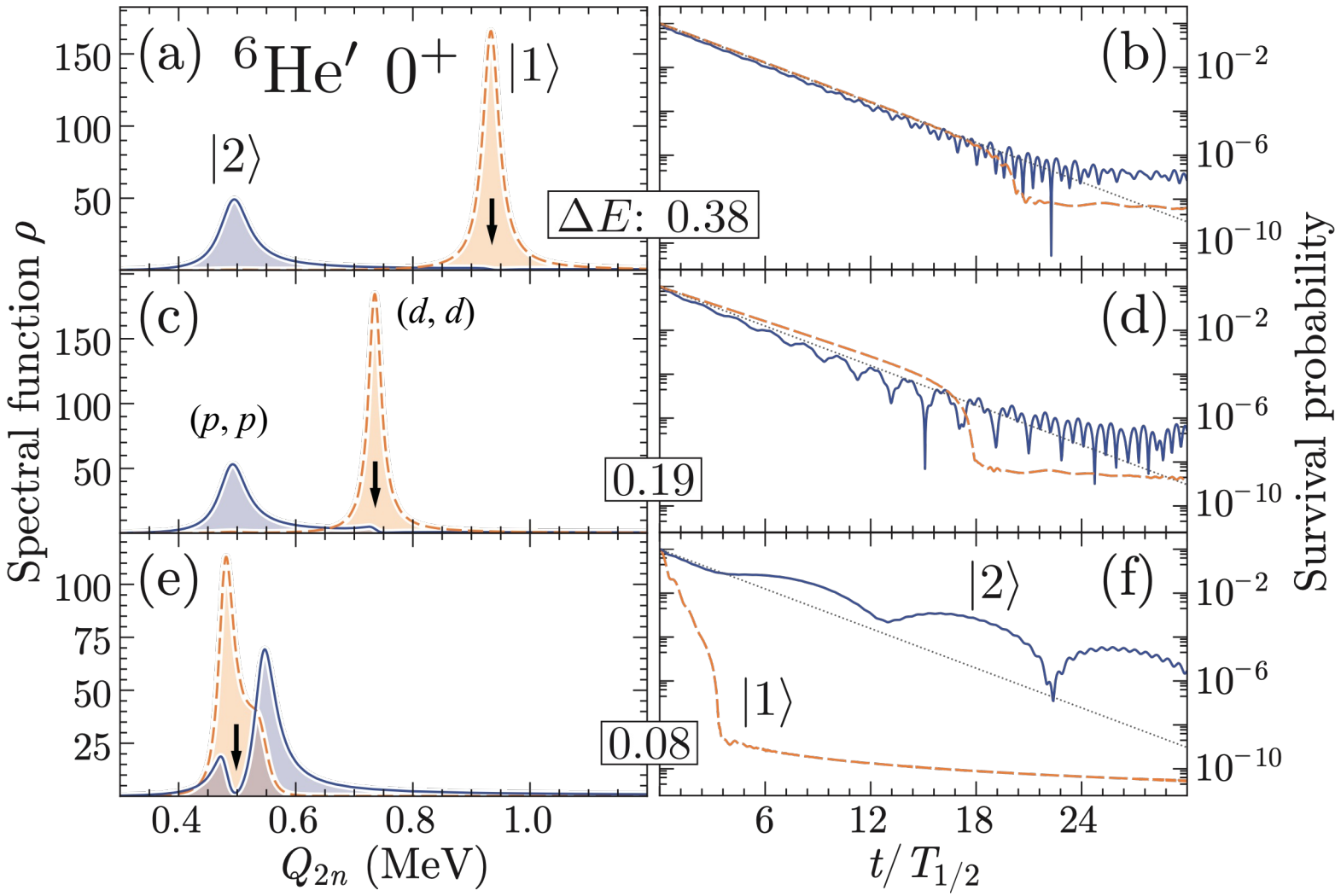


G. Kuechler *et al.*, Z. Phys. A 326, 447454 (1987)

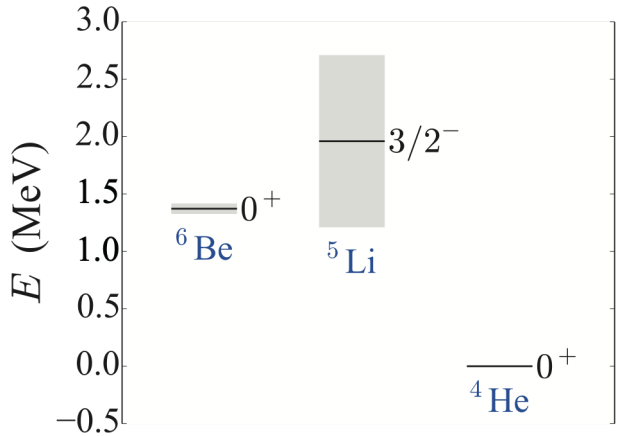


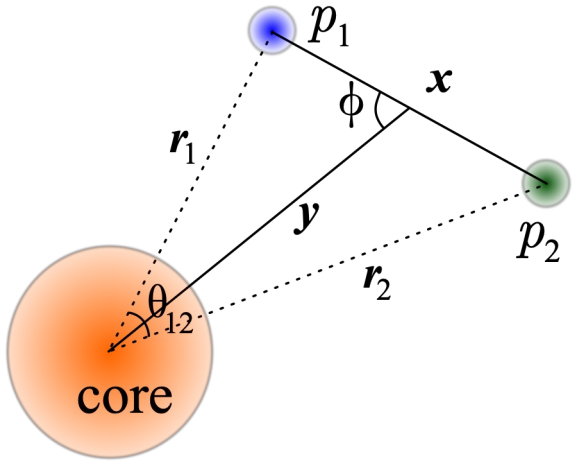
- Non-exponential decay can be studied through the asymmetric spectral function
- High resolution data are anticipated

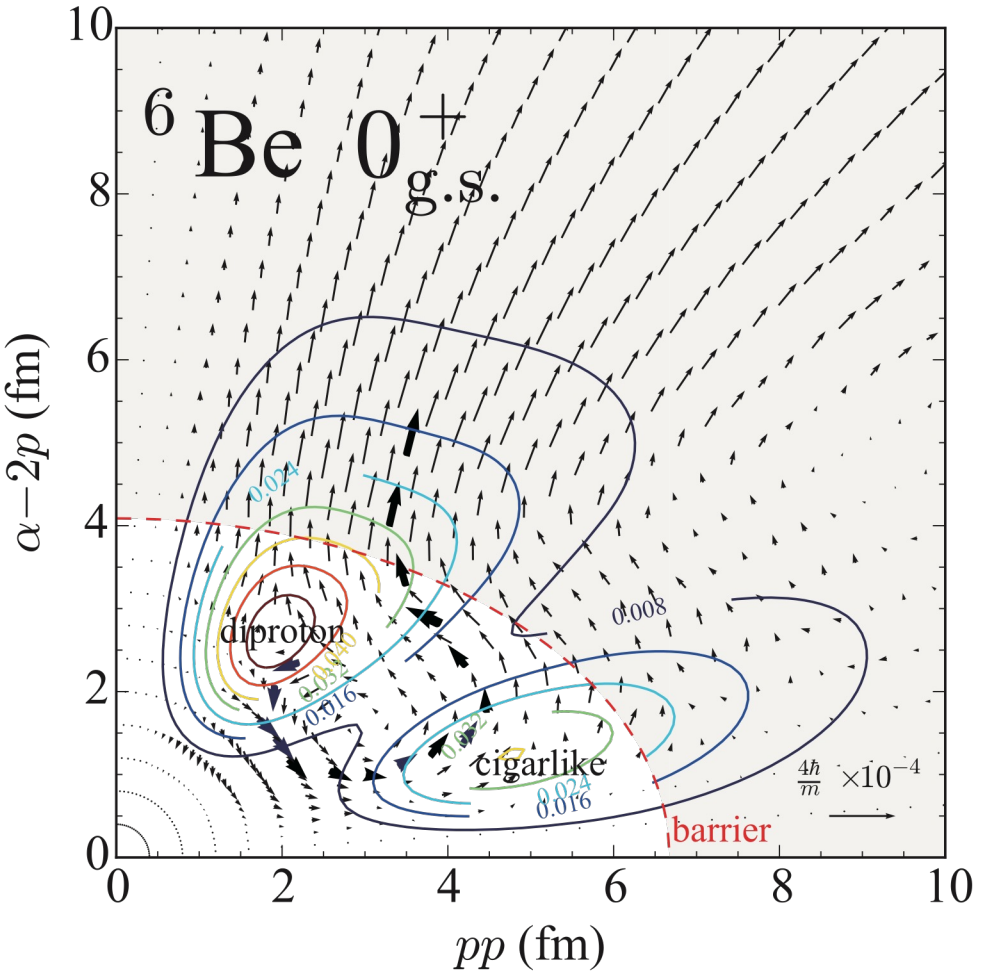
Near-lying resonances with the same spin



Ground-state of ^{6}Be



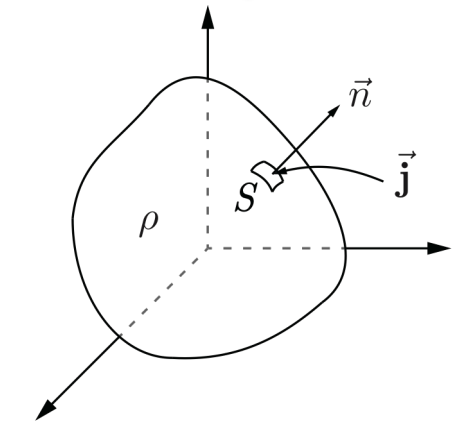




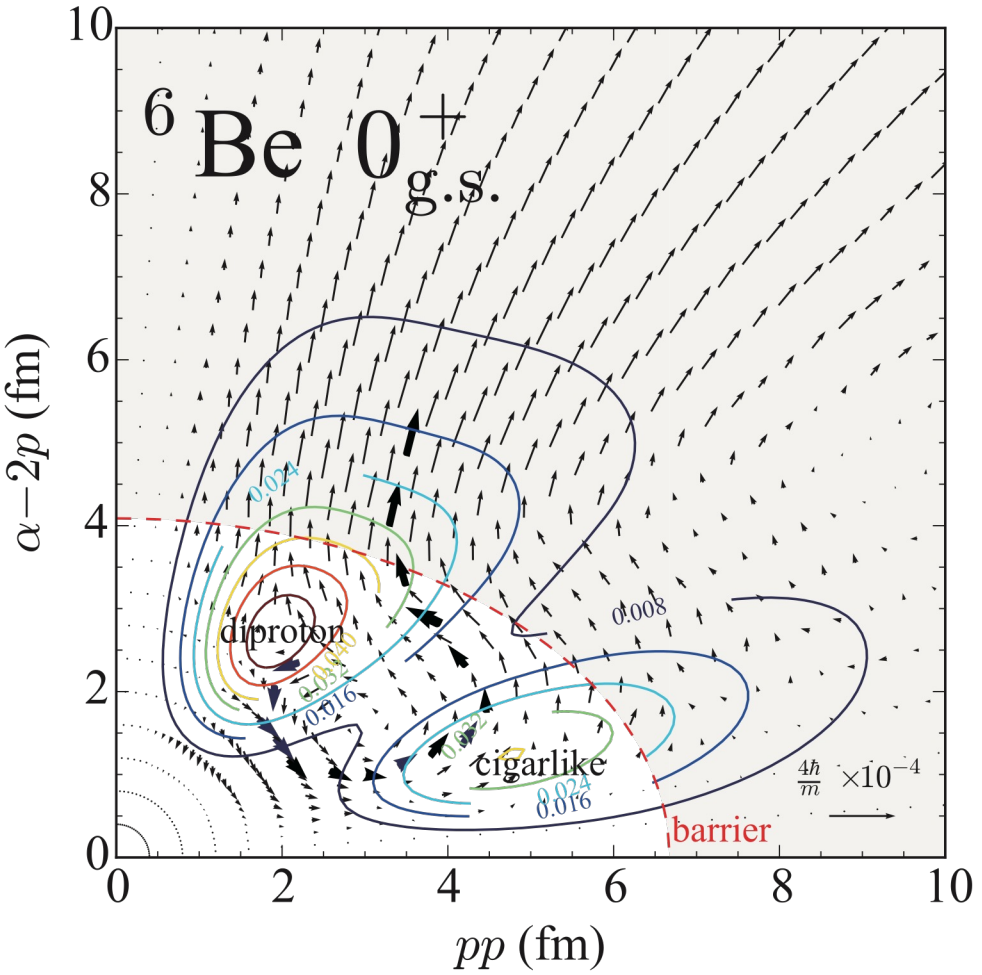
SW *et al.*, Phys. Rev. C 99, 054302 (2019)

Ground-state of ^{6}Be

Probability current

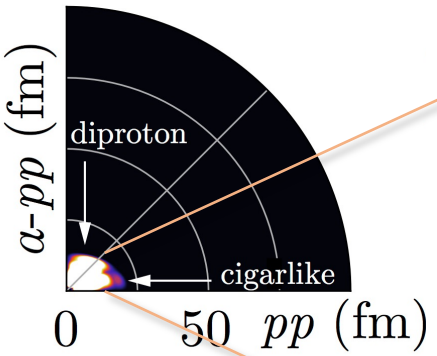


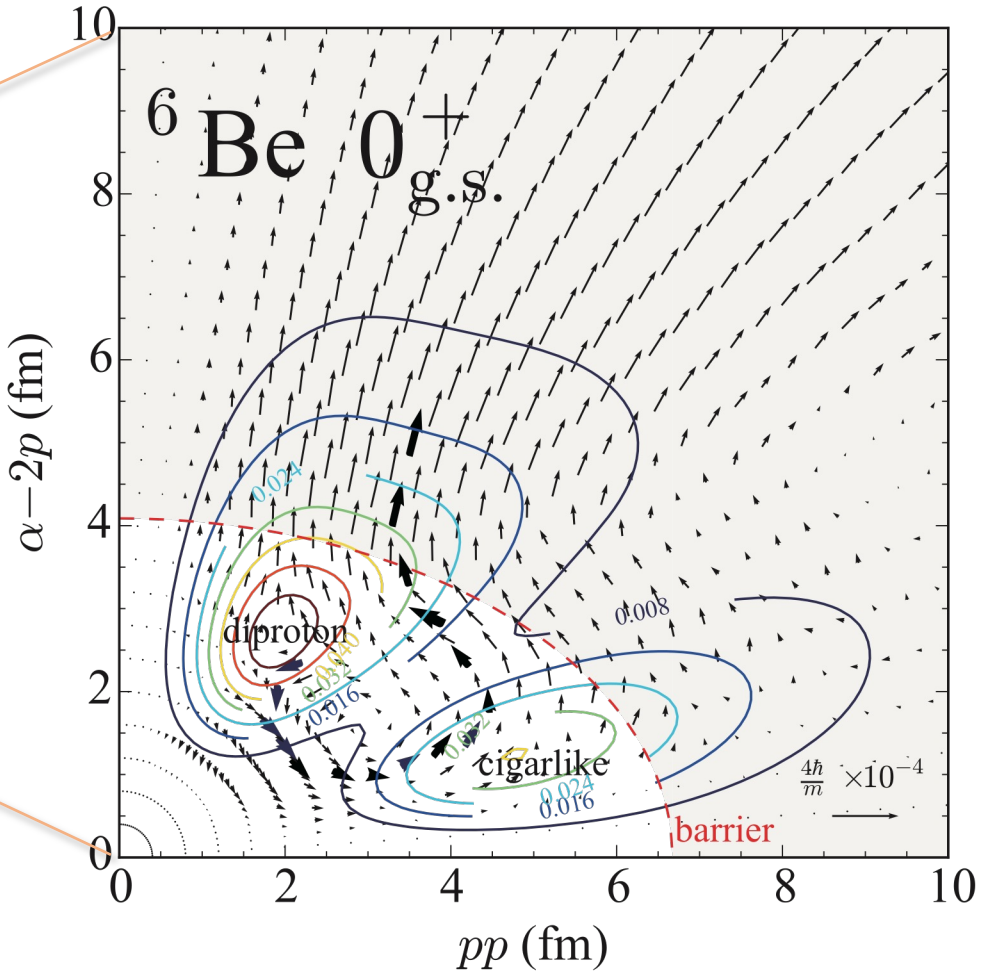
$$\iiint \frac{\partial \rho}{\partial t}\,\mathrm{d}V = -\oiint \vec{\mathbf{j}}\cdot\vec{n}\,\mathrm{d}S$$



SW *et al.*, Phys. Rev. C 99, 054302 (2019)

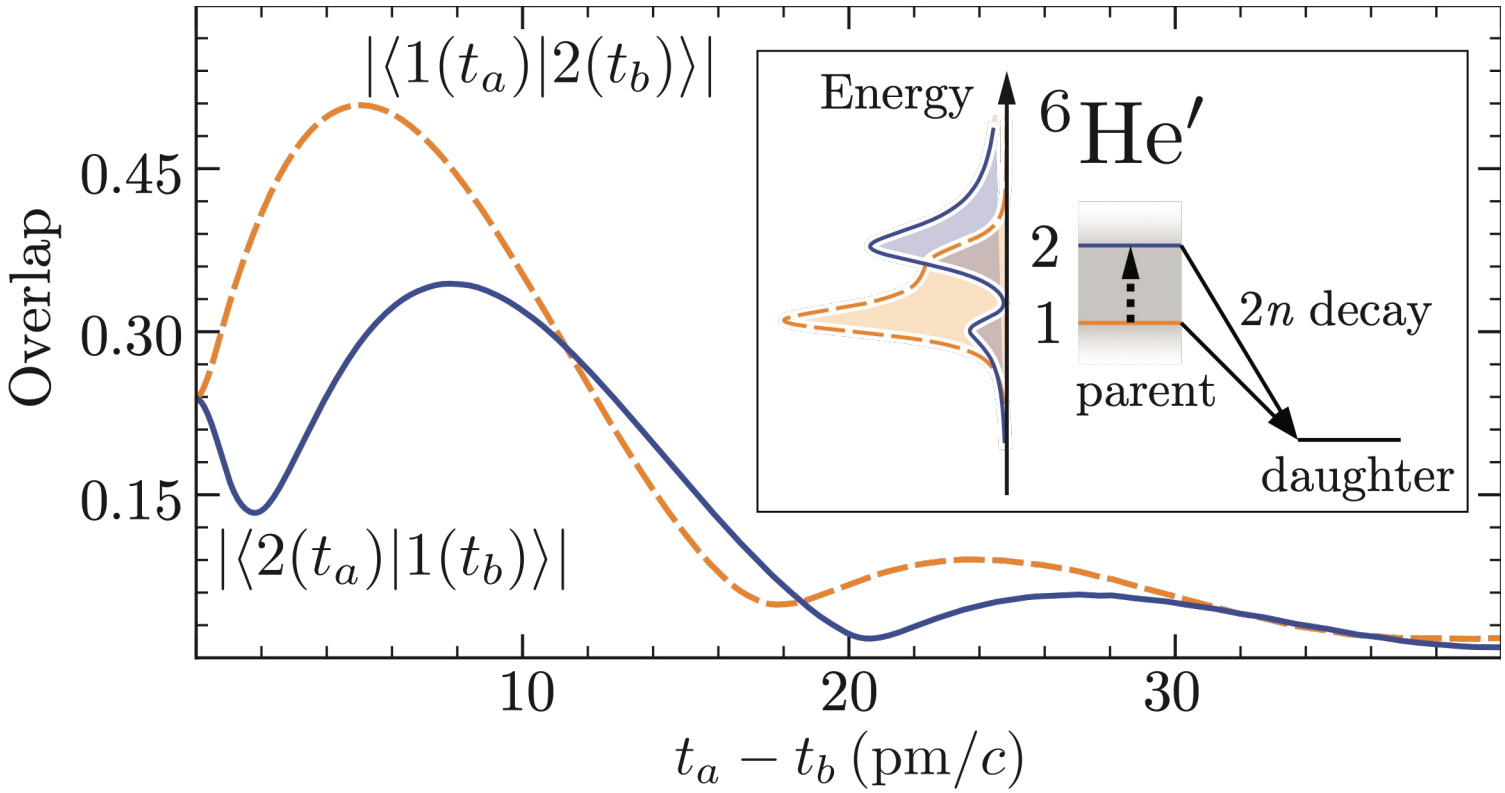
Ground-state of ^{6}Be





SW *et al.*, Phys. Rev. C 99, 054302 (2019)

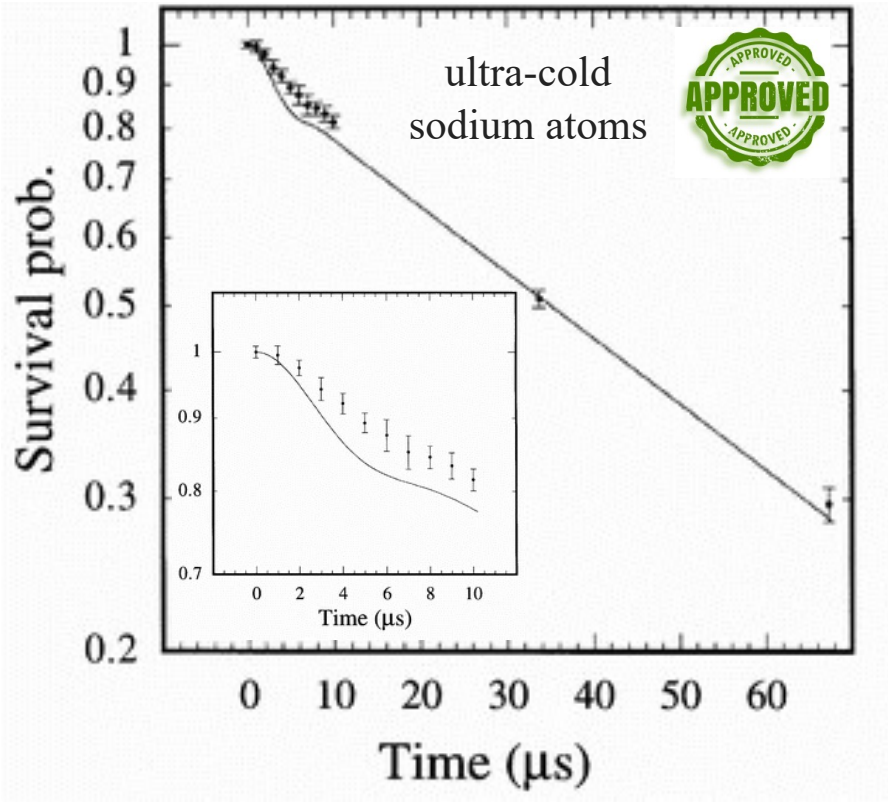
Virtual transition



SW, W. Nazarewicz, A. Volya, and Y.G. Ma, Phys. Rev. Res. 5, 023183 (2023)

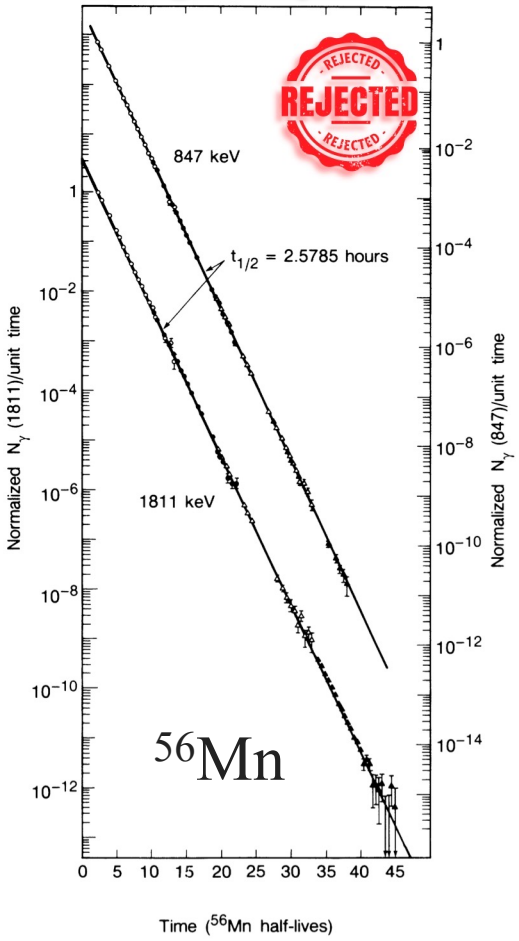
Probe non-exponential decay experimentally

Initial stage



S. R. Wilkinson *et al.*, Nature 387, 575 (1997)

Long-time period

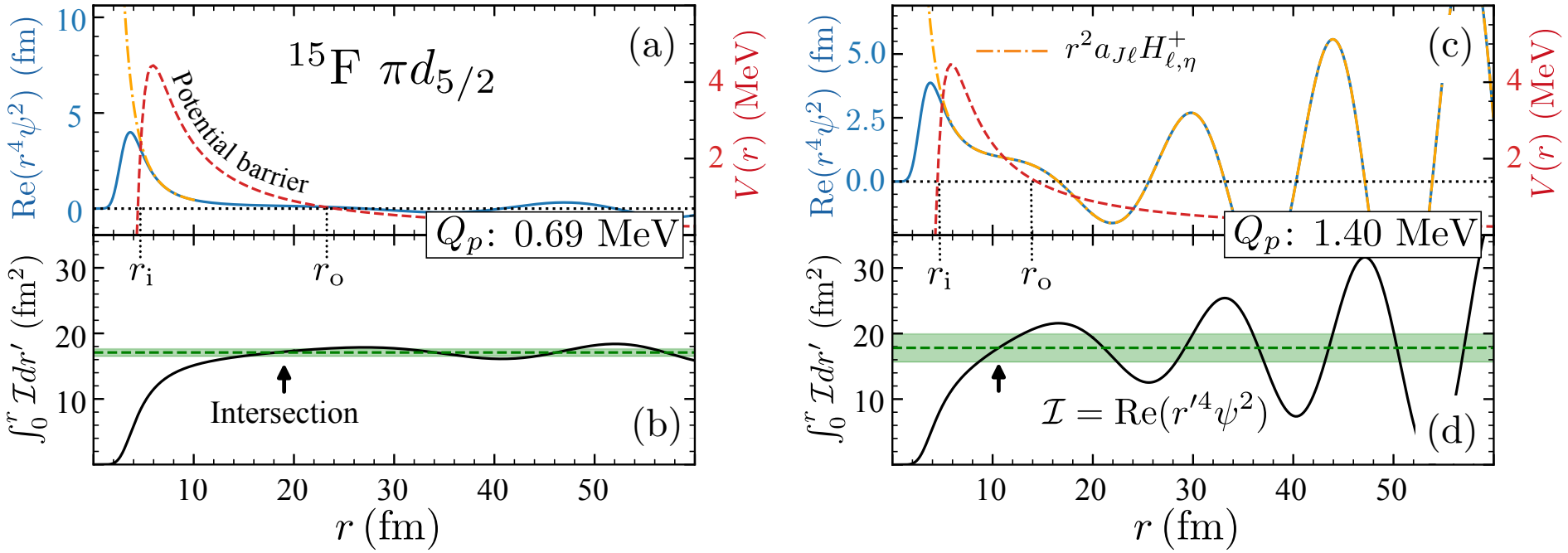


E. B. Norman *et al.*, Phys. Rev. Lett. 60, 2246 (1988)

The objective of this work is to offer experimentally accessible scenarios to probe post-exponential decay.

Complex radius of 1*p* emitter ^{15}F

Wavefunction & radius integrand at Q = 0.69, 1.40 MeV

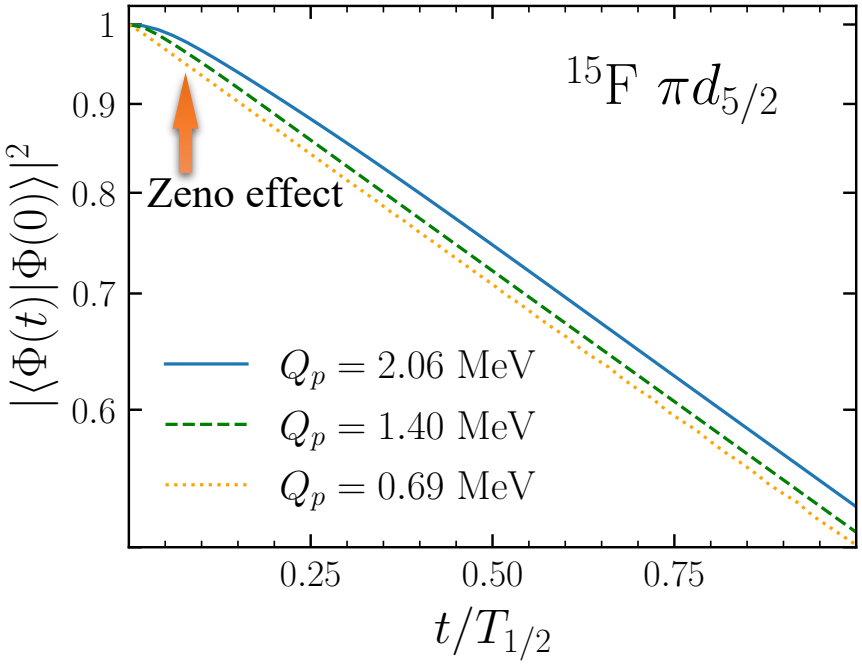


Y. R. Lin, SW *et al.*, Arxiv 2511.10238 (2025)

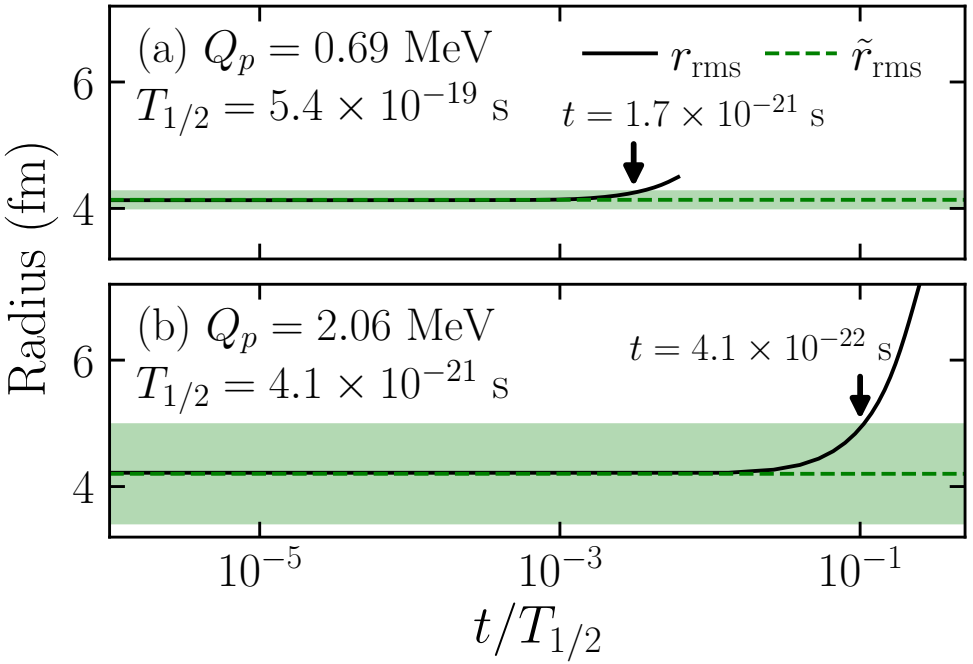
- The contribution to the complex radius from the asymptotic region is largely canceled out.
- The match point for the complex radius is located inside the barrier.

RMS radius evolution during the decay

Survival probability



Radius evolution at Q = 0.69, 2.06 MeV

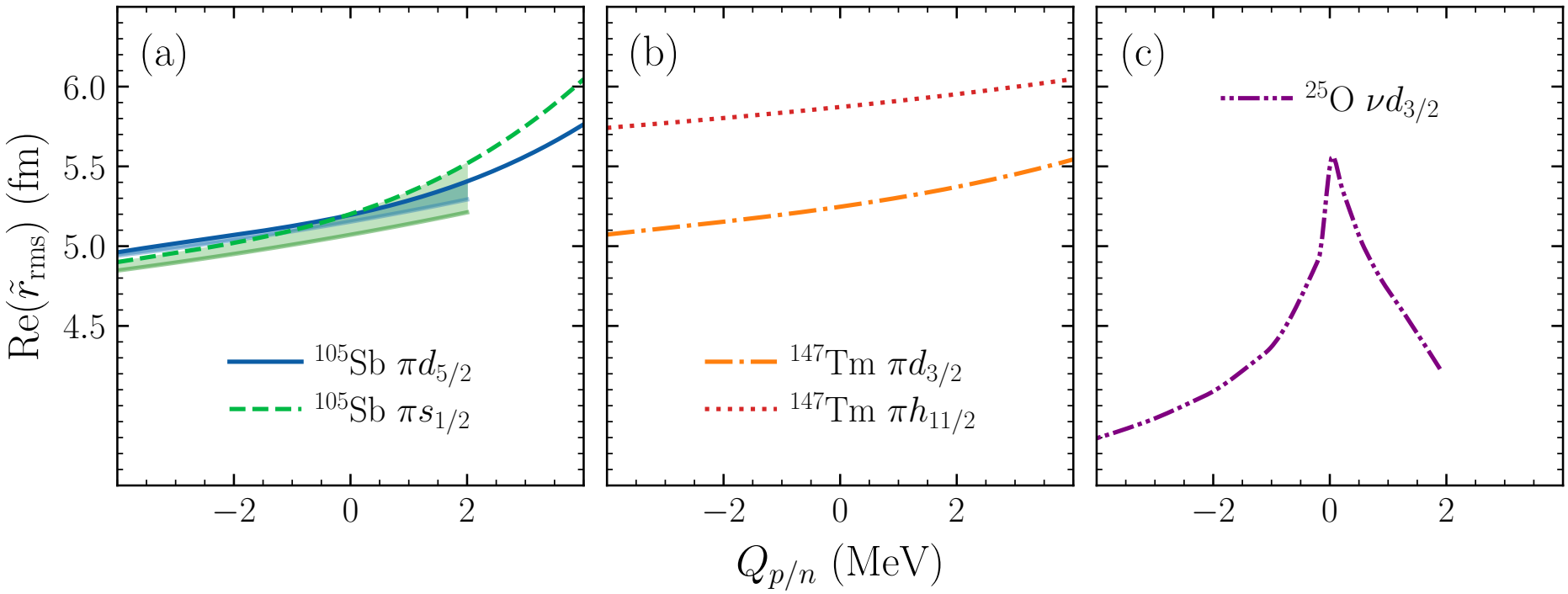


Y. R. Lin, SW *et al.*, Arxiv 2511.10238 (2025)

- Initially, the rms radius matches with the complex one.
- There is a plateau for the rms radius at the early stage of the decay due to the quantum Zeno effect.
- For long-lived system, one can extract the radius experimentally.

Radius enhancement around the dripline

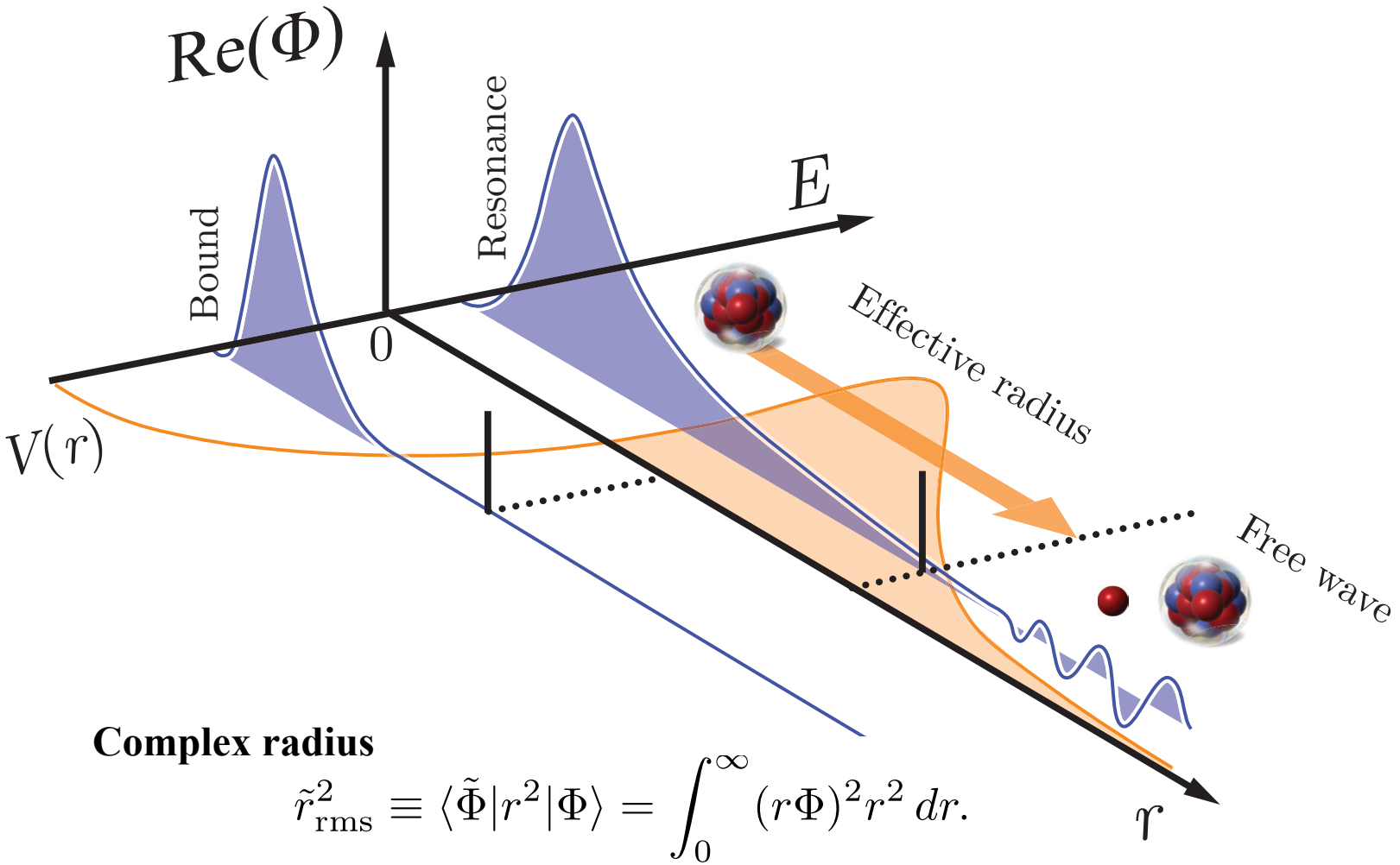
Radius predictions for ^{105}Sb, ^{147}Tm, and ^{25}O



Future test with laser spectroscopy?

- The radii of all the dripline systems are enhanced by the continuum.
- Neutron-rich nuclei are more sensitive to the continuum.

Complex radii of particle emitters

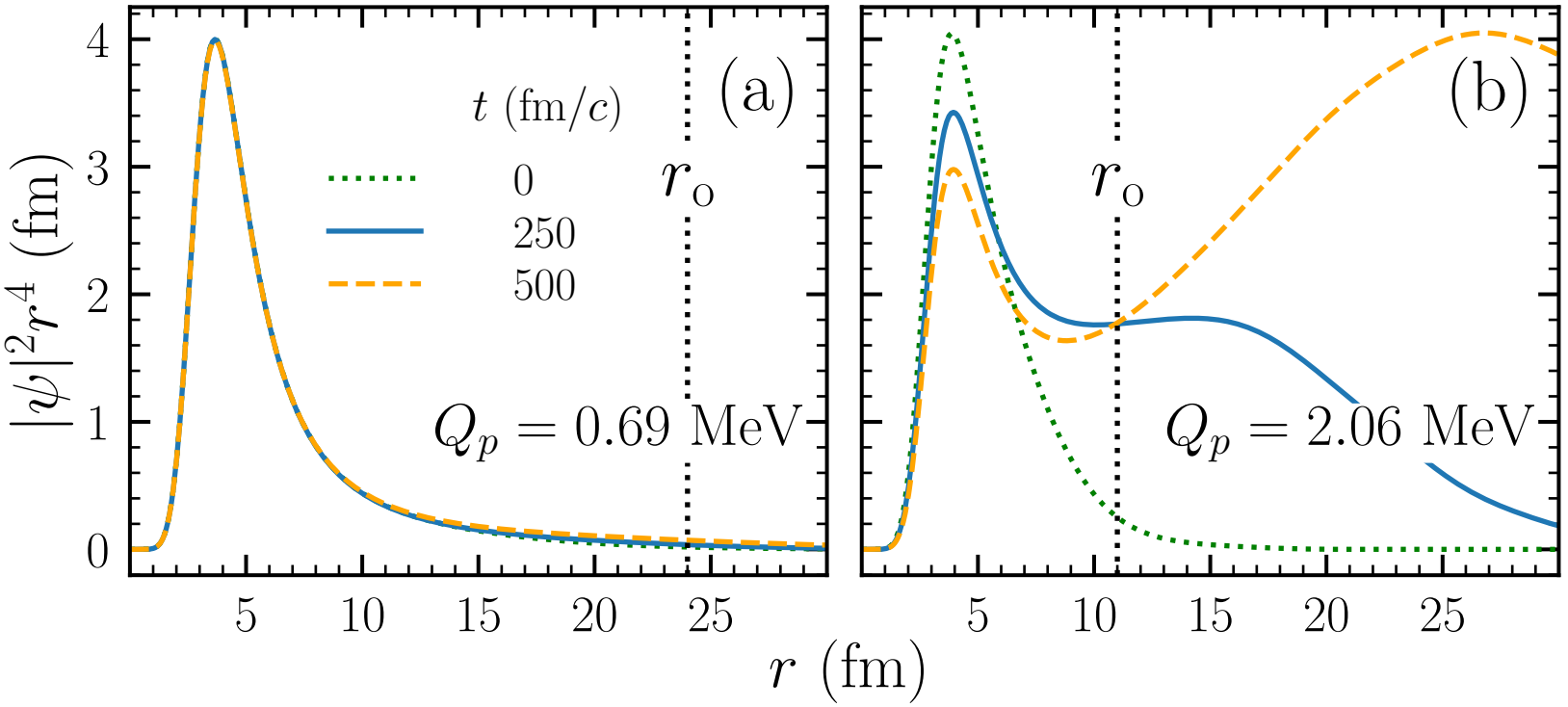


Complex radius

$$\tilde{r}^2_{\rm rms} \equiv \langle \tilde{\Phi} | r^2 | \Phi \rangle = \int_0^\infty (r\Phi)^2 r^2 \, dr.$$

RMS radius evolution during the decay

Wavefunction evolution at Q = 0.69, 2.06 MeV

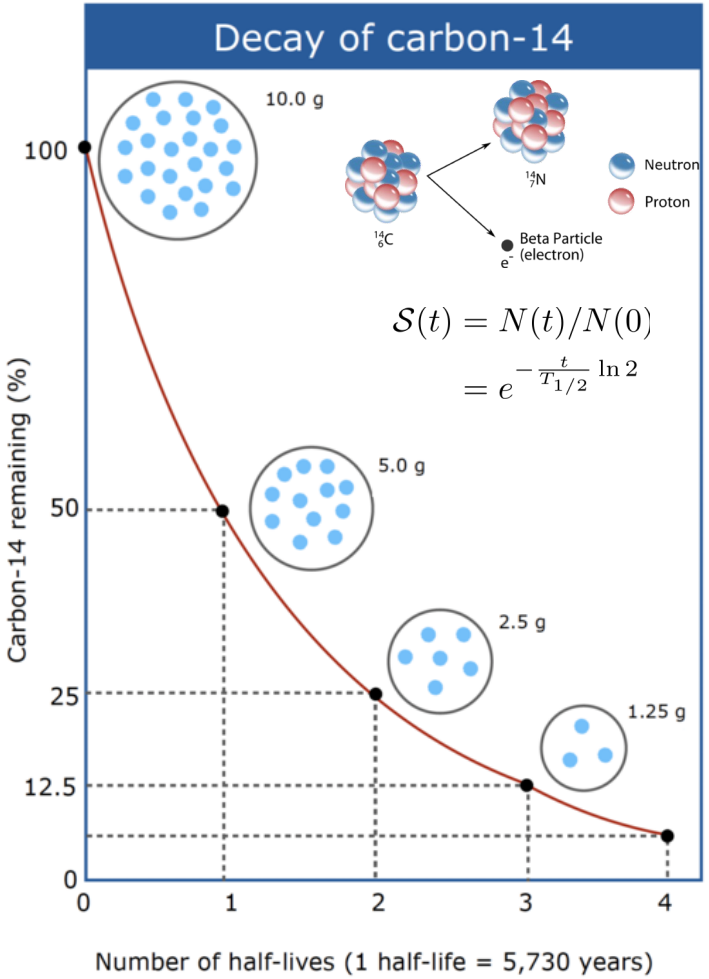


- The density inside r_i gradually decreases.
- Beyond r_o is the free space for particle emission.

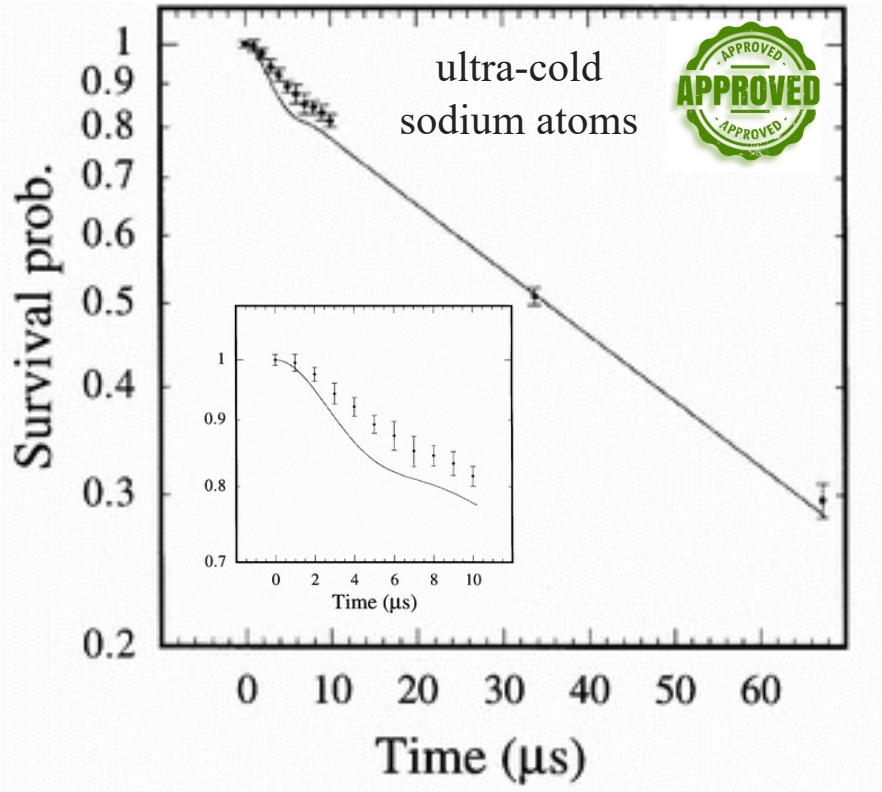
Y. R. Lin, SW *et al.*, Arxiv 2511.10238 (2025)

Quantum Zeno effect

Classical picture of decay



Quantum tunneling

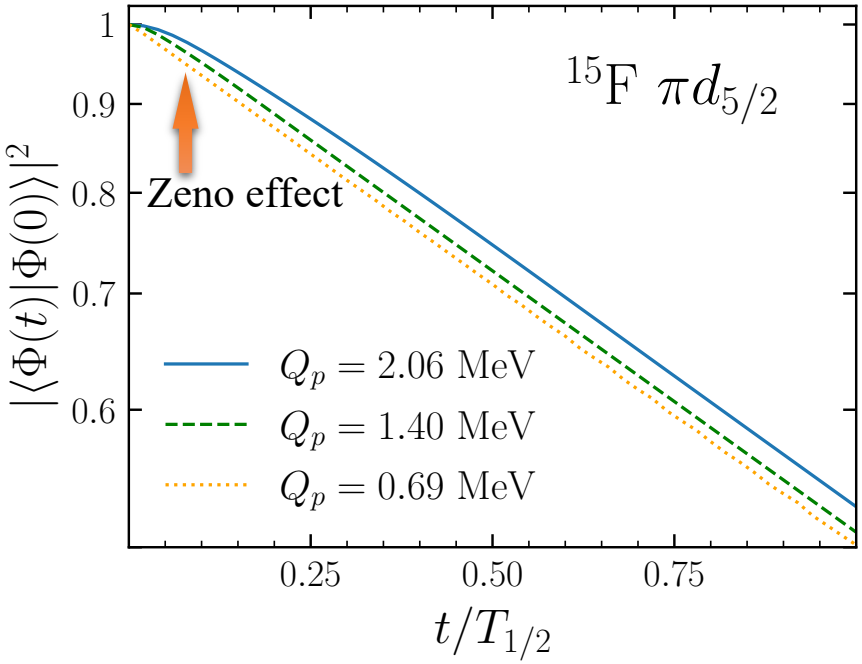


S. R. Wilkinson *et al.*, Nature 387, 575 (1997)
M. Ji and C. Xu, Chinese Phys. Lett. 38 032301 (2021)

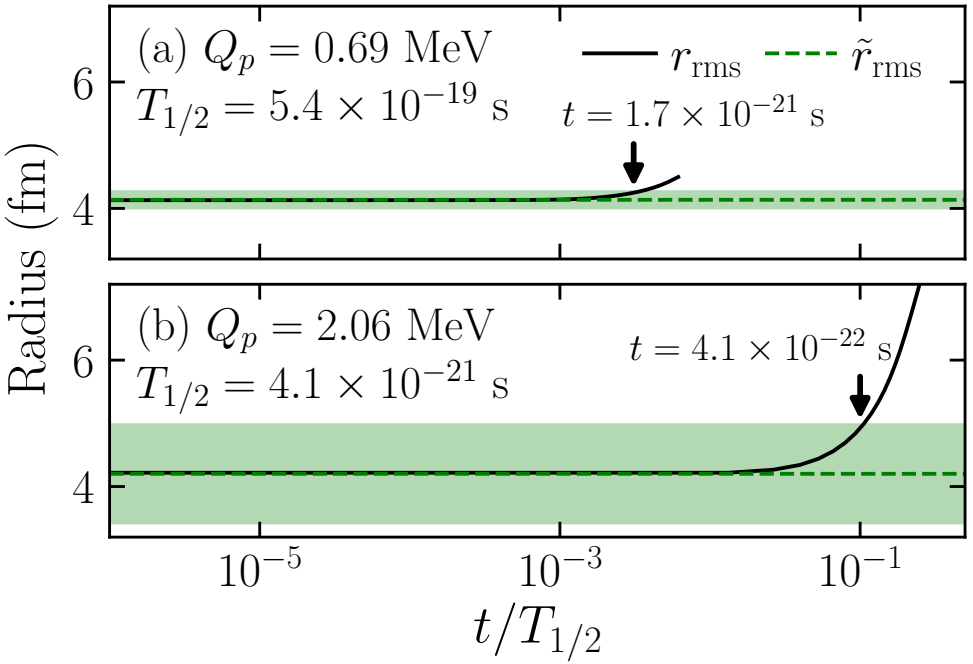
- Decay rate is a constant in classical decay.
- Memory effect in quantum decay.

RMS radius evolution during the decay

Survival probability



Radius evolution at Q = 0.69, 2.06 MeV

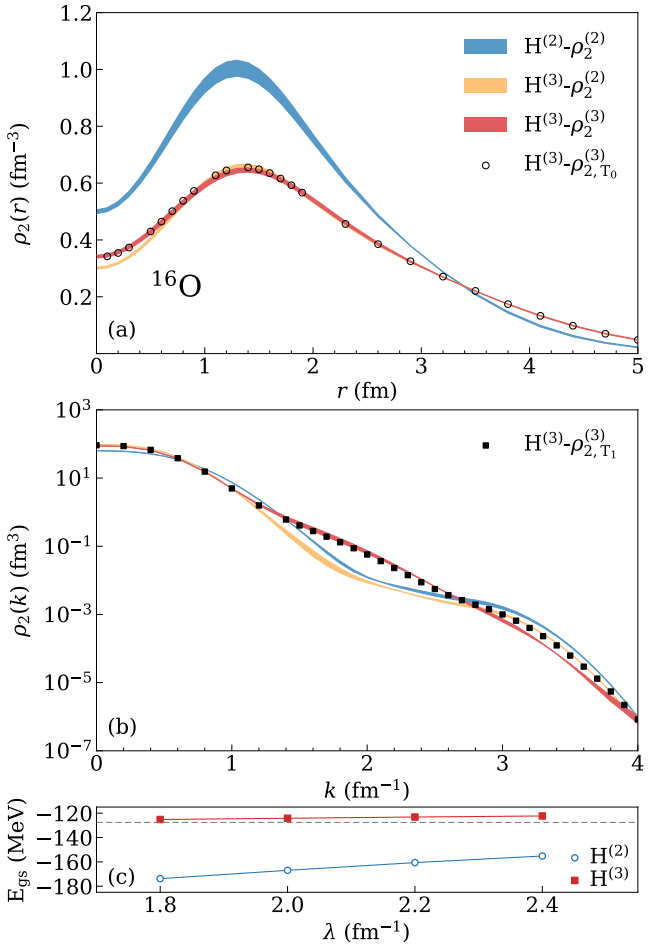


Y. R. Lin, SW *et al.*, Arxiv 2511.10238 (2025)

- Initially, the rms radius matches with the complex one.
- There is a plateau for the rms radius at the early stage of the decay due to the quantum Zeno effect.
- For long-lived system, one can extract the radius experimentally.

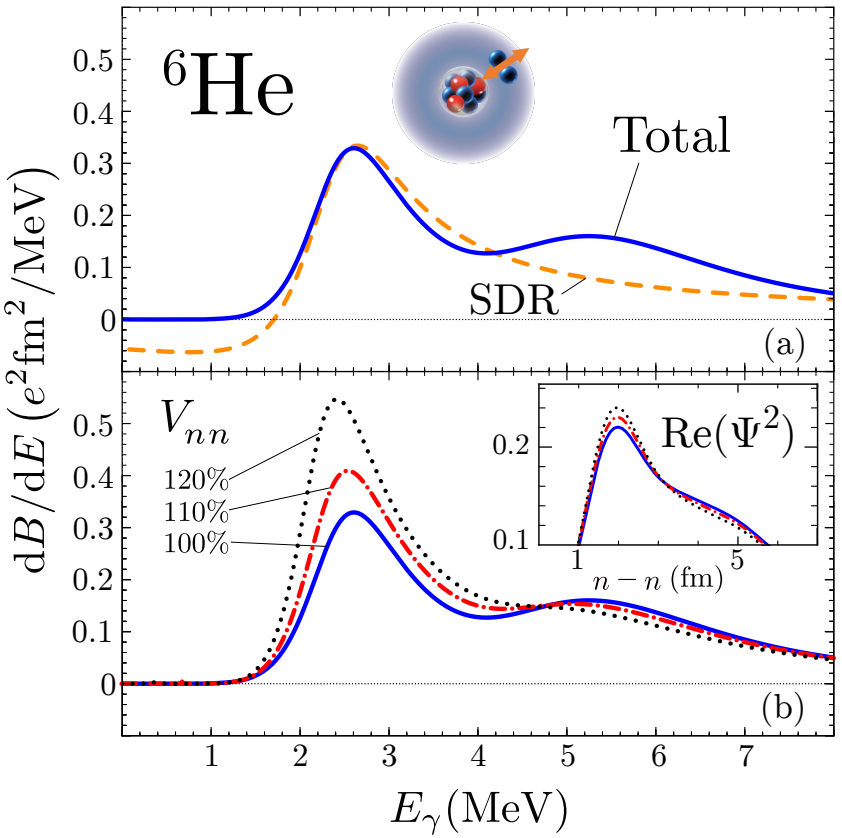
Short & mid ⟷ long range correlations

3-body effect on short-range correlation



H. Y. Shang *et al.*, in preparation

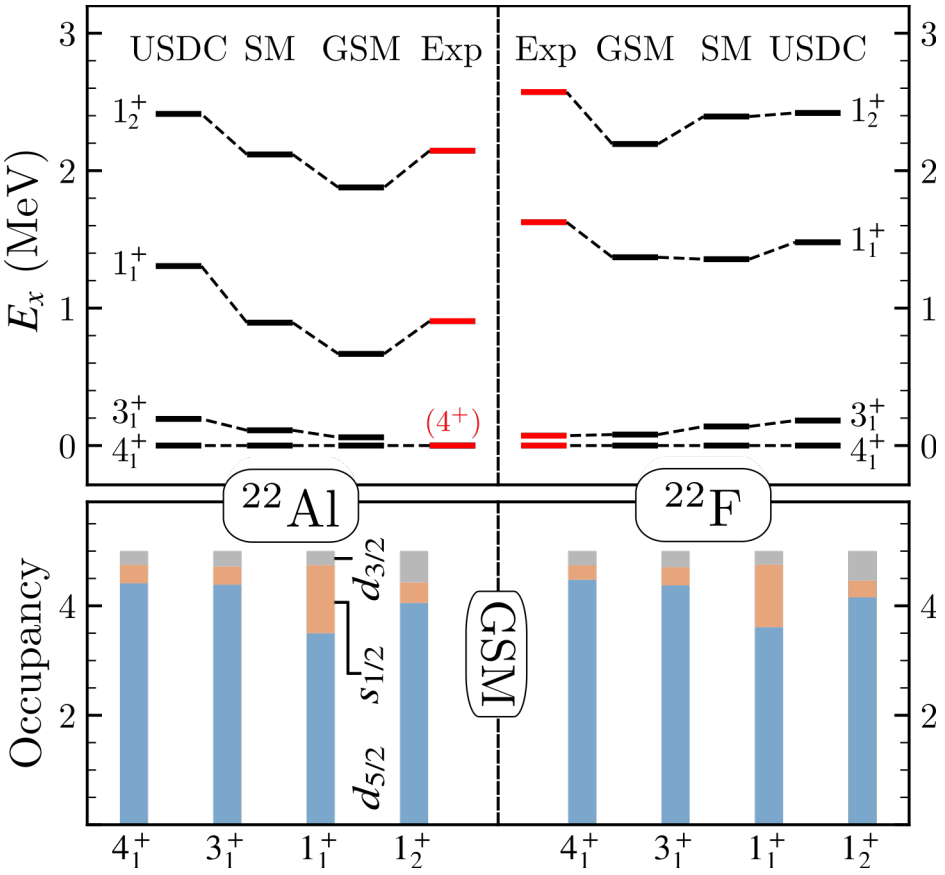
*E*1 response



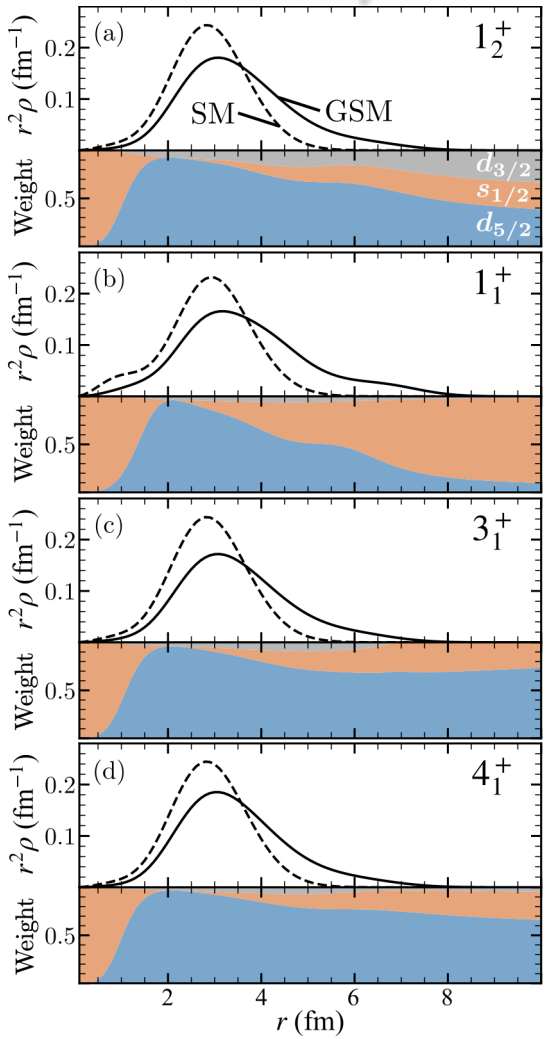
Y. H. Yang *et al.*, Eur. Phys. J. A
T. Nakamura *et al.*, Phys. Rev. Lett 96, 252502(2006)
Y. L. Sun *et al.*, Phys. Lett. B 814, 136072

Halo structure in ^{22}Al?

Spectroscopy of ^{22}Al and ^{22}F



Density

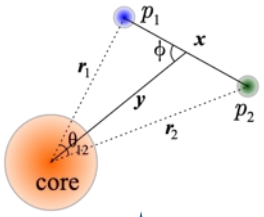


Z. C. Xu, H. Y. Shang, SW, and Y. G. Ma, Phys. Rev. C (Letter) accepted

Summary: selected progresses in multi-*p* decay

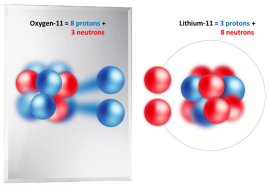
GCC model

SW, Michel, Nazarewicz *et al.*
PRC 122, 122501 (2017)



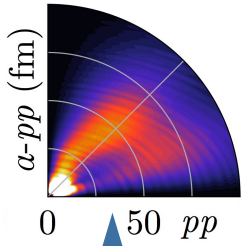
2*p* emitter ^{11}O

Webb, **SW**, Brown *et al.*
PRL 122, 122501 (2019)



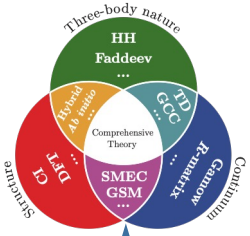
2*p* dynamics

SW and Nazarewicz
PRL 126, 142501 (2021)



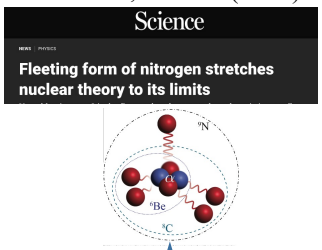
2*p* Review

Pfützner, Mukha, **SW** *et al.*
PPNP 132, 104050 (2023)



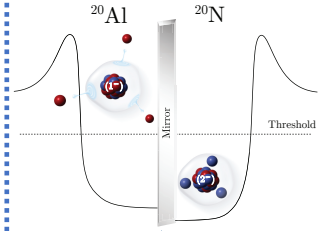
5*p* emitter ^{9}N

Charity, Wylie, **SW** *et al.*
PRL 131, 172501 (2023)

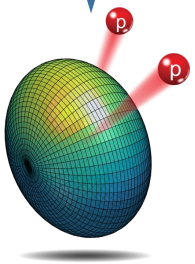


3*p* emitter ^{20}Al

Xu, Mukha, Li, **SW** *et al.*
PRL 135, 022502 (2025)

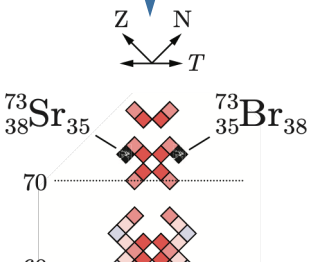


2017 2018 2019 2020 2021 2022 2023 2024 2025 2026



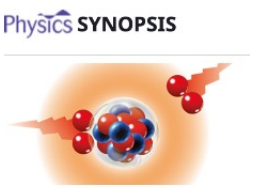
SW and Nazarewicz
PRL 120, 212502 (2018)

Deformed 2*p*



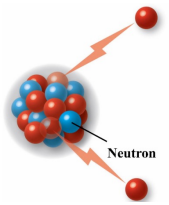
Hoff, Rogers, **SW** *et al.*
Nature 580, 52 (2020)

Mirror symmetry



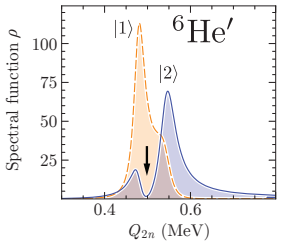
Jin, Niu, Brown, Li *et al.*
PRL 127, 262502 (2021)

4*p* emitter ^{18}Mg



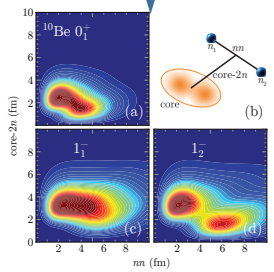
Liu, Xu, Sun, Yuan *et al.*
PRL 129, 242502 (2022)

β*-delayed 2*p



SW, Nazarewicz, Ma
PRR 5, 023183 (2023)

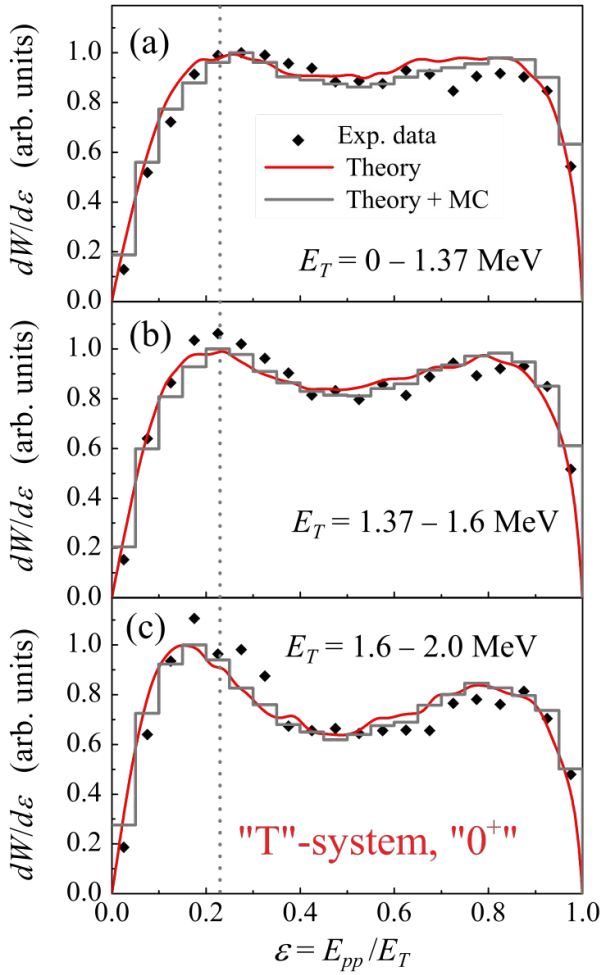
Non-exp decay



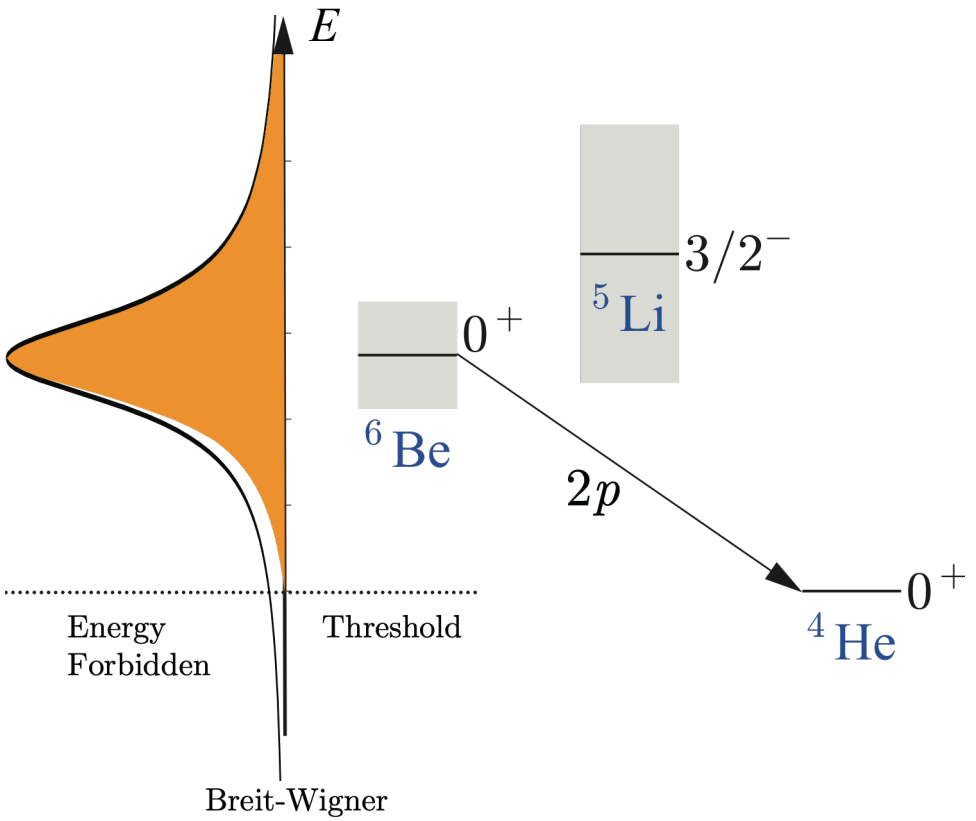
Chen, Ayyad, Bazin *et al.*
PRL 134, 012502 (2025)

Threshold 1$^-$

Energy dependence of the correlation in ^{6}Be

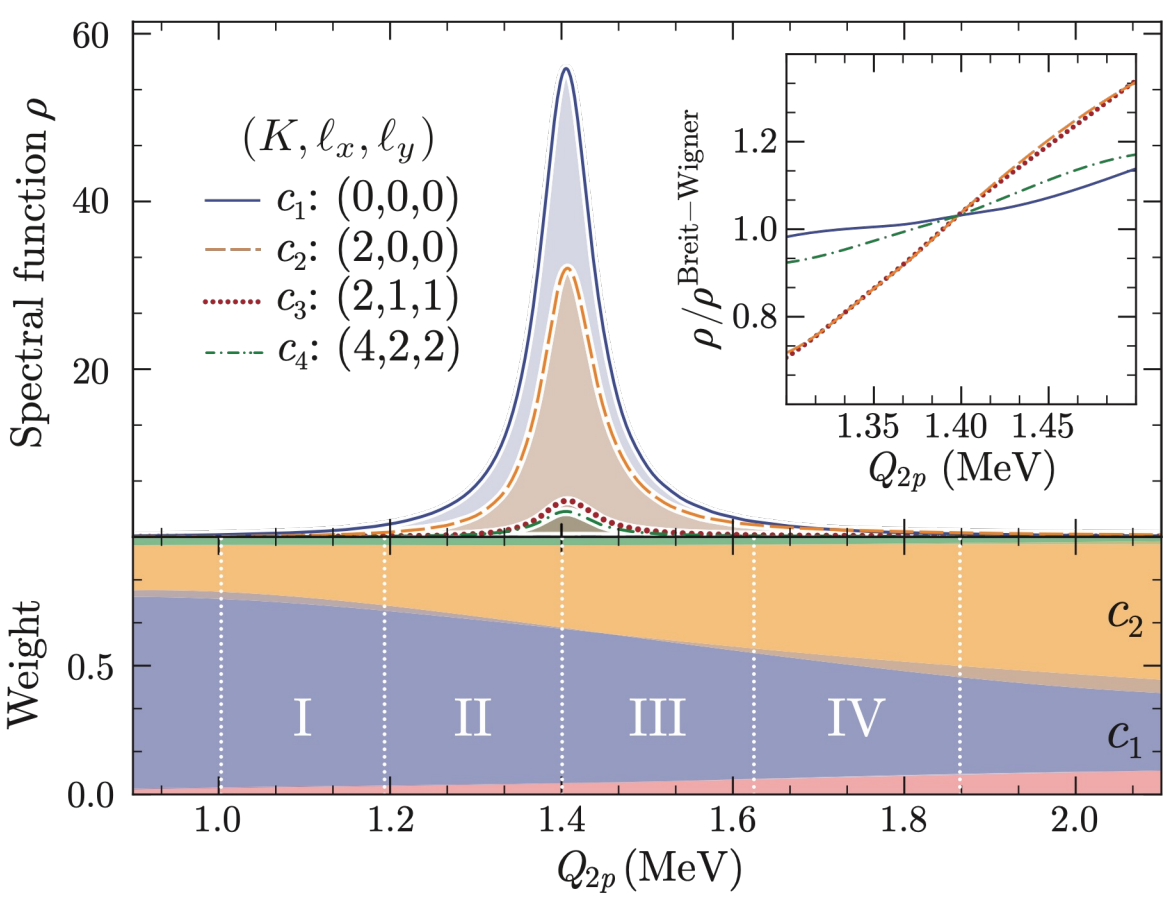


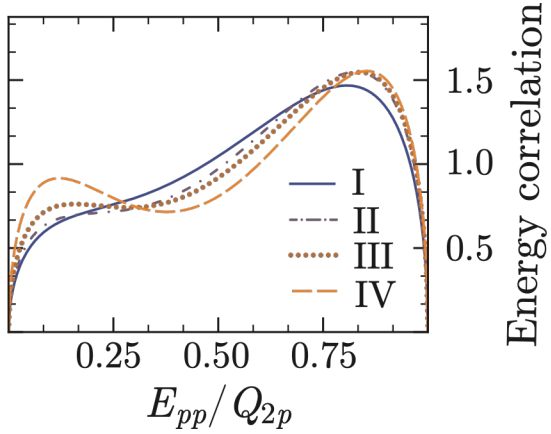
I. A. Egorova *et al.*, Phys. Rev. Lett. 109, 202502 (2012)

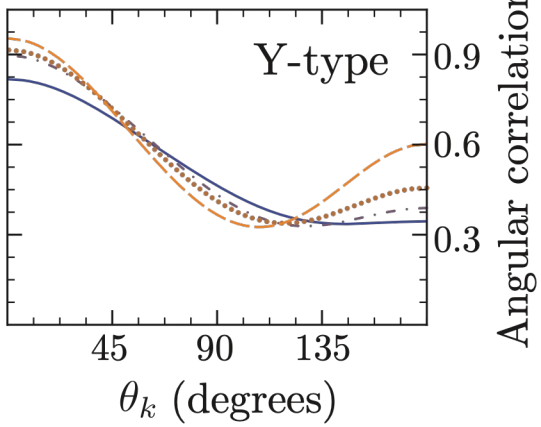


- Deviates from Breit-Wigner due to the threshold proximity.
- The threshold effect is channel-dependent.

Energy dependence of the correlation in ^{6}Be







- The weights of different components change as energy increases.
- Result in a energy-dependent correlation.

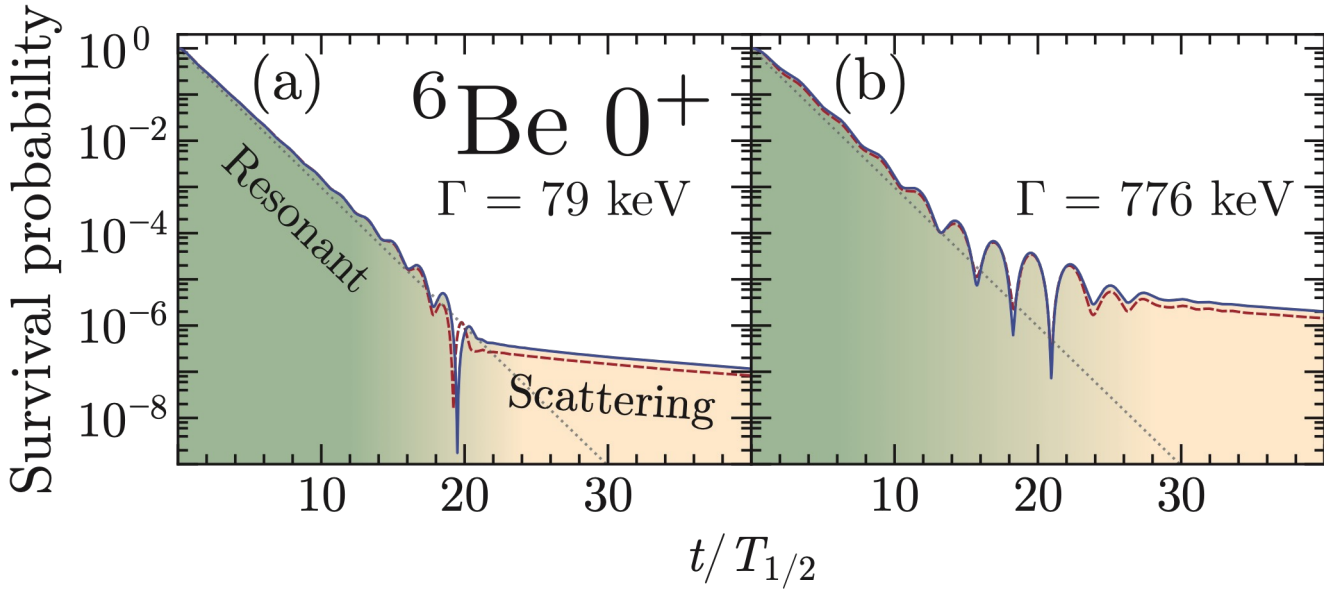
SW, W. Nazarewicz, A. Volya, and Y.G. Ma, Phys. Rev. Res. 5, 023183 (2023)

Non-exponential decay

Survival probability

$$\mathcal{S}(t) = |\langle\Psi(0)|\Psi(t)\rangle|^2 = \left|\int_0^{+\infty} \underline{\rho(E)} e^{-i\frac{E}{\hbar}t} \mathrm{d}E\right|^2$$

Spectral function



Ψ

Complex-energy Gamow state

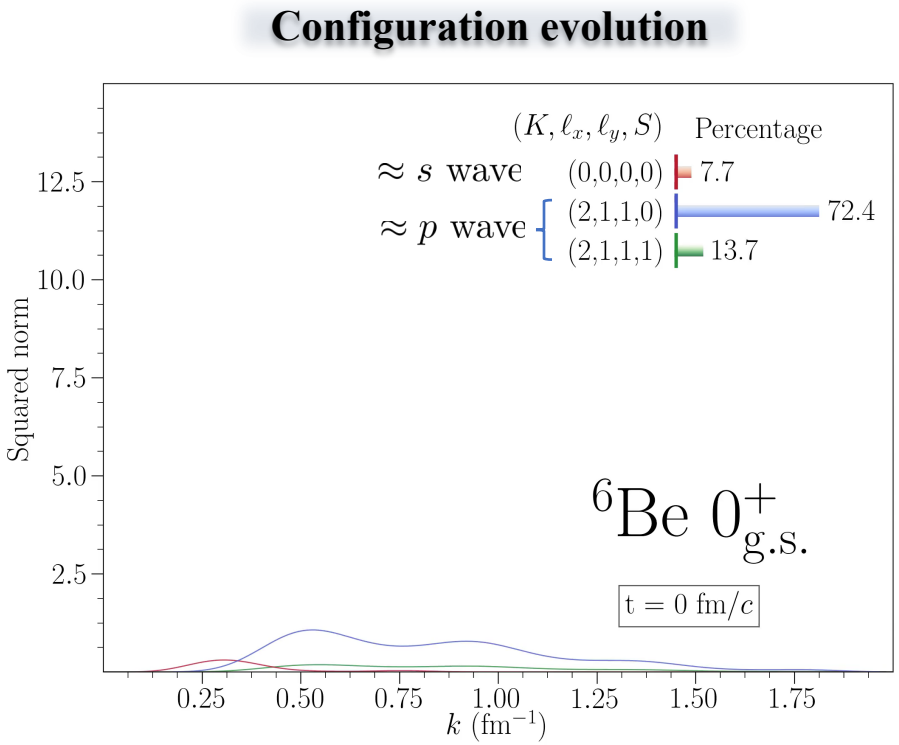
Ψ'

Expanded on harmonic oscillator basis

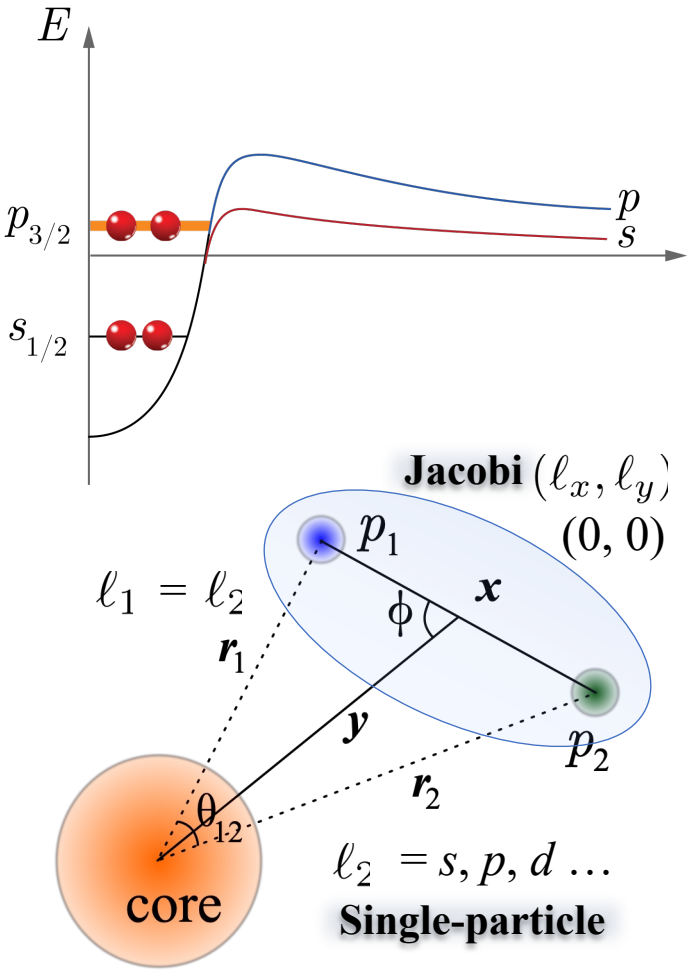
- The time evolution of a resonance contains exponential (resonant) and powered (scattering) decays.
- When the decay width is large enough, scattering feature is dominated.

SW, W. Nazarewicz, A. Volya, and Y.G. Ma, Phys. Rev. Res. 5, 023183 (2023)

Configuration evolution of ^{6}Be



Kinetic energy: $T = \dfrac{\hbar^2}{2m}k^2$

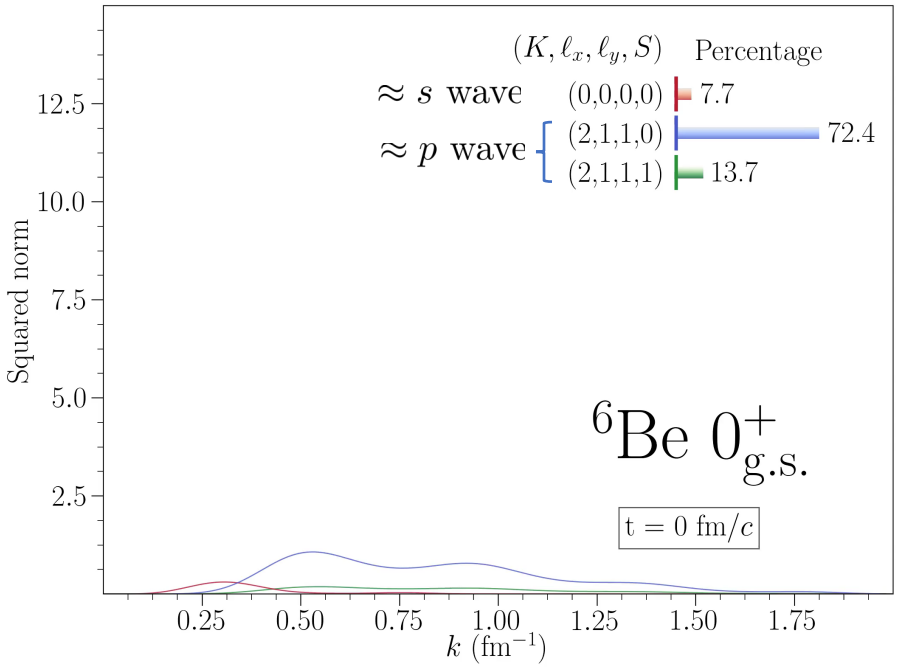


- p wave gradually transfers to s wave.
- The formation of diproton benefits tunneling process.

SW and W. Nazarewicz, Phys. Rev. Lett. 126, 142501 (2021)

Configuration evolution of ^{6}Be

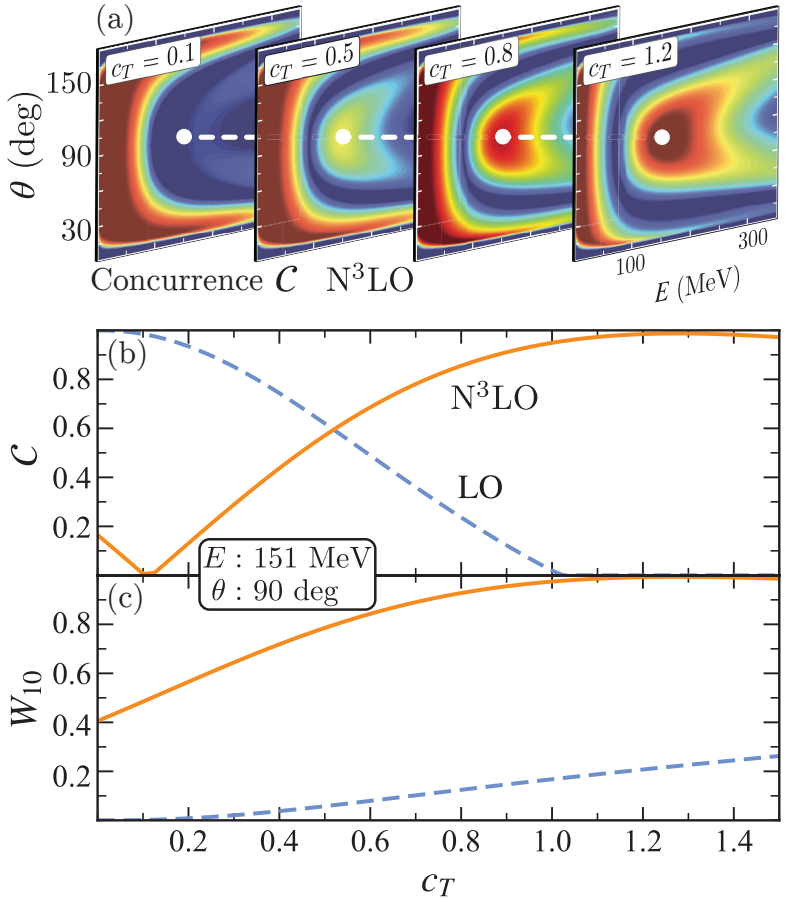
Configuration evolution



Kinetic energy: $T = \dfrac{\hbar^2}{2m}k^2$

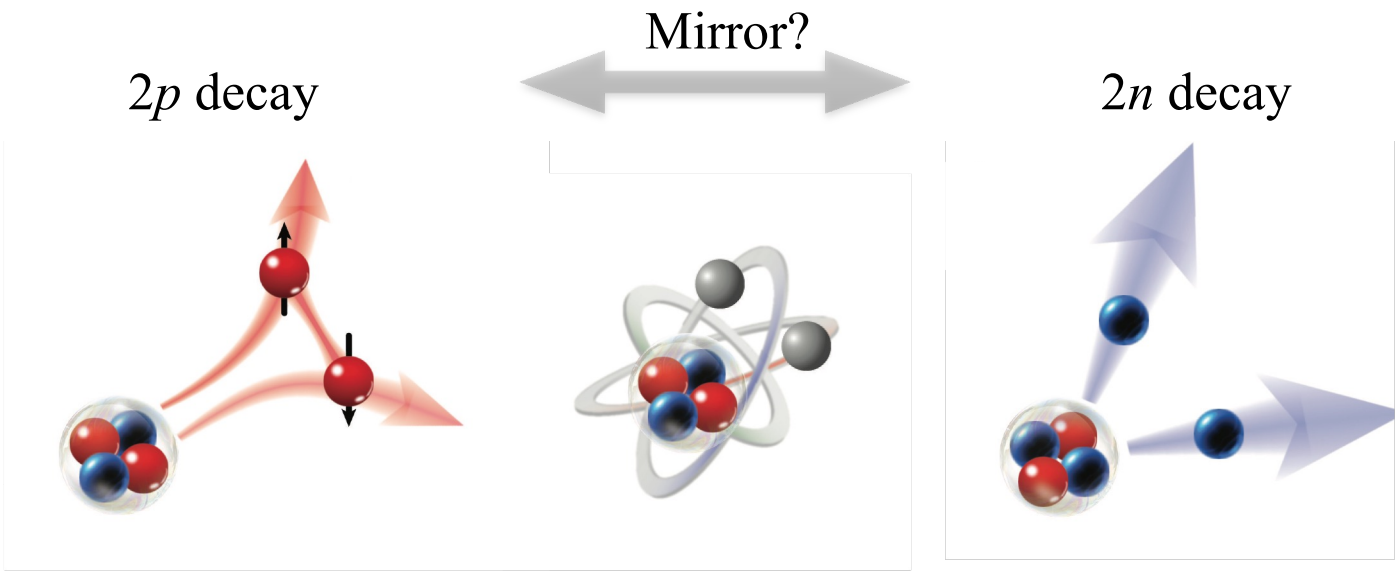
- p wave gradually transfers to s wave.
- The formation of diproton benefits tunneling process.

Probe nuclear force



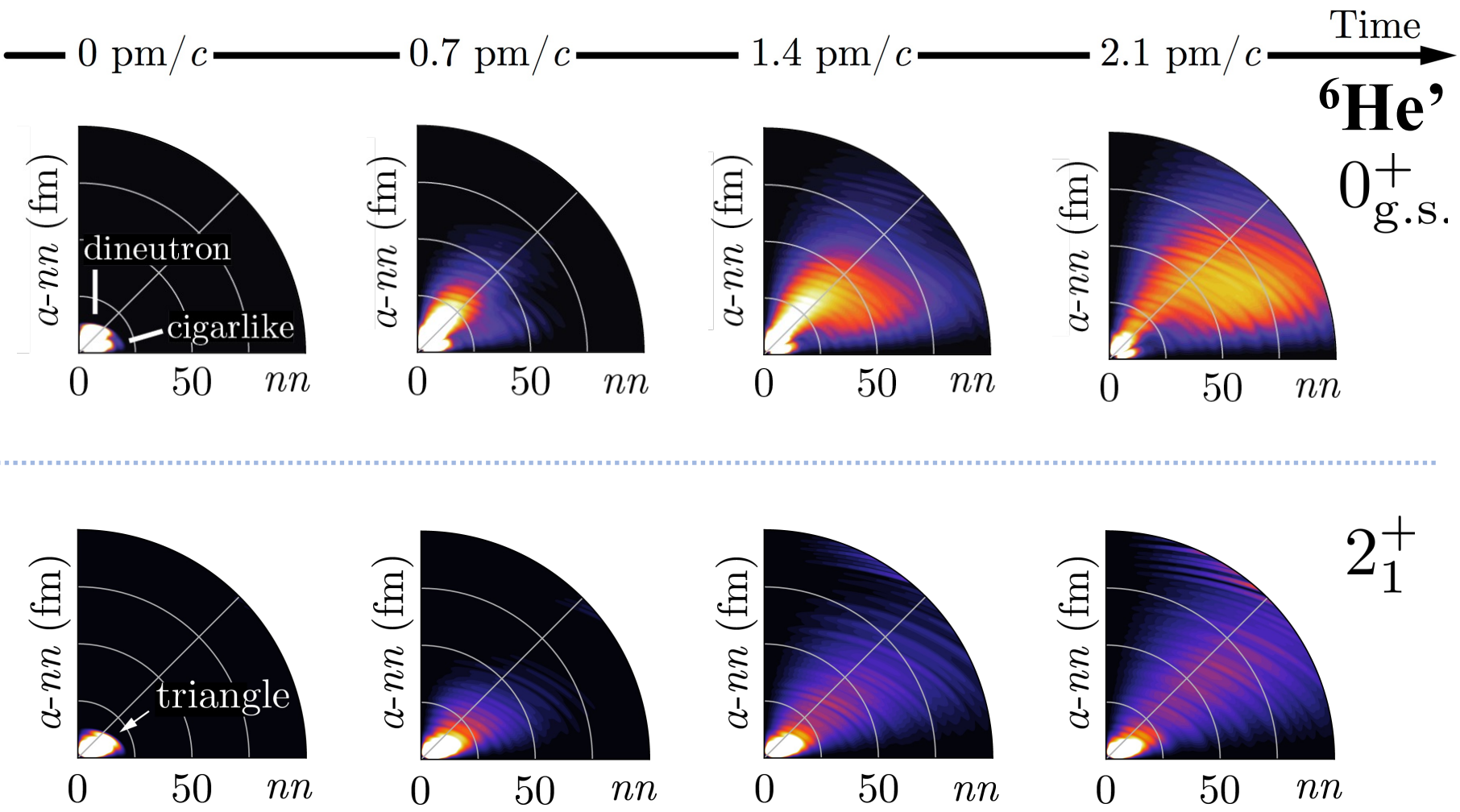
S. Z. Xin *et al.*, Arxiv 2510.24325 (2025)

2*p*/2*n* decay

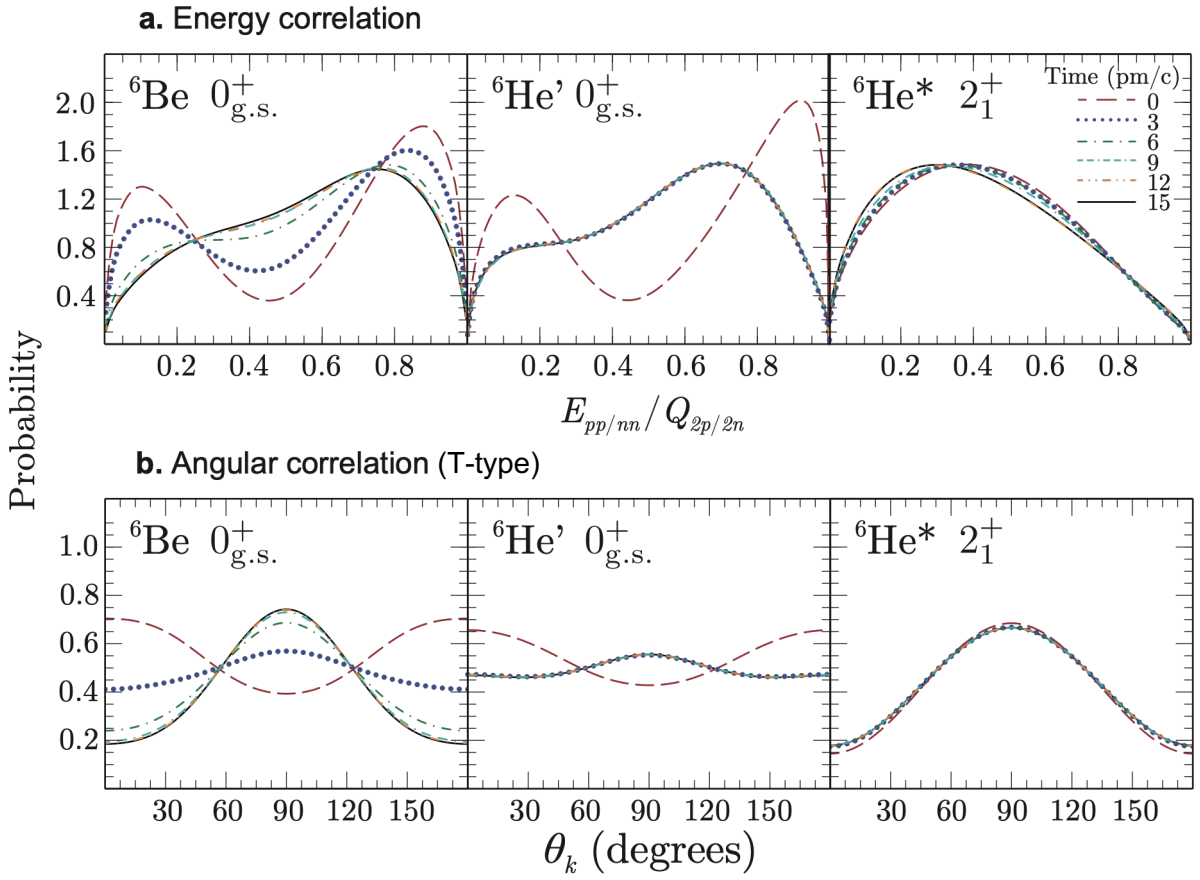


- The symmetry and asymmetry between 2*p* and 2*n* decays.
- Candidates: ^{16}Be, ^{26}O, ^{14}Be* …

Time evolution of ^{6}He’



Evolution of 2*p*/2*n* correlations

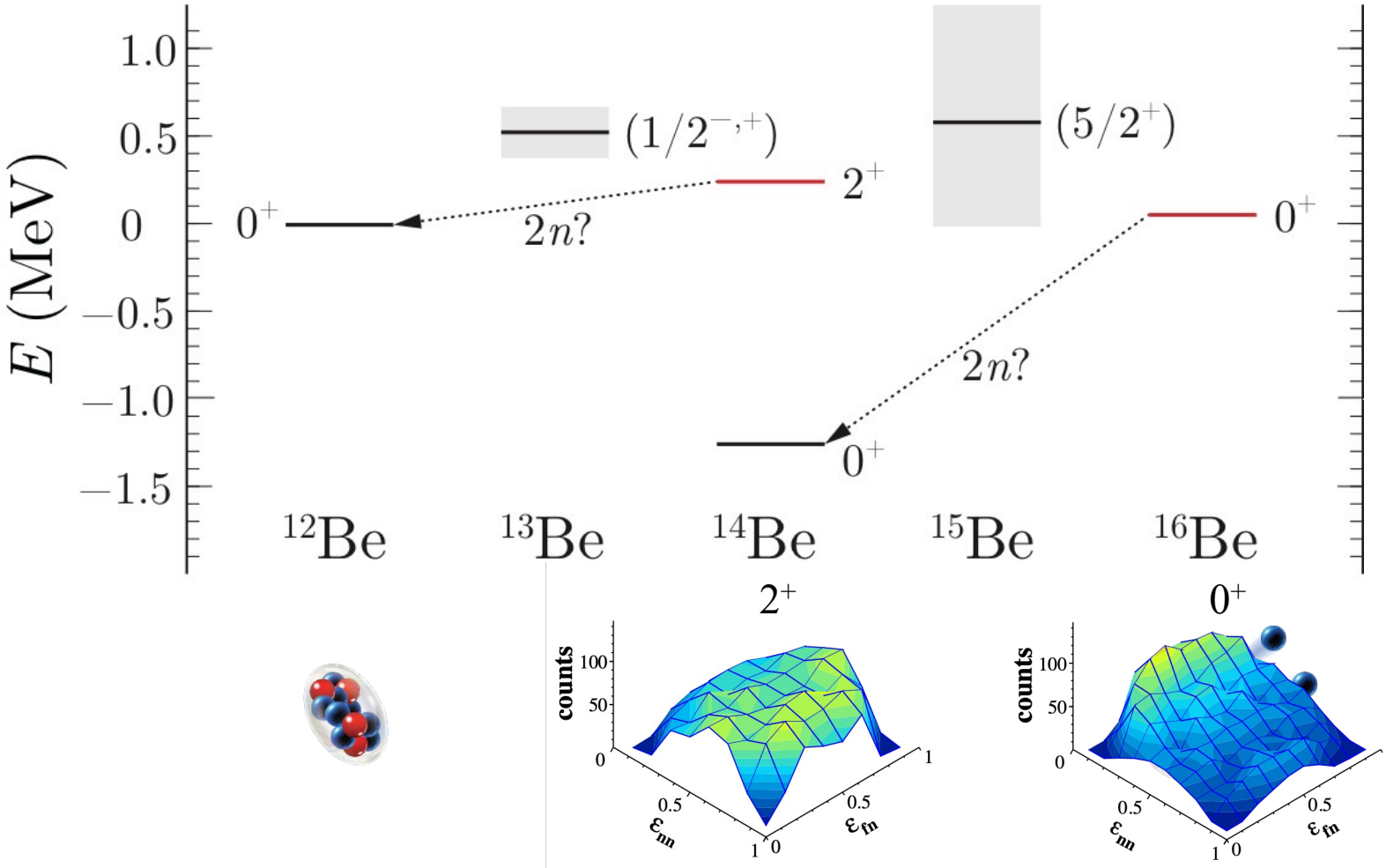


- ***pp***: subthreshold resonance L.P. Kok, PRL 45, 427 (1980)

  $k = 0.0647–i0.0870$ fm^{-1}; $E = –140$ keV; $\Gamma = 934$ keV

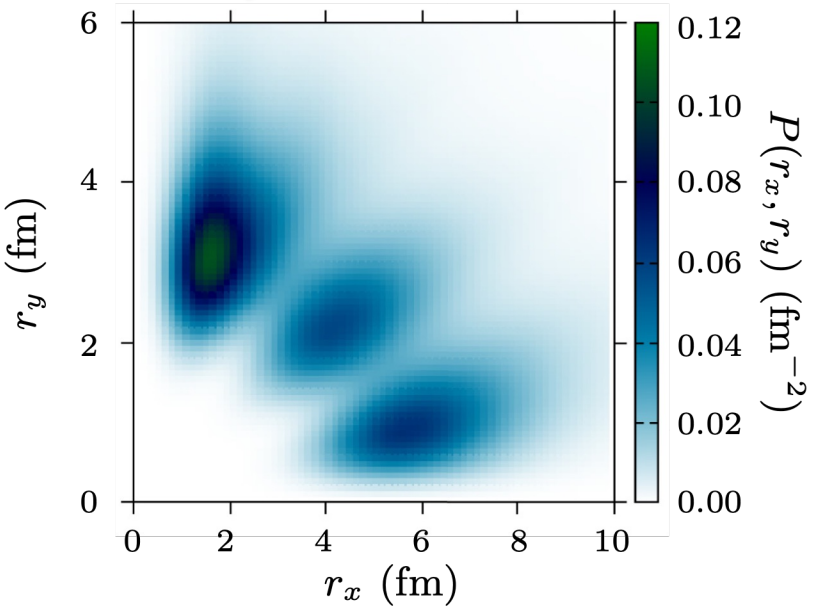
- ***nn***: antibound state, $k = –i0.0559(33)$ fm^{-1} V.A. Babenko, PAN 76, 684 (2013)

2*n* decay of ^{14,16}Be



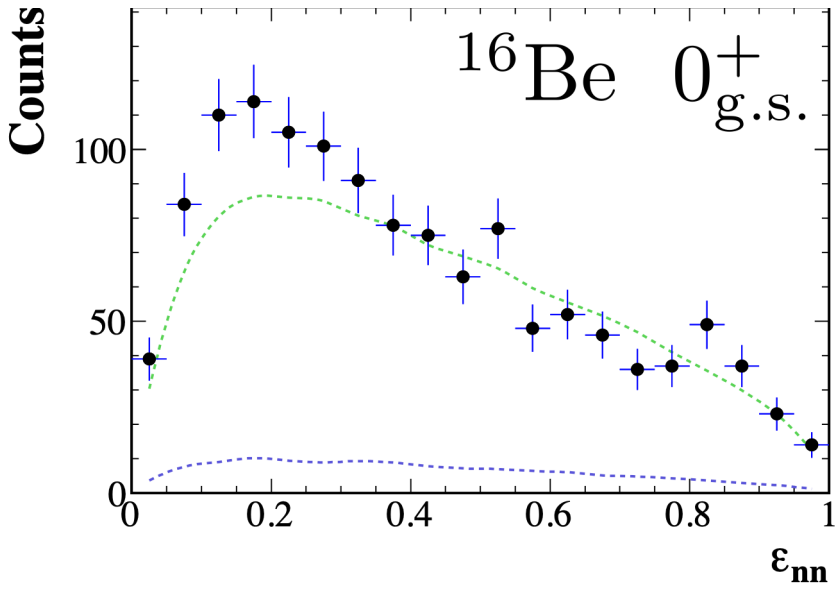
Structure and and correlation of ^{16}Be

Density distribution of ^{16}Be

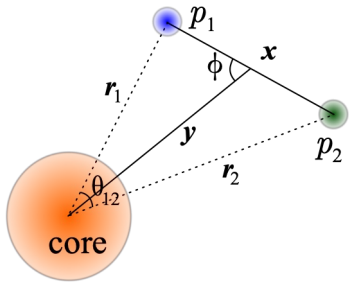


J. Casal *et al.*, Phys. Rev. C 99, 014604 (2019)
A. E. Lovell *et al.*, Phys. Rev. C 95, 034605 (2017)

***nn* energy correlation**



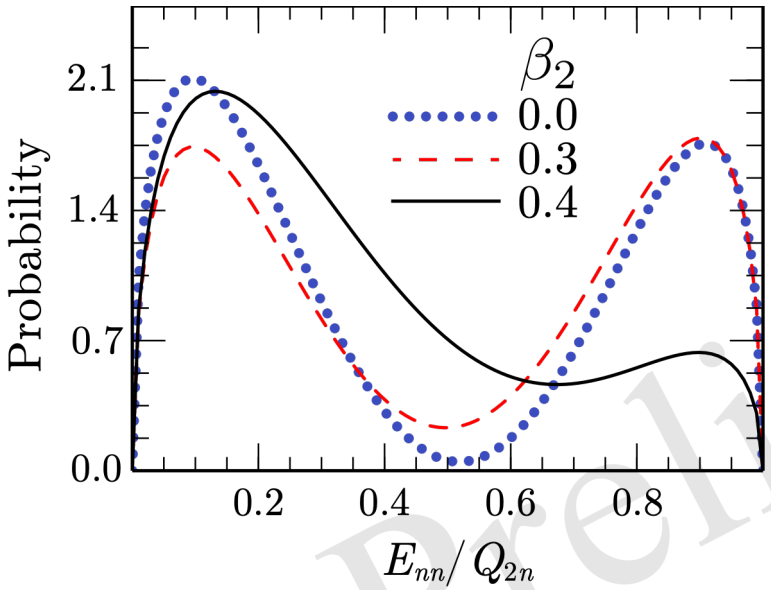
B. Monteagudo, J. Casal *et al.*, Phys. Rev. Lett. 132, 082501(2024)



- The inner structure of ^{16}Be is dominated by *d*-wave component.
- Asymptotic correlation indicates *s*-wave component.
- *pp* & *nn* correlations of *sd*-shell nuclei.

Impact of deformation

nn energy correlation of ^{16}Be



Decay widths and configurations of ^{16}Be

	β_2	E (MeV)	Γ (keV)	Configuration
	0.0	1.486	24	90.1% $(d_{5/2})^2$
				2.6% $(p_{3/2})^2$
				2.1% $(p_{1/2})^2$
				0.2% $(s_{1/2})^2$
	0.4	1.286	547	3.4% $(d_{5/2})^2$
				5.8% $(p_{3/2})^2$
				2.1% $(p_{1/2})^2$
				72.8% $(s_{1/2})^2$

Preliminary

- In spherical case, $s_{1/2}$ orbital is occupied by the core due to the halo structure.
- Deformation causes the mixing among different orbitals.
- $s_{1/2}$ component dramatically changes the decay width and energy correlations.